Using flotsam lines for improving predictions of hydraulic loads on coastal dikes

G.J.W. van Lente

Technische Universiteit Delft

Using flotsam lines for improving predictions of hydraulic loads on coastal dikes

by

G.J.W. van Lente

to obtain the degree of Master of Science
at the Delft University of Technology,
to be defended publicly on Wednesday May 29, 2019 at 14:00 PM.

Student number:	4233255	
Thesis committee:	Prof. Dr. Ir. M. Kok,	Delft University of Technology
	Ir. R. Slomp,	Rijkswaterstaat
	Dr. Ir. V. Vuik,	Delft University of Technology & HKV
	Dr. Ir. G.Ph van Vledder,	Delft University of Technology & Van Vledder Consulting

An electronic version of this thesis is available at http://repository.tudelft.nl/.

TU Delft

Rijkswaterstaat
Ministerie van Verkeer en Waterstaat

Preface

This thesis concludes the master track Hydraulic Engineering, with specialization Hydraulic structures and Flood Risk at Delft University of Technology. This research was carried out at Rijkswaterstaat.

I would like to thank my entire thesis committee: Matthijs Kok, Robert Slomp, Vincent Vuik and Gerbrant van Vledder, for their expertise, feedback and inspiration. I would especially like to thank Robert Slomp, for his critical view, his feedback and his advice about the subject during all the meetings we had. Also Vincent Vuik, for his critical view and sharing his knowledge about the subject. I would like to thank you both for the support and to make time whenever I needed advice. Vincent, also thank you for making it possible to work on my thesis at HKV. Many thanks to Gerbrant van Vledder for his critical view at my approach and especially sharing his expertise regarding the SWAN model. I would also like to thank my colleagues at Rijkswaterstaat, especially Robert Vos and Marcel Bottema for their personal involvement, discussions and interest in my research. Furthermore, thanks to Henry Rijploeg and his team of water authority Noorderzijlvest which made it possible to perform recordings (during stormy conditions) and measurements at the Wadden Sea dike between Noordpolderzijl and Eemshaven. Another thank you goes to Patrick Oosterlo, he has helped me to perform SWAN computations on one of the Linux clusters of the TU Delft.

Last but not least, I want to thank my girlfriend and family for their support and my fellow graduate students at Rijkswaterstaat and HKV for their interest, advice and the enjoyable time during the lunch and coffee-breaks.

G.J.W. van Lente
Middelharnis, May 2019

Abstract

The purpose of this thesis is to investigate the (added) value of spatial information obtained from flotsam lines. These lines may arise at coastal dikes in the vicinity of vegetated foreshores. Flotsam (pieces of floating debris) exist mainly of organic material and is transported onto the dike by waves during a storm surge. The position of the flotsam line on the dike slope gives an indication of the hydraulic loads along the dike. The line is expected to mark the highest wave run-up (maximum wave run-up).

In the past, measured flotsam lines were used to predict hydraulic loads on coastal dikes, but models (SWAN and WAQUA) fulfill currently this function. This may result in losing the value of flotsam lines. By investigating the spatial information obtained from flotsam levels, this study may be used for improving predictions of hydraulic loads on coastal dikes. The study of Witteveen+Bos [2010] used flotsam lines measurements instead of wave buoys to assess the performance of SWAN. The remaining questions and recommendations of Witteveen+Bos [2010] were the main reason for Rijkswaterstaat to conduct this study. By performing this study, it should become clear how the information obtained by flotsam lines can be used by hydraulic engineers in the future.

Recordings and observations were performed for this study during the storm of 8 January 2019. Based on the findings, it was determined that the upper side of the flotsam line marked the maximum wave run-up in case of a small layer of flotsam. Besides, a relative thick layer of flotsam was able to absorb the force of the wave run-up and remained in position. This means that the amount of flotsam can disturb the wave run-up and eventually flotsam levels.

The applied method in this study was used to compare calculated and measured flotsam lines for the Wadden Sea dike trajectory between Lauwersoog and Eemshaven in the Netherlands. The method existed of a sequence of models and wave run-up formulas, which were used to calculate flotsam levels for three different occurred storms. Four stationary SWAN simulations (hindcasts) were performed to compute wave conditions for four time instants around the peak water level for each storm. These wave conditions were used to calculate the (maximum) wave run-up. This was done with help of the EurOtop [2016] and 'Delft' wave run-up formulas and by applying a Rayleigh or Battjes-Groenendijk wave height distribution in calculation of the flotsam levels (maximum wave run-up).

By comparing the calculated and measured flotsam lines it became clear that the EurOtop [2016] and 'Delft' formula together with an applied Battjes-Groenendijk and Rayleigh wave height distribution respectively approximated the highest measured flotsam levels (5.5 - 6.5 m+NAP) quite well. Nevertheless, the calculated lines, using the EurOtop [2016] formula, tend to overestimate the measured flotsam lines. Based on the systematic comparison between modelled and measured data (wind, water level and wave conditions), it was determined that modelled wave conditions at Uithuizerwad overestimated significantly the measurements. This means that the analysis of (calculated) flotsam lines gives an indication of the performance of the applied set of models (SWAN and WAQUA) and wave run-up formulas, provided that a systematic comparison between modelled and measured data is performed.

In addition, flotsam levels were also calculated using measured wave conditions at the toe of the dike instead of computed wave conditions by SWAN. Pressure sensors measured water level and wave conditions at four locations (positioned over a length of 1.5 km) near the toe of the Wadden Sea dike close to Eemshaven. Again, the same wave run-up and wave height distributions were used to calculate the (maximum) wave run-up.

The calculated flotsam levels (EurOtop [2016] and an applied Battjes-Groenendijk distribution) at the four locations, based on the measurements near the toe of the dike, resulted in smaller overestimations (up to +0.5 m) than the overestimations (up to +1.5 m) based on computed wave conditions by SWAN.

Finally, it can be said that the information obtained from flotsam levels gives an indication of the hydraulic loads along a dike. This study showed that the upper side of the flotsam line marked the maximum wave run-up in case of a small layer of flotsam. Besides, a relative thick layer of flotsam was able to absorb the force of the wave run-up and remained in position. This means that the amount of flotsam can disturb the wave run-up and eventually flotsam levels. It also became clear that the used method is able to give an indication of the performance of the applied set of models (SWAN and WAQUA) and wave run-up formulas. A large database of detailed flotsam lines with corresponding storm conditions (water level, wave conditions, wind, etc) can provide valuable information to low costs. This database can be used to detect spatial variations which might give more insight in certain processes during storm conditions. It may also serve as the starting point for follow-up studies using new methods for analysing flotsam lines.

Contents

1 Introduction

In the Netherlands, the majority of the population is located in flood prone areas. The primary flood defence system along the rivers, coasts and lakes is thus of critical importance for the nation. Waterwet [2009] prescribes that primary flood defences should be assessed each 12 years to the required safety standards. The managing institution of a primary flood defence must assess at least once every 12 years whether their flood defences meet the required safety standards and must report this to the Minister of Infrastructure and Water Management (IenW), who is responsible for the primary flood defences.

In which way the safety assessment for primary flood defences has to be performed is prescribed in a legal safety assessment method. Rijkswaterstaat (RWS) is updating this instrument for each round on behalf of the Ministry of IenW. This is done on the basis of new knowledge, insights from research and experiences from the past. The upcoming assessment round is called WBI2017 (Wettelijk Beoordelingsinstrumentarium) and runs from 2017 till 2023. In the safety assessment of dikes, different failure mechanisms are used to describe different processes of how a dike can lose its primary function. The primary function of a coastal dike is to prevent flooding of the hinterland. The most commonly encountered failure mechanisms for dikes are shown in Figure 1.1. Wave overtopping is typically relevant for coastal dikes, overtopping occurs if waves running up the outer slope of the dike will flow over the top of the dike.

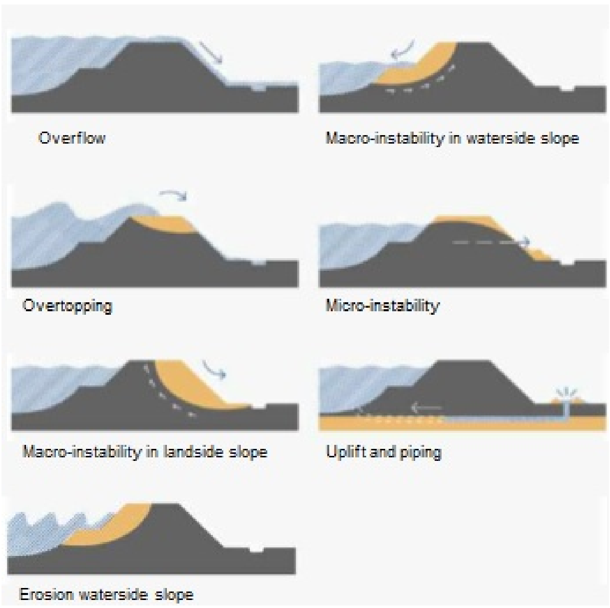

Figure 1.1: Failure mechanisms in earthen structures [ENW, 2017]

In the past, some hydraulic engineers used measurements of flotsam lines (each in their own way) to assess the safety of coastal dikes along the Wadden Sea dikes in the Netherlands. Flotsam lines (in Dutch: veekranden) may arise on dikes after a storm surge (Figure 1.2). These lines are generated when material due to debris accumulation on the foreshore has been transported onto the dike surface by wave run-up. Hydraulic engineers who used flotsam line measurements, interpreted a flotsam line as a line which is marking the highest wave run-up (maximum wave run-up).

Figure 1.2: Two flotsam levels along the dike are clearly visible after two high waters during the storm surge of 5/6 December 2013. [Photo: Regional water authority Hunze en Aa's]

1.1. Problem statement

Sanders [1962], IJnsen [1983], Niemeyer et al. [1995] and Grüne [2005] showed with their studies that flotsam lines can provide valuable information for determining hydraulic loads and to perform safety assessments on dikes. Sanders [1962] investigated wave run-up and wave overtopping at the Emmapolderdike (dike section along the Wadden Sea in the Netherlands between Lauwersoog and Eemshaven). He used eight flotsam line measurements, which were measured between January 1958 and March 1962, to determine a relation between wave run-up and water levels. The purpose of this was to get an impression of wave run-up for storms with higher water levels. IJnsen [1983] investigated also flotsam line measurements. He wanted to obtain an estimate for the significant wave height and angle of wave attack under design conditions for the dike beneath Hollum at Ameland. Based on a schematized probabilistic model, IJnsen developed a method to translate the measured flotsam line to the commonly used 2% wave run-up. A more recent study, Witteveen+Bos [2010], used flotsam lines measurements instead of wave buoys to assess the performance of SWAN. These measurements were used because no wave buoys were deployed at the time of the storm.

All these studies indicate that flotsam lines can provide valuable information, but there is still a lack of knowledge about how this spatial information can be used to obtain more insight in water levels, wave conditions and wave run-up during storm conditions. Flotsam lines were measured if there was a certain reason to measure them, but they are currently not consequently measured in a structured way after a storm. And if measured, it is unknown whether Rijkswaterstaat can use the spatial information obtained from flotsam lines, to improve the models which predict the hydraulic loads on coastal dikes. The main reason for Rijkswaterstaat to conduct this study are the remaining questions and recommendations of Witteveen+Bos [2010].

1.2. Objectives

The objective of this study is to investigate the (added) value of spatial information obtained from flotsam lines. By investigating the spatial information obtained from flotsam levels, this study may be used to improve the models, which predict the hydraulic loads on coastal dikes, used by Rijkswaterstaat. By performing this study, it should become clear how the information obtained by flotsam lines can be used by hydraulic engineers in the future.

1.3. Research questions

The main question which follows from the objectives is:

- How can flotsam lines be used in the safety assessment of flood defences?

Sub-questions:

1. How was the obtained information from flotsam lines used in the past?
2. How can flotsam lines be used to assess the quality of the models used by Rijkswaterstaat?
3. How can the obtained information from flotsam levels give more insight in wave physics during storm conditions?
4. In which way should flotsam lines be measured to obtain useful information?

1.4. Approach and report structure

This study focusses on the (added) value of spatial information obtained from flotsam lines. The first chapter gives a brief introduction in flotsam lines, followed by a problem statement along with objectives and research questions. In Chapter 2 the theoretical background about waves and wave run-up and a model to calculate the maximum wave run-up (flotsam level) is provided. In Chapter 3 former studies containing flotsam line measurements are analysed. The aim is to see how obtained information from flotsam lines was used in the past. This chapter contains also a collection of the gathered flotsam lines. This is followed by a discussion of recordings and observations made on 8 January 2019 during storm conditions in Chapter 4. The method to calculate flotsam levels, using a set of models (SWAN) and formulas, is explained in Chapter 5. This chapter also contains an elaboration of the model set-up to perform the hindcasts in the wave model SWAN. In Chapter 6 the calculated flotsam lines, based on computed wave conditions by SWAN, and a comparison with measured flotsam lines is presented. This is followed by Chapter 7 in which measured wave conditions were used to calculated flotsam levels. A general discussion is given after the obtained results (Chapter 8). Followed by a conclusion by answering the research questions in Chapter 9.

A more elaborated collection of flotsam lines is given in Appendix I. Appendix II contains properties of the considered dike-foreshore trajectory. In Appendix III, IV and V measured and modelled water levels, wind and wave data is presented. Furthermore, these appendices contain SWAN output such as spatial figures of all hindcast moments. Lastly, Chapters VI and VII contain measured data at the salt marsh edge between Lauwersoog and Eemshaven close to the toe of the dike.

2
Literature overview

The purpose of this chapter is to provide necessary background information regarding the generation of flotsam lines. This study focuses mainly on flotsam lines in the Wadden Sea area. Literature about wind waves and wave run-up is described. In these sections wave parameters and different wave run-up formulas are expressed.

2.1. Wind waves

A wave is the general term for any disturbance in water height, velocity or pressure. Wind-generated waves are locally generated at open water, where the driving force (wind) is active. Wind waves that have been generated elsewhere will transform over distance and time into swell. Wind-generated waves from the North Sea can propagate into the Wadden Sea and reach the coastal dikes along the Wadden Sea. Additionally, the generation of local wind waves in the Wadden Sea is also possible. Waves travelling from the storm area will disperse across the water surface due to two processes: frequency-dispersion and direction-dispersion. During these processes waves become more regular [Holthuijsen, 2007]. Finally, waves that reach the coastal dikes along the Wadden Sea result in wave run-up onto the slopes.

2.2. Wave parameters

The wave height H and wave period T can be defined through zero-crossing analysis of a surface elevation time series. The surface elevation η(t) is defined as the change in water surface relative to some reference level. A wave is defined as the profile of a time series between two successive zero up or down crossings. Figure 2.1 shows the defined wave height and wave period.

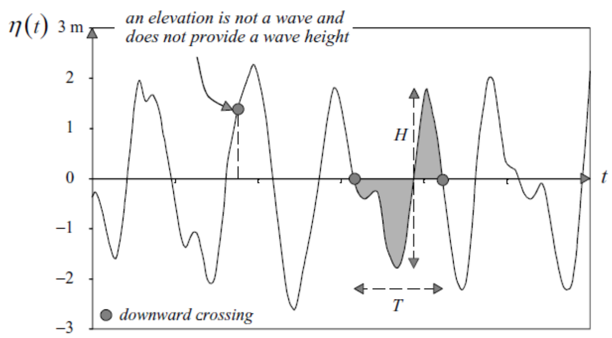

Figure 2.1: Wave height and wave period defined with a zero-crossing analysis performed on a surface elevation time series. Figure from Holthuijsen [2007].

The significant wave height (H_s) is used to define the characteristic wave height $H_{1/3}$: the mean wave height of the 1/3 highest waves in a wave record [Holthuijsen, 2007]. This significant wave height ($H_{1/3}$) is close to the value to the visually estimated wave height H_v by trained observers. Currently, the significant wave height can also estimated from the wave spectrum and defined as H_{m0}. This wave height, obtained from a wave spectrum is explained in more detail in Section 2.2.1.

The mean wave period can be expressed as T_m, $\overline{T}_0$ or $\overline{T}_z$ and is defined as the mean of all wave periods in a surface elevation time series. The mean wave period $\overline{T}_0$ can also be obtained from a wave spectrum and is expressed as T_{m02} (Eq. 2.9). The significant wave period (T_s) is defined in accordance with $H_{1/3}$ as the mean period of the 1/3 highest waves in a wave record and is expressed as $T_{1/3}$ [Holthuijsen, 2007].

2.2.1. Statistical description

The short-term statistical characteristics of wind waves are based on the assumption that the surface elevation is a stationary, Gaussian process [Holthuijsen, 2007]. This is usually a reasonable assumption for a wave record duration of 15-30 min. Nevertheless, it is sometimes also assumed for the duration of a storm (6-12 hours), but only if the duration is divided into multiple smaller time records. From Holthuijsen [2007] follows that statistical characteristics of wind waves can be determined by the variance density spectrum *E(f)*. The spectrum gives a complete description of the surface elevation of waves in a statistical sense. It shows how the sea surface elevation is distributed over the frequencies. Figure 2.2 shows an one-dimensional wave spectrum of a swell combined with a locally generated wind sea. This wave spectrum may occur along the coast of the Netherlands.

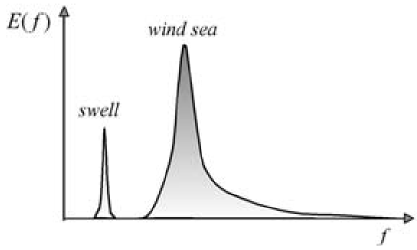

Figure 2.2: An one-dimensional wave spectrum of a swell meeting a locally generated wind sea. Figure from Holthuijsen [2007].

The characteristics can be expressed in terms of the moments (n = ...,-3, -2, -1, 0, 1, 2, 3,...) of that spectrum, which are defined as:

$$m_n = \int_0^\infty f^n E(f) df \tag{2.1}$$

Statistical characteristics of the wave height is an important wave parameter. Lonquet-Higgins [1952] stated that all statistical characteristics of $\underline{H}$ can be obtained from the Rayleigh distribution (Figure 2.3). An underscore means that the value is a random variable. This can be described by:

$$\mathrm{F}_{\underline{H}} \equiv \Pr\{\underline{H} < H\} = 1 - \exp\left(-\frac{H^2}{H_{rms}}\right) \tag{2.2}$$

where $\underline{H}$ is a random wave height and H_{rms} the root-mean-square wave height.

For waves with a narrow frequency spectrum in deep water, all characteristic wave heights become proportional to the standard deviation of the water surface elevation. The root-mean-square value of the wave height can be written as [Holthuijsen, 2007]:

$$H_{rms} = \sqrt{8m_0} \tag{2.3}$$

The significant wave height can not only obtained by zero crossing analysis ($H_s = H_{1/3}$) but also with a wave spectrum. An estimate of the significant wave height can be made using the zeroth-order moment of the wave spectrum. The estimate of the significant wave height H_s for Rayleigh distributed waves using a wave spectrum is expressed as H_{m0} [Holthuijsen, 2007]:

$$H_{m0} \approx 4\sqrt{m_0} \tag{2.4}$$

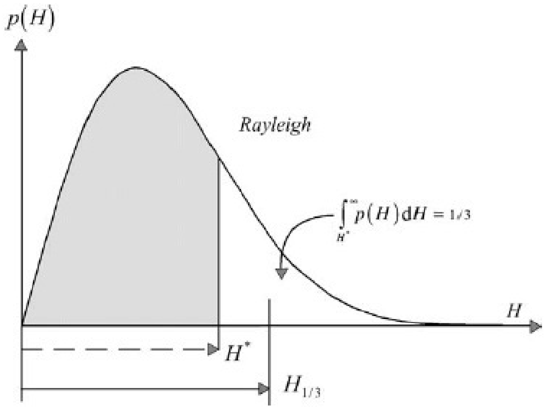

Figure 2.3: The probability density function of the wave height following a Rayleigh distribution. Figure from Holthuijsen [2007].

The maximum wave height can be obtained by the given that the probability density function of $\underline{H}_{\text{max}}$ is a narrow spectrum. Due to this, the most probable value (mod($\underline{H}_{\text{max}}$)) is almost equal to $\underline{H}_{\text{max}}$. The mode of $\underline{H}_{\text{max}}$ can be approximated by [Holthuijsen, 2007]:

$$\text{mod}(\underline{H}_{max}) \approx H_{m0}\sqrt{\frac{1}{2}\ln N} \tag{2.5}$$

where N is the number of individual waves.

Based on the above, the maximum wave height (H_{max}) can be estimated by [Holthuijsen, 2007]:

$$\underline{H}_{max} \approx 2H_s \tag{2.6}$$

Statistical characteristics of the wave period can also be obtained from a wave spectrum. Different mean periods are defined [Holthuijsen, 2007]:

$$T_{m-1,0} = \frac{m_{-1}}{m_0} \tag{2.7}$$

$$T_{m01} = \frac{m_0}{m_1} \tag{2.8}$$

$$T_{m02} = \overline{T}_0 = \sqrt{\frac{m_0}{m_2}} \tag{2.9}$$

where the spectral wave height $T_{\text{m-1,0}}$ puts more emphasis on the presence of longer waves compared to T_{m01} and T_{m02}

In shallow water the distribution of the wave height deviates from the distribution in deep water, due to effects of non-linear phenomena (shoaling, triad interactions and depth-induced breaking). Due to this, Battjes and Groenendijk [2000] replaced the tail of the Rayleigh distribution with the tail of the more general Weibull distribution, the so-called Composite Weibull distribution (CWD):

$$\text{F}_{\underline{H}} \equiv \Pr\{\underline{H} \leq H\} = 1 - \exp\left[-2\left(\frac{H}{H_{ch,i}}\right)^{ki}\right] \tag{2.10}$$

For wave height lower than a transition wave height H_{tr}, the index i = 1, the characteristic wave height is $H_{ch,1}$ and the power in the exponent is k_1. For $H > H_{tr}$, the index i = 2, the characteristic wave height is $H_{ch,2}$ and the power is k_2. Battjes and Groenendijk [2000] suggested the following values for the powers: $k_1 = 2$ and $k_2 = 3.6$

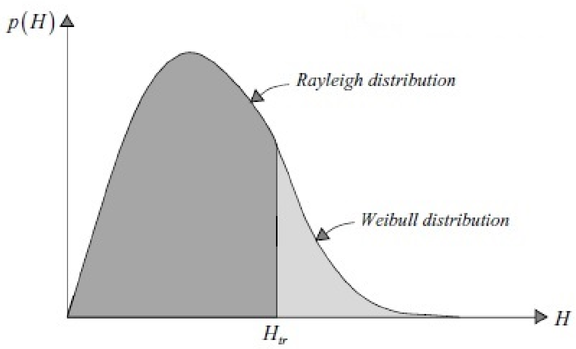

Figure 2.4: The probability density function of a Battjes and Groenendijk [2000] wave height distribution. Figure from Holthuijsen [2007].

In shallower water the wave height distribution of Battjes and Groenendijk [2000] deviates from a Rayleigh wave height distribution and changes to a Weibull-distribution. The result of this is a smaller ratio of H_{max} over $H_{2\%}$ compared to a Rayleigh distribution [van Vledder et al., 2013].

2.2.2. Breaking waves

The wave run-up height strongly depends whether or not the waves will break onto the slope of a dike. Waves will break due to a too large wave steepness (on deep-water) or because the water is very shallow or a combination of both. The limit is described with the breaking criterion of Miche. In Figure 2.5 this breaking limit together with different wave theories based on the wave steepness (H/gT^2) and relative water depth (h/gT^2) can be seen. Inside the breaking limit (blue area) waves are not breaking. For deep water the breaking criterion is $H_b/L = 0.142$ and for shallow water the solitary wave theory leads to the following limit: $H_b/h \approx 0.78$.

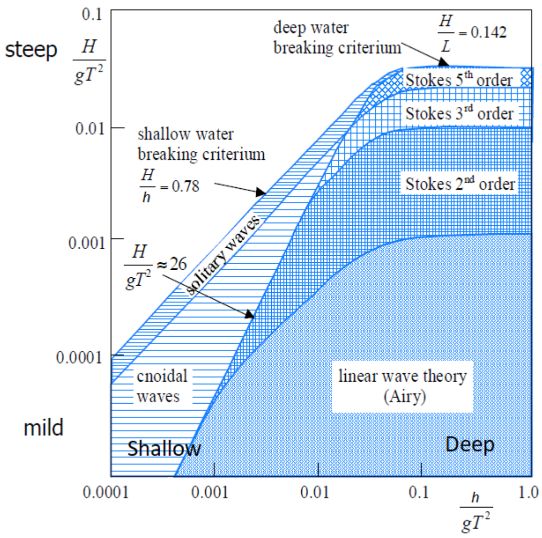

Figure 2.5: Validity of wave theories, after Le Méhauté [1976]

H_b is the wave height at breaking point, L is the wave length and h is the water depth.

Battjes [1974] defined a parameter to describe different breaker types. This parameter is called the dimensionless Iribarren number, breaker parameter or surf similarity parameter. It is derived from a situation with periodic long crested waves that approach a plane and impermeable slope. It is given by:

$$\xi = \frac{\tan\alpha}{\sqrt{\frac{H}{L_0}}} \tag{2.11}$$

The breaker parameter represents the ratio of slope steepness and wave steepness, where α is the outer slope angle of the dike and H/L_0 is the wave steepness (s_0) in deep-water. L_0 is the deep-water wave length: $L_0 = \frac{g \cdot T^2}{2\pi}$, in which g is the gravitational acceleration (9.81 m/s^2) and T the wave period. For irregular waves H_s and L_{0p} (wave length based on peak period T_p) are normally used in Eq. 2.11.

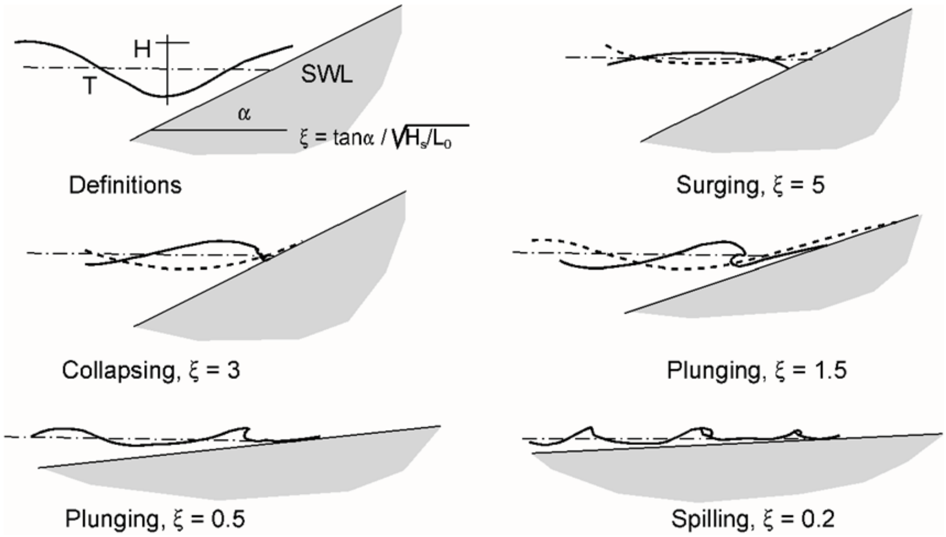

Figure 2.6: Breaker types based on Battjes [1974]. Figure from Schiereck and Verhagen [2016].

In EurOtop [2016] the following equation, based on the wave period $T_{m-1,0}$, is used to calculate the breaker parameter, surf similarity or Iribarren number:

$$\xi_{m-1,0} = \frac{\tan\alpha}{\sqrt{\frac{H_{m0}}{L_{m-1,0}}}} \tag{2.12}$$

where α is the outer slope angle of the dike and $L_{m-1,0}$ is the deep water wave length based on $T_{m-1,0}$. The ratio $H_{m0}/L_{m-1,0}$ represents the wave steepness ($s_{m-1,0}$). From EurOtop [2016] it follows that for values $\xi_{m-1,0}$ < ~2 the waves will break onto the slope. The breaker parameter also gives an indication of how waves will break. In EurOtop [2016] four breaker types are defined. These can be described with help of the breaker parameter based on $T_{m-1,0}$:

- Spilling ($\xi_{m-1,0} < 0.2$)
- Plunging ($0.2 < \xi_{m-1,0} <$ 2-3)
- Collapsing ($\xi_{m-1,0} \pm$ 2-3)
- Surging ($\xi_{m-1,0} >$ 2-3)

2.2.3. Wave run-up

Wave run-up formed an important part in the design or safety assessment of dikes in the past. Currently, the design or safety assessment is based on allowable overtopping. However, the wave run-up can still be valuable in certain cases. The wave run-up is defined as the vertical difference between the highest level reached by the run-up and still water level (SWL), this is shown in Figure 2.7 as R_u. As result of this run up, an amount of water may flow over the top of the dike if the top is below the (theoretical) run-up level. This is called wave overtopping.

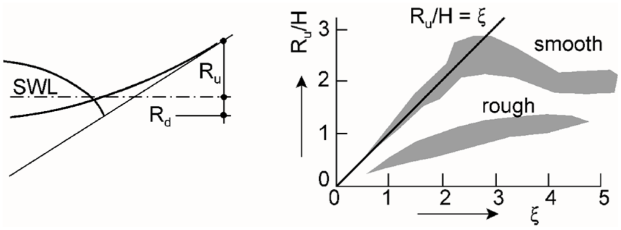

Figure 2.7: Left, the definitions of run-up R_u and run-down R_d. Right, experimental results (grey area) and the wave run-up based on Hunt [1959] (black line). Figure from Schiereck and Verhagen [2016].

Early formulas for regular wave run-up were presented by Hunt [1959] and are based on measurements performed in the United Sates of America. For periodic waves of perpendicular incidence breaking (ξ < 2.5-3) on plane and impermeable slopes, Hunt [1959] gives the following formulas:

$$R = \sqrt{HL_0} \cdot \tan(\alpha) = \xi \cdot H \tag{2.13}$$

where ξ is the Iribarren number (Eq. 2.12), α the outer slope angle of the dike, L_0 the deep-water wave length and H the wave height. The above formula can also be written in terms of the wave period T as follows:

$$R = 0.4 \cdot T\sqrt{g \cdot H} \cdot \tan(\alpha) \tag{2.14}$$

To calculate the wave run-up of irregular waves, the wave conditions at the toe of the dike should be used. Experiments have showed that the spectral wave height H_{m0} and period $T_{m-1,0}$ provide the most accurate prediction of wave run-up, also in non-standard cases such as double-peaked spectra and (very) shallow foreshores. The distribution of the incoming wave heights is commonly taken as a Rayleigh distribution, however several shallow water wave height distributions exist. In this study the shallow water wave height distribution of Battjes and Groenendijk [2000] is used. This distribution deviates from a Rayleigh distribution in shallow water due to depth-induced breaking.

In EurOtop [2016] the currently recommended formulas to calculate the 2% wave run-up are based on a large dataset which consists of measured conditions such as oblique wave attack, roughness, berms, etc. The wave run-up, based on measured data, for a mean value approach is expressed as:

$$\frac{R_{u2\%}}{H_{m0}} = 1.65 \cdot \gamma_b \cdot \gamma_f \cdot \gamma_\beta \cdot \xi_{m-1,0} \tag{2.15}$$

with a maximum of

$$\frac{R_{u2\%}}{H_{m0}} = 1.0 \cdot \gamma_f \cdot \gamma_\beta \cdot \left(4 - \frac{1.5}{\sqrt{\gamma_b \cdot \xi_{m-1,0}}}\right) \tag{2.16}$$

where $R_{2\%}$ is the run up value exceeded by 2% of the incoming waves. Several factors can reduce the wave run-up, the effect of these factors is given as a value between 0 and 1 ($\gamma = 1$ means no reduction). γ_b is the influence factor for a berm, γ_f is the influence factor for roughness elements on a slope and γ_β is the influence factor for oblique wave attack.

For a design and assessment approach a partial safety factor of one standard deviation is used. This results in the following equations of EurOtop [2016]:

$$\frac{R_{u2\%}}{H_{m0}} = 1.75 \cdot \gamma_b \cdot \gamma_f \cdot \gamma_\beta \cdot \xi_{m-1,0} \tag{2.17}$$

with a maximum of

$$\frac{R_{u2\%}}{H_{m0}} = 1.07 \cdot \gamma_f \cdot \gamma_\beta \cdot \left(4 - \frac{1.5}{\sqrt{\gamma_b \cdot \xi_{m-1,0}}}\right) \tag{2.18}$$

Measured data of model tests together with equations 2.15 and 2.16 are shown in Figure 2.8. Preference is given to the mean value approach (continuous black line in Figure 2.8) for this study, because this gives the best representation of actually occurring wave run up.

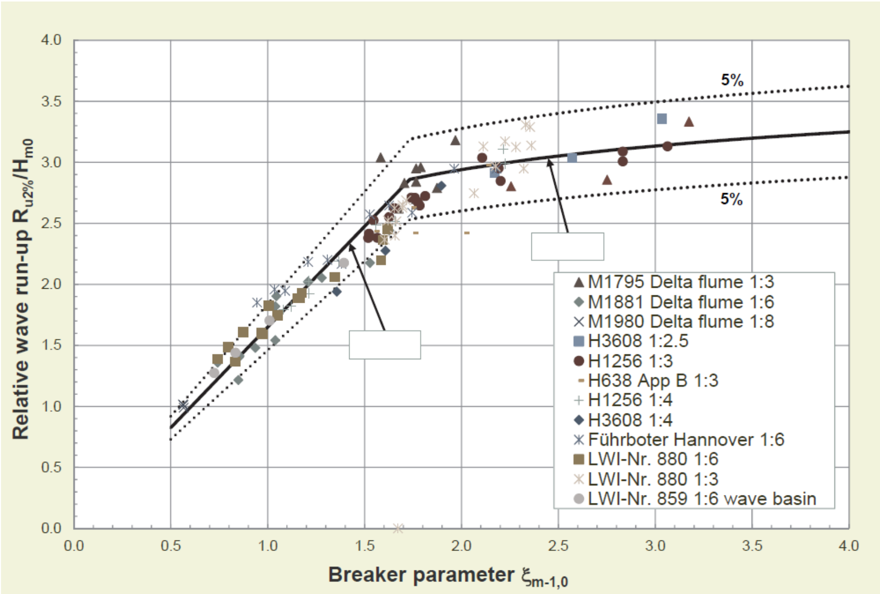

Figure 2.8: Relative wave run-up as function of the breaker parameter [EurOtop, 2016]

Delft formula

An equation developed in the Netherlands which is only valid for "typically Dutch" wave conditions is the 'Delft' formula. It gives a first estimate for run up levels and is expressed as follows [Jonkman et al., 2018]:

$$R_{u2\%} = 8 \cdot H_s \cdot \tan\alpha \tag{2.19}$$

This formula is originating from the context of the Zuiderzee works in the Netherlands during the construction of the Afsluitdike in 1932. In the past this formula was used in the design of dikes. Currently, it is used to obtain a quick first estimate of the wave run-up.

2.3. Flotsam models

To calculate flotsam levels a number of models can be used. In this section the models of IJnsen [1983] and Grüne [2005] are described. The preference is given to the flotsam method of IJnsen to calculate flotsam levels for this study. The main reason is the complete description of the model in IJnsen [1983] compared to Grüne [2005]. Besides, it has also been applied in a previous flotsam level calculation ([Witteveen+Bos, 2010]).

2.3.1. Flotsam model of IJnsen

IJnsen [1983] developed a model to calculate the flotsam level. The model is based on flotsam line measurements at the outer slope of the Wadden Sea dike of Ameland. In Section 3.1.3 more background information about IJnsen [1983] is given. IJnsen [1983] defined the flotsam level as Z_v in [m+NAP] and maximum still high water level as h_x in [m+NAP]. The difference between Z_v and h_x is assumed to be equal to the maximum individual wave run-up height z_x in [m+SWL]. Due to this the maximum wave run-up Z_x is equal to Z_v. A graphical representation is shown in Figure 2.9.

IJnsen [1983] defined a ratio between the maximum and 2% wave run-up. He used the 'Delft' formula (Eq. 2.19) to calculate the 2% wave run-up ($z_{0.02}$):

$$\zeta = \frac{z_x}{z_{0.02}} \tag{2.20}$$

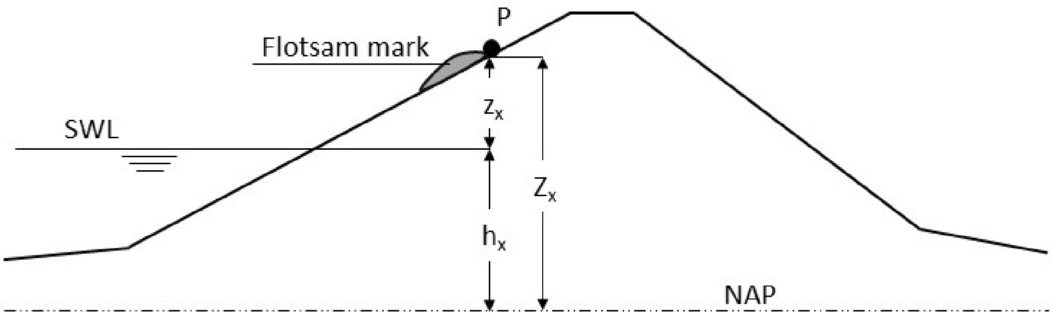

Figure 2.9: Definition of flotsam parameters

The model has a number of assumptions:

- The flotsam level is assumed to be equal to the highest wave run-up (Maximum wave run-up) during the storm. Visual observations of wave run-up against the slope of the same dike confirm that it is a valid approach [de Reus, 1983]. Results from large-scale laboratory investigations Grüne [2005] also confirms that it is a valid approach.
- The upper side of the flotsam line is used as input for the model (Point P in Figure 2.9).
- Wave run-up is Rayleigh distributed [Battjes, 1972].
- Shape of the tidal curve is schematized as a sinusoidal function.

The flotsam level or maximum wave run-up is Z_x calculated as:

$$Z_x = h_x + z_x \tag{2.21}$$

The highest still water level h_x can be written as a function of a time period τ, because IJnsen [1983] assumed that the shape of the tidal curve can be schematized as a sinusoidal function (Figure 2.10). Due to this equation (2.21) turns into:

$$Z_x = \overline{h}(\tau) + z_x \tag{2.22}$$

The mean water level $\overline{h}(\tau)$ can be approximated using the tidal amplitude A for a tidal period T = 12.4 hours and storm duration up to 6 hours. This gives:

$$\overline{h}(\tau) = h_x - 0.01 \cdot A \cdot \tau^2 \tag{2.23}$$

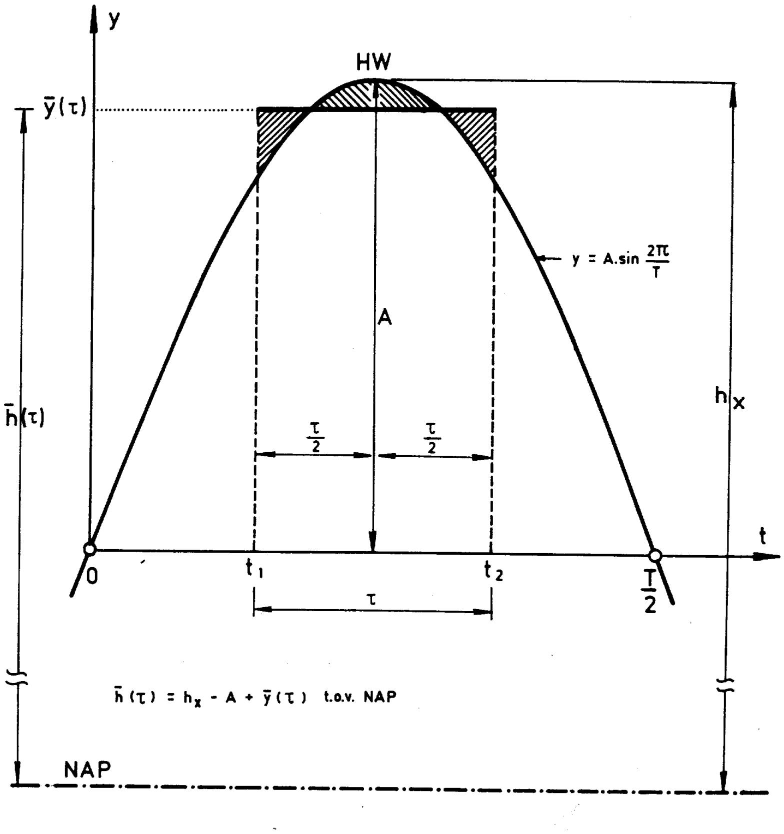

Figure 2.10: Tidal water curve schematized as a sinusoidal shape [IJnsen, 1983]

IJnsen [1983] assumed a Rayleigh distribution for the wave run-up according to Battjes [1972]. Therefore the maximum wave run-up can be calculated using the following equation, which follows from the defined ratio ζ in equation (2.20):

$$z_x = 0.5056 \cdot z_{0.02} \cdot \sqrt{-ln\left(\frac{\overline{T}z}{\tau}\right)} \tag{2.24}$$

where τ is the storm duration and $\overline{T}_z$ the mean wave period.

By substitution equations (2.23) and (2.24) into equation (2.22), the maximum wave run-up Z_x or as assumed the flotsam level can be written as:

$$Z_x = h_x - 0.01 \cdot A \cdot \tau^2 + 0.5056 \cdot z_{0.02} \cdot \sqrt{-ln\left(\frac{\overline{T}z}{\tau}\right)} \tag{2.25}$$

The first part of Eq. 2.25 is a basically a correction on the peak water level. In this study the maximum wave run-up is calculated around the high water level peak for different time instants. Flotsam heights are therefore obtained by adding the maximum wave run-up and corresponding water level for certain time instants. Therefore no reduction on the water level is applied and the following formula is used in this study:

$$Z_x = h_x + 0.5056 \cdot z_{0.02} \cdot \sqrt{-ln\left(\frac{\overline{T}z}{\tau}\right)} \tag{2.26}$$

2.3.2. Flotsam model of Grüne

Grüne [2005] developed a method for a safety analysis within a coast protection master plan of the German North Sea from Denmark to Hamburg. Along the coastline of the state Schleswig-Holstein a lot of flotsam level surveys have been performed for two decades. Grüne [2005] used this data to develop a method for the evaluation of wave parameters. In Section 3.1.4 this is described in more detail.

Grüne [2005] compared the spatial distribution of the calculated wave run-up with the measured flotsam levels. A linear regression approach was used to find a relation between significant wave height $H_{1/3}$ and measured sea water level (SWL) by means of determination parameters *Dz* and *GR*. The parameter *Dz* represents the wave inactive part of the local water depth in [m] and *GR* is the vertical difference of the slope (continuous black line in left panel of Figure 2.11). Based on Grüne [2005], the significant wave height $H_{1/3}$ is expressed as:

$$H_{1/3} = (SWL - Dz) \cdot GR \tag{2.27}$$

Linear regression is also used to determine a relation between the wave period T_m and $H_{1/3}$ by means of the determination parameters *a* and *b*:

$$T_m = a + b \cdot H_{1/3} \tag{2.28}$$

The determination parameters *Dz*, *GR*, *a* and *b* have to be varied step by step to calculate the corresponding T_m and $H_{1/3}$ which will result in the best fit according to the measured flotsam levels.

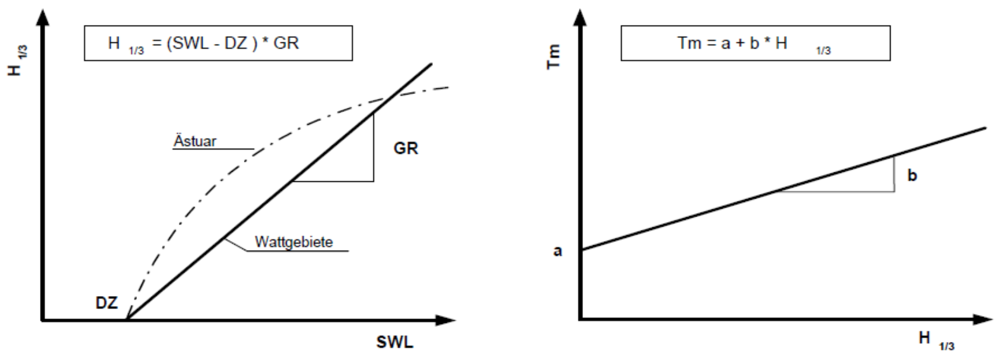

Figure 2.11: Left, $H_{1/3}$ based on determination parameters *Dz* and *GR* and measured SWL. Right, relation of T_m and $H_{1/3}$ based on determination parameters *a* and *b*.

3

Usage of flotsam lines in the past

In this chapter exists of two parts, in the first part an analysis of former studies in which flotsam lines were used is performed. The second part contains an inventory of flotsam lines with corresponding background information.

3.1. The usage of flotsam lines in former studies

Four studies which contain flotsam line measurements are discussed in this section. The aim is to analyse how obtained information from flotsam lines was used in the past and what lessons can we learn from them. Two studies, Niemeyer et al. [1995] and Grüne [2005], both focussed on flotsam level measurements at the Wadden Sea coast of Germany (especially along the coast of Dithmarschen, a district in Schelswig-Holstein). In the Netherlands Sanders [1962] and IJnsen [1983] used flotsam line measurements for their studies. The most recent study was performed in 2010 by Witteveen+Bos [2010].

3.1.1. Sanders [1962]

Sanders [1962] investigated the wave run-up and overtopping at Emmapolderdike. An objective of this study was to obtain an impression of the wave run-up during higher water levels. He supposed that the wave movements are in a certain state correlated to the sea bottom and therefore he made a relation between measured flotsam levels (with an interval of 500 meters) and water levels for certain locations and multiple years along the Emmapolderdike. All flotsam line measurements can be found in Appendix I.

Sanders [1962] derived a scatter plot between wave run-up and water level for each location. The resulting plots were widely spread, therefore he concluded that wind direction and speed were seriously disturbing the correlation between wave run-up and water level. By using the obtained scatter plots he defined a line which represents the relation between wave run-up and water level for each location along the Emmapolderdike. These lines were almost straight, because the fetch over the Wadden Sea is likely to generate mature waves and the height of these mature waves is almost in direct proportion to the water depth.

An objective of this study was to obtain an impression of the wave run-up during higher water levels. This was achieved by extrapolation of the above discussed lines for each location. A remark should be made that these lines are slightly bended upwards, this because the foreshores are losing their dissipating wave energy effect during higher water levels

3.1.2. Niemeyer et al. [1995]

Niemeyer et al. [1995] used two flotsam level measurements to verify the extrapolation method of Niemeyer [1976]. This extrapolation method is used to obtain a design wave run-up which is also based on flotsam level measurements. The method is elaborated in more detail in Niemeyer et al. [1995] and Niemeyer et al. [1999].

Flotsam levels measurements of two severe storms surges in two distinct areas at the German Sea coast, Dithmarschen and East Frisian island of Norderney (Figure 3.1), are used to test the extrapolation method.

The first data set of flotsam levels corresponds to 3 January 1976 and the second one to 27 February 1990. There were 13 measurements and 9 measurements available for respectively the coast of Dithmarschen and the island Norderney. These storm surges have been selected to minimize berm effects due to water level differences.

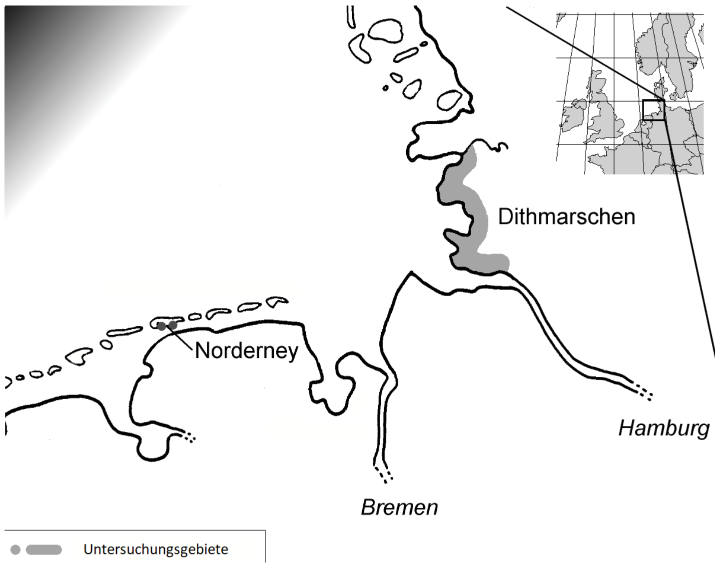

Figure 3.1: The two investigations areas Dithmarschen and Norderney [Niemeyer et al., 1995].

The extrapolation method exists of three formula's, these are shown in Figure 3.2

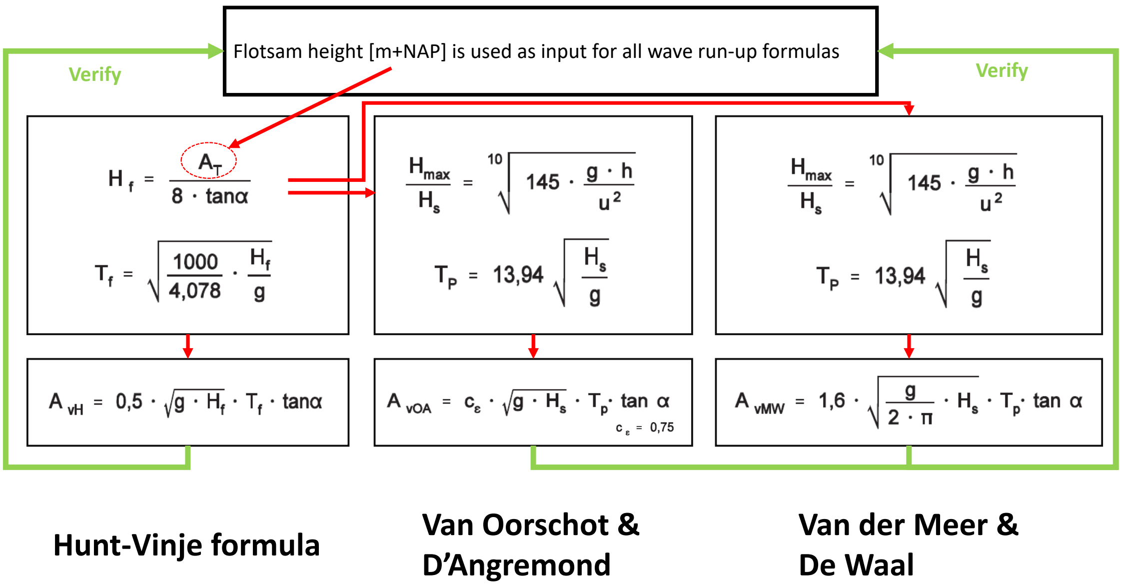

Figure 3.2: The extrapolation methods used by Niemeyer et al. [1995]

The flotsam level is used as input to calculate a fictional wave height H_f. Niemeyer et al. [1995] assumed that this fictional wave height corresponds with the maximum wave height, with this assumption the Van Oorschot & D'Angremond and Van der Meer & De Waal can be used.

The verification tests have shown that the output from the formulas (Figure 3.2) differs from the measured flotsam levels. The measured flotsam levels do not always represent an adequate derivation of the maximum wave run up. Niemeyer et al. [1995] stated that the flotsam may be blown by wind into a higher position than it reached due to wave run-up or the amount of flotsam is so large that the wave run-up is damped.

In the verification tests the Van Oorschot & D'Angremond formula gives the lowest variation. For the coast of Ditmarschen this is shown in Figure 3.3. Niemeyer et al. [1995] concluded that the extrapolation method must be regarded as a useful tool which allows to estimate the design wave run-up in a economical way.

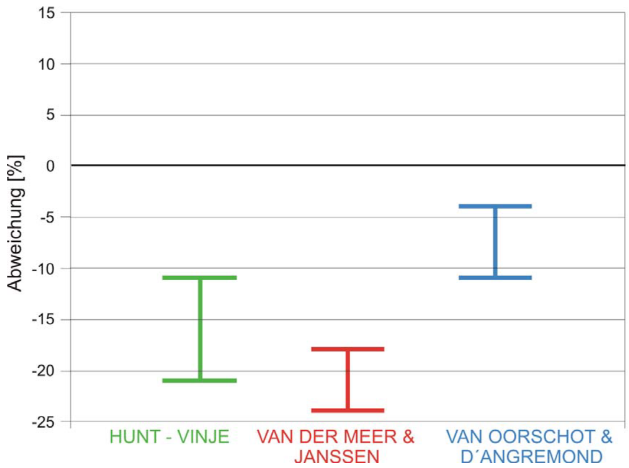

Figure 3.3: Verification of the extrapolation method at the coast of Dithmarschen: wave run-up is always underestimated. Van Ooschot & D'Angremond formula gives the lowest variation. [Niemeyer et al., 1995]

3.1.3. IJnsen [1983] and de Reus [1983]

For an assessment of a dike at Ameland, IJnsen [1983] used flotsam level measurements from 38 high waters starting form November 1977 onwards. IJnsen used measured flotsam levels to determine an estimate of the significant wave height and angle of wave incidence under design conditions. Also the model, as described in Section 2.3.1, is developed during this study of IJnsen [1983]. The flotsam levels were measured from the upper side of the flotsam line. He assumed that the upper side of the line shows the maximum wave run-up. His estimate is supported by visual observations. The study of de Reus [1983] is a reaction on IJnsen [1983] and stated also that the flotsam line represents the maximum wave run-up, based on visual observations.

IJnsen [1983] concluded that the spatial variation of all the flotsam lines followed a similar pattern. In Figure 3.4 the flotsam line of 1 February 1983 is shown. This was the highest flotsam line measured by IJnsen [1983] and also the only line that was included in the paper.

IJnsen [1983] concluded the following:

- The flotsam lines were a factor 1.4 higher than the 2% wave run-up. Therefore he stated that the ratio between maximum wave run-up and the 2% wave run-up is $\zeta = \bar{z}_x \;/\; \bar{z}_{0.02} = 1.4$ under design conditions in the Wadden Sea area.
- The estimated significant wave height under design conditions agrees well with previous studies for the same area.
- Foreshores have a reducing effect on the wave run-up. This can be seen in Figure 3.4, from point 15 to the left the foreshore increases in depth and width and the measured flotsam levels decreases.

The reaction on the study of IJnsen [1983] by de Reus [1983] concluded:

- The probability of the wave run-up is not following the Rayleigh distribution for measured run-ups between 18:20 and 21:19 at 06-12-1973. The method as described in Section 2.3.1, should therefore be

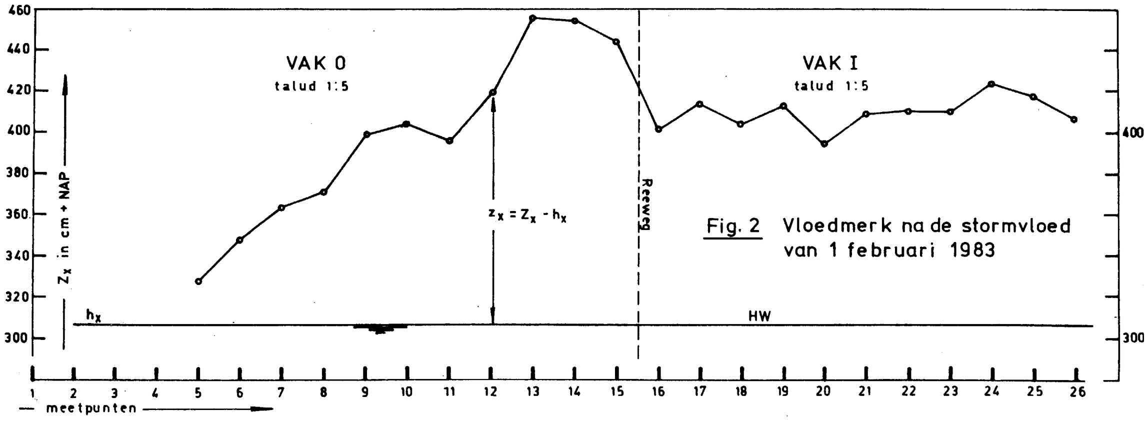

Figure 3.4: The flotsam line of 01-02-1983. The y-axis shows the measured flotsam level [m+NAP] [IJnsen, 1983].

reviewed if the wave run-up distribution follows a Rayleigh distribution, but for a first approximation the method of IJnsen [1983] can be used.

3.1.4. Grüne [2005]

Based on flotsam levels, measured at the upper side of the flotsam line, Grüne [2005] developed a method to assess the safety of coastlines in Germany. He used flotsam levels which were measured along the coastline of the state Schleswig-Holstein for two decades. In Figure 3.5 the flotsam level survey stations can be seen. In Grüne [2005] a ratio of 1.1 between the maximum and 2% wave run-up is applied.

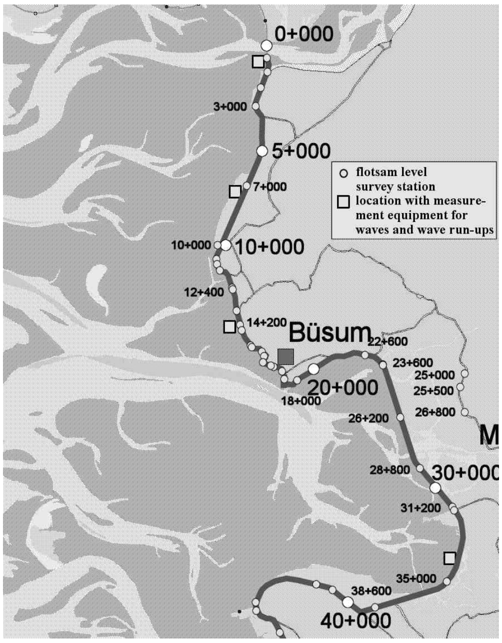

Figure 3.5: The coast of Dithmarschen was selected by Grüne to obtain wave parameters from flotsam level measurements [Grüne, 2005].

The method of Grüne [2005] obtains indirectly wave parameters ($H_{1/3}$ and T_{m}) by using the comparison of two different spatial wave run-up distributions on the outer slopes of dykes:

- A spatial wave run-up distribution of flotsam level measurements of one dike profile. Each point represents the maximum wave run-up of one storm surge event and thus one point of the spatial wave run-up distribution.

- The second spatial wave run-up is calculated by using a composite model which uses parameters Dz, Gr, a and b as input, see Section 2.3.2. This model is particularly applicable in conditions with a natural sea state and irregular dike profiles [Grüne and Wang, 2000] and is explained in more detail in Grüne [2008].

To obtain the wave parameters $H_{1/3}$ and T_{m} the composite model from Grüne [2008] is used in reverse mode. This is done by comparing the spatial distribution of measured flotsam levels with the calculated spatial wave run-up distribution using the composite model in its regular way. By using the method of trail-and-error (changing the input parameters Dz, Gr a and b) a distribution is obtained which coincides the best according the spatial distribution of the measured flotsam levels. In Figure 3.7 this trail-and-error process is shown for one of the survey locations (Stinteck). The obtained spatial wave parameter distribution of all survey stations along the selected coast trajectory is shown in Figure 3.6. In Figure 3.6, this distribution is also compared to data of 4 wave measurement locations along the 40 km coastline.

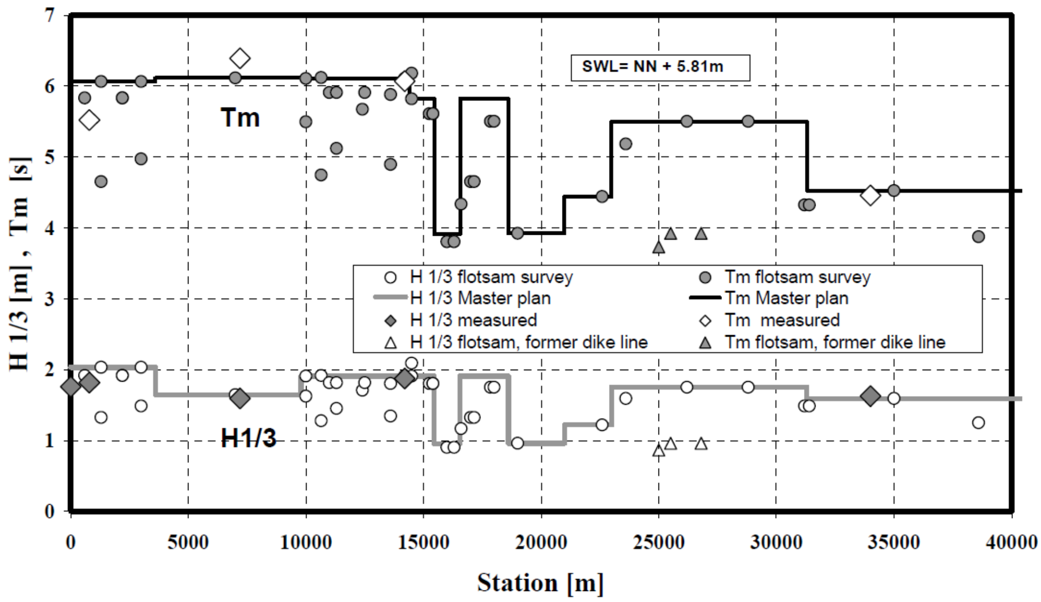

Figure 3.6: Spatial distribution of $H_{1/3}$ and T_{m} along coast trajectory (Figure 3.5) for a coast master plan [Grüne, 2005].

Grüne [2005] stated that both spatial wave run-up distributions have to be in agreement with the following idealised boundary conditions:

- Homogeneity of flotsam level data: The flotsam level only depends on the still water level and dike profile and which is not affected by other boundary conditions.

- Homogeneity of the sea state: In the influence of variations in wind on the real occurring wave conditions is minimal. Only the still water level and local morphological foreshore conditions are responsible for the change in the occurring wave conditions.

- The composite model considers all possible natural sea states.

Grüne [2005] mentioned also that results from former large-scale laboratory investigations confirmed that the flotsam level after a storm surge event corresponds to the highest wave run-up during the highest still water level of a storm surge. These large scale test have been performed in the Large Wave Channel (GWK) of the Coastal Research Centre (FZK) in Hannover and natural debris material from the coast of the German Bight was used as flotsam.

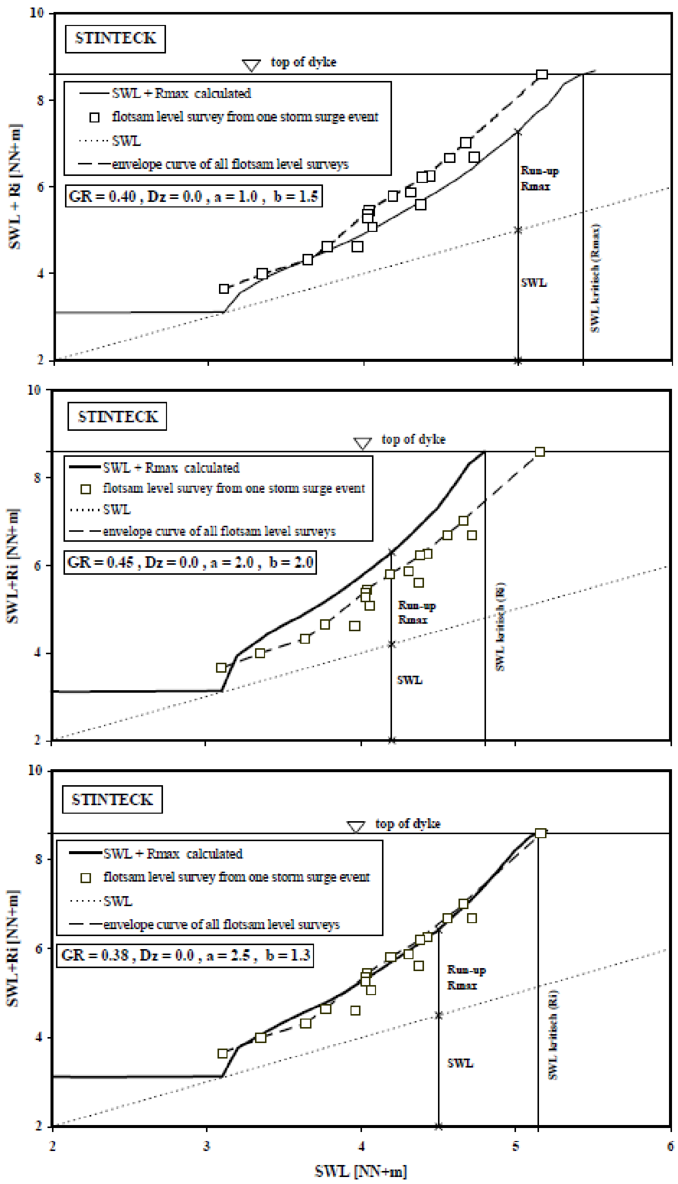

Figure 3.7: The best fit with the spatial distribution of measured flotsam levels at location Stinteck [Grüne, 2005].

3.1.5. Witteveen+Bos [2010]

Witteveen+Bos [2010] used flotsam level measurements to investigate the value of these measurements for model improvement by comparing measured and calculated flotsam levels. Measured flotsam levels of the 1 November 2006 (Section 3.2.2) storm were used to perform this study.

Calculated flotsam levels were obtained by applying the flotsam model of IJnsen [1983]. This model requires the upper side of the flotsam line as input. Therefore the height of the flotsam line was added to measured flotsam levels in order to be able to compare measured flotsam levels with computed flotsam levels. This was done because the line of 1 November 2006 was measured at the lower side of the highest flotsam levels.

Witteveen+Bos [2010] obtained differences between measurements and calculated lines: the calculated lines overestimated the measured lines (0.6 to 1.5 m) between x RD = 210 and 235 km and underestimated the measured lines (1.4 m) between x RD = 235 and 245 km. Witteveen+Bos [2010] concluded that the reason for this was most likely primarily caused by the translation of spectral wave results to wave run-up/flotsam levels. This was expected to be caused by the applied wave height distribution (Rayleigh) in the wave run-up/flotsam levels formulas.

A sensitivity analysis of Witteveen+Bos [2010] showed that the calculated flotsam level is not sensitive to the number of waves, angle of wave attack and a limiter on refraction. But it showed that the calculated line is sensitive to the water level, the wave period $T_{\text{m-1,0}}$, the dike characteristics and the wave height distribution.

Witteveen+Bos [2010] concluded that it is not possible to assess the performance of SWAN by using flotsam line measurements due to the combined uncertainty of the applied set of models/formulae needed to compute flotsam levels. The study also concluded that the alongshore variation in measured flotsam level cannot be explained with SWAN as results showed almost no alongshore variation in wave conditions (H_{m0} = 1.4 - 1.6 m and $T_{\text{m-1,0}}$ = 3.7 - 4.4 s) over a dike length of 35 km. Apparently, the flotsam level is affected considerably by local processes that vary along the dike;

Recommendations about flotsam lines from the study of Witteveen+Bos [2010] were:

- Measure at a fixed interval of 20 m along the highest flotsam line. This to map the alongshore variation in flotsam level.
- Measure the upper side of the line in order to be consistent with the model of IJnsen.
- The 'raw' data of the measured flotsam line should be registered and reported. Due to this the level of detail of the flotsam level calculation can be increased.
- Continue measuring flotsam lines after storm surges to create a database. The flotsam level is a valuable indicator of the maximum load on a dike and because of its spatial extent it gives insight in the spatial variation of wave conditions along the dike rather than point measurements like buoys.

3.2. Inventory flotsam lines

This chapter includes all flotsam line measurements from the past. In Table 3.1 a brief overview of the collected flotsam line measurements is shown. RD-coordinates (Rijksdriehoekscoördinaten) were used as a coordinate system. Each measurement was analysed on its quality on a scale[1-5]. A higher number means a higher density of measured points, this resulted in a higher quality. Each flotsam line measurement is elaborated in the following sections. Most of the flotsam lines were measured along the Wadden Sea dike between Lauwersoog and Eemshaven (Figure 3.8). Appendix I contains a collection of visual maps of each flotsam line measurement. The flotsam line measurements were stored in several Excel files.

Table 3.1: Inventory of flotsam line measurements

		Start location of flotsam line		End location of flotsam line			
Storm date	**Dike traject**	**x RD [m]**	**y RD [m]**	**x RD [m]**	**y RD [m]**	**Quality**	**Source**
10-1-1958	Emmapolderdike	239790	608385	248575	608520	4	P. Sanders
17-10-1958	Emmapolderdike	239790	608385	248575	608520	3	P. Sanders
2/3-1-1959	Emmapolderdike	239790	608385	248575	608520	3	P. Sanders
20-1-1960	Emmapolderdike	239790	608385	248575	608520	2	P. Sanders
20/21-3-1961	Emmapolderdike	239790	608385	248575	608520	5	P. Sanders
18-10-1961	Emmapolderdike	239790	608385	248575	608520	5	P. Sanders
6-12-1961	Emmapolderdike	239790	608385	248575	608520	4	P. Sanders
13-2-1962	Emmapolderdike	239790	608385	248575	608520	5	P. Sanders
14-10-1963	Emmapolderdike	239790	608385	248575	608520	5	P. Sanders
17-11-1964	Emmapolderdike	239790	608385	248575	608520	5	P. Sanders
3/4-12-1964	Emmapolderdike	239790	608385	248575	608520	5	P. Sanders
13-2-1965	Emmapolderdike	239790	608385	248575	608520	5	P. Sanders
2-11-1965	Emmapolderdike	239790	608385	248575	608520	5	P. Sanders
10/11-12-1965	Emmapolderdike	239790	608385	248575	608520	5	P. Sanders
30-11-1966	Emmapolderdike	239790	608385	248575	608520	5	P. Sanders
23-2-1967	Emmapolderdike	239790	608385	248575	608520	5	P. Sanders
1-3-1967	Emmapolderdike	239790	608385	248575	608520	5	P. Sanders
4-12-1967	Emmapolderdike	239790	608385	248575	608520	5	P. Sanders
28/29-11-1969	Emmapolderdike	239790	608385	248575	608520	5	P. Sanders
3/4-11-1970	Emmapolderdike	239790	608385	248575	608520	5	P. Sanders
9-11-1970	Emmapolderdike	239790	608385	248575	608520	5	P. Sanders
21-11-1971	Emmapolderdike	239790	608385	248575	608520	5	P. Sanders
1-11-2006	Lauwersoog - Delfzijl	210122	602876	257831	595309	1	Noorderzijlvest
9-11-2007	Noordpolderzijl - Emmapolderdike	230920	604819	245639	609669	4	Noorderzijlvest
5/6-12-2013	Delfzijl - Nieuwe Statenzijl	257659	594544	276490	584395	5	Hunze en Aa's
11-1-2015	Lauwersoog - Eemshaven	219009	602360	249702	609451	5	Vincent Vuik
13-1-2017	Emmapolderdike	230920	604819	247545	609096	4	Vincent Vuik
8-1-2019	Noordpolderzijl - Eemshaven	234358	605845	248886	608669	4	Myself

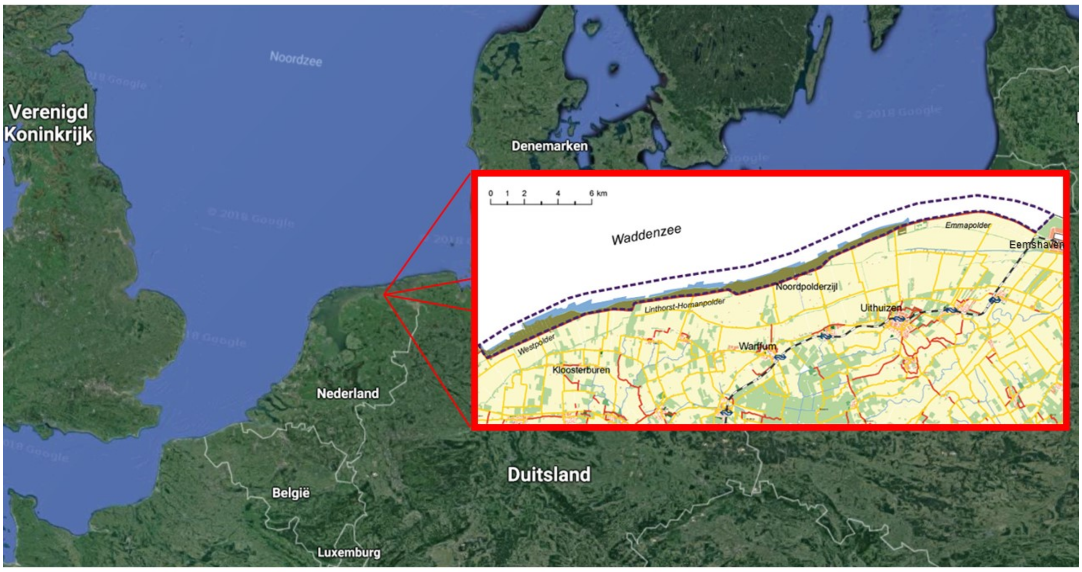

Figure 3.8: Wadden Sea coast between Lauwersoog and seaport Eemshaven [Source: https://www.avifaunagroningen.nl]

3.2.1. Flotsam lines in the period between 1958 and 1971

In Sanders [1962] eight flotsam lines measurements were used to assess the wave run-up and overtopping at the Emmapolderdike by determining a relation between wave run-up and water levels. These lines were measured between January 1958 and February 1962. In Figure 3.9 one of the flotsam line measurements is shown. The y-axis shows the flotsam level [m+NAP] and these were measured along hectometre posts/mile markers [x-axis].

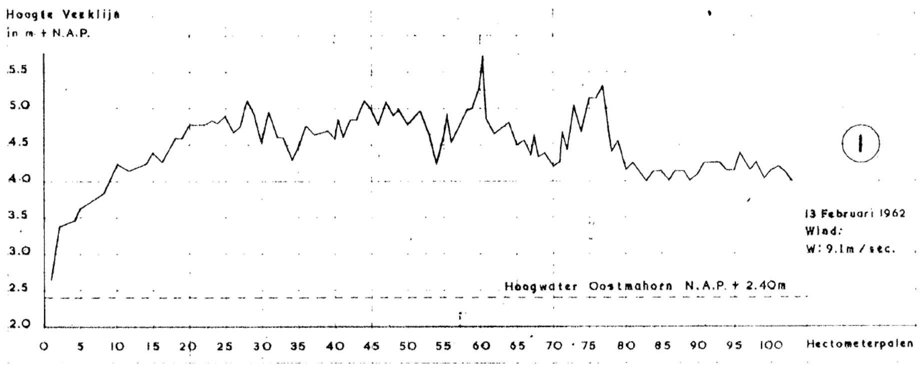

Figure 3.9: One of the 22 measured flotsam lines of Sanders [1962]

All flotsam lines were measured from an assumed fixed height with respect to NAP. The distance from this fixed point to the top of the flotsam line was measured to along the slope. Flotsam levels with respect to NAP were obtained with help of the slope gradient. Back then, it should have cost a lot of time and effort to visualize these flotsam lines. Sanders [1962] measured the flotsam lines along hectometre posts. These posts are currently situated at the inner side of the dike and are numbered west-east.

Flotsam lines as result of extreme storm conditions were not measured in the time period of Sanders study. This was caused by three reasons; the fact that flotsam was pushed over the dike during extreme conditions (useless measurement for this study), the short available time period to measure the flotsam line and after a severe storm which caused a lot of dike damage the priority to perform flotsam measurement was low. [Sanders, 1962]

These flotsam line measurements were performed in the period between 1958 and 1971. Due to harbour construction, harbour channel dredging and changes in the Wadden Sea, the bathymetry in Eastern Wadden Sea and Eems has changed. The Emmapolderdike has also been upgraded throughout the years. The seaport Eemshaven was constructed between 1970-1973, it is situated at the eastern side of the Emmapolderdike. The measurements performed for Sanders [1962] are overlapping with the current location of the Eemshaven seaport. Due to this, statistics of water levels obtained from this study are likely to differ with water level statistics after construction of the seaport.

3.2.2. Flotsam line of 1 November 2006

The flotsam line, generated during the 1 November 2006 storm, was used in Witteveen+Bos [2010]. The objectives of this study were: performing a hindcast of this storm in the Eastern Wadden Sea (Lauwersoog-Delfzijl) and to investigate the value of flotsam lines for model improvement by comparing measured and calculated flotsam levels. Flotsam lines were used instead of wave buoys to assess the performance of SWAN. This was done because no wave buoys were deployed at the time of the storm in the Eastern Wadden Sea.

Regional water authority Noorderzijlvest supplied the measured flotsam line. This line was constructed by measuring several high flotsam levels corresponding to the upper flotsam line between Lauwersoog and Delfzijl. The highest flotsam levels were selected by visual observation and were measured at the lower side of this upper flotsam line. Deltares provided the measured flotsam level averaged per dike section, which consists of six levels over 39 km of dike. The 'raw' measurements of this flotsam line do not exist any more and the study of Witteveen+Bos [2010] included three photographs of flotsam lines.

3.2.3. Flotsam line of 9 November 2007

Regional water authority Noorderzijlvest (Peter Lalkens) provided aerial photographs of the flotsam line corresponding to the storm of 9 November 2007. These photographs were made between Noordpolderzijl and the Emmapolderdike. The aerial photographs are roughly "translated" with help of dike profiles to obtain flotsam levels. This was done to get a first impression of the spatial variation along the dike. The accuracy of this translation is ± 0.5 m + NAP.

By analysing the obtained flotsam line multiple variations appeared. The transition from a vegetated high foreshore to a lower and non-vegetated foreshore was clearly visible in the flotsam line (Figure 3.10) and at one location the flotsam line almost reached the dike crest (Figure 3.11) which is situated around 9.0 m + NAP. The spatial variability as shown in Figure 3.11 is likely caused by one individual high wave run-up.

Figure 3.10: Transition in the flotsam line of 9 November 2007 is visible. Line shifts from 4.5 to 7.0 m + NAP. [Photo: Regional water authority Noorderzijlvest]

Figure 3.11: Highest flotsam level at 9 November 2007 is marked by a person of the regional water authority Noorderzijlvest. [Photo: Regional water authority Noorderzijlvest]

3.2.4. Flotsam lines of 5 and 6 December 2013

Regional water authority Hunze en Aa's (Henk van Norel) provided a shape file with flotsam line measurements from Delfzijl to Nieuwe Statenzijl. The regional water authority also supplied one photograph which showed an upper and a lower flotsam line (Figure 1.2). These lines correspond to the two high waters from 5 and 6 December 2013.

3.2.5. Flotsam lines of 11 January 2015 and 13 January 2017

Vuik [2019] developed new methods to assess how, and how much vegetated foreshores can contribute to flood risk reduction. This study was part of the project BE-SAFE in the framework of Building with Nature. In his study he used flotsam line measurements between Lauwersoog and Eemshaven. These measurements were done after high waters at 11 January 2015 and 13 January 2017. The water level (≈ 3.25 m) didn't reached high enough to call one of these high waters a severe storm surge. Nevertheless at some locations the flotsam level was shifted quite high on the outer slope, especially in 2017.

3.2.6. Flotsam lines of 8 January 2019

During this study, the high water of 8 January 2019 created a flotsam line. The development of the flotsam line was observed and captured with photographs and videos. At 9 January 2019 flotsam levels were measured between Noordpolderzijl and Eemshaven by myself. The water level was in the same order as 11 January 2015 and 13 January 2017 (≈ 3.0 m+NAP)

3.2.7. Conclusion

Our inventory resulted into 28 flotsam lines measured and registered from January 1958 until now. Most of the measurements were performed between Lauwersoog and Eemshaven except one flotsam line from 2013 which was measured between Delfzijl and Nieuwe Statenzijl. In Figure 3.8 the area between Lauwersoog and seaport Eemshaven is shown.

In Figure 3.12 the flotsam line measurements of 1 November 2006, 9 November 2007, 11 January 2015, 13 January 2017 and 8 January 2019 are shown.

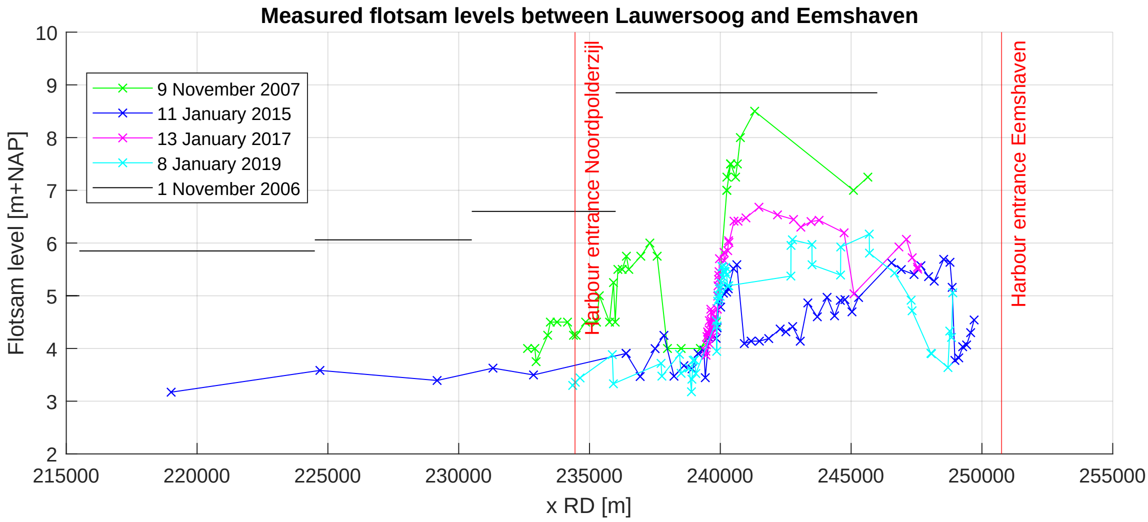

Figure 3.12: Inventory of flotsam level measurements between Lauwersoog and Eemshaven

4

Observations of the 8 January 2019 storm

This section presents the background and a description of the made observations during the 8 January 2019 storm on the Wadden Sea dike in the Netherlands between Noordpolderzijl and Eemshaven. The main objectives of this field trip were: recording the development of flotsam line during the storm and performing flotsam level measurements after the storm. During the high water of 8 January 2019 multiple photographs and videos were made to capture the temporal development of the flotsam line. On 9 January 2019 a flotsam line measurement was performed between Noordpolderzijl and Eemshaven. This was made possible by regional water authority Noorderzijlvest. A description of the storm is given in the first section. This is followed by an elaboration of observations made at 8 January 2019 (MET 11:00) around the high water peak. In Section 4.2.1 the measured flotsam line is analysed and the chapter ends with a discussion.

4.1. Description of the storm

On Monday 7 January 2019 a low pressure area was propagating from Iceland via southern Norway towards Denmark. Between high and low pressure areas, a storm field (8-10 Bft) was present at the central North Sea. The cold front of this depression passed the Dutch coast in the night of 7/8 January 2019. The wind direction then changed from a south-westerly direction to a north-westerly direction. The wind developed to a gale (8 Bft) along the entire coast. More seaward, the wind reached strong gale force (9 Bft). The wind direction then changed to a northerly direction and the wind speed decreased in strength during the afternoon and evening of 8 January 2019. Around midnight the wind decreased to a near gale (7 Bft) along the entire coast.
The north-westerly storm caused a significant set-up of the water level especially around the Wadden Sea. The water level set-up was 99 cm at Vlissingen and 246 cm at Delfzijl. The highest set-up, measured at Delfzijl, has an average recurrence frequency of once per five years. Figure 4.1 shows the predicted wind field (HIRLAM) for 8 January 2019 as well as the weather chart for 7 January 2019. HIRLAM (High Resoluation Limited Area model) is a metrological model which is used by The Royal Netherlands Meteorological Institute (KNMI) to provide weather forecasts.

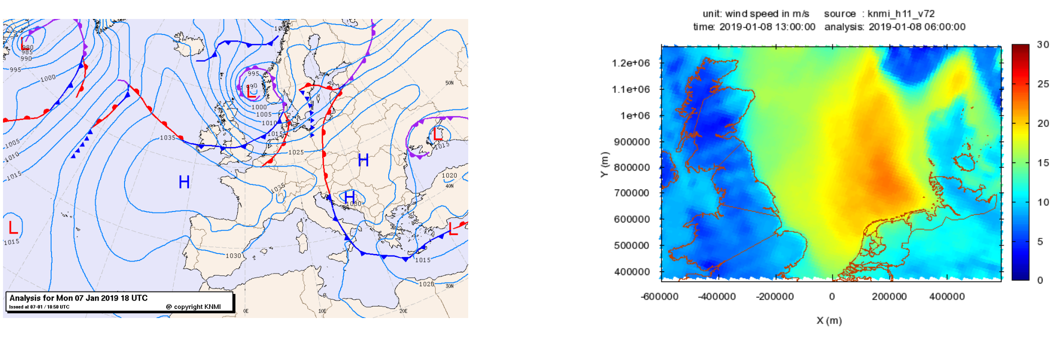

Figure 4.1: Overview of the north-westerly storm at 8 January 2019. Left, the weather chart for 7 January 2019 18:00 (UTC). Right, predicted HIRLAM wind field for 8 January 2019 13:00 (UTC).

4.2. Development of flotsam line

On 8 January 2019 (11:00 MET) video recordings have been made to capture the interaction between wave run-up and flotsam level during storm conditions. A couple of interesting high wave run-up moments were captured in the recordings. Figures 4.2, 4.3, 4.4 and 4.5 represent each a different individual wave run-up. These figures are subdivided into multiple figures which are displayed in chronological order in a total time frame of approximately 5 seconds. Each figure shows in which way the flotsam line changes by one individual wave run-up at a particular location.

In Figure 4.2 an upward movement of flotsam can be seen. This is followed by a breaching in the flotsam line (Figure 4.2d) next to an upward movement. The backwash of this individual wave run-up causes a downward movement of flotsam at the left side. It seems also that the flotsam at the right side is able to stay in position while getting hit by the wave run-up. Presumably the flotsam is able to absorb the force of the wave run-up and therefore doesn't shift upward.

(a)

(b)

(c)

(d)

(e)

(f)

Figure 4.2: Development of the flotsam line at 8 January 2019 11:31 (MET)

In Figure 4.3 the same behaviour is captured as shown in Figure 4.2. On the left an upward movement of flotsam can be seen and is followed by some downward movement of flotsam due to the backwash of the wave run-up. In the middle there is also some upward movement initially. After this it seems that a relative thick amount of flotsam is able to absorb the force of the wave run-up and remains in position.

(a)

(b)

(c)

(d)

(e)

(f)

Figure 4.3: Development of the flotsam line at 8 January 2019 11:33 (MET)

In Figure 4.4, especially Figure 4.4d and 4.4e, the dampening effect of a relative large amount of flotsam can be seen. At the corners of this amount, the run-up tongue breaches through the flotsam line, but the flotsam in the middle remains in position and seems to be able to absorb the force of the wave run-up.

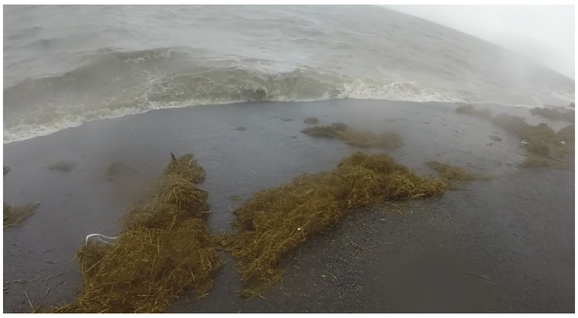

(a)

(b)

(c)

(d)

(e)

(f)

Figure 4.4: Development of the flotsam line at 8 January 2019 11:36 (MET)

In Figure 4.5 a significant higher flotsam level can be seen compared to surrounding flotsam levels. In Figure 4.5a a very thin run-up tongue can be seen which resulted in the flotsam line in Figure 4.5b (red circle). Again, a relative large amount of flotsam remained in position and in between a thin layer of flotsam was shifted to the maximum run-up height of this individual wave due to a thin layer of water.

(a) (b)

Figure 4.5: Flotsam line shifted onto the dike by the wave run-up tongue at 8 January 2019 11:36 (MET)

4.2.1. Flotsam level measurements

On 9 January 2019 (11:00 MET) a flotsam line measurement was performed using a Leica Viva GPS. The flotsam levels were measured between Noordpolderzijl and Eemshaven (x RD = 234 - 249 km). In front of this dike trajectory two vegetated foreshores are present (x RD < 240 km and between x RD = 247 - 248 km). However, along a significant part (x RD = 240 - 247 km) lower mudflats are present. Due to the lack of flotsam at the mudflats, the flotsam line faded at this part and no flotsam levels were measured here (red line). At some point, a line of seashells was visible and has been measured instead of the flotsam line. More easterly, near Eemshaven, the flotsam line was visible again. In Figure 4.6 the flotsam measurement points with description is displayed.

Figure 4.6: Overview of measured flotsam points and properties corresponding to the flotsam line of 8 January 2019

Multiple photographs were made while performing the flotsam level measurements. Two photographs can be seen in Figure 4.7. In Figure 4.7a two flotsam levels are visible: a higher line of flotsam corresponding to a relative thin layer of flotsam and a lower line of flotsam corresponding to a relative thick layer of flotsam. In Figure 4.7b the measured line of seashells is visible. On this photograph also two lines of flotsam are visible (one at SWL and one in between SWL and seashell line), despite no vegetated foreshore is present here in front of the dike. The highest of these two flotsam lines corresponds presumably to the high water after the highest water of 8 January 2019 (Figure V.1). The reason that the second high water generated a flotsam line is most likely caused by the fact that the flotsam was able to spread out in the water by making use of the currents.

(a)

(b)

Figure 4.7: Left, a flotsam line in the vicinity of salt marshes. Right, a seashell line in the vicinity of mud flats. Both lines correspond to the storm of 8 January 2019.

In Figure 4.8 the measured flotsam line is shown. This line exists of 40 measured flotsam and 12 seashell levels. Between x RD = 240.5 and 242.5 km no measurements were performed due to unclear flotsam line.

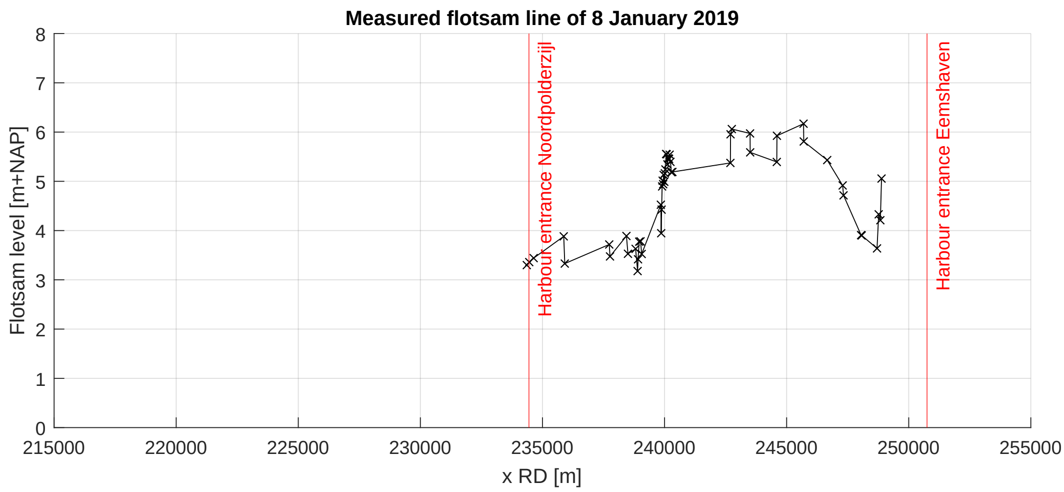

Figure 4.8: Measured flotsam line of 8 January 2019.

4.3. Discussion

The objective of recording the spatial and temporal development of a flotsam line was to gain insight in the interaction between wave run-up and flotsam levels. Based on observations and analysing the video recordings, it becomes clear that:

- the upper side of the flotsam line marked the highest occurred wave run-up (maximum wave run-up). In Figure 4.5 can been seen that a small layer of flotsam was shifted to the maximum wave run-up height by a very thin run-up tongue. The observations and recordings of this study confirm the assumption of previous studies (Sanders [1962], IJnsen [1983] and de Reus [1983]). These studies stated that the flotsam line is representing the maximum wave run-up. However, it should be mentioned that observations and recordings of 8 January 2019 showed that a relative thick layer of flotsam may disturb the final level of the flotsam line;
- a relative thick flotsam layer is able to withstand the force of the wave run-up compared to a relative small layer of flotsam. The recordings confirmed the finding of Niemeyer et al. [1995], he stated that the wave run-up can be damped by a large amount of flotsam. The recordings of 8 January 2019 (Figures 4.2, 4.3 and 4.4) showed that a relative thick layer of flotsam was able to absorb the force of the wave run-up and remained in position. The wave run-up should considerably have reached higher compared to the same situation without a flotsam line on the dike. This has presumably a significant impact on the spatial variability of the flotsam line, which can be seen in Figure 4.7a;
- water is the driving force in the development of the flotsam line. The study of Niemeyer et al. [1995] stated that the flotsam may be blown by wind into a higher position than it reached due to the wave run-up. However, this can be rejected based on the observations and recordings. The flotsam levels were not situated higher than the wave run-up during the storm of 8 January 2019;
- evident flotsam lines occurred on locations in the vicinity of vegetated foreshores. In Figure 4.7b a line of seashells can be seen as a result of the highest water level on 8 January 2019. No flotsam line at this trajectory was generated due to the high water. Mainly caused by the fact that in front of this part of the dike no vegetated foreshore was present. However, the high water after the highest water level was able to generate a small line of flotsam, but this was most likely caused by the assumption that the flotsam was spread out by making use of the currents in the Wadden sea.

The driving process behind the developing flotsam line is shown in Figures 4.2, 4.3, 4.4 and 4.5. During rising water and increasing wind speed, a high individual wave run-up may cause flotsam to shift upward. On the other hand, the wave run-up was also be able to take up some flotsam from the dike if the force of the wave run-up was high enough. After this the flotsam was transported again onto the dike by one of the following incoming waves. This behaviour repeated itself and eventually a flotsam line was formed.

Figure 4.9: Coiled shape of flotsam line at 9 January 2019. Seaside on the right of the figure.

In Figure 4.9 an interesting shape of flotsam can be seen. The wave run-up was perhaps be able to flow beneath the flotsam line and to condense the flotsam line with its backwash. A coiled line of flotsam as in Figure 4.9 might have been a result of the above.

5

Method and data availability

This chapter presents a brief introduction of the method which is used to calculate flotsam levels. This method is based on a sequence of models which is used for the derivation of the Hydraulic Boundary Conditions on behalf of Rijkswaterstaat. This was done to investigate if flotsam levels can be used to assess the quality of these models. In Section 5.1 the derivation of the HBC, performed with the models WAQUA and SWAN, is briefly described. Followed by a method description to calculate flotsam levels. In Section 5.5 it was determined which storms are hindcasted by SWAN. This is followed by a summary of the used method to calculate flotsam levels. Finally, the SWAN model set-up is explained in Section 5.7.

5.1. Models used for derivation HBC

In compliance with the Dutch Water Act ('Waterwet, 2009'), the safety of the Dutch primary water defences must be assessed every twelve years (in practise every six years: 2011, 2017, 2023, etc) for the required level of protection. The water authorities have to submit a report on the general structural condition of a primary flood defence structure to the Provincial Executive. In which way this safety assessment has to be performed is prescribed in legal safety assessment tool which is called WBI2017 for the current assessment round. The Hydraulic Broundary Conditions (HBC) are also derived every six years and approved by the Minister of Infrastructure and Water Management (IenW). This derivation was performed with help of a sequence of physical models. The start of the derivation is a large database of standardised storms. This dataset was used to calculate different states of the water system by using a hydrodynamic model and a wave model and to obtain in the end the HBC.

It was investigated whether flotsam levels can be used to assess the quality of the above models and corresponding programs used by Rijkswaterstaat. Hereby, the value of flotsam lines was investigated by comparing calculated and measured flotsam levels, where the above models were used to calculate flotsam levels. In Section 5.1.1 and 5.1.2 these models and corresponding programs are explained in more detail and in Section 5.2 the method, consisting of models and equations, to calculate flotsam levels is described.

5.1.1. Hydrodynamic model

The program WAQUA (WAter movement and water QUAlity modddeling) performed the hydrodynamic modelling in the derivation of the HBC. WAQUA is able to calculate water levels, currents and concentrations of dissolved substances. Wind and pressure conditions were required to perform a calculation in WAQUA. The computation in WAQUA was done with a cascade of three models. The first model is a Dutch Continental Shelft Model (DSCM) and has the largest grid of the three models. It has a resolution of 9.3 to 6.5 km in West - East direction and 9.25 km in South - North direction [Rijkswaterstaat and Deltares, 2009c]. The ZUidelijke NOordzee (ZUNO) model is a finer model compared to DSCM. ZUNO uses sea boundary conditions obtained from DCSM. The resolution of this model is 1-2 km along the Dutch coast [Rijkswaterstaat and Deltares, 2009a]. The finest model is named Kuststrook-Fijn model. It requires sea boundary conditions obtained from the ZUNO model and has a resolution of 300 meters in the Wadden Sea [Rijkswaterstaat and Deltares, 2009b]. The most detailed modelling is obtained by performing all models after each other. In Section 5.7.2 is explained which WAQUA models were used to perform a flotsam level calculation.

5.1.2. Wave model

Wave parameters were modelled with a spectral wave model named, Simulating WAves Nearshore (SWAN). The model can be used to obtain realistic estimates of wave parameters in coastal areas and it is based on the wave action balance equation with sources and sinks. The computation in SWAN was performed by using water level and current field output from the hydrodynamic model WAQUA. The calculation in SWAN also required wind conditions, bottom level and roughness information. The HBC were determined at predefined locations which are located 100 meters from the crest of the dike. This set of locations is defined as *HRbasis set* and is explained in more detail in Section 5.7.2.

The model set up of SWAN which was used to perform flotsam level calculations is explained in Section 5.7.

5.2. Method

In this section the method to calculate flotsam levels is explained. The method was composed in such a way that realistic estimates of flotsam levels were obtained. This implies that measured wind data instead of a HIRLAM wind field was used. In addition, due to the limited time frame of this study it was decided to use previously computed water level and current fields in WAQUA to perform hindcasts with SWAN. The wave conditions were modelled with SWAN in stationary mode. In Section 5.7.2 it is explained in more detail which data sources were used. Our research plan consisted of seven aspects: the first five bullets are elaborated in Section 5.7 and last two bullets are explained in this section.

The following method/approach was used to calculate flotsam levels:

- Determine four hindcast moments at and around the storm peak to catch the highest wave run-up, leading to the highest flotsam levels;
- Based on measurements around the storm peak which an average wind speed and direction is determined and applied as an uniform wind condition in SWAN;
- Regridding computed water level and current fields to serve as input in SWAN;
- Define wave boundary conditions for the computational grid in SWAN;
- Simulate four hindcast moments with SWAN in stationary mode for each storm;
- Calculate the 2% wave run-up;
- Calculate the flotsam level (maximum wave run-up) by applying the flotsam model of IJnsen.

5.2.1. Calculation of 2% wave run-up

Wave run-up formulas were used to calculate flotsam levels for each hindcast. The 2% wave run-up was calculated using obtained wave parameters from SWAN and this was then translated to the maximum wave run-up (upper side of the flotsam line). For each hindcast the 2% wave run-up was calculated with wave parameters obtained from the HRbasis set. These set is located 100 m from the crest of the dike (Figure 5.7).

The general formulas that currently can be applied are described in Section 2.2.3 and were obtained from EurOtop [2016]. This study used the mean value approach for irregular waves to calculate the 2% wave run-up:

$$\frac{R_{u2\%}}{H_{m0}} = 1.65 \cdot \gamma_b \cdot \gamma_f \cdot \gamma_\beta \cdot \xi_{m-1,0} \tag{5.1}$$

with a maximum of:

$$\frac{R_{u2\%}}{H_{m0}} = 1.0 \cdot \gamma_f \cdot \gamma_\beta \cdot \left(4 - \frac{1.5}{\sqrt{\gamma_b \cdot \xi_{m-1,0}}}\right) \tag{5.2}$$

The flotsam model of IJnsen was derived from an older 2% wave run-up formula. This formula is based on Dutch Wadden Sea wave conditions (4% wave steepness ($s_{\text{m-1,0}}$) and gentle smooth slopes) and is originating from the context of the Zuiderzee works in the Netherlands during the construction of the Afsluitdijk in 1932. The formula was used for designing dikes until 1980, but currently it provides a first estimate for the run-up height [EurOtop, 2016]. [IJnsen, 1983] did take the influence of roughness (r) and permeability and oblique wave incidence (β) into account. This resulted in the following formula:

$$R_{u2\%} = 8 \cdot r \cdot H_s \cdot \tan(\alpha) \cdot \cos(\beta) \tag{5.3}$$

Formulas 5.1 and 5.2 as well as formula 5.3 were used to calculate the wave run-up. The following parameters were required to calculate this:

- Wave conditions at toe of the dike: spectral wave height H_{m0} [m], spectral wave period $T_{\mathrm{m\text{-}1,0}}$ [s] and wave direction [°N].
- Dike characteristics: slope of the dike ($\tan(\alpha)$), influence of dike orientation (γ_β), friction coefficient (γ_{f}) and coefficient to account for a berm (γ_{b}).

Dike dimensions, orientation and revetment types were supplied by HKV. The slope of the dike and berm factor depend on the local water level and wave height. These parameters are time dependent and were determined for each hindcast moment. The revetment of the considered dike trajectory consists mostly of an asphalt and a grass cover. This means a friction factor (γ_f) of 1.0 was used in the calculations. In Appendix II the applied dike slope and reduction factor for oblique wave incidence (γ_β) are shown.

5.2.2. Calculation of flotsam lines (maximum wave run-up)

The maximum wave run-up height [m+NAP], Z_{x}, was calculated by applying the flotsam model of IJnsen as explained in Section 2.3.1. The spectral wave period $T_{\mathrm{m\text{-}1,0}}$ obtained from the HRbasis set was used as input for the mean wave period, T_{z}, during the storm. The effect on the calculated flotsam levels when using $T_{\mathrm{m\text{-}1,0}}$ instead of T_{z} was minimal (reduction of 0.1 m). For all hindcasts the storm duration, τ, was estimated at three hours.

The model is based on the assumption that the wave run-up height distribution follows a Rayleigh distribution, which resulted in the following equation for the maximum wave run-up z_{x} in [m] [IJnsen, 1983]:

$$z_x = 0.5056 \cdot z_{0.02} \cdot \sqrt{-ln\left(\frac{\bar{T}z}{\tau}\right)} \tag{5.4}$$

Battjes and Groenendijk [2000] showed that the wave height distribution is less steep in shallower water than a Rayleigh distribution. In other words: the Battjes-Groenendijk distribution leads to a lower flotsam height. In Witteveen+Bos [2010] the Battjes-Groenendijk wave height distribution was integrated in the flotsam model of IJnsen and led to the following equation for z_{x}:

$$z_x = 0.68 \cdot z_{0.02} \cdot \left(-ln\left(\frac{\bar{T}z}{\tau}\right)\right)^{\frac{1}{3.6}} \tag{5.5}$$

In the end, flotsam levels [m+NAP] were obtained by adding the water level [m+NAP] to the 2% wave run-up [m]. The flotsam lines were computed using both equation 5.4 (Rayleigh distribution) and 5.5 (Battjes-Groenendijk distribution). In combination with both 2% wave run-up formulas, this resulted in four calculated flotsam lines for each hindcast.

5.3. Comparison

The calculated flotsam lines are compared to measured flotsam lines in the end and evaluated if these measured lines can be used to assess the quality of the used models. The method exists of multiple models and formulas, which were required to calculate flotsam levels as explained earlier in Section 5.2. Each step in this method incorporates sources of uncertainty, therefore a systematic comparison between calculated and measured data needs was performed. By doing this, the quality of the used set of models and formulas was not evaluated as a whole but rather as individual components. The following systematic comparison was performed:

- Measured wind speed and direction are compared to HIRLAM wind.*
- Measured water levels are compared with WAQUA water level fields.
- Calculated SWAN wave parameters are compared with wave parameters obtained at measurement locations in the Eastern Wadden Sea.

* Measured wind data was used to perform the SWAN hindcasts. The computation of the water and current fields in WAQUA is based on the wind model HIRLAM and was therefore compared to measured wind.

5.4. Data availability

The required data to perform a flotsam level calculation is explained above. However, more data was required in this study. In Section 5.4.1 the database DONAR which contains measured data in the Eastern Wadden Sea is elaborated. This is followed by Section 5.4.2 in which the web-based system MATROOS is explained. This system was used to request model as well as measured data.

5.4.1. DONAR

To be able perform a systematic comparison as explained above, measured data was required. This measured data was obtained from measurement locations in the Eastern Wadden Sea. These locations are shown in Figure 5.1 and can provide real data of wind, water or wave parameters. Table 5.1 shows the measured parameters for each location. This data is stored in a database called DONAR (Data Opslag NAtte Rijkswaterstaat) and was requested by mailing the servicedesk-data of Rijkswaterstaat, via the website https://waterinfo.rws.nl or https://waterberichtgeving.rws.nl.

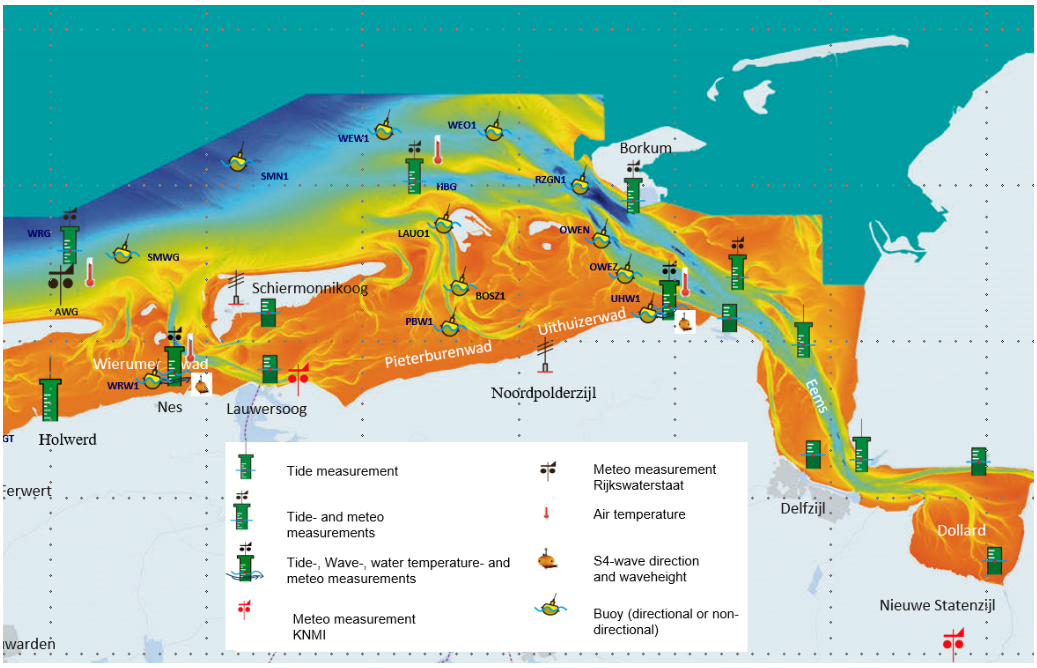

Figure 5.1: Measurement locations in the Eastern Wadden Sea. [Source: Rijkswaterstaat]

Table 5.1: Overview measurement locations in the eastern Wadden Sea

Location	Abbrevation(s)	x RD [m]	y RD [m]	Parameter(s)
Ameland Westgat	AWG/AWGPFM	191767	611861	Wind, air temp
Borkum (DE)	Borkum	237154	639323	Water level, wind
Borkum Noord	BRKN1/BORKND	236460	639460	Directional waves, water temp
Boschgat Zuid	BOSZ1/BOSCHGZD	226200	612700	Directional waves
Delfzijl	DLFZB/DELFZL	258017	594451	Water level
Eemshaven Binnen	EMSH/EEMSHVN	250810	607815	Water level, water temp
Eemshaven Stroommeetpaal	SPE/SPE11/EEMSHVSMPL	250250	610750	Water level, waves, flow dir, wind
Emshorn (DE)	EMSHN/EMH1	251486	612774	Wind
Holwerd	HOLWD	187550	601850	Water level
Huibertgat	HUIB/HUB1/HUIBGT	221990	621330	Water level, wind, air temp
Lauwersoog	LAUW/LAUWOG	208850	602790	Water level, wind
Lauwers Oost	LAUWOT/LAUO1	225500	617700	Directional waves
Nes	NES	179743	604897	Water level, waves, wind, water temp, air temp
Nieuwe Statenzijl	NWST/NIEUWSTZL	276540	584310	Water level
Nieuwe Beerta	NIEUWBTA/NIBE	272759	580081	Wind, air temp
Oude Westereems Noord	OWEN/OWE1/OUWDWTENBI1	240557	614915	Directional waves
Oude Westereems Zuid	OWEZ/OWE2/OUDWTEZBI1	243806	612177	Directional waves
Pieterburenwad	PBW1/PIETBRWD1	225792	608394	(Directional) waves
Randzelgat Noord	RZGN1/RANDZGND	237439	621340	Directional waves, water temp
Schiermonnikoog	SCHI/SCHIERMNOG	209221	609493	Water level, waves
Schiermonnikoog Noord	SON/SMN1/SCHIERMNOND	206527	623484	Directional waves,water temp
Schiermonnikoog Westgat	SMWG/SCHIERMNOWGT	195585	615149	Directional waves
Uithuizerwad	UHW1	245500	609810	Directional waves
Uithuizerwad	UHW2/UHW3/UHWD	245996	609772	Water level, waves, wind, water temp
Westereems Oost	WEO1/WESTEOT	230086	626634	Directional waves, water temp
Westereems West	WEW1/WESTEWT	219900	626397	Directional waves, water temp
Wierumergronden	WIERMGDN	192882	614562	Water level, wind, air temp
Wierumerwad	WRW1	200000	602587	Directional waves
Wierumerwad	WRW2/WRW3/WRWD	199957	602618	Water level, waves, wind, water temp

5.4.2. MATROOS

WAQUA water level and current fields were requested via MATROOS (Multifunctional Access Tool foR Operational Oceandata Services). This is a web-based system of operational predictions of water level, flow rates, waves and more. This system offers an interface which is used to visualize time series or grid data. Grid data of water level and current fields for the hindcast moments were requested via MATROOS and is explained in more detail in Section 5.7.2. Data in MATROOS is automatically deleted after 10 years. Unfortunately, this had it consequences on selecting the storms which were hindcasted. In the next section this is explained in more detail.

HIRLAM wind was requested in MATROOS via the interface Timeseries. HIRLAM wind speed and direction was compared to measured wind speed and direction for each hindcast moment. This was done because the computation of water level and current fields in WAQUA was based on HIRLAM wind.

5.5. Storm date selection

In Section 3.2 an inventory of measured flotsam lines is shown in Table 3.1. The first measured lines were originating from 1958-1971 and the last one was measured at 8 January 2019. As explained in Section 5.2, flotsam lines were calculated with help of hindcasts in SWAN. To obtain realistic estimates for each calculated flotsam line, accurate input data in SWAN and comparison data was crucial. Due to the time frame of this study, the quality of available data and location of measured flotsam lines it was decided to perform hindcasts of the following storms:

- 11 January 2015
- 13 January 2017
- 8 January 2019

The measured flotsam lines of 1 November 2006 and 8/9 November 2007 were not taken into account. The main reason for this was the absence of water level and current fields in MATROOS for these storms (data is automatically deleted after 10 years). The measured line of 2006 had also a low quality compared to the other lines. The line of 1 November 2006 had only six averaged measured flotsam levels over 40 km dike. Whereas the key feature of a flotsam line is the spatial variation and this cannot be seen in the measured flotsam line of the 1 November 2006 storm. The flotsam line of 9 November 2007 was obtained by translating aerial photographs with help of dike profiles. As a consequence of this, the vertical accuracy of the flotsam line is ±0.5 m.

The measured flotsam lines of 5/6 December 2013 were neither taken into account. As can be seen in Figure 3.12 and Table 3.1 almost all flotsam lines were measured between Lauwersoog and Eemshaven, except the two of 5/6 December 2013. These flotsam lines were measured between Delfzijl and Nieuwe Statenzijl and were therefore not used as comparison to the other flotsam lines.

5.6. Method flow scheme

In this section a flow scheme for the selected storms is presented. This flow scheme is a graphical summary of the method and comparison as described in Section 5.2 and Section 5.3. Three dates, as determined in Section 5.5, were selected to be examined in this study. In Figure 5.2 the flow scheme is shown. Models and formulas are presented in the blue boxes, input/output is shown in red and grey boxes. The input/output in the red boxes was compared to measured data as explained in Section 5.3. In the end measured flotsam lines were compared to the calculated flotsam lines for 11 January 2015, 13 January 2017 and 8 January 2019. The computations in the bounded red dashed area, which resulted in water level and current fields obtained from WAQUA, were already calculated and have been requested via MATROOS.

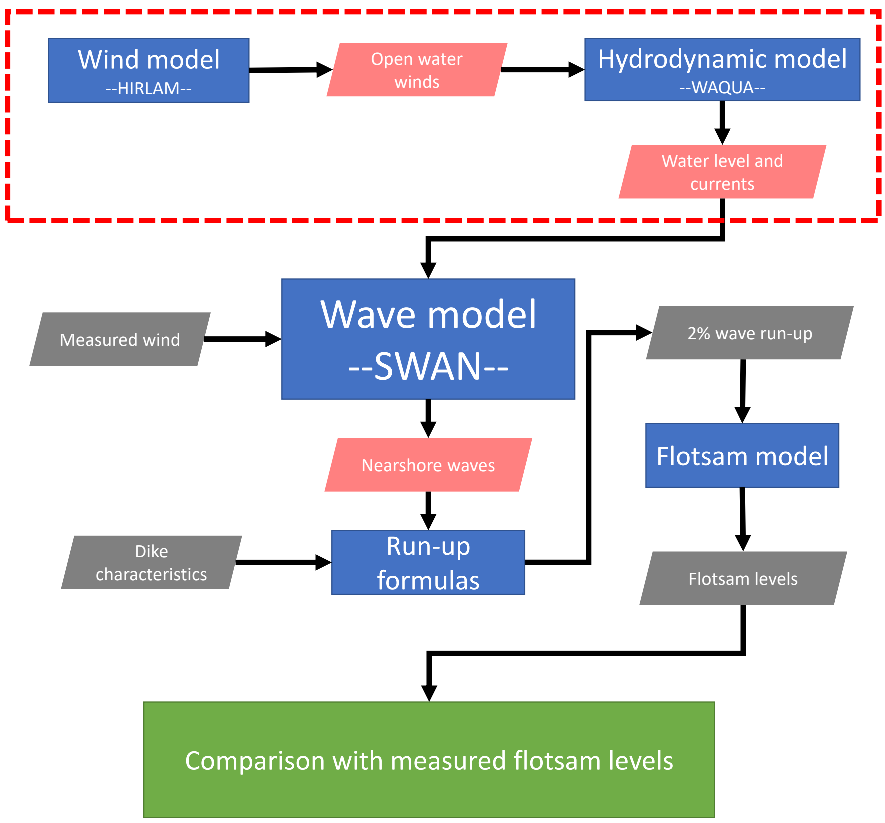

Figure 5.2: Flow scheme to calculate and compare flotsam lines

5.7. The SWAN model

This section describes the model set-up for the hindcasts in the wave model SWAN in stationary mode. Three storms were selected to be hindcasted: 11 January 2015, 13 January 2017 and 8 January 2019. Each storm had four time instants that were hindcasted. The selection of these time instants is described in the first subsection. In the following subsection, first the computational grid, spectral resolution and bathymetry are described. This is followed by a description of the model input conditions which consists of wind, water level and currents fields as well as the wave boundary conditions. In Subsection 5.7.2 is also the model output is presented. In the end, the SWAN version and used hardware as well as the physical and numerical settings of the model is described.

5.7.1. Selection of hindcast moments

Each hindcast consists of four time instants at and around the storm peak. These time moments were chosen such that they captured the highest wave conditions at the toe of the dike, which were leading to the highest predicted flotsam levels. The moments during the storms of 11 January 2015, 13 January 2017 and 8 January 2019 included:

- 2015 (Table 5.2): the peak water levels measured at Huibertgat, Lauwersoog, Eemshaven, Delfzijl and high wave heights at the offshore wave buoys Pieterburenwad (PBW1) and Randzelgat Noord (RZGN1);
- 2017 (Table 5.3): the peak water levels measured at Huibertgat, Lauwersoog, storm peak at Lauwersoog (highest windspeed) and peak wave height at the offshore wave buoy Pieterburenwad (PBW1);
- 2019 (Table 5.4): the peak water levels measured at Huibertgat, Eemshaven, high wind speed at Uithuizerwad (UWH1) and (peak) wave height at the offshore wave buoys Pieterburenwad (PBW1), Randzelgat Noord (RZGN1) and Uithuizerwad (UWH1).

Table 5.2: Selected time instants for SWAN hindcast of 11-01-2015

RunID	Time instant	Event
2015-001	11-01-2015 01:10	Highest water level (2.74 m+NAP) at Huibertgat
2015-002	11-01-2015 01:30	Highest water level (2.97 m+NAP) at Lauwersoog High H_{m0} (1.01 m) at PWB1
2015-003	11-01-2015 02:10	Highest water level (3.27 m+NAP) at Eemshaven High H_{m0} (2.22 m) at RZGN1
2015-004	11-01-2015 02:40	Highest water level (3.77 m+NAP) at Delfzijl

Table 5.3: Selected time instants for SWAN hindcast of 13-01-2017

RunID	Time instant	Event
2017-001	13-01-2017 22:20	Highest water level (2.57 m+NAP) at Huibertgat
2017-002	13-01-2017 22:30	Highest water level (2.99 m+NAP) at Lauwersoog
2017-003	13-01-2017 22:50	Highest H_{m0} (1.14 m) at PWB1
2017-004	13-01-2017 23:00	Highest wind speed (20.83 m/s) at Lauwersoog

Table 5.4: Selected time instants for SWAN hindcast of 08-01-2019

RunID	Time instant	Event
2019-001	08-01-2019 11:20	High H_{m0} (1.12 m) at PWB1 High H_{m0} (2.57 m) at RZGN1 Highest water level (2.55 m+NAP) at Huibertgat
2019-002	08-01-2019 11:40	Highest H_{m0} (1.07 m) at UHW1 (Radac) High wind speed (18.56 m/s) at UHW1
2019-003	08-01-2019 11:50	Highest water level (3.11 m+NAP) at Eemshaven
2019-004	08-01-2019 13:10	High H_{m0} (1.08 m) at PWB1

5.7.2. SWAN model set up

This section describes the model set-up for SWAN hindcasts as performed for this study. The time instants for each hindcast are selected in Section 5.7.1. The settings were chosen such that they are in line with the SWAN model settings as used in the derivation of the HBC, these settings were obtained from Svašek Hydraulics/ HKV [2011]. The used settings are elaborated in this section.

Computational grid, spectral resolution and bathymetry

The hindcasts were performed on two curvilinear grids, G1 and G3. The outline of these grids is shown in Figure 5.3. Grid G1 has a red outline and G3 a blue outline. G1 was used to generate wave boundary conditions for the other grids (G2,G3 and G4). Due to the scope of this study, the area between Lauwersoog and Eemshaven is of interest. The Southern boundary of G3 coincides with this area and was therefore used to calculate wave parameters. G3 covers the Eastern Wadden Sea and it extents from halfway the island Ameland at the west side to the eastern shore of the Eems-Dollard.

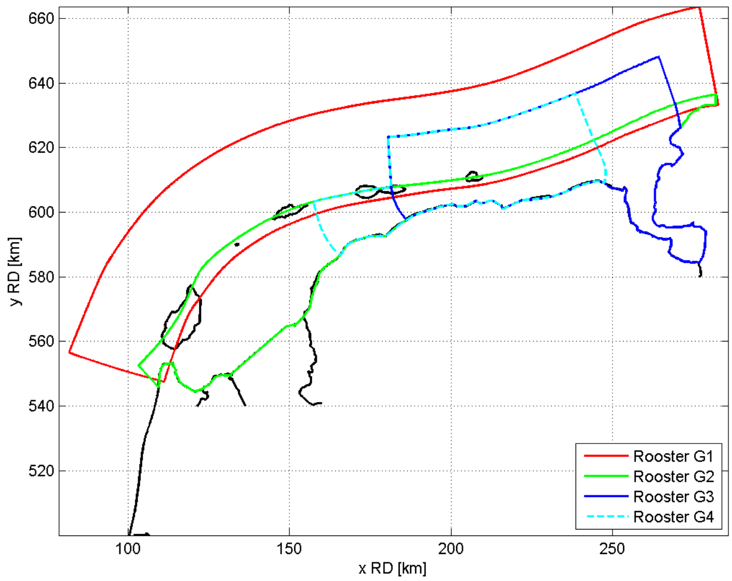

Figure 5.3: Computational grids G1 in red and G3 in dark blue [Svašek Hydraulics/ HKV, 2011]

The used bathymetries for G1 and G3 are shown in Figure 5.4. The spectral resolution for G1 and G3 consists of 36 directional bins of 10° and the frequency is fixed with a minimum and maximum frequency of respectively 0.015 Hz and 1.00 Hz. The minimum frequency differs from the minimum recommended frequency of 0.03 Hz by [Gautier and Groeneweg 2009]. A minimum frequency of 0.015 Hz was applied because some spectra may contain a significant amount of energy below 0.03 Hz [Svašek Hydraulics/ HKV, 2011]. In Table 5.5 the characteristics of both grids is summarised.

Table 5.5: Characteristics of the three SWAN computational grids

Grid	Nx	Ny	Ntotal	Nactive	Cell size min [m]	Cell size max [m]	Min frequency [Hz]	Max frequency [Hz]	Nbins
G1	2363	574	1.356.362	1.356.362	29	158	0.015	1	36
G3	990	1258	1.245.420	942.96	14	184	0.015	1	36

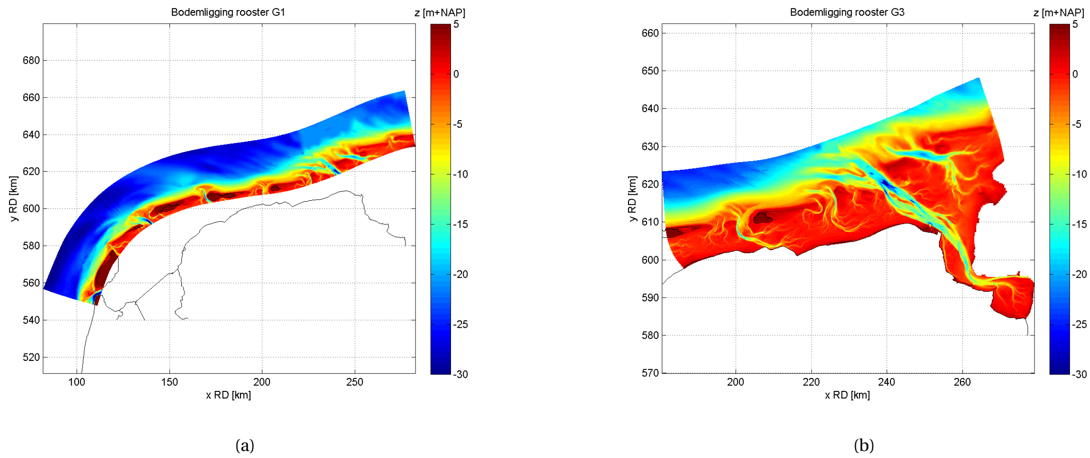

Figure 5.4: Bottom levels of grid G1 and G3 [Svašek Hydraulics/ HKV, 2011]

Wind

SWAN requires wind conditions to perform the hindcasts. Wind speed and direction or a complete wind field can serve as input. The hindcasts, each existing of four time instants, were performed using an averaged measured wind speed and direction over the whole computational domain. Measured wind was used to obtain in the end a realistic estimate for the calculated flotsam levels. Measured wind fields do not exists, therefore the wind at platform Ameland Westgat (AWG) was used as wind condition for both grid G1 and G3. The wind at AWG provided a conservative approach because this offshore wind speed was often higher compared to wind speeds closer to the coast. From Figures 6.8 , 6.9 and 6.10 it becomes clear that no major deviations occurred between the measured wind speed and wind direction for the concerned measurement locations in the Eastern Wadden Sea.

Table 5.6 shows averaged wind conditions obtained from a certain measured time period at AWG. These wind conditions were uniformly applied for each hindcast.

Table 5.6: Wind conditions, based on measurements at AWG, for each hindcasts.

Date	Time period [MET]	Wind speed [m/s]	Wind direction [°N]
11-01-2015	20:00 - 03:00	14.5	281
13-01-2017	18:40 - 23:50	20.4	319
08-01-2019	09:00 - 14:00	18.9	315

The measured wind at AWG was requested via DONAR and was supplied as a 10 min scalar average of measured wind. HIRLAM wind speed, used for the computation in WAQUA, is a potential wind, this is a fictive hour averaged wind speed in a standardised situation. This is in a situation with a measurement height of 10 m above an area with a roughness (z_0) which coincides with an open and flat grass environment (z_0 = 0.03 m) [KNMI, 1983]. The translation of a measured wind to potential wind is performed by taking into account the local roughness in the area of the measurement location. At open water the wind speed is higher than potential wind. The reason for this is the lower roughness of the water surface (z_0 = 0.0002 m) compared to the standardised roughness [KNMI, 1983]. HIRLAM wind speeds should be increased with 1.0 m/s to be compared to measured wind. (Personal communication with Robert Slomp)

Water level and current fields

Predicted water level and current fields, computed by WAQUA with HIRLAM wind, were used as input of each SWAN hindcast. These fields were obtained from the web-system MATROOS. The used source in MATROOS is called 'dd zuno-v4 hirlam kf(dscmv6-zunov4)'. This source presents the most accurate water level and current fields which are available in MATROOS. The sequence of models used in this source, dcsmv6-zunov4, is supported with a kalman filter. This filter is integrating a network of 32 water level measurement stations to improve the prediction. The water level and current fields from MATROOS were translated to the dimensions and conditions of the computational grids G1 and G3 to serve as input in the hindcasts. A matlab script was used to perform this translation. In Figure 5.5a a water level field from MATROOS for 13 January 2017 23:00 is shown. Besides this figure, the interpolated water level field to G1 is shown. The remaining water level and current fields for G1 and G3 were obtained in a similar way.

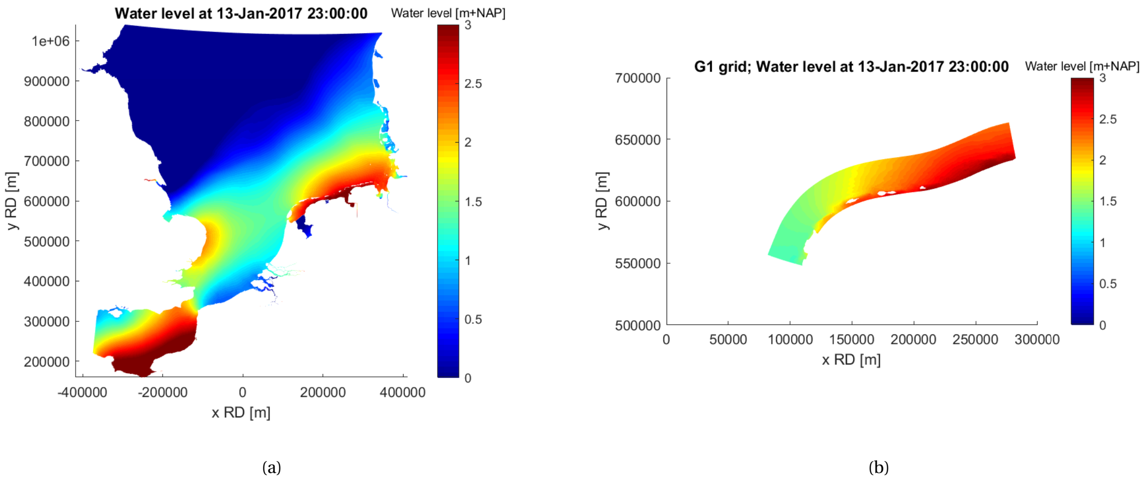

Figure 5.5: Left, the original water level field from MATROOS for 13 January 2017 23:00. Right, the same time instant interpolated to G1.

Wave boundary conditions

Wave boundary conditions at G1 were required to perform the hindcasts on the G1 grid. G1 was used to compute boundary conditions for the G3 grid. The wave boundary conditions were derived from measurement at the following buoys: Schiermonnikoog Noord (SMN1), Eierlandse Gat (ELD1) and Amelander Zeegat 11 (ABZ11). These wave buoys are located inside the computational grid and can be seen in Figure 5.6. Wave boundary conditions for the hindcast of 11 January 2015 were based on the Amelander Zeegat 11 buoy instead of the offshore wave buoy ELD, this is due to lack of data for this date.

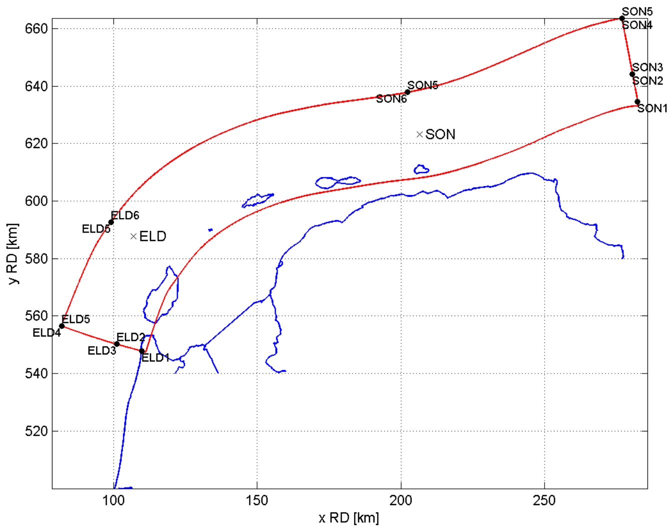

Figure 5.6: The boundary segments of grid G1 are made of 12 spectra files

In Figure 5.6, wave boundary segments of G1 are illustrated. It exists of two lateral boundaries divided into two segments each and a northern seaward boundary divided into three segments. Each segment consist of a starting and ending point. Measured 1D spectra were applied as wave boundary conditions at these points and data for in between points were computed by SWAN internally by linear interpolation.

There were 12 spectra files required, 6 for ELD and 6 for SON. SON1 and ELD1 contain no energy, for the other locations the measured spectra's at SON and ELD (or AZB11) were directly applied at respectively SON2 - SON6 and ELD2 - ELD6. Boundary data at intermediate points were obtained by interpolation (done in SWAN).

The wave boundary conditions for G3 were obtained via nesting from the hindcast simulations of G1. This nesting exists of writing a wave boundary file for G3 directly after the G1 simulation was performed.

Output
A specific set of locations (defined as *HRbasis set*) was used to generate wave conditions close as possible to the dike. This set of points was initially constructed to determine the HBC in WBI2017 and was used to calculate flotsam levels along the dike in this study. Besides this output set of wave parameters other output was also generated such as, spatial fields for a number of parameters and 1D and 2D spectra for certain locations.

The main output of each SWAN hindcast is the HRbasis set with wave parameters. This set exists of 1395 point locations. These points are located 100 meters from the crest of the dike and have at least 2 active cells between dike and output locations. The spacing between the output locations is not greater than 250 meters. However, this study focusses at the location between Lauwersoog and Eemshaven. Due to this only 144 points between x RD = 220 and 250 km were taken into account. An overview of these points can be seen in Figure 5.7. One point (x RD = 224678 m, y RD = 603965 m) in this HRbasis set remained dry in the hindcasts and was therefore not included in the flotsam level calculation.

Figure 5.7: Selected 144 points of the HRbasis set

Spatial fields were computed with help of a general generated Matlab Data file. These spatial fields served as comparison. The same holds for the generated spectra output files. These files contain 1D and 2D spectra and wave conditions for measurement locations in the eastern Wadden Sea.

Appendix III, IV and V contain spatial figures that present the results of the four time moments for 11 January 2015, 13 January 2017 and 8 January 2019. For each time instant the following parameters are shown:

- the significant wave height, H_{m0} [m];
- the spectral wave period, $T_{\mathrm{m-1,0}}$ [s];
- difference in significant wave height ΔH_{m0} [m] for the last two iterations;
- difference in spectral wave period ΔRT_{m01} [s] for the last two iterations;

- mean wave direction (nautical), *DIR* [°N];
- directional spreading, *DSPR* [°];
- wave height over water depth ratio, H_{m0}/d [-];
- water level [m+NAP];
- fraction of breaking waves, Q_b [-] (logarithmic);
- ratio of the spectral periods, $T_{m01}/T_{m\text{-}1,0}$ [-].

The ratio $T_{m01}/T_{m\text{-}1,0}$ can be considered as an indicator of low-frequency waves. The spectral wave height $T_{m\text{-}1,0}$ puts more emphasis on the presence of longer waves compared to T_{m01} and T_{m02}. A decreasing ratio means an increase in the relatively amount of energetic long wave components.

The ratio H_{m0}/d can be considered as an indication of the finite depth wave growth limit. The study of van der Westhuysen and de Waal [2008] showed that maximum ratios of H_{m0}/d in the Wadden Sea should be in the order of 0.43.

SWAN version and hardware
The SWAN version 4072ABCDE was used to perform the stationary SWAN hindcasts. This version was supplied by Deltares. The simulations were performed on a TU Delft LINUX computational cluster 'HPC08'. One hindcast had a computational time of 2 hours, because all instants were performed simultaneously.

Physical and numerical settings
The model simulations were performed with the same physical settings as used for the derivation of the HBC for WBI2017. These settings have been obtained from [Svašek Hydraulics/ HKV, 2011] and were originally supplied by Deltares.

```
GEN3 WESTH
WCAP WESTH cds2=5.0e-05 br=0.00175 p0=4.0 powst=0.0 powk=0.0 & nldisp=0.0 cds3=0.8 powfsh=1.0
QUAD iquad=2 lambda=0.25 Cnl4=3.0e+07
LIMITER ursell=10.0 qb=1.0
FRIC JONSWAP cfjon=0.0380000
BREA WESTH alpha=0.96 pown=2.5 bref=-1.39630 shfac=500.0
TRIAD trfac=0.1 cutfr=2.5
```

Inspection of the SWAN results of the hindcast 13 January 2017 showed that the average number of required iterations used in our set of computations was 27 for G1 grid and 32 for G3 grid. These numbers indicated that the maximum of 80 iterations was on the safe side.

The convergence behaviour was checked by performing a test run for the hindcast of 13 January 2017 with a stricter criterion of 99.8% accepted points. The results of this test run were compared to the original run with a required percentage of 99.0%. This comparison is shown in Figure IV.4 and Figure IV.5. The number of required iterations was 52 and 58 for respectively G1 and G3 grid, still on the safe side.

The results of the test computations indicate that for both the significant wave height H_{m0} and spectral wave period $T_{m\text{-}1,0}$ have sufficiently converged at the output locations. Although a criterion of 99.0% seems sufficient, it was decided to perform all subsequent SWAN computations with a convergence criterion of 99.8% accepted points (Recommendation of Gerbrant van Vledder)

The following numerical settings were applied for grid G1:

```
NUM STOPC dabs=0.00 drel=0.01 curvat=0.001 npnts=99. STAT mxitst=80 alfa=0.001
```

Refraction was partly deactivated for the computations with G3. This means that the penetration of longer waves was stimulated. The following numerical settings were applied for this grid:

```
NUM  STOPC  dabs=0.00  drel=0.01  curvat=0.001  npnts=99.  STAT  mxitst=80  alfa=0.001  REFRL  0.2  2
```

6

Calculated flotsam lines with SWAN

In this chapter presents the results of calculated flotsam lines using computed wave conditions by SWAN in stationary mode. The lines were calculated following the method as described in Chapter 5. In Section 6.2 a systematic comparison between modelled data and measured data is performed, this to analyse the sequence of models and formula's. In Chapter 8 the results are discussed.

6.1. Calculated flotsam levels

The flotsam levels are calculated as explained in Section 5.2. A graphical illustration of the method can be seen in Figure 5.2. The flotsam lines (maximum wave run-up) are calculated with wave parameters from the HRbasis set. The 144 selected locations from this set are located between x RD = 220 and 250 km (Figure 5.7).

The maximum computed flotsam lines of each hindcast are presented in Figures 6.1, 6.2 and 6.3. These lines correspond for the time instants of 11 January 2015 01:30 (Figure 6.1), 13 January 2017 22:50 (Figure 6.2) and 8 January 2019 11:20 (Figure 6.3). These time instants were leading to the highest maximum wave run-up of the considered time instants for each hindcast.

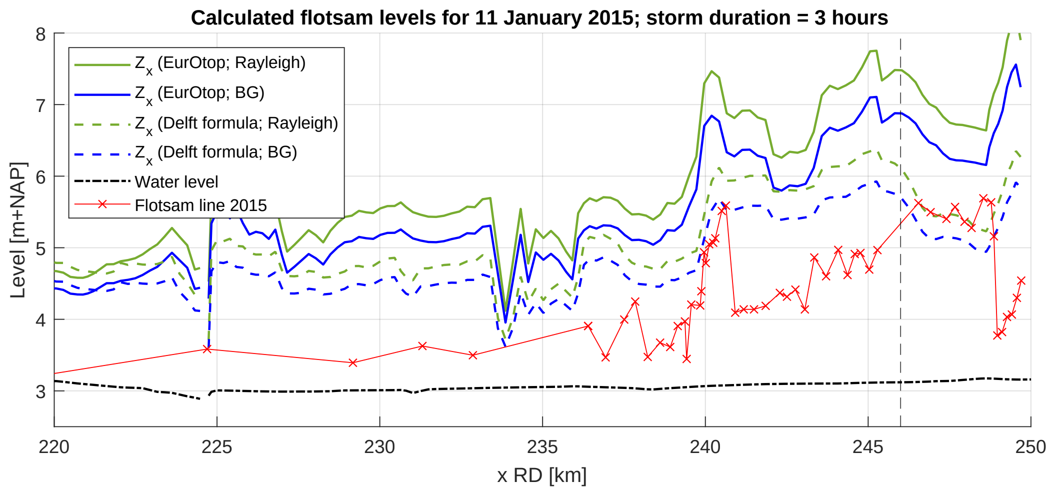

Figure 6.1: Calculated flotsam lines for 11 January 2015 01:30. The dashed line at x RD = 246 km corresponds to the location of the measurement pole Uithuizerwad.

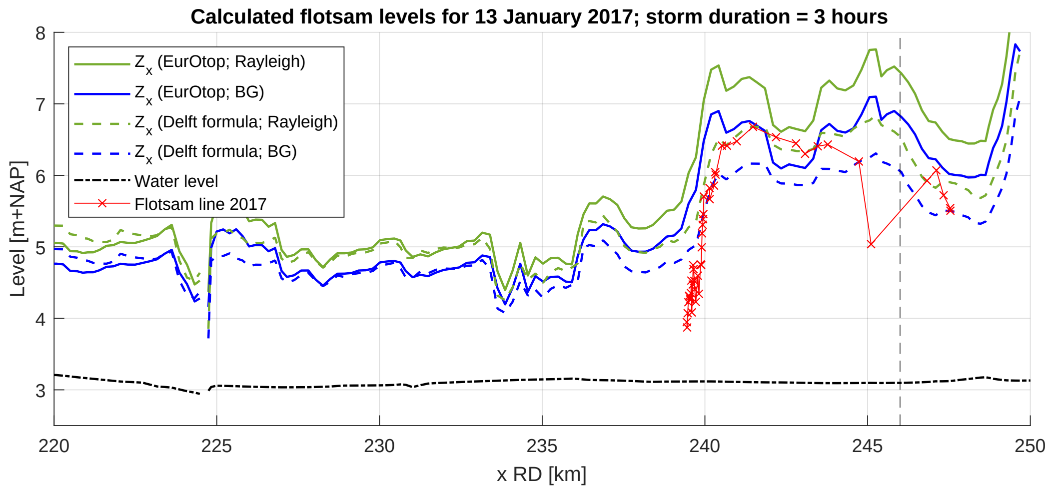

Figure 6.2: Calculated flotsam lines for 13 January 2017 22:50. The dashed line at x RD = 246 km corresponds to the location of the measurement pole Uithuizerwad.

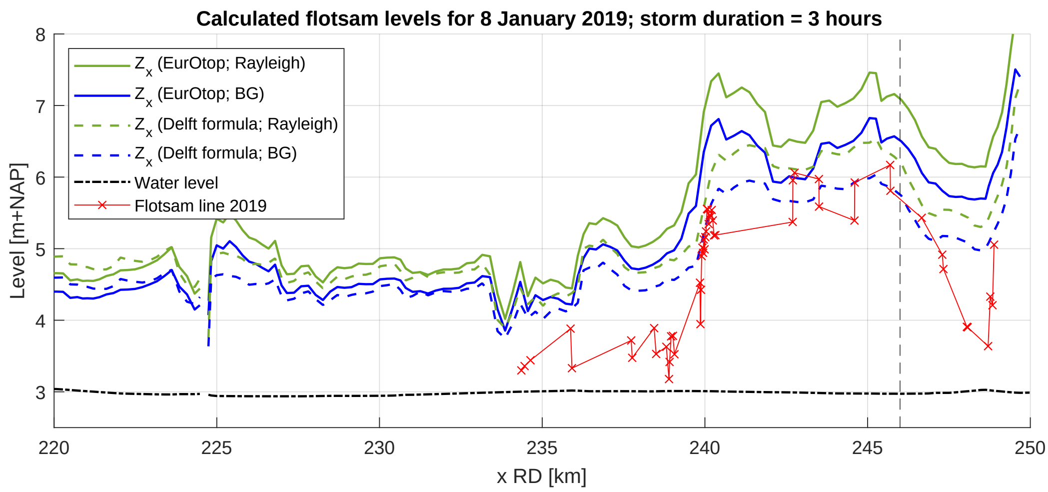

Figure 6.3: Calculated flotsam lines for 8 January 2019 11:20. The dashed line at x RD = 246 km corresponds to the location of the measurement pole Uithuizerwad.

As can be seen in Figures 6.1, 6.2 and 6.3 each figure exists of six different lines: four lines corresponding to calculated flotsam levels, a red line for the measured flotsam line and a dashed black line for the water level. Flotsam levels were calculated in four ways, as described in Section 5.2. The continuous lines were using the EurOtop [2016] formula (Eq. 2.15 and 2.16) and the dashed lines were calculated using the 'Delft' formula (Eq. 2.19). The flotsam model of IJnsen was applied with both the Rayleigh (green lines) and the Battjes Groenendijk (blue lines) wave height distribution.

IJnsen [1983] used the 'Delft' formula and a Rayleigh wave height distribution in his study to construct the flotsam model. Back then, the 'Delft' formula was used commonly to calculate the wave run-up. However, currently the formulas in EurOtop [2016] are used to calculate the wave run-up. Due to this, flotsam lines were calculated using both formulas. In addition to the Rayleigh wave height distribution, the Battjes-Groenendijk was height distribution was also used to calculate flotsam levels. The reason for this was the suggestion by Witteveen+Bos [2010] that this distribution led to a better agreement with measured flotsam lines between x RD = 210 and 235 km.

The spectral wave height, wave period, breaker parameter and wave steepness are presented in Figures 6.4, 6.5, 6.6 and 6.7 for the considered time instants with the highest maximum wave run-up.

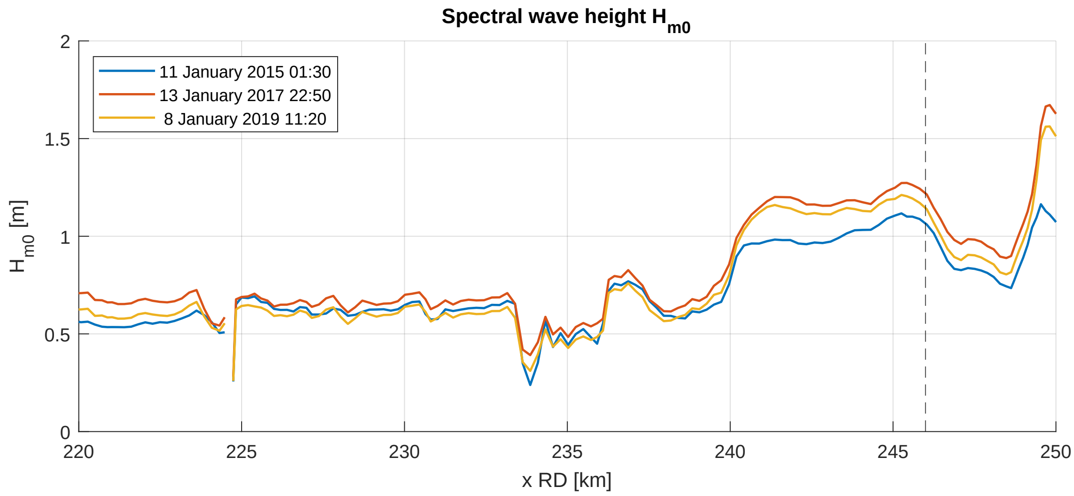

Figure 6.4: Computed spectral wave heights (H_{m0}) for the considered storms.

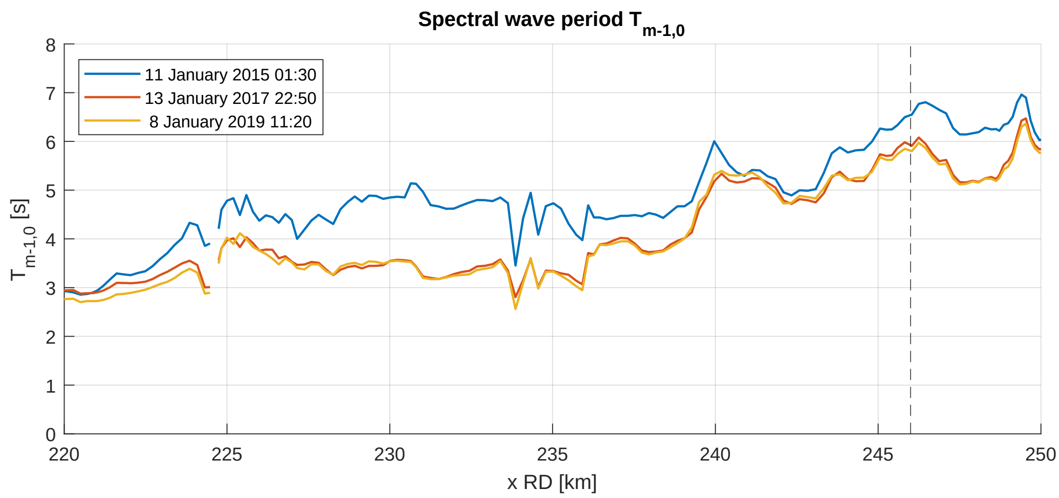

Figure 6.5: Computed spectral wave periods ($T_{\mathrm{m-1,0}}$) for the considered storms.

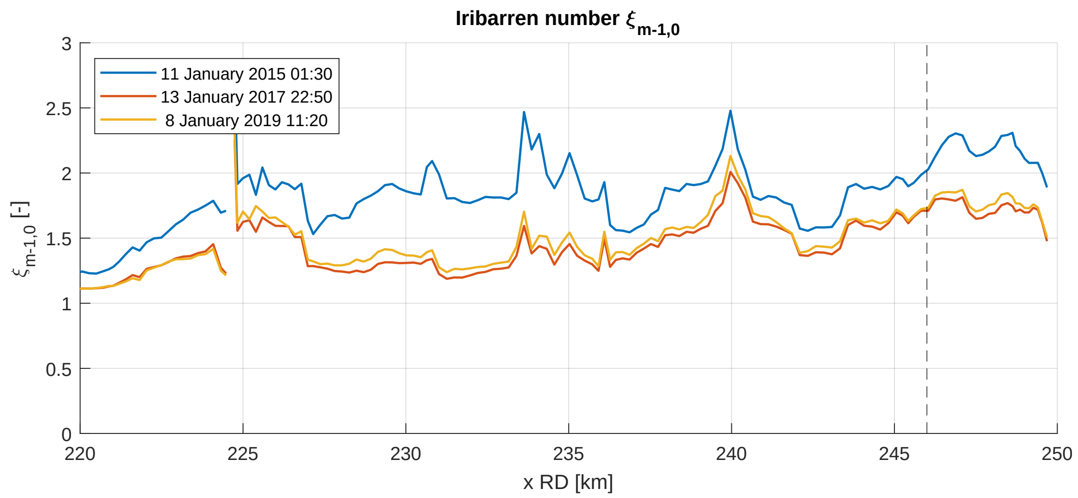

Figure 6.6: Calculated Iribarren numbers ($\xi_{m-1,0}$) for the considered storms.

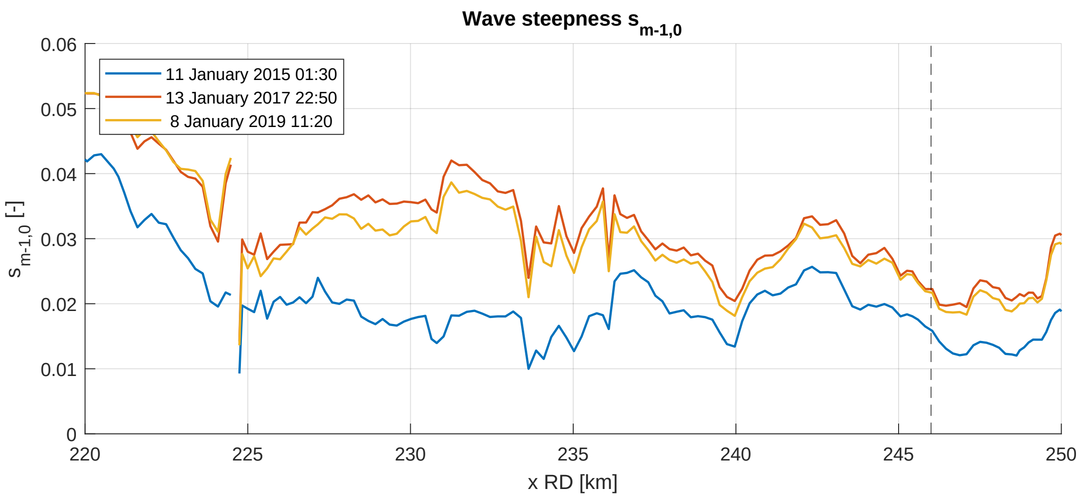

Figure 6.7: Calculated wave steepness ($s_{m-1,0}$) for the considered storms.

In Figure 6.1 the calculated flotsam lines of 11 January 2015 overestimates the measured line between x RD = 220 and 239 km. The area in front of this dike section exists mainly of vegetated foreshores. At x RD = 240 km an increase of both the calculated as measured flotsam line can be seen. At this point the vegetated foreshore stops and the bed level (Figure II.4) decreases and remains more or less constant till x RD = 246 km. The measured line shows a sudden drop after x RD = 241 km. Between x RD = 246 and 249 km another (vegetated) foreshore is present with almost same bed level as between x RD = 220 and 239 km. A sudden drop of the measured flotsam line can be seen at x RD = 248.5 km followed by a small increase towards the east (x RD > 248.5 km).

The identical increase at x RD = 240 km as in 2015 for both calculated and measured flotsam lines can be seen in Figure 6.2 for 2017. Unfortunately, there are no measurements from x RD = 239 km towards the west and between x RD = 246 and 249 km.

Again, an increase for both calculated and measured flotsam line of 8 January 2019 at the same location (x RD = 240 km) can be seen in Figure 6.3. In comparison to the measured flotsam line of 2017, this flotsam line is a more fluctuating line, because it contains not only the highest flotsam levels but also the lower levels of the flotsam line. Westward of x RD = 240 km, the same behaviour as in 2015 is observed; the calculated flotsam lines are overestimating the measured line. Another similar increasing pattern with 2015 can be seen eastward of x RD = 248.5 km.

Figures 6.1, 6.2 and 6.3 show that:

- the water levels are almost identical for the considered storms (3.0 - 3.25 m+NAP);
- the measured flotsam levels are different for each storm. The lines of 2017 and 2019 have a more similar pattern and differ from the measured line of 2015;
- the measured flotsam lines have more spatial variability than the calculated lines. Besides this, not one of the four calculated flotsam lines is in favour to approximate the entire measured flotsam line for each year. However, two lines give the best approximation with respect to highest measured flotsam levels (5.5 - 6.5 m+NAP): the 'Delft' formula together with an applied Rayleigh wave height distribution (dashed green line) and the EurOtop [2016] formula together with an applied Battjes-Groenendijk wave height distribution (continuous blue line);
- both measured and calculated lines show an increase in flotsam line around x RD = 240 km and x RD = 248.5 km;
- the calculated levels in 2017 and 2019 using the EurOtop [2016] formula with a wave steepness $s_{\text{m-1,0}}$ of around 0.035 - 0.04 are almost identical to calculated levels using the 'Delft' formula;
- the four calculated lines of 2015 show a larger variation between each other compared to the lines of 2017 and 2019. This is caused by a significant higher wave period $T_{\text{m-1,0}}$ for 2015, especially between x RD = 220 and 239 km;
- the applied wave height distribution (Rayleigh or Battjes-Groenendijk) in flotsam model results in a reduction between 0.3 and 0.5 m in calculated flotsam levels when applying a Battjes-Groenendijk distribution.

Figures 6.4, 6.5, 6.6 and 6.7 show that:

- the spectral wave height at the salt marsh (x RD = 220 - 240 km) is around 0.6 - 0.7 m. Between x RD = 240 and 246 km H_{m0} is significantly higher for 2017 and 2019 (1.2 - 1.3 m) compared to 2015 (1.0 m);
- the spectral wave height is comparable for 2017 and 2019. $T_{\text{m-1,0}}$ is significantly higher (> 10 %) for 2015 compared to 2017 and 2019, especially at the salt marsh (x RD = 220 - 240 km);
- the Iribarren number is higher for 2015 than 2017 and 2019. This is the result of a higher spectral wave period $T_{\text{m-1,0}}$ for the storm of 2015. However, the breaker type (plunging waves) is the same for all years;
- the wave steepness is significantly lower (> 20 %) for 2015 compared to 2017 and 2019. The reason for this is the higher wave period $T_{\text{m-1,0}}$ for the storm of 2015.

6.2. Comparison between model and measurement data

This section presents the systematic comparison between model and measurements data results as described in Section 5.3. This comparison was performed to analyse the performance of the sequence of models and formulas (Figure 5.2). In Sections 6.2.1 - 6.2.3 modelled wind, water level and wave parameters are compared to measurements in the Eastern Wadden Sea. The specific measurements were obtained from measurement locations as shown in Figure 5.1 and Table 5.1.

6.2.1. Wind

Measured wind speed and direction at locations Lauwersoog, Nieuwe Beerta, Uithuizerwad and Ameland Westgat (AWG) is shown in Figures 6.8, 6.9 and 6.10 for the considered storms.

Wind speed and direction plots are shown in Appendix III (2015), IV (2017) and V (2019). Figures III.2, IV.2 and V.2 contain measured wind speed as well as HIRLAM wind speed. Measured and HIRLAM wind direction is shown in Figures III.3, IV.3 and V.3.

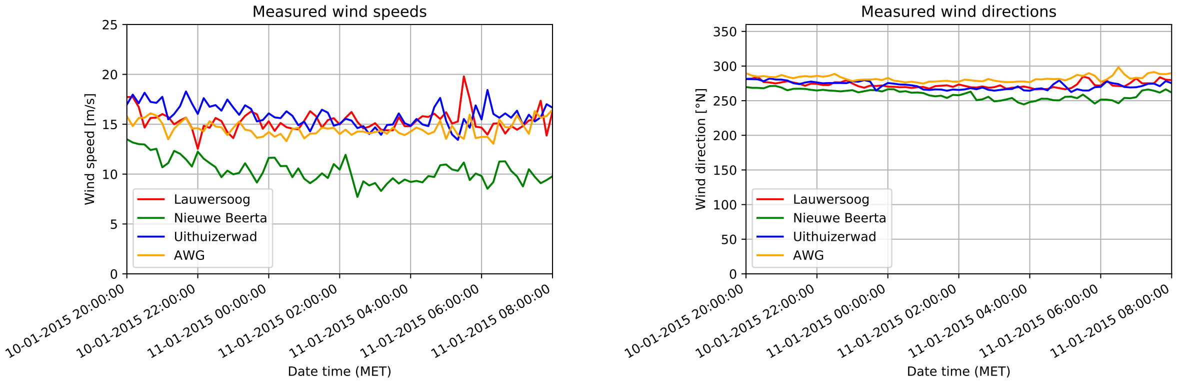

(a) (b)

Figure 6.8: Measured wind speed and direction for 11 January 2015

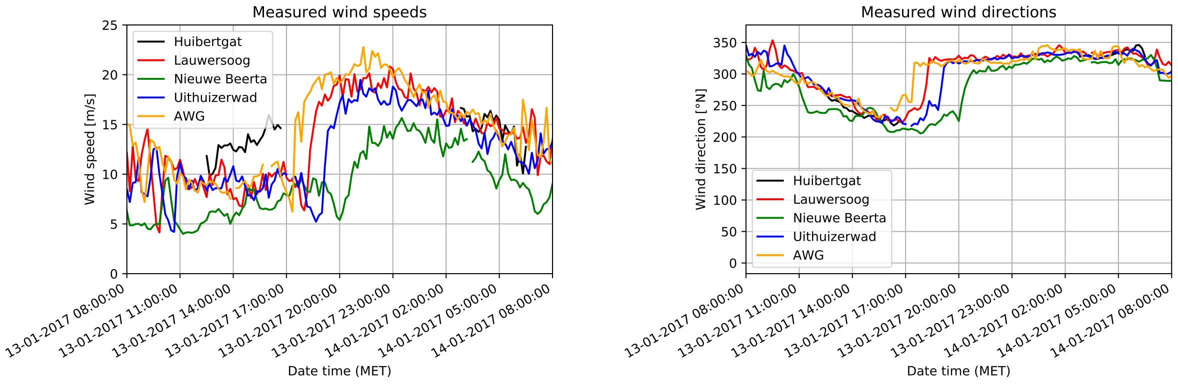

(a) (b)

Figure 6.9: Measured wind speed and direction for 13 January 2017

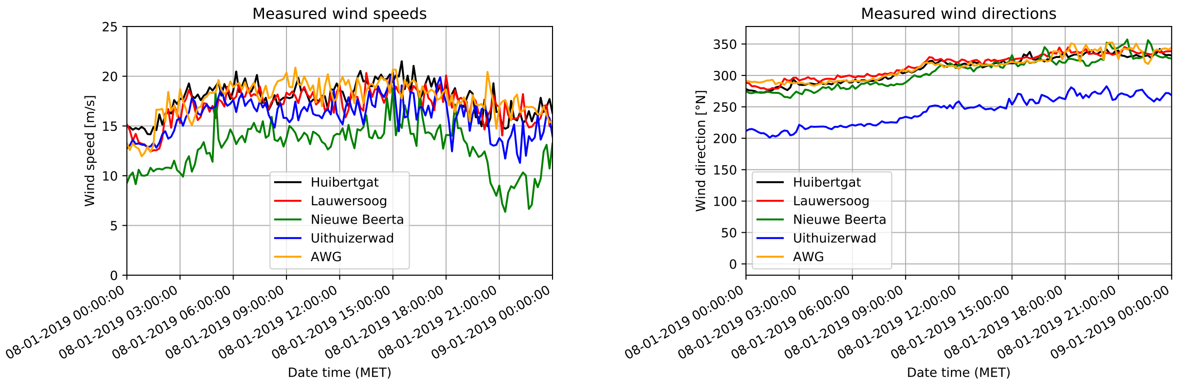

(a) (b)

Figure 6.10: Measured wind speed and direction for 8 January 2019

Figures 6.8, 6.9 and 6.10 show that:

- the applied western wind (14.5 m/s, 281 °N) in the hindcast of 11 January 2015 was almost uniform in wind speed and direction at the considered time interval. One can recognize lower wind speeds above land (10 m/s at Nieuw Beerta);

- The applied wind speed (20.4 m/s) and direction (319 °N) in the hindcast of 13 January 2017 were averaged measurements at AWG and has been applied uniformly over the computational grid. In the hours before the peak of the storm (MET 22:00), wind speed and direction suddenly shifted from a western direction with lower wind speeds (u≈10 m/s) to a NW/NNW wind with higher wind speeds. This can be seen in Figure 6.9;
- for the hindcast of 8 January 2019 also averaged measurements at AWG were applied uniformly over the computational grid. A wind speed of 18.9 m/s and a direction of 315 °N was used in the SWAN computation. Figure 6.10 shows a more gradual change in wind speed and wind direction compared to 2017. The wind direction was NW/NNW during the peak of the storm. The measured wind direction at Uithuizerwad is most likely to be incorrect, but the measured wind speed seems to be correct.

Figures III.2, III.3, IV.2 IV.3, V.2 and V.3 (In appendices III (2015), IV (2017) and V (2019)) show that:

- in 2015 HIRLAM wind speed at Lauwersoog and Nieuw Beerta agrees quite well to measured wind speeds, but HIRLAM overestimated the wind speed with a value of around 2 m/s at AWG. In Figures 6.8 small deviations between HIRLAM and measured wind directions at AWG and Nieuwe Beerta can be seen. These small deviations increase after the high water level peak. At Lauwersoog the HIRLAM wind direction was almost identical to measured values. At Huibertgat, no comparison can be made due to lack of measurements for both wind speed and direction;
- HIRLAM underestimated the wind speed at the peak of the storm (13 January 2017 22:00 MET) at the locations AWG, Lauwersoog and Nieuw Beerta. Figures IV.3 and IV.3 shows small deviations between HIRLAM and measured wind directions at AWG and Lauwersoog. On the other hand, significant deviations in wind direction (≈ 20°) occurred at Nieuw Beerta in the hours before the peak of the storm (MET 22:00). Again, due to lack of data measured at Huibertgat. No good comparison can be made;
- HIRLAM wind speed and direction were almost identical to measured wind speed and direction for the locations Huibertgat, AWG, Lauwersoog and Nieuw Beerta. However, after the peak of the storm (8 January 2019 12:00 MET) small deviations in wind speed can be seen at Lauwersoog and Nieuw Beerta (Figure V.2).

6.2.2. Water level

Measured water levels at locations Huibertgat, Schiermonnikoog, Lauwersoog, Eemshaven, Delfzijl and Nieuwe Statenzijl are shown in Figures 6.11, 6.12 and 6.13 for the considered storms. WAQUA water level fields served as input in the SWAN hindcasts. These fields were obtained from the source 'dd zuno-v4 hirlam kf(dcsmv6-zunov4) via MATROOS. For the same source, time series were obtained to serve as comparison with measured water levels. In Tables 6.1, 6.2 and 6.3 the peak value of measurements and modelled WAQUA water levels are shown for each location.

Time series plots of modelled and measured water levels are shown in Appendix III (2015), IV (2017) and V (2019). This can be seen in Figures III.1, IV.1 and V.1 for the locations: Huibertgat, Wierumergronden, Nes, Schiermonnikoog, Lauwersoog, Eemshaven, Delfzijl and Nieuwe Statenzijl.

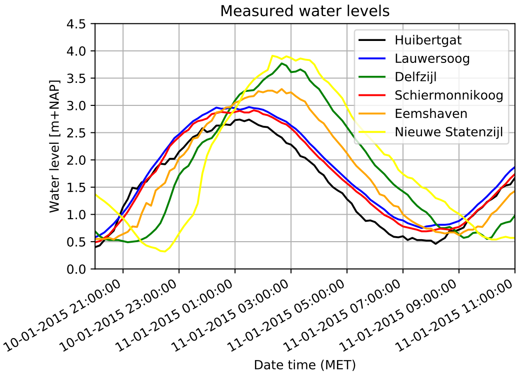

Figure 6.11: Measured water levels for 11 January 2015

Hindcast 11-01-2015	**Maximum water level [m+NAP]**	
	Measured	Model
Huibertgat	2.74	2.82
Schiermonnikoog	2.91	2.90
Lauwersoog	2.97	2.92
Eemshaven	3.3	3.14
Delfzijl	3.77	3.57
Nieuwe Statenzijl	3.91	3.91

Table 6.1: Measured maximum water levels compared to maximum water levels from the source 'dd zuno-v4 hirlam kf(dcsmv6-zunov4)' for 11 January 2015

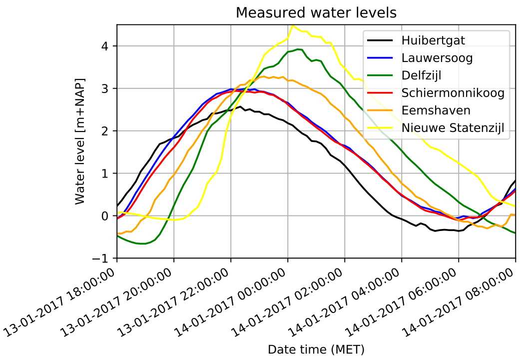

Figure 6.12: Measured water levels for 13 January 2017

Hindcast 13-01-2017	**Maximum water level [m+NAP]**	
	Measured	Model
Huibertgat	2.57	2.66
Schiermonnikoog	2.94	2.80
Lauwersoog	2.99	2.90
Eemshaven	3.28	3.07
Delfzijl	3.92	3.5
Nieuwe Statenzijl	4.49	4.07

Table 6.2: Measured maximum water levels compared to maximum water levels from the source 'dd zuno-v4 hirlam kf(dcsmv6-zunov4)' for 13 January 2017

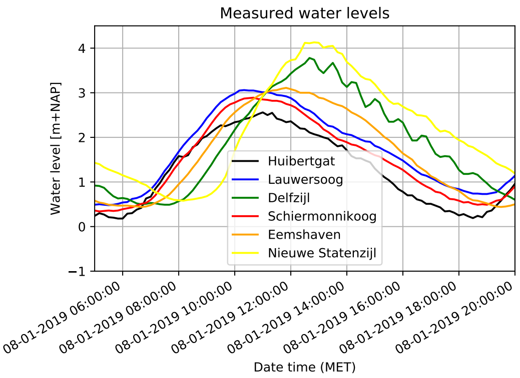

Figure 6.13: Measured water levels for 8 January 2019

Hindcast 08-01-2019	**Maximum water level [m+NAP]**	
	Measured	Model
Huibertgat	2.56	2.67
Schiermonnikoog	2.89	2.79
Lauwersoog	3.06	2.87
Eemshaven	3.11	3.07
Delfzijl	3.78	3.51
Nieuwe Statenzijl	4.13	3.92

Table 6.3: Measured maximum water levels compared to maximum water levels from the source 'dd zuno-v4 hirlam kf(dcsmv6-zunov4)' for 8 January 2019

Figures 6.11 - 6.13 and Tables 6.1 - 6.3 show that:

- in 2015 the largest deviations between measured and modelled water levels occurred at Eemshaven (16 cm) and Delfzijl (20 cm);
- in 2017 the largest deviations between measured and modelled water levels occurred at Eemshaven (21 cm), Delfzijl (42 cm) and Nieuwe Statenzijl (42 cm);
- in 2019 the largest deviations between measured and modelled water levels occurred at Lauwersoog (19 cm), Delfzijl (26 cm) and Nieuwe Statenzijl (21 cm).

Figures III.1, IV.1 and V.1 (appendices) show that:

- in 2015, 2017 and 2019 the modelled high water peaks were slightly higher than measurements for the locations Huibertgat and Wierumergronden. Inside the Wadden Sea measurements were somewhat higher than the model peak values. The reason for this can be the omission of wave setup due to wave breaking at the northern sides of the Wadden islands and in the Wadden Sea;
- modelled water levels at the area of interest (Lauwersoog - Eemshaven) do not show significant differences with measured water levels. The largest deviation occurred at the peak of the storm in 2017 at Eemshaven (21 cm)

6.2.3. Waves

Wave parameters modelled in SWAN and measured wave parameters are compared in this section. This comparison was done for measurement locations from Figure 5.1 and Table 5.1. Modelled and measured wave parameters (H_{m0} and $T_{m\text{-}1,0}$) for each time instant and storm are shown in Appendix III (2015), IV (2017) and V (2019).

For two locations, Uithuizerwad and Schiermonnikoog Noord, the spectral wave height H_{m0} and wave period $T_{m\text{-}1,0}$ are presented in this section. Tables 6.4, 6.5 and 6.6 show the spectral wave height H_{m0} and wave period $T_{m\text{-}1,0}$ at Uithuizerwad. These parameters were measured with a Radac wave radar and a Etrometa stepgauge. For 2015, only measurements with the Etrometa stepgauge were registered.

Table 6.4: H_{m0} and $T_{m\text{-}1,0}$ at location Uithuizerwad for time instants of hindcast 11 January 2015

Uithuizerwad	**H_{m0} [m]**			**$T_{m\text{-}1,0}$ [s]**		
11-01-2015	Radac	Etrometa	Model (G3)	Radac	Etrometa	Model (G3)
01:10 (001)	-	0.67	1.07	-	4.9	6.45
01:30 (002)	-	0.67	1.09	-	5	6.45
02:10 (003)	-	0.73	1.11	-	4.9	6.60
02:40 (004)	-	0.74	1.08	-	4.9	6.34

Table 6.5: H_{m0} and $T_{m\text{-}1,0}$ at location Uithuizerwad for time instants of hindcast 13 January 2017

Uithuizerwad	**H_{m0} [m]**			**$T_{m\text{-}1,0}$ [s]**		
13-01-2017	Radac	Etrometa	Model (G3)	Radac	Etrometa	Model (G3)
22:20 (001)	1.06	1.21	1.16	4.9	5	5.84
22:30 (002)	1.09	1.17	1.19	4.5	4.6	5.89
22:50 (003)	1.08	1.02	1.22	5.2	5.1	5.91
23:00 (004)	1.10	1.03	1.24	5.2	5.2	5.90

Table 6.6: H_{m0} and $T_{m\text{-}1,0}$ at location Uithuizerwad for time instants of hindcast 8 January 2019

Uithuizerwad	**H_{m0} [m]**			**$T_{m\text{-}1,0}$ [s]**		
08-01-2019	Radac	Etrometa	Model (G3)	Radac	Etrometa	Model (G3)
11:20 (001)	0.99	0.62	1.16	5.37	5.6	5.79
11:40 (002)	1.05	0.62	1.17	5.1	5.5	5.70
11:50 (003)	1.07	0.63	1.16	5.1	5.4	5.73
13:10 (004)	0.95	0.79	0.96	4.6	4.5	4.85

In Tables 6.7, 6.8 and 6.9 the wave parameters H_{m0} and $T_{m-1,0}$ are shown for Schiermonnikoog Noord buoy (SMN1). Both model results of G1 and G3 are present for this location.

Table 6.7: H_{m0} and $T_{m-1,0}$ at location Schiermonnikoog Noord buoy (SMN1) for time instants of hindcast 11 January 2015

SMN1		$\mathbf{H_{m0}}$ **[m]**			$\mathbf{T_{m-1,0}}$ **[s]**	
11-01-2015	Measured	Model (G1)	Model (G3)	Measured	Model (G1)	Model (G3)
01:10 (001)	5.85	5.02	4.88	10.7	10.75	10.47
01:30 (002)	5.74	5.3	5.14	10.7	10.79	10.64
02:10 (003)	6.2	6.02	5.83	11.7	11.59	11.54
02:40 (004)	5.67	4.76	4.59	11.0	10.28	10.29

Table 6.8: H_{m0} and $T_{m-1,0}$ at location Schiermonnikoog Noord buoy (SMN1) for time instants of hindcast 13 January 2017

SMN1		$\mathbf{H_{m0}}$ **[m]**			$\mathbf{T_{m-1,0}}$ **[s]**	
13-01-2017	Measured	Model (G1)	Model (G3)	Measured	Model (G1)	Model (G3)
22:20 (001)	7.51	7.41	7.13	12.2	11.53	11.27
22:30 (002)	7.12	7.41	7.18	12.1	11.55	11.22
22:50 (003)	7.07	7.31	7.19	12.1	11.65	11.36
23:00 (004)	7.0	7.3	7.17	12.1	11.65	11.37

Table 6.9: H_{m0} and $T_{m-1,0}$ at location Schiermonnikoog Noord buoy (SMN1) for time instants of hindcast 8 January 2019

SMN1		$\mathbf{H_{m0}}$ **[m]**			$\mathbf{T_{m-1,0}}$ **[s]**	
08-01-2019	Measured	Model (G1)	Model (G3)	Measured	Model (G1)	Model (G3)
11:20 (001)	6.53	6.78	6.58	11.1	10.59	10.36
11:40 (002)	6.72	7.2	6.95	11.3	10.55	10.44
11:50 (003)	6.86	7.41	7.13	11.8	10.85	10.76
13:10 (004)	6.23	6.58	6.39	11.1	10.65	10.49

Tables 6.4 - 6.9 show that:

- SWAN overestimated both H_{m0} and $T_{m-1,0}$ for each storm at Uithuizerwad;
- the measured wave height and period differs between the measurement types (Radac vs Etrometa). A significant difference in measured wave height (≈ 50%) compared to modelled wave height can be seen at 8 January 2019. Experts at Rijkswaterstaat expect that the Etrometa stepgauge had a malfunction;
- small deviations between H_{m0} and $T_{m-1,0}$ occurred for each storm at offshore wave buoy Schiermonnikoog Noord;
- differences between model output of grids G1 and G3 at SMN1 can be seen;
- the wave conditions at 8 January 2019 were close to the conditions of 2017. However, the wave conditions occurred at 13 January 2017 contains the highest values of these three hindcasts.

6.3. Summary

Table 6.10 shows a summary of model and measured data. Measured wind direction, wind speed, maximum water level and wave parameters (H_{m0} and $T_{m-1,0}$) are presented. For each storm the difference between model and measurement is shown inside brackets (A positive value represents an overestimation of the model). The presented wind speeds are averaged measured values around the storm peak. These averaged values have served as wind input in SWAN to perform the hindcasts in this study. However, modelled wind (HIRLAM) was used to calculate the water level and current fields. These fields were directly obtained from the web-based system MATROOS and have served as input in the stationary SWAN computations. This means that the made errors in wind modelling can have feed through into the water level and current modelling in WAQUA.

Table 6.10: Summary of the comparison between model and measured data. The difference between model and measurements is given inside brackets.

	11 January 2015		**13 January 2017**		**8 January 2019**	
	Measured	**Difference**	**Measured**	**Difference**	**Measured**	**Difference**
Wind direction *AWG*	W	(±5°)	NNW	(±5°)	NNW	(±9°)
Wind direction *Lauwersoog*	W	(±5°)	NNW	(±7°)	NNW	(±2°)
Wind speed *AWG*	14.5 m/s	(+2 m/s)	20.5 m/s	(± 0.5 m/s)	19.0 m/s	(±0.25 m/s)
Wind speed *Lauwersoog*	15.0 m/s	(±0.25 m/s)	19.0 m/s	(-1.0 m/s)	17.5 m/s	(-0.75 m/s)
Max water level *Eemshaven*	3.3 m+NAP	(-0.16 m)	3.28 m+NAP	(-0.21 m)	3.11 m+NAP	(-0.04 m)
Max water level *Lauwersoog*	2.97 m+NAP	(-0.05 m)	2.99 m+NAP	(-0.09 m)	3.06 m+NAP	(-0.19 m)
$\boldsymbol{H_{m0}}$ *Uithuizerwad*	0.7 m	(+0.4 m)*	1.1 m	(+0.1 m)	1.0 m	(+0.15 m)
$\boldsymbol{T_{m-1,0}}$ *Uithuizerwad*	4.9 s	(+1.5 s)	5.0 s	(+0.9 s)	5.2 s	(+0.5 s)

* In 2015 the wave height at Uithuizerwad was only measured with an Etrometa stepgauge. Experts at Rijkswaterstaat cannot validate the measured wave heights at the storm peak of 11 January 2015. Due to this, it cannot be excluded that the Etrometa stepgauge had the same malfunction as expected at the storm peak of 8 January 2019.

7

Analysis flotsam lines with measurements BE-SAFE

This chapter presents the calculated flotsam lines by using measurements instead of computed water level and wave conditions as used in Chapter 6. This means that only the last two steps of the method as described in Section 5.2 were performed.

The project BE-SAFE performed measurements in 2015 and 2017 at the salt marsh edge (x RD ≈ 240 km) between Lauwersoog and Eemshaven. Several pressure sensors measured water level and wave conditions. These measurements were used in this chapter to calculate flotsam levels for 11 January 2015 and 13 January 2017. First the area of interest is described. This is followed by an approach description to calculate flotsam levels using the data of BE-SAFE. In Section 7.3 the calculated flotsam levels are compared to measured flotsam levels at each specific location. In the end, measured data from BE-SAFE locations is compared to measurements at Uithuizerwad.

7.1. Location

Water level and wave conditions were measured with pressure gauges 1-4; A and B corresponds to respectively measurements in 2015 and 2017. These gauges were located at the eastward edge of the salt marsh along the toe of the Emmapolderdike (Figure 7.1). There were positioned over a length of 1.5 km to measure the differences in wave conditions caused by vegetation and bed level. In Appendix VI and VII the time-varying measured wave parameters and water levels are presented for respectively 11 January 2015 and 13 January 2017.

7.2. Flotsam level calculation

The performed measurements for both years were used to calculate time-varying flotsam levels. The method as described in Section 5.2.1 was used to perform these calculations. The different calculated flotsam levels showed large differences between the EurOtop [2016] formula and the 'Delft' formula, especially between x RD = 240 and 247.5 km.

In addition to the previously used wave run-up formulas another wave run-up formula was taken into account for these calculations. The wave run-up formula from Hunt [1959] (Eq. 2.14) was also used to calculate flotsam levels:

$$R = 0.4T\sqrt{gH} \cdot \tan\alpha \tag{7.1}$$

The above formula of Hunt [1959] was derived in wave conditions with periodic waves. However, in this study it is assumed that it can also be applied for individual waves in a random wave train. Due to this, the formula of Hunt [1959] gave the possibility of using an arbitrary wave period T and wave height H as input.

Figure 7.1: Locations of the pressure gauges. Yellow pins (2015) and red pins (2017)

Time-varying flotsam levels were calculated using three wave run-up formulas. The 'Delft' formula and EurOtop [2016] formula used the spectral wave height H_{m0} and period $T_{\mathrm{m\text{-}1,0}}$ as input. These parameters (in a 15-min interval) were obtained by a performed spectral analysis on the measured wave records of the project BE-SAFE. The wave run-up formula of Hunt [1959] used the maximum of $\mathrm{T}\sqrt{gH}$ in a 15-min interval which was obtained by performing a zero crossing analysis on the same wave records. It is assumed that the maximum individual wave run-up height is equal to the flotsam observations and according to Battjes [1972] and Battjes and Janssen [1978] the wave run-up follows the same distribution as the wave height distribution, because the wave run-up is the result of individual waves. Therefore, to obtain the highest wave run-ups (flotsam levels), the maximum of $\mathrm{T}\sqrt{gH}$ is used in the equation of Hunt [1959].

7.3. Results

Figures 7.2 and 7.3 show the calculated time-varying flotsam levels for respectively 11 January 2015 and 13 January 2017 for locations 1-4. In each figure the black line corresponds to the calculated wave run-up with the formula of Hunt [1959] (Eq. 2.14). The four coloured calculated lines were calculated using the wave run-up formulas as described in Sections 5.2.1 and 5.2.2: the continuous lines used the EurOtop [2016] formula (Eq. 2.15 and 2.16) and the dashed lines were calculated using the 'Delft' formula (Eq. 2.19). The flotsam model of IJnsen was applied with both the Rayleigh (green lines) and the Battjes-Groenendijk (blue lines) wave height distribution.

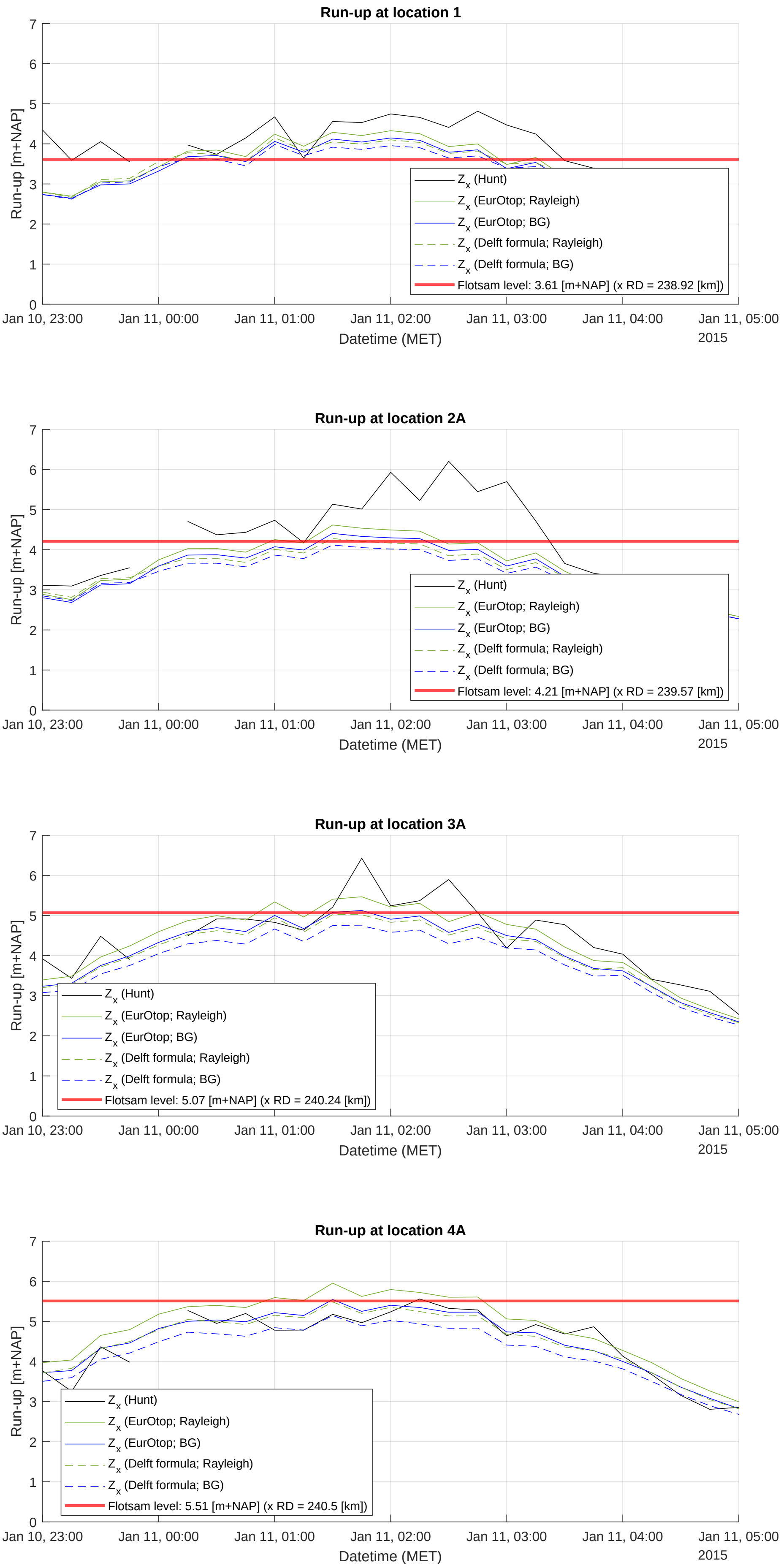

Figure 7.2: Calculated time-varying flotsam levels for 10/11 January 2015.

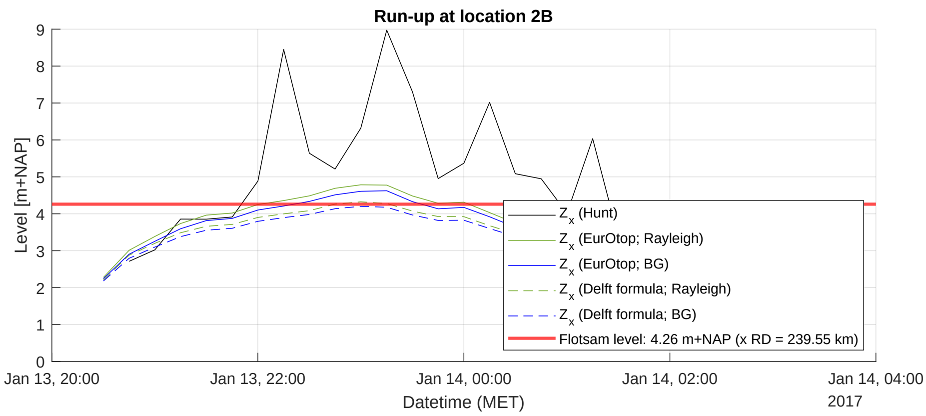

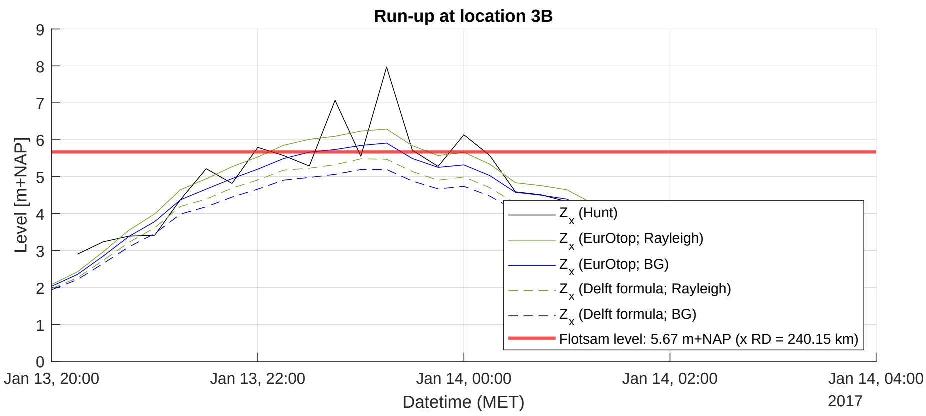

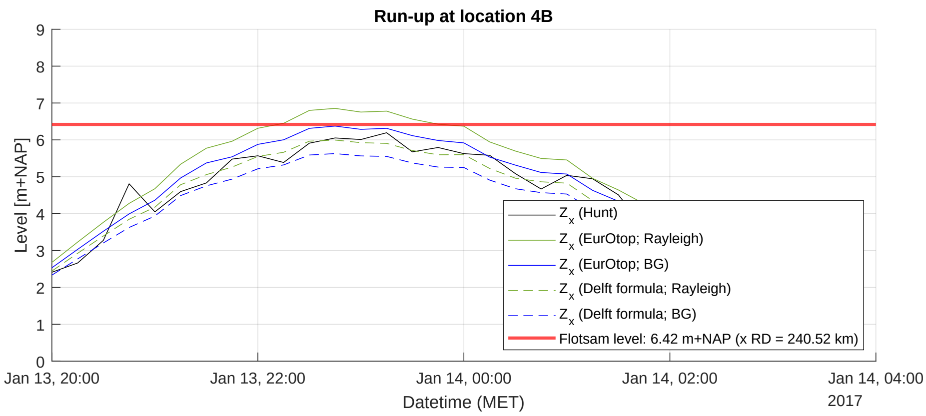

Figure 7.3: Calculated time-varying flotsam levels for 13/14 January 2017.

7.3.1. Measured data

Data from measurement locations 1-4 at the toe of the Emmapolderdike has been used to calculate flotsam levels. Measurement pole Uithuizerwad (UHW) is also located in the area of interest and was used as comparison to verify or to detect irregularities in the measurements. The measurement pole UHW is positioned 100 m seawards from the Emmapolderdike and 6 km Eastwards from measurements locations 1-4. In 2015 data at UHW was measured with an Etrometa stepgauge. For 2017 data was also measured with a Radac wave radar.

Appendix VI (2015) and VII (2017) are containing Figures VI.1 and VII.1. These figures represent the comparison between UHW and locations 1-4 for the spectral wave height H_{m0}, maximum wave height H_{max}, spectral wave periods $T_{\mathrm{m\text{-}1,0}}$ and T_{m02}. These figures show that:

- the effect of bed level and vegetation is visible. The spectral wave height, maximum wave height and spectral wave period T_{m02} were higher for locations with a lower bed level for both years;
- the spectral wave height $T_{\mathrm{m\text{-}1,0}}$ showed an opposite behaviour in both years: $T_{\mathrm{m\text{-}1,0}}$ increased with increasing bed level in 2015 (Figure VI.1d) and $T_{\mathrm{m\text{-}1,0}}$ decreased with increasing bed level in 2017 (Figure VII.1d).
- low spectral wave heights ($H_{\mathrm{m0}} < 0.35$ m) with high spectral wave periods ($T_{\mathrm{m\text{-}1,0}} \approx$ 10-20 s) were measured at location 2B in 2017.

In Appendix VI (2015) and VII (2017) Figures VI.4 and VII.4 are containing the following measured parameters:

(a) Spectral wave height, H_{m0} [m];

(b) Maximum wave height, H_{max} [m];

(c) Spectral wave period, $T_{\mathrm{m\text{-}1,0}}$ [s];

(d) Spectral wave period, T_{m02} [s];

(e) Spectral wave period, T_{m01} [s];

(f) T_{m01} over $T_{\mathrm{m\text{-}1,0}}$ ratio [-];

(g) Water level [m+NAP];

(h) Wave height over water depth ratio, H_{m0}/d [-].

The following observations can be made when analysing Figures VI.4 and VII.4:

- Spectral wave height H_{m0} and maximum wave height H_{max} were higher in 2017 than in 2015;
- All spectral wave periods ($T_{\mathrm{m\text{-}1,0}}$, T_{m01} and T_{m02}) were higher in 2017 than in 2015. $T_{\mathrm{m\text{-}1,0}}$ shows the largest increase and was in 2017 at least twice as large for locations 2-4 compared to 2015;
- The ratio $T_{\mathrm{m01}}/T_{\mathrm{m\text{-}1,0}}$ was lower in 2017 than in 2015. This is due to relative high values of $T_{\mathrm{m\text{-}1,0}}$ in 2017;
- Maximum water levels are 3.25 m+NAP and 3.28 m+NAP for 2015 and respectively 2017;
- Wave height H_{m0} over water depth ratios were lower in 2017 compared to 2015. At maximum water level, location 4A gives a ratio of 0.57 where location 4B gives a ratio of 0.42. The study of van der Westhuysen and de Waal [2008] showed that maximum ratios of H_{m0}/d in the Wadden Sea should be in the order of 0.43.

Based on Figures 7.2 and 7.3 and the above findings, the calculated flotsam lines using the measurements of BE-SAFE show that:

- two calculated time-varying levels gave at most locations the best approximation with respect to measured flotsam levels: the EurOtop [2016] formula together with an applied Battjes-Groenendijk wave height distribution (continuous blue line) and the 'Delft' formula together with an applied Rayleigh wave height distribution (dashed green line);
- the maximum value of calculated time-varying flotsam levels (EurOtop [2016] together with an applied Battjes-Groenendijk distribution) overestimated the measured flotsam levels with a maximum of 0.5 m and 0.3 m for respectively 2015 and 2017;
- the difference between EurOtop [2016] (continuous lines) and the 'Delft' formula (dashed lines) increased when moving away from the salt marsh;
- the applied formula of Hunt [1959], where the maximum of T$\sqrt{gH}$ in a 15-min interval was used as input, presented only for locations 4A and B a good approximation. This was caused by the obtained T$\sqrt{gH}$ from the zero-crossing analysis.

8
Discussion

The main objective of this study was to evaluate the (added) value of spatial information obtained from flotsam lines. It was investigated whether these lines can be used for improving predictions of hydraulic loads on coastal dikes in the future. This was done by first analysing studies about flotsam line measurements in the past and followed by a comparison between calculated flotsam lines and measured flotsam lines. By doing this comparison, it should became clear whether flotsam level measurements can be used to assess the quality of the models used by Rijkswaterstaat and if the spatial variations in flotsam level can give more insight in wave physics during storm conditions.

Flotsam line measurements in the past

Former studies of Sanders [1962], Niemeyer [1976], IJnsen [1983] and Grüne [2005] used flotsam lines to estimate the design wave run-up for the assessment of coastal dikes. Back then, wave run-up formulas were based on the ('Delft') formula $R_{u2\%} = 8 \cdot H_s \cdot \tan(\alpha)$. This formula was used for the design of dikes until 1980. Currently, the wave run-up is no longer used in the design or safety assessment of dikes and has been changed to allowable overtopping. However, wave run-up formulas provide still valuable information.

During this study, it was assumed that the maximum wave run-up is marked by the upper side of the flotsam line. Observations during the storm of 8 January 2019 confirm this. Also former studies, both in Germany (Niemeyer [1976]) as well as in the Netherlands (Sanders [1962] and IJnsen [1983]) stated that the flotsam levels represented the maximum wave run-up. However, the study of IJnsen [1983] determined a ratio of 1.4 between the maximum wave run-up and the 2% wave run-up on the dike of Ameland (Netherlands). On the other hand, Grüne [2005] used a ratio of 1.1 in his study. Both studies were based on the formula $R_{u2\%} = 8 \cdot H_s \cdot \tan(\alpha)$, but probably the difference in wave conditions played a role in determining the empirical ratio between the maximum and 2% wave run-up.

Comparison of measured flotsam lines

The comparison of measured flotsam lines showed a lot of variability. The flotsam lines of 13 January 2017 and 8 January 2019 have a similar pattern and differ from the line of 11 January 2015. The main reason for this is likely the wind direction of the storm. Both storms 2017 and 2019 had a NW/NNW wind direction during the peak of the storm, where the storm of 2015 was orientated mainly more western. This might explain the different patterns in flotsam levels between x RD = 240 and 245 km. The storm of 9 November 2007, not hindcasted in this study, had also a comparable pattern to the measured lines of 2017 and 2019. From Alkyon [2008] it follows that at the peak of the storm the wind direction was also orientated NW.

The measured lines between Lauwersoog and Eemshaven had two things in common: a steep increase in flotsam level at the edge of the salt marsh (x RD ≈ 240 km) and lower measured flotsam levels at locations were salt marshes are present (x RD = 220 - 239 km and x RD = 247 - 248 km). This shows that salt marsh height, width and vegetation have likely a reducing effect at flotsam levels at the dike. Findings in the studies of IJnsen [1983] and Vuik [2019] support this phenomenon.

Fieldwork findings and observations
During the storm of 8 January 2019 the interaction between wave run-up and flotsam was recorded and on 9 January 2019 flotsam line measurements have been performed. As discussed earlier in Section 4.3, it became clear that:

- the upper side of the flotsam line marked the highest occurred wave run-up (maximum wave run-up) in case of a small layer of flotsam. The observations and video recordings at 8 January 2019 showed that a relative thick layer of flotsam may disturb the final level of the flotsam line;
- a relative thick layer of flotsam was able to absorb the force of the wave run-up and remained in position. This means that the amount of flotsam can disturb the wave run-up and eventually flotsam levels. This effect can be seen in Figure 4.7a: here, differences in flotsam level and amount of flotsam were observed along the dike;
- water is the driving force in the final level of the flotsam line. The flotsam levels were not positioned higher than the wave run-up during the storm of 8 January 2019. In addition, the wind was unlikely to be responsible for the spatially varying pattern flotsam line along the dike. Perhaps, the wind was able to relocated small pieces of flotsam into a higher position, but it seems unlikely that it was responsible for the occurring patterns along the dike (e.g Figure 3.11)

Calculated flotsam lines with SWAN
Flotsam lines were calculated for three different storms (11 January 2015, 13 January 2017 and 8 January 2019). This was done, by following a sequence of models and formulas (Figure 5.2), to investigate whether measured flotsam lines can be used to asses the quality of certain models, such as SWAN. All components (wind model, hydrodynamic model, wave model, etc) of this sequence were used and analysed as explained in Section 5.6. The EurOtop [2016] (Eq. 2.15 and 2.16) formula and the 'Delft' formula (Eq. 2.19) for wave run-up were used to calculate the 2% run-up. Followed by a calculation with the flotsam model of IJnsen which was applied with a Rayleigh and a Battjes-Groenendijk wave height distribution to calculated flotsam levels. By analysing the calculated and measured flotsam lines and by performing a systematic comparison between model and measured data it becomes clear that:

- all calculated flotsam lines were overestimating the measured lines between x RD = 220 - 239 km. The calculated lines with EurOtop [2016] formula showed significant higher levels (+0.5 m) in 2015 than the calculated lines with EurOtop [2016] formula in 2017 and 2019 between x RD = 220 - 239 km. This is caused mainly by higher computed wave periods $T_{\text{m-1,0}}$ by SWAN for 11 January 2015;
- it seems that the applied 2% wave run-up formula had a significant influence on the calculated flotsam levels. The currently used EurOtop [2016] formula for wave run-up calculated significantly higher flotsam levels between x RD = 240 and 245 km than the 'Delft' formula. The largest deviation (+1.5 m) occurred for the hindcast of 2015. The calculated flotsam lines of 2017 and 2019 showed deviations of +1.0 m. These deviations were mainly the reason of assumed wave conditions ($s_{\text{m-1,0}} \approx 0.04$) in the 'Delft' formula. Instead, the wave period ($T_{\text{m-1,0}}$) and thus the wave steepness is a variable in the EurOtop [2016] formula. Figures 6.1, 6.2 and 6.3 show the same calculated levels, regardless of the used formula (EurOtop [2016] or 'Delft' formula) for a wave steepness of $s_{\text{m-1,0}} \approx 0.04$ (Figure 6.7).
- the highest measured flotsam levels (5.5 - 6.5 m+NAP) for 2017 and 2019 were well approximated by two lines: the 'Delft' formula together with an applied Rayleigh wave height distribution (dashed green line) and the EurOtop [2016] formula together with an applied Battjes-Groenendijk wave height distribution (continuous blue line);
- by comparing modelled data and measurements for wind, water level and waves it is shown that in this part (wind, hydrodynamic and wave model) of the set of models and formulas, the largest deviations were found in the wave conditions (Table 6.10) calculated by SWAN. The calculated wave parameters at Uithuizerwad overestimated the measurements for all three storms. This means that the calculated lines should be lower than the current calculated lines. The largest deviations occurred for the flotsam

line of 2015: modelled $T_{\text{m-1,0}}$ and H_{m0} were respectively 1.5 s and 0.5 m higher than the measurements. However, the measured wave heights for 11 January 2015 cannot be validated (Table 6.10). The measurement device (Etrometa stepgauge) had possibly the same malfunction as expected at the peak of the storm of 8 January 2019;

- an applied Rayleigh wave height distribution leads to a higher calculated flotsam line (+0.3 to +0.5 m) than an applied Battjes-Groenendijk distribution. The largest differences occurred where lower bottom levels are situated (x RD = 240 - 245 km). However, due to the vertical variability in flotsam level (±0.5 m) it can not be determined that the Battjes Groenendijk distribution leads to a better agreement with measured flotsam levels which was suggested by Witteveen+Bos [2010];
- that the measured flotsam levels (2015 and 2019) were lower at locations with salt marshes (x RD = 220 - 239 km and x RD = 247 - 248 km) compared to the calculated lines, even regardless the applied wave run-up formula or wave height distribution. The amount of flotsam plays a role in the final height of the flotsam lines as discussed in Section 4.3. This might be a reason for the overestimation of flotsam levels between x RD = 220 - 239 km and x RD = 247 - 248 km.

Calculated flotsam levels with measurements BE-SAFE
Flotsam levels were also calculated by using measured wave records instead of computed wave conditions by stationary SWAN runs. The project BE-SAFE performed measurements in 2015 and 2017 at four locations (Figure 7.1) at the salt marsh edge (x RD ≈ 240 km) between Lauwersoog and Eemshaven. These measurements have been used to calculate time-varying flotsam levels for 11 January 2015 and 13 January 2017. This means that only the last two bullets of the method as described in Section 5.2 were performed to calculate the flotsam levels for the four locations (Figures 7.2 and 7.3).

In addition to the EurOtop [2016] and 'Delft' formula, the wave run-up formula (Eq. 2.14) of Hunt [1959] was used to calculate flotsam levels. The wave run-up formula of Hunt [1959] used the maximum of $\mathrm{T}\sqrt{gH}$ in a 15-min interval which was obtained by performing a zero crossing analysis on the measured wave records. Wave parameters H_{m0} and $T_{\text{m-1,0}}$ were obtained by a performed spectral analysis on the same measured wave records. These parameters (15-min interval) served as input for the EurOtop [2016] formula and 'Delft' formula.

The general trend is that two calculated time-varying levels approximated the measured flotsam levels at most locations quite well: the EurOtop [2016] formula together with an applied Battjes-Groenendijk wave height distribution (continuous blue line) and the 'Delft' formula together with an applied Rayleigh wave height distribution (dashed green line).

The maximum value of calculated time-varying flotsam levels using the EurOtop [2016] formula together with an applied Battjes-Groenendijk wave height distribution (continuous blue line) were in better agreement with measured flotsam levels than the calculated levels, considered at the same four locations, based on computed wave conditions by SWAN. The calculated levels, based on computed wave conditions by SWAN, overestimated the measured flotsam levels with a maximum of 1.5 m and 1.2 m for 2015 and 2017 respectively. Whereas the calculated levels, based on measured wave conditions, differences up to +0.5 m and +0.3 m for respectively 2015 and 2017 occurred.

9 Conclusions and recommendations

The objective of this study was to gain more insight in the (added) value obtained from flotsam lines and by doing so, investigate whether flotsam levels can be used to improve models, such as SWAN. In this chapter the conclusions of this study are presented by means of answering the research questions posed in Chapter 1. The subquestions are answered first. Hereafter, the main question is answered.

At the start of this study four research subquestions were formulated:

1. **How was the obtained information from flotsam lines used in the past**
   The spatial information obtained from flotsam lines in the past was mainly used for design purposes and to perform safety assessments at coastal dikes. This was done by applying an extrapolation method on the measured flotsam levels to gain insight in wave run-up or wave parameters at a design water level. It can be concluded that it was not only studied in the Netherlands (Sanders [1962] and IJnsen [1983]), but also in Germany flotsam lines (in German: Teekgrenzen) were used in different studies (Niemeyer et al. [1995] and Grüne [2005]). Niemeyer et al. [1995] mentioned that the idea of measuring flotsam lines was already recommended by the coastal engineer Brahms in 1754.

2. **How can flotsam lines be used to assess the quality of the models used by Rijkswaterstaat?**
   It can be concluded that not one of the calculated flotsam lines, based on computed wave conditions by SWAN, approximated the entire measured flotsam line. However, two lines were able to approximate the highest measured flotsam levels (5.5 - 6.5 m+NAP) quite well: the EurOtop [2016] and 'Delft' formula together with an applied Battjes-Groenendijk and Rayleigh wave height distribution respectively in the flotsam model of IJnsen. Nevertheless, the EurOtop [2016] formula tends to overestimate the measured flotsam lines. Based on the systematic comparison between modelled and measured data (wind, water level and wave conditions), it was determined that modelled wave conditions at Uithuizerwad overestimated significantly the measurements. This means that the used method (Section 5.6) gives an indication of the performance of the applied set of models and formulas.

   The calculated flotsam lines of Witteveen+Bos [2010] showed also differences with measured lines: the calculated lines overestimated the measured lines (+0.6 to +1.5 m) between x RD = 210 and 235 km and underestimated the measured lines (-1.4 m) between x RD = 235 and 245 km. They concluded that this was likely caused by the translation of spectral wave results to wave run-up/flotsam levels. In this study the calculated lines (EurOtop [2016]), based on computed wave conditions by SWAN, tend to overestimate the measured flotsam lines for the entire trajectory (x RD = 220 - 250 km). However, overestimated wave conditions by SWAN have feed through into the flotsam level calculations. In addition, calculated flotsam levels (EurOtop [2016] and an applied Battjes-Groenendijk distribution) at four locations (Figure 7.1), based on the measurements of BE-SAFE at the toe of the dike, resulted in smaller overestimations (up to +0.5 m) than the overestimations (up to +1.5 m) based on computed wave conditions by SWAN. Furthermore, the applied wave height distribution (Battjes-Groenendijk) results only in 0.3 to 0.5 m lower lines than calculated lines with an applied Rayleigh distribution. This means that the overestimation is caused primarily by the computation of spectral wave parameters. This contradicts the findings of Witteveen+Bos [2010]. Witteveen+Bos [2010] concluded that the difference between calculated and measured lines was caused primarily by the translation of spectral wave results to wave run-up/flotsam levels which was expected to be caused by the applied wave heigh distribution.

The calculated pattern obtained by the applied set of models and formulas showed the same features as the measured flotsam lines. This means that the calculated flotsam levels can serve as an useful indicator of local wave conditions, when applying the used set of models and formulas in this study. Taking into account the model/formulas and flotsam level (± 0.5 m) uncertainties, it becomes clear that flotsam lines cannot be used to calibrate the models used by Rijkswaterstaat such as SWAN and WAQUA. However, flotsam lines may show variations in wave conditions which are not modelled.

3. **How can the obtained information from flotsam levels give more insight in wave physics during storm conditions?**
The information obtained from flotsam lines is the spatial variability of the flotsam height above NAP along a dike. Flotsam level measurements may indicate unexpected behaviour of waves and water level at certain locations. However, multiple factors play a role in this: the width, height and vegetation of a salt marsh, water level and wave conditions and the amount of flotsam. It seems that if a large database of detailed flotsam lines with corresponding storm conditions (water level, wave conditions, wind, etc) is organized, it is possible to detect (recurring) spatial variations which might give more insight in certain processes during storm conditions.

4. **In which way should flotsam lines be measured to obtain useful information?**
The inventory of flotsam lines (Table 3.1) exists of multiple measured unique flotsam lines. In the past, flotsam lines were measured if there was a specific reason to measure them. However, there are no guidelines to measure flotsam levels in a structured way after a storm to obtain useful information from them. Based on this study it becomes clear that the alongshore variation of the flotsam levels in [m+NAP] provides very useful information. However, this holds that the density of measurement points should be high enough to map the alongshore variation (x,y,z). Observations and recordings have shown that:

    - the upper side of the flotsam line marked the maximum wave run-up. This means that the upper side of the flotsam line should be measured. This is also in consistency with the previously measured flotsam lines (Table 3.1);
    - a relative thick layer of flotsam was able to absorb the force of the wave run-up and remained in position. This means that the amount of flotsam can disturb the wave run-up and eventually flotsam levels. This holds that also the amount of flotsam (depth and width) should be measured and attached to each measured flotsam level.

   In addition to measured flotsam lines, predicted and measured data (wind, water level, wave conditions, etc) of corresponding storm events should be stored for each measured flotsam line. Not only predicted and measured time series, but also predicted 2D field data of wind, water level, currents and wave conditions are of great value and should be stored. All these data and measured flotsam lines should always be accessible. Such that flotsam level calculations, following the method (Section 5.6) of this study, of important storm dates can be performed in the future.

The main question is:

How can flotsam lines be used in the safety assessment of flood defences?
The information obtained from flotsam levels gives an indication of the hydraulic loads along a dike. This study showed that the upper side of the flotsam line marked the maximum wave run-up in case of a small layer of flotsam. Besides, a relative thick layer of flotsam was able to absorb the force of the wave run-up and remained in position. This means that the amount of flotsam can disturb the wave run-up and eventually flotsam levels. It also was determined that the analysis of (calculated) flotsam lines gives an indication of the performance of the applied set of models (SWAN and WAQUA) and wave run-up formulas, provided that a systematic comparison between modelled and measured data is performed. A large database of detailed flotsam lines with corresponding storm conditions (water level, wave conditions, wind, etc) can provide valuable information to low costs. This database can be used to detect spatial variations which might give more

insight in certain processes during storm conditions. It may also serve as the starting point for follow-up studies using new methods for analysing flotsam lines.

Recommendations

The following recommendations are based on the study findings and experiences while performing this study:

1. Having more data (predicted 2D water level and current fields) of the 1 November 2006 and 9 November 2007 storms available at MATROOS, could have added a lot of value to this study. The conditions during these storms were a lot heavier compared to the hindcasted storms (2015, 2017 and 2019) in this study. However, data in MATROOS is automatically deleted after 10 years and data of such important/major storm events (November 2006 and 9 November 2007) should always be accessible for research in the future;

2. It would be very interesting to investigate the interaction between flotsam line and wave run-up in an experimental facility. Observations showed that the flotsam line, at the parts with relatively more flotsam, was able to remain at those position under the force of the wave run-up tongue. Therefore it is interesting to investigate the wave energy absorbing property of the flotsam line;

3. Niemeyer et al. [1995] mentioned that parts of the flotsam line were blown higher onto the dike by wind. The wind seems unlikely to be responsible for the spatially varying patterns in flotsam line along the dike. Perhaps, the wind is able to relocated small pieces of flotsam into a higher position, but it seems unlikely that it can be responsible for the large-scale occurring patterns along the dike. Nevertheless, it is interesting to investigate the influence of wind on flotsam levels in an experimental facility under storm conditions;

4. Regional water authority Noorderzijlvest is performing field measurements at its coastal dikes with the aim to use the gathered data to improve or validate the used models for dike design. These measurements are performed in the context of the project Meerjarige Veldmetingen Eems-Dollard for the coming 12 years in the estuary Eems-Dollard. In addition to their planned measurements at Uithuizerwad, they should definitely investigate the development of flotsam lines during storm conditions. IJnsen [1983] and Grüne [2005] are based on an old wave run-up formula ($R_{u2\%} = 8 \cdot H_{m0} \cdot \tan(\alpha)$). It would therefore be of great value to investigate the relation between the EurOtop [2016] wave run-up formulas and flotsam level (maximum wave run-up).

5. Performing quality checks on the measured wave conditions at measurement pole Uithuizerwad if these measurements are used. The reason for this is the probable malfunction of the Etrometa step-gauge during the storms of 11 January 2015 and 8 January 2019.

6. Enlarging the used database of flotsam lines in this study for all coastal dikes around the Wadden Sea in the future. It should also be extended to other areas where flotsam can be transported onto (coastal) dikes such as Zeeland or the IJsselmeer (Lake IJssel). A proposed guideline to measure flotsam levels is elaborated below.

Finally, based on this study and previous recommendations the following guidelines are composed to provide useful information obtained from flotsam lines in the future:

- Flotsam levels [m+NAP] should be measured from the upper side of the flotsam to be consistent with already measured flotsam lines;

- In addition to each flotsam measurement point (x,y,z), the amount of flotsam (depth and width) should be measured and attached to each measured flotsam level;

- Measure with an interval of 100 m to map the alongshore spatial variability. In this interval the highest and lowest flotsam level of the highest flotsam line should be measured in order to obtain the bandwidth of the measured line;

- The flotsam level measurements are recommended to be performed with a GPS mounted on a quad or car to increase the speed of measuring flotsam levels;

- (Aerial) recordings of the flotsam line should be made to check the measurements or to serve as a backup;
- All 'raw' measured data (flotsam location, level, depth and width) and possibly corresponding remarks should be registered (database for flotsam lines) and reported in a structured way;
- Predicted and measured time series, but also predicted 2D field data of wind, water level, currents and wave conditions are of great value and should be stored. All these data and measured flotsam lines should always be accessible, especially data of important/major storm events.

In the future, also the possibility to use LIDAR technology to obtain flotsam levels [m+NAP] might be used. Another possible method is to use a specific computer model, which is able to obtain flotsam levels from performed recordings (photographs and videos). Both methods will probably increase the quality of the measured flotsam line.

Bibliography

Alkyon. SWAN hindcast in the Eastern Wadden Sea and Eems-Dollard estuary: storm of 9 November 2007. Technical report, 2008.

J.A. Battjes. Golfoploop en golfoverslag. Technische Adviescommissie voor de Waterkeringen, 1972.

J.A. Battjes. Computation of set-up, longshore currents, run-up and overtopping due to wind-generated waves. *Phd thesis*, 1974.

J.A. Battjes and H.W. Groenendijk. Wave height distributions on shallow foreshores. *Coastal Engineering*, 40 (3):161–182, 2000.

J.A Battjes and J.P.F.M. Janssen. Energy loss and set-up due to breaking of random waves. *Proc. 16th International Conference on Coastal Engineering*, pages 569–588, 1978.

J.H. de Reus. Reactie op het rapport: Analyse van vloedmerkwaarnemingen op de dijk onder Hollum op Ameland. (83), 1983.

ENW. Grondslagen voor hoogwater- bescherming. page 83, 2017.

EurOtop. EurOtop - Manual on wave overtopping of sea defences and related structures. page 252, 2016.

J. Grüne. Evaluation of wave climate parameters from benchmarking flotsam levels. *International Conference on Coastlines*, pages 1–10, 2005.

J. Grüne and Z. Wang. Wave Run – up on sloping seadykes and revetments. *Proc. 27th International Conference on Coastlines Engineering (ICCE)*, III(July):2044–2057, 2000.

L.H. Holthuijsen. *Waves in Oceanic and Coastal Waters*. Cambridge University Press, 2007.

I.A. Hunt. Design of seawalls and breakwaters. *Journal of the Waterways and Harbors Division*, 85(3):123–152, 1959.

F. IJnsen. Analyse van vloedwaarnemingen op de dijk onder Hollum op Ameland. Technical report, 1983.

S.N. Jonkman, T. Schweckendiek, R.E. Jorissen, and J.P. van den Bos. Flood Defences - Lecture notes CIE5314. Technical report, Department of Hydraulic Engineering Faculty of Civil Engineering and Geoschiences, 2018.

KNMI. Windklimaat van Nederland. pages 1–261, 1983.

B. Le Méhauté. *An Introduction to Hydrodynamics & Water Waves*. Springer, 1976.

M.S. Lonquet-Higgins. On the Statistical Distribution of the Heights of Sea waves.pdf. *Journal of Marine Research*, 11(3), 1952.

H.D. Niemeyer. Zur Abschätzung des maximalen Wellenauflaufs an Seedeichen aus der Einmessung von Teekgrenzen. *Die Küste, H.29.*, 1976.

H.D. Niemeyer, R. Kaiser, K.H. Peters, and O. Schneider. The estimation of design wave run-up on sea dykes in consideration of overtopping security. pages 1–12, 1995.

H.D. Niemeyer, R. Kaiser, J. Gärtner, K.H. Peters, and O. Schneider. Verifikation des Extrapolationsverfahrens zur Ermittlung des Bemessungswellenauflaufs aus der Einmessung von Teekgrenzen. 1999.

Rijkswaterstaat and Deltares. Modelbeschrijving Zuidelijke Noordzee Model (ZUNO). page 2, 2009a.

Rijkswaterstaat and Deltares. Modelbeschrijving Kuststrook-fijn Model. page 2, 2009b.

Rijkswaterstaat and Deltares. Modelbeschrijving Dutch Continental Shelf Model (DCSM). page 2, 2009c.

P. Sanders. De golfoploop tegen en de golfoverslag over de Emmapolderdijk. 1962.

G.J. Schiereck and H.J. Verhagen. *Introduction to Bed, bank and shore protection. Engineering the interface of soil and water*. Delft Academic Press / VSSD, 2016.

Svašek Hydraulics/ HKV. Productieberekeningen Waddenzee voor WTI-2011 : rapportage fase 1. 2011.

A .J. van der Westhuysen and J.P. de Waal. Observed finite depth wave growth limit in the Wadden Sea: SBW Wadden Sea. page 129 pp., 2008.

G.Ph. van Vledder, G. Ruessink, and D.P. Rijnsdorp. Individual wave height distributions in the coastal zone: Measurements and simulations and the effect of directional spreading. *Coastal Dynamics*, (229), 2013.

V. Vuik. *Building Safety with Nature - Salt marshes for flood risk reduction*. PhD thesis, 2019.

Waterwet. Waterwet. 2009. URL https://wetten.overheid.nl/BWBR0025458/2018-07-01.

Witteveen+Bos. Hindcast of the flotsam levels of the 1 November 2006 storm in the Eastern Wadden Sea. Technical Report November, 2010.

Inventory of flotsam lines

In this appendix an extended overview of measured flotsam line inventory is given. This appendix exists of the following flotsam line measurements:

- Period between 1958 and 1971
- 1 November 2006
- 9 November 2007
- 5 and 6 December 2013
- 11 January 2015
- 13 January 2017
- 8 January 2019

I.1. Period between 1958 - 1971

Measured flotsam lines obtained from Sanders [1962] are digitalised with help of the program 'Engauge Digitizer'. The data is stored in several Excel files. In Table I.1 a summary of corresponding properties and occurred conditions for each storm is shown.

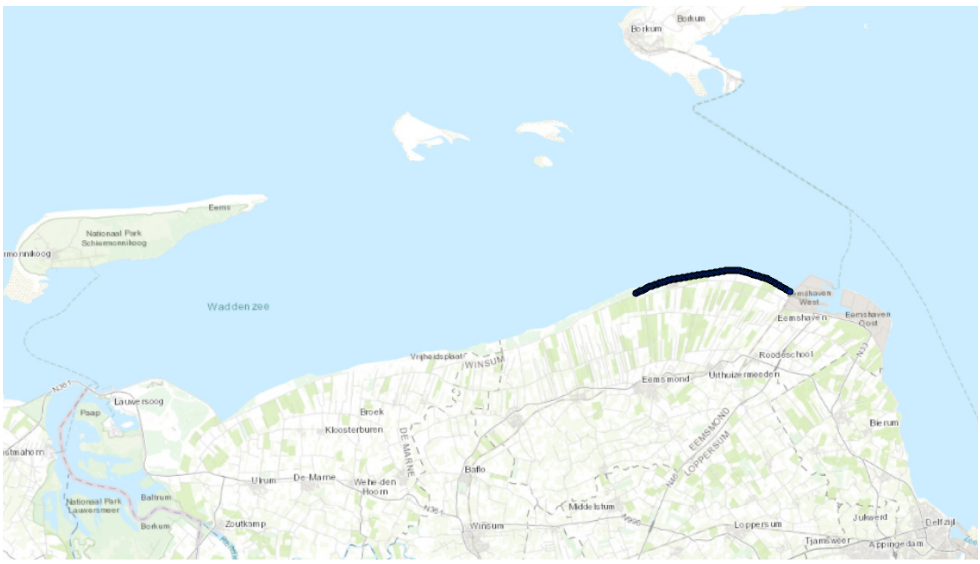

Figure I.1: Flotsam line trajectory corresponding to the high waters of the period between 1958 - 1971

Table I.1: Properties of flotsam lines Sanders [1962]

Date	Highest flotsam level [m+NAP]	Location (x-axis) highest flotsam level	Measurements	Mean	Std	Wind speed [m/s]	Wind direction [°]	Highest water level [m+NAP]	Location highest water level
10-1-1958	5.75	77.26	35	4.92	0.42	8.9	NW	2.84	Oostmahorn
17-10-1958	4.39	59.87	15	3.92	0.367	14.8	NW	2.53	Oostmahorn
2/3-1-1959	4.71	77.22	18	3.89	0.43	11.7	WNW	2.58	Oostmahorn
20-1-1960	4.62/4.61	61.32/76.97	11	3.93	0.41	17.5	NW	2.41	Oostmahorn
20/21-3-1961	5.52	30.87	109	4.79	0.31	18.2	NW	2.90	Oostmahorn
18-10-1961	4.40	59.73	149	4.08	0.43	16.6	NW	2.27	Oostmahorn
6-12-1961	5.13	60.63	38	4.25	0.36	14.8	W	2.63	Oostmahorn
13-2-1962	5.68	60.13	92	4.52	0.45	9.1	W	2.4	Oostmahorn
14-10-1963	5.54	48.00	93	4.66	0.49	16.8	NW	2.65	Oostmahorn
17-11-1964	5.32	76.13	65	4.59	0.46	13.6	WNW	2.57	Oostmahorn
3/4-12-1964	5.65	43.24	91	4.84	0.45	13.9	NW	2.95	Zoutkamp
13-2-1965	6.15	45.05	94	5.20	0.43	15.3	WNW	2.81	Oostmahorn
2-11-1965	5.57	35.99	95	4.76	0.39	17.1	WZW	2.6	Oostmahorn
10/11-12-1965	5.95	75.59	116	4.99	0.41	14.9	WNW	2.84	Oostmahorn
30-11-1966	5.91	76.13	108	4.95	0.40	16.1	W	2.78	Oostmahorn
23-2-1967	6.38	43.92	101	5.60	0.48	18.4	W	3.09	Oostmahorn
1-3-1967	6.36	47.29	87	5.54	0.36	16.2	W	2.96	Oostmahorn
4-12-1967	5.66	47.0	95	4.65	0.43	12.4	NW	2.62	Oostmahorn
28/29-11-1969	5.64	42.11	117	4.85	0.37	16.4	NW	2.7 2.84	Lauwersoog Oude Westereems
3/4-11-1970	6.14	46.88	91	4.96	0.42	17.4	W	2.9	Oude Westereems
9-11-1970	5.74	45.18	79	4.79	0.47	16.9	W	2.82	Oude Westereems
21-11-1971	5.43	86.30	74	4.87	0.31	17.0	N	2.79	Oude Westereems

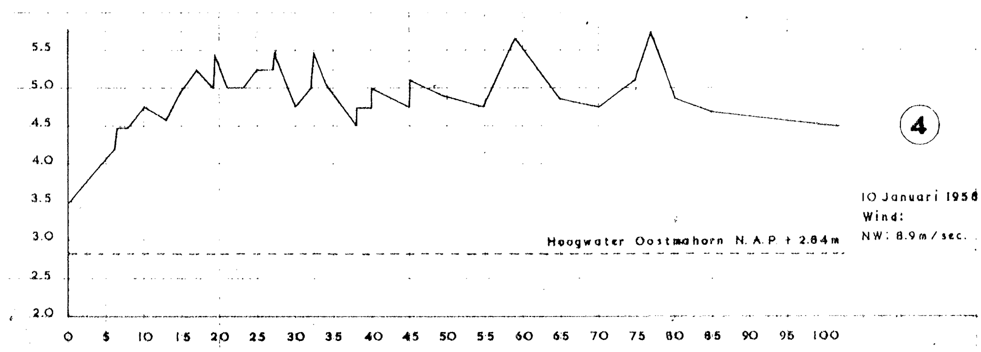

Figure I.2: Flotsam line of 10 January 1958 [Sanders, 1962]

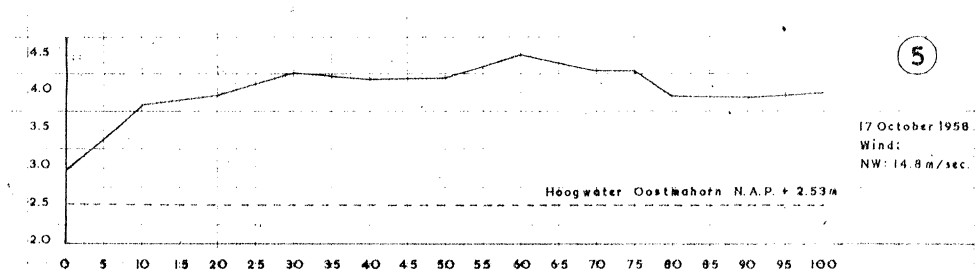

Figure I.3: Flotsam line of 17 October 1958 [Sanders, 1962]

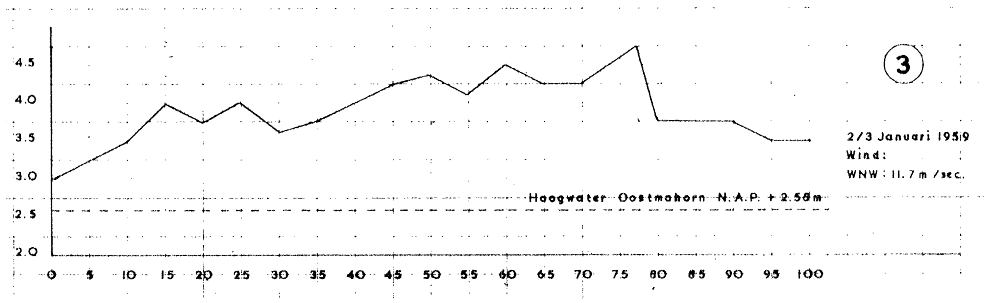

Figure I.4: Flotsam line of 2/3 January 1959 [Sanders, 1962]

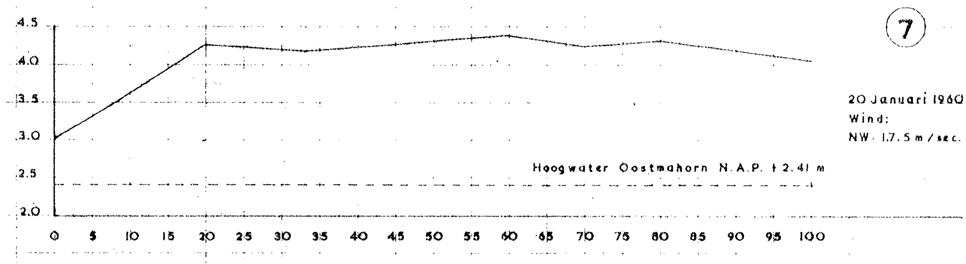

Figure I.5: Flotsam line of 20 January 1960 [Sanders, 1962]

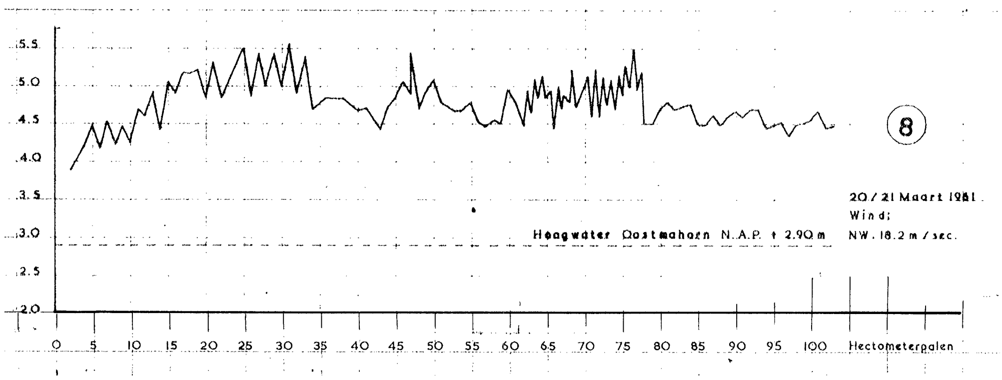

Figure I.6: Flotsam line of 20/21 March 1961 [Sanders, 1962]

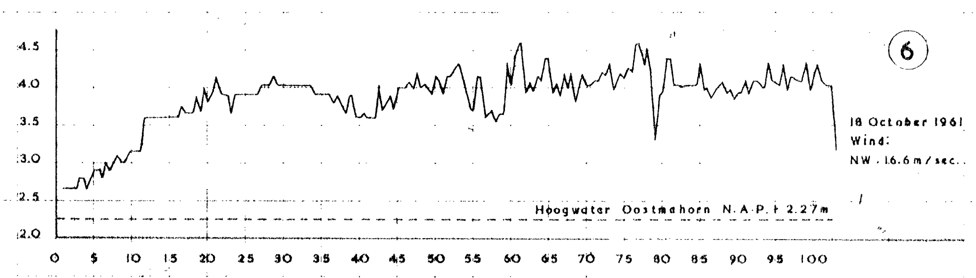

Figure I.7: Flotsam line of 18 October 1961 [Sanders, 1962]

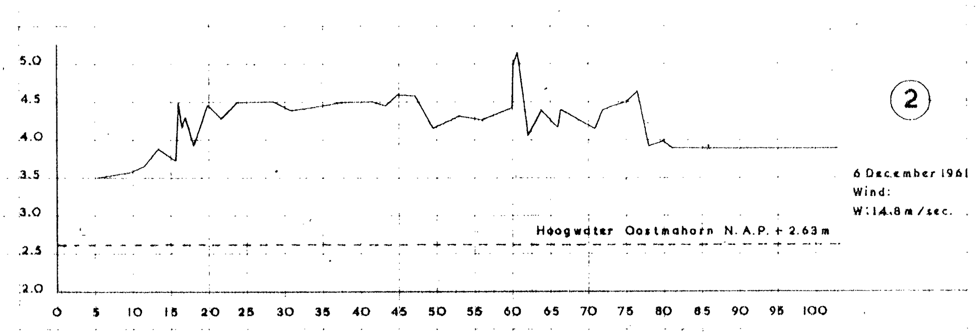

Figure I.8: Flotsam line of 6 December 1961 [Sanders, 1962]

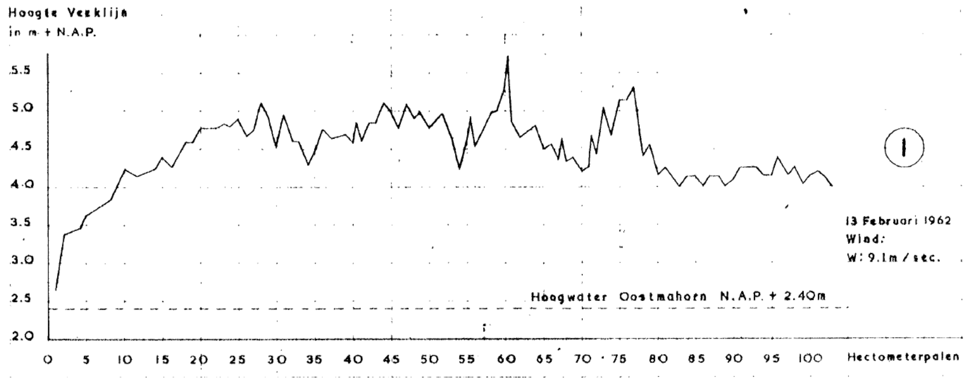

Figure I.9: Flotsam line of 13 February 1962 [Sanders, 1962]

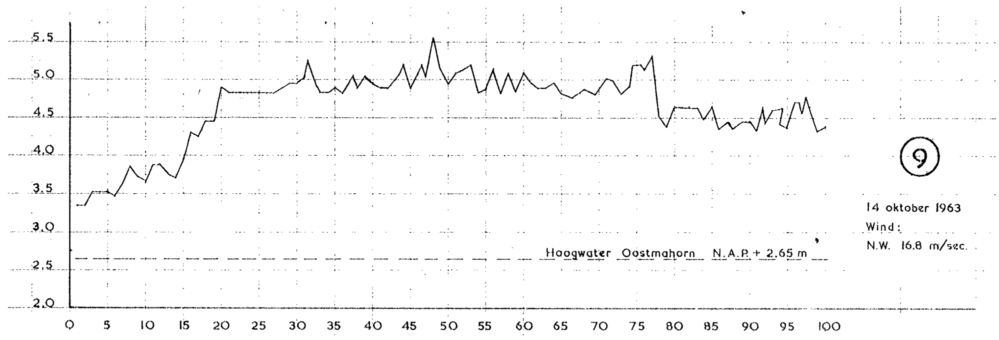

Figure I.10: Flotsam line of 14 October 1963 [Sanders, 1962]

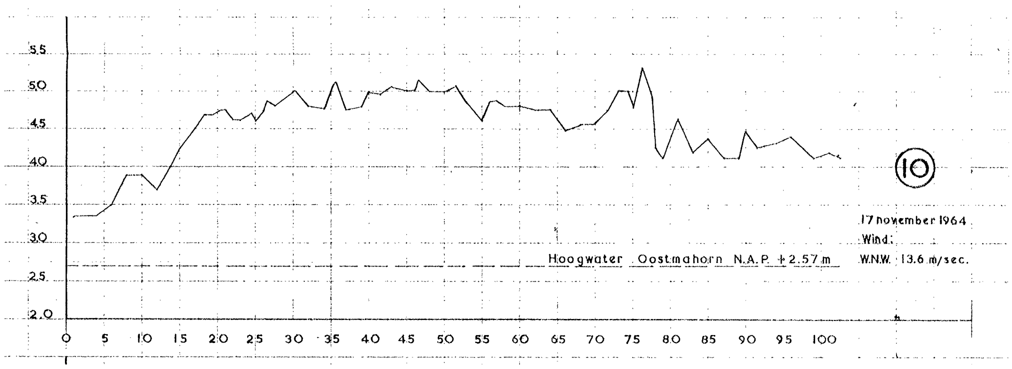

Figure I.11: Flotsam line of 17 November 1964 [Sanders, 1962]

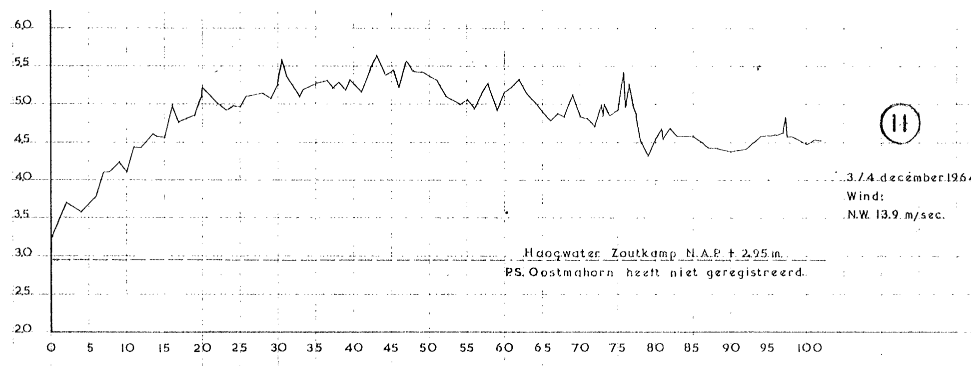

Figure I.12: Flotsam line of 3/4 December 1964 [Sanders, 1962]

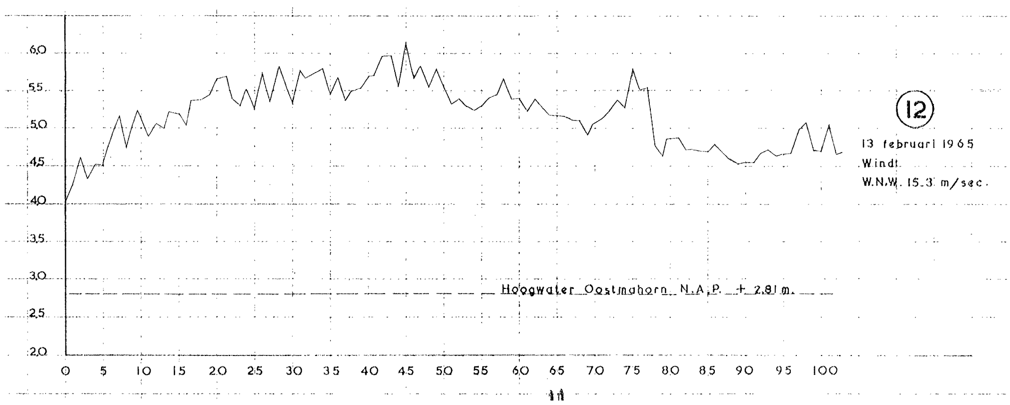

Figure I.13: Flotsam line of 13 February 1965 [Sanders, 1962]

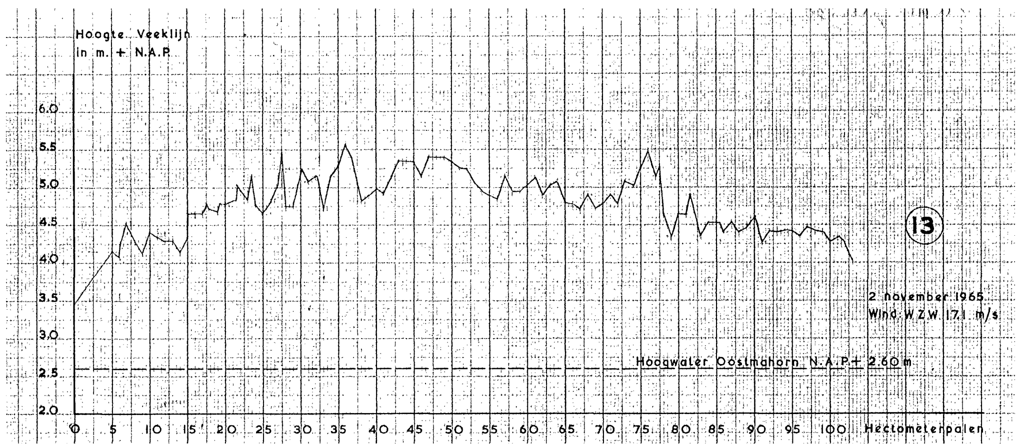

Figure I.14: Flotsam line of 2 November 1965 [Sanders, 1962]

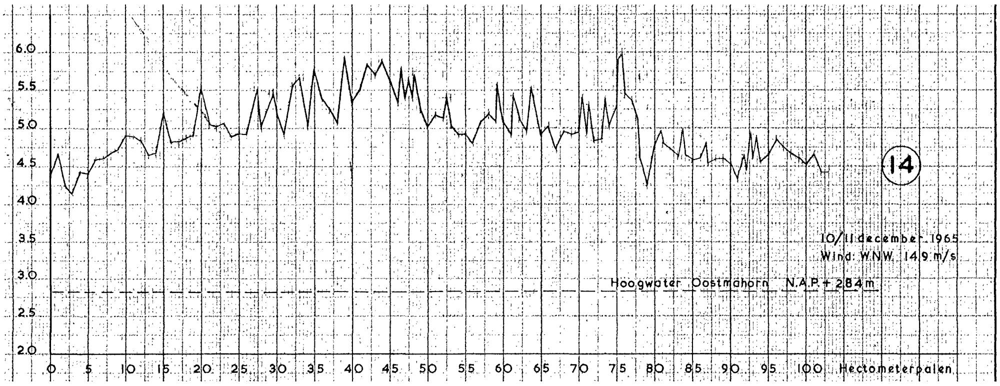

Figure I.15: Flotsam line of 10/11 December 1965 [Sanders, 1962]

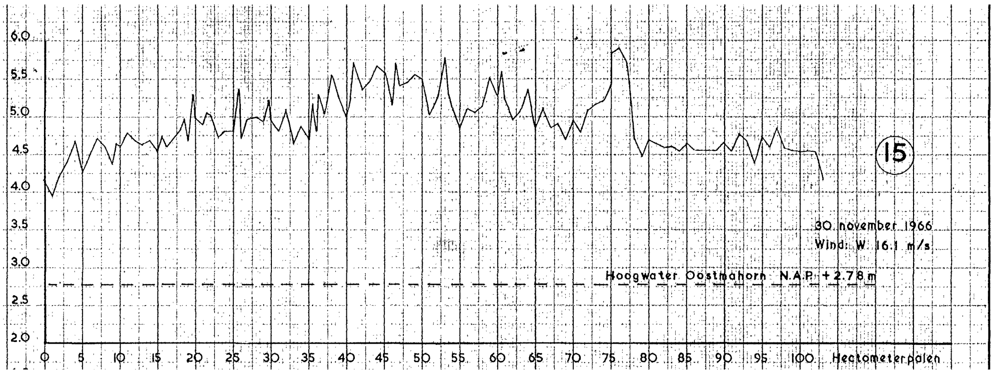

Figure I.16: Flotsam line of 30 November 1966 [Sanders, 1962]

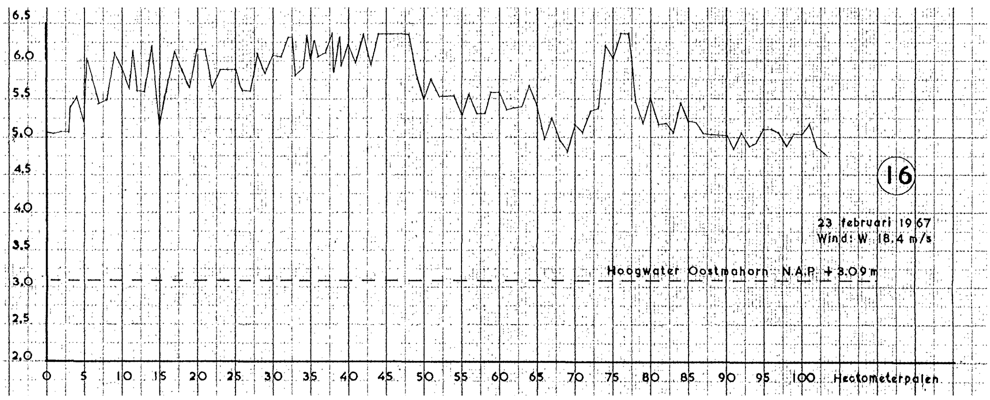

Figure I.17: Flotsam line of 23 February 1967 [Sanders, 1962]

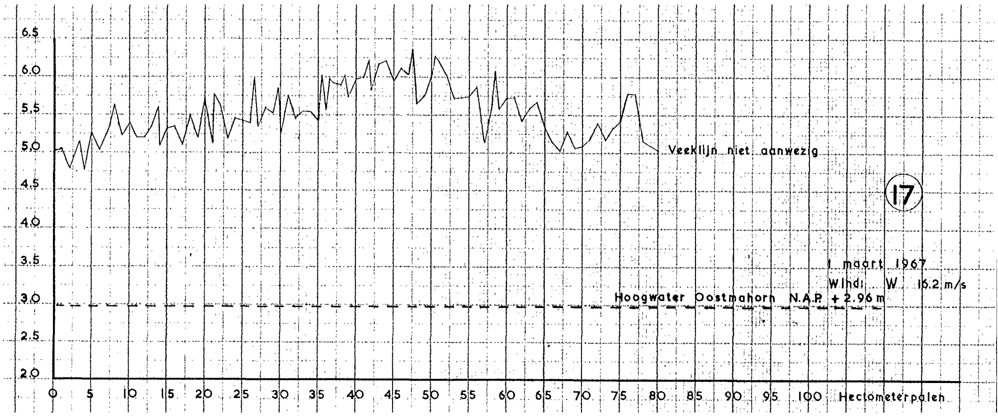

Figure I.18: Flotsam line of 1 March 1967 [Sanders, 1962]

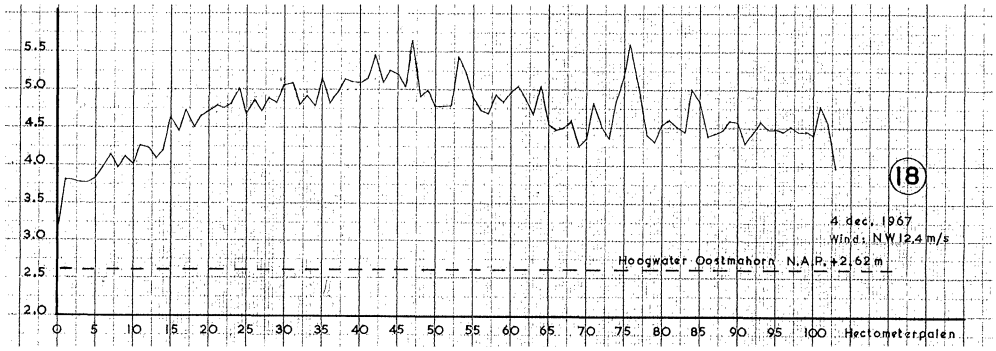

Figure I.19: Flotsam line of 4 December 1967 [Sanders, 1962]

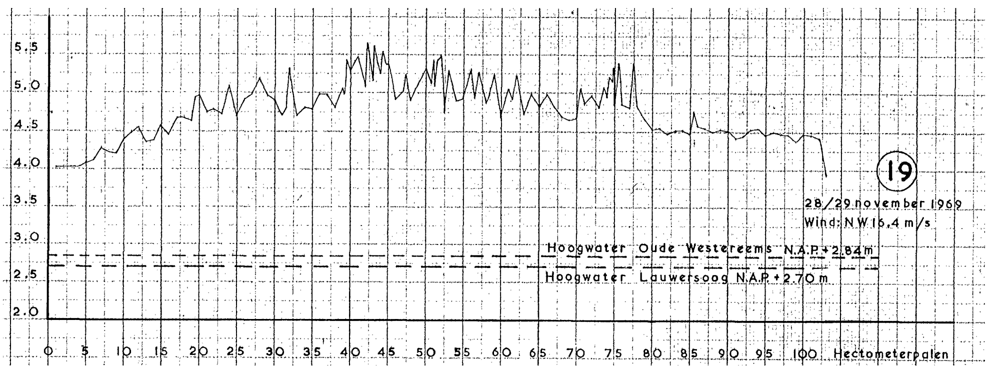

Figure I.20: Flotsam line of 28/29 November 1969 [Sanders, 1962]

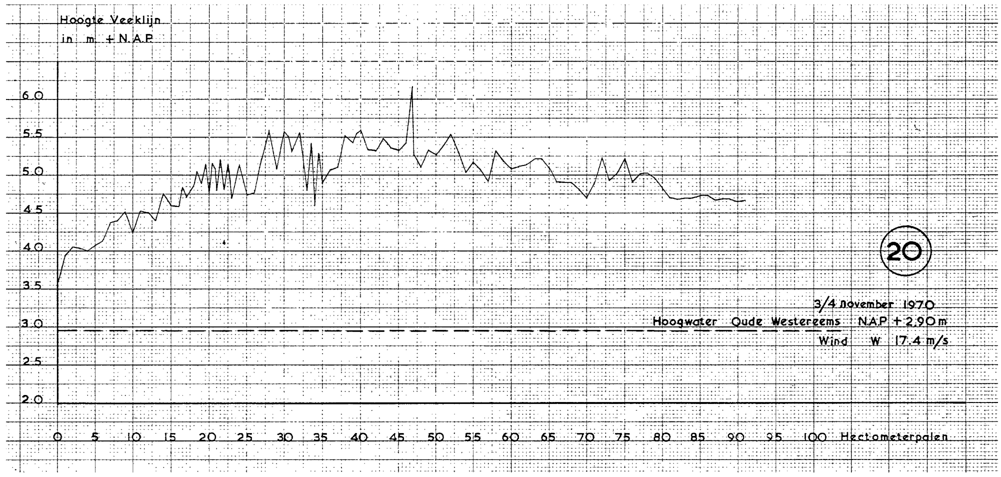

Figure I.21: Flotsam line of 3/4 November 1970 [Sanders, 1962]

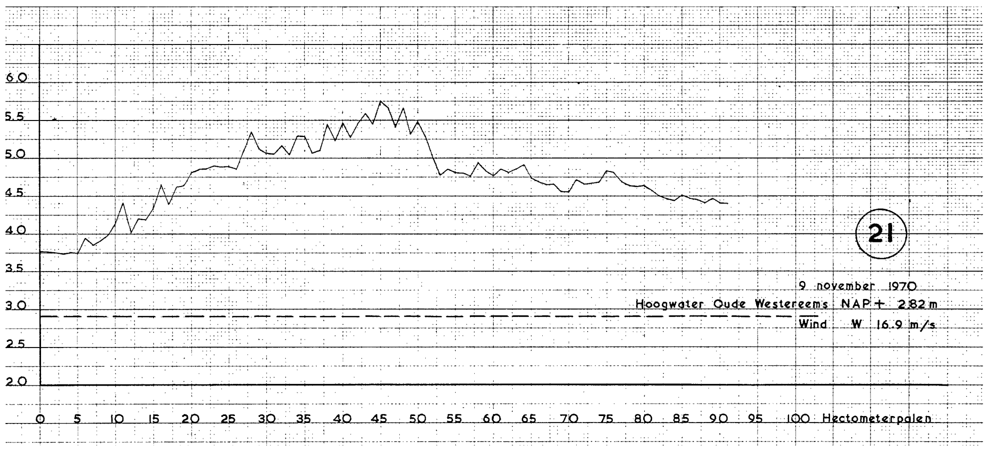

Figure I.22: Flotsam line of 9 November 1970 [Sanders, 1962]

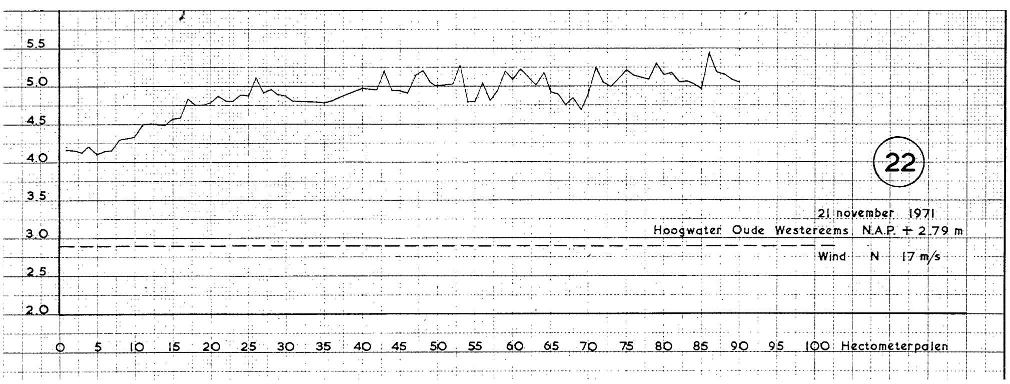

Figure I.23: Flotsam line of 21 November 1971 [Sanders, 1962]

I.2. 1 November 2006

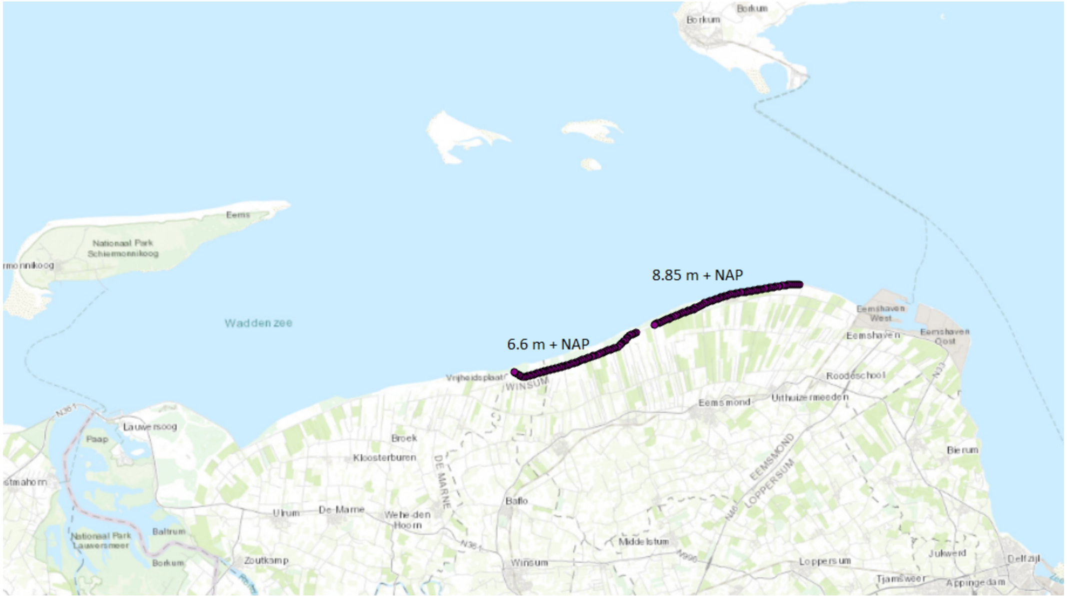

Figure I.24: Flotsam line trajectory corresponding to the high water of 1 November 2006

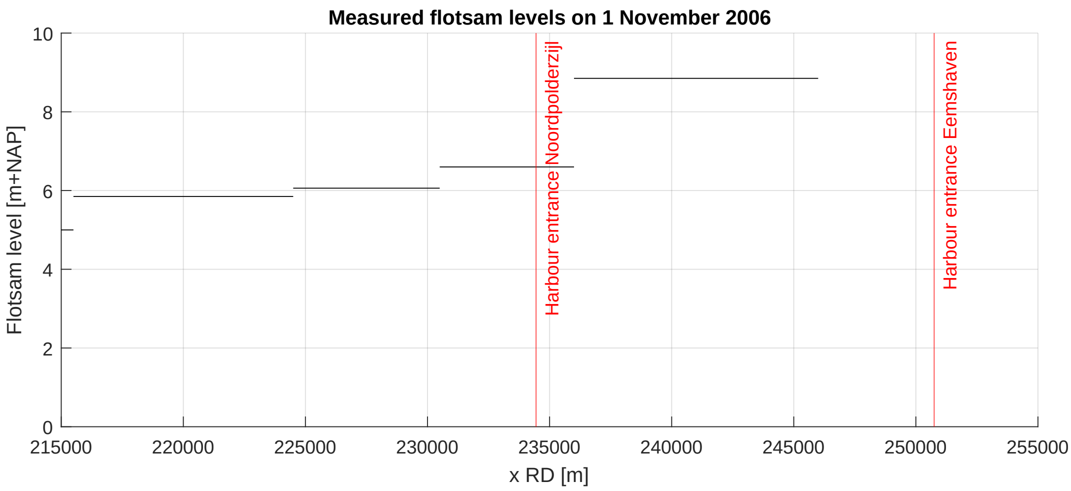

Figure I.25: Flotsam line corresponding to the high water of 1 November 2006

I.3. 9 November 2007

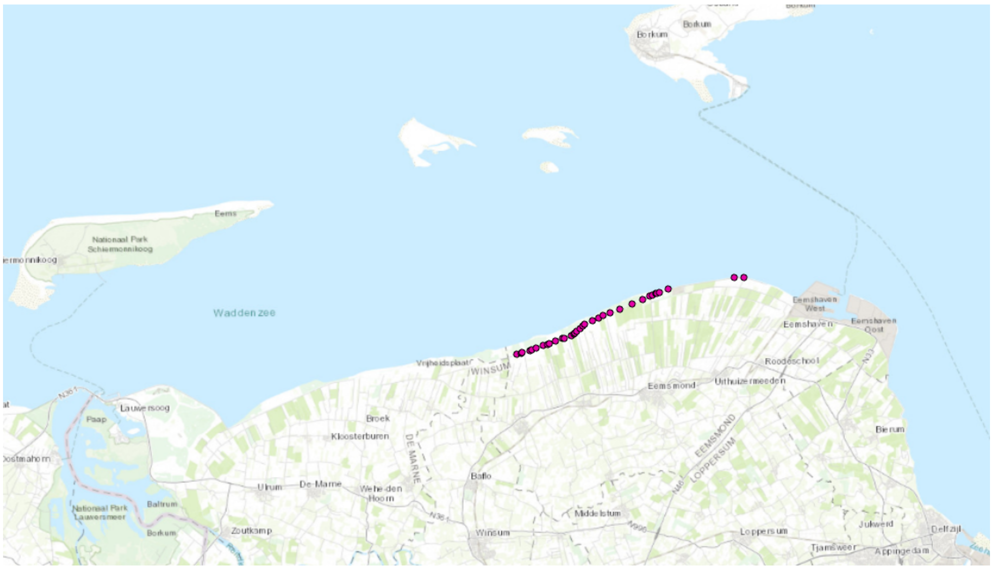

Figure I.26: Flotsam line trajectory corresponding to the high water of 9 November 2007

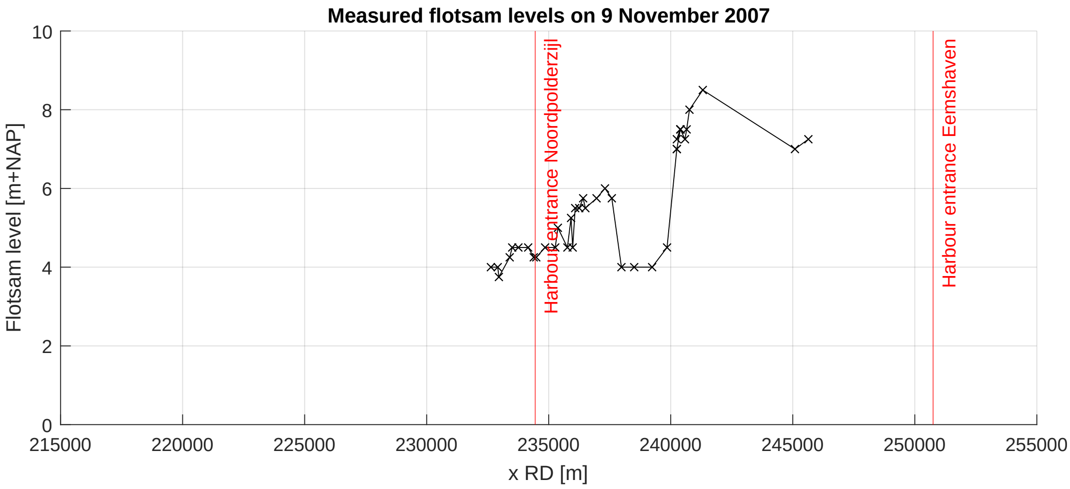

Figure I.27: Flotsam line corresponding to the high water of 9 November 2007

I.4. 5 and 6 December 2013

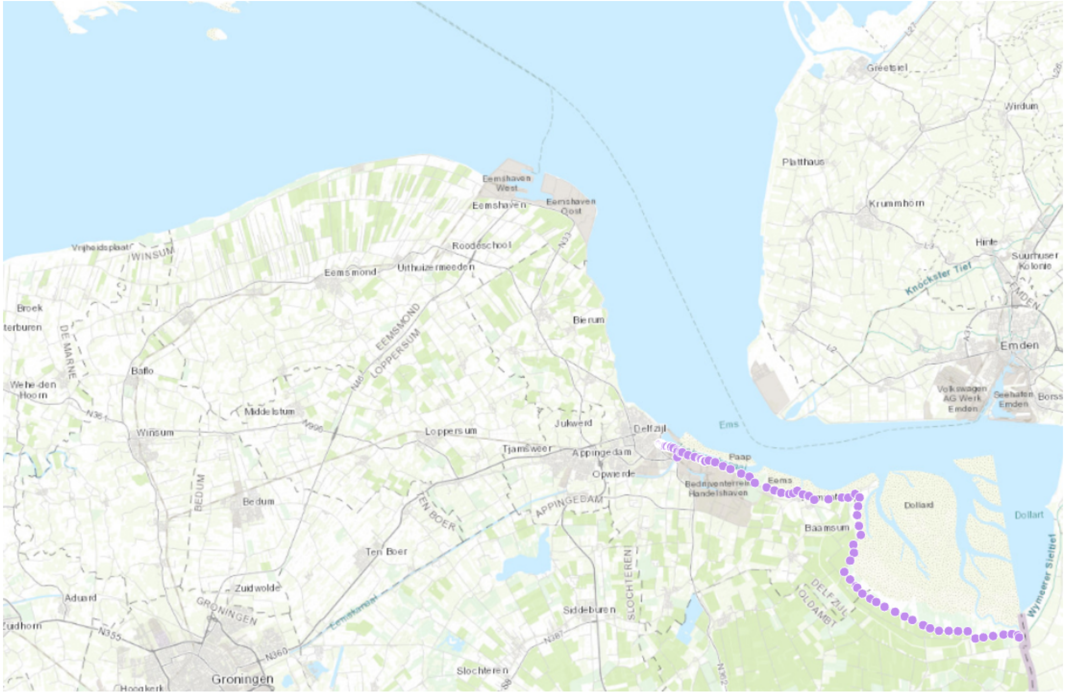

Figure I.28: Flotsam line trajectory corresponding to the two high waters of 5 and 6 December 2013

The two flotsam lines are corresponding to the high waters of 5 and 6 December 2013. The lines are measured between Delfzijl (L = 0 km) and Nieuwe Statenzijl (L = 27 km). Maximum measured water levels at Eemshaven and Delfzijl were respectively 4.15 and 4.82 m+NAP for the highest flotsam line. For the lower flotsam line maximum water levels of respectively 3.58 and 4.26 m+NAP were measured.

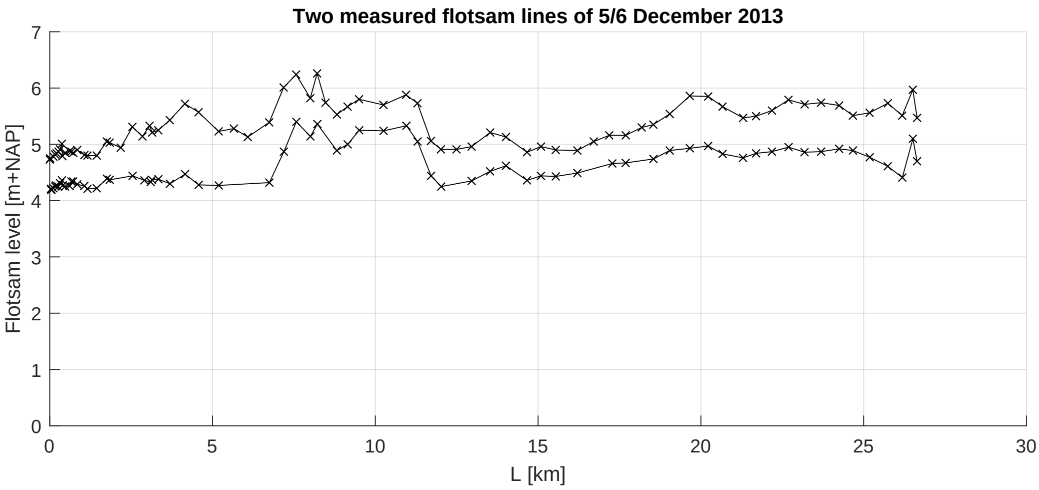

Figure I.29: Two flotsam lines corresponding to the high waters of 5 and 6 December 2013

I.5. 11 January 2015

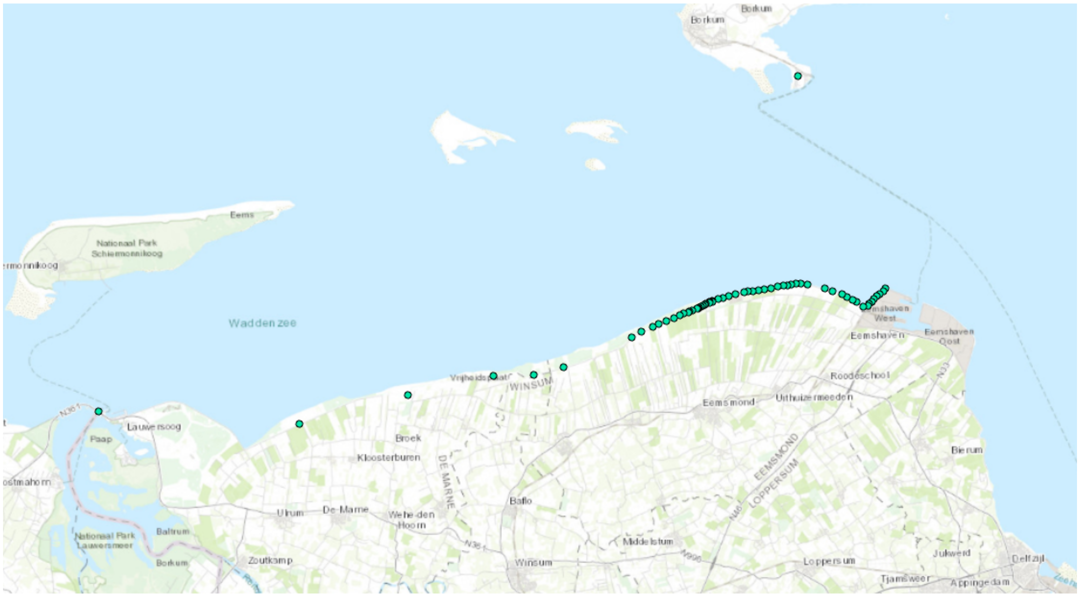

Figure I.30: Flotsam line trajectory corresponding to the high water of 11 January 2015

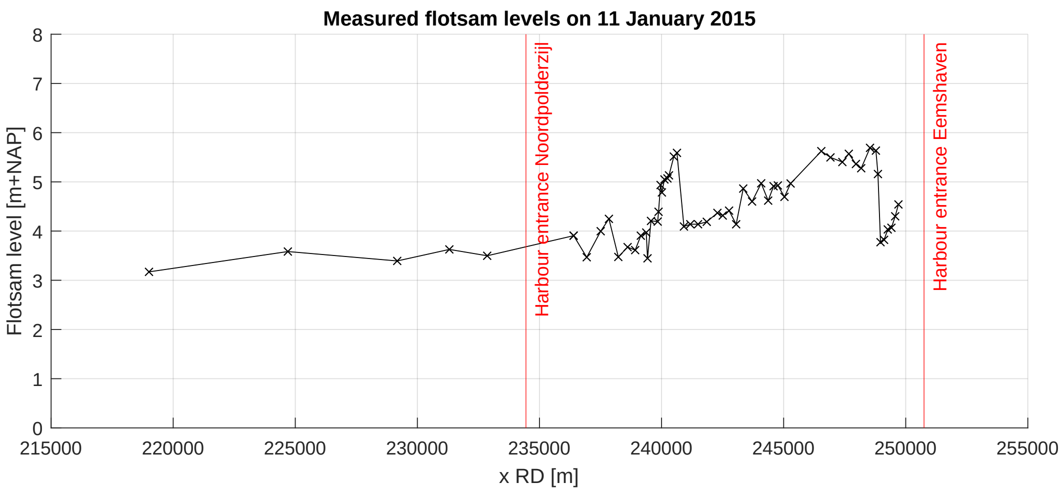

Figure I.31: Flotsam line corresponding to the high water of 11 January 2015

I.6. 13 January 2017

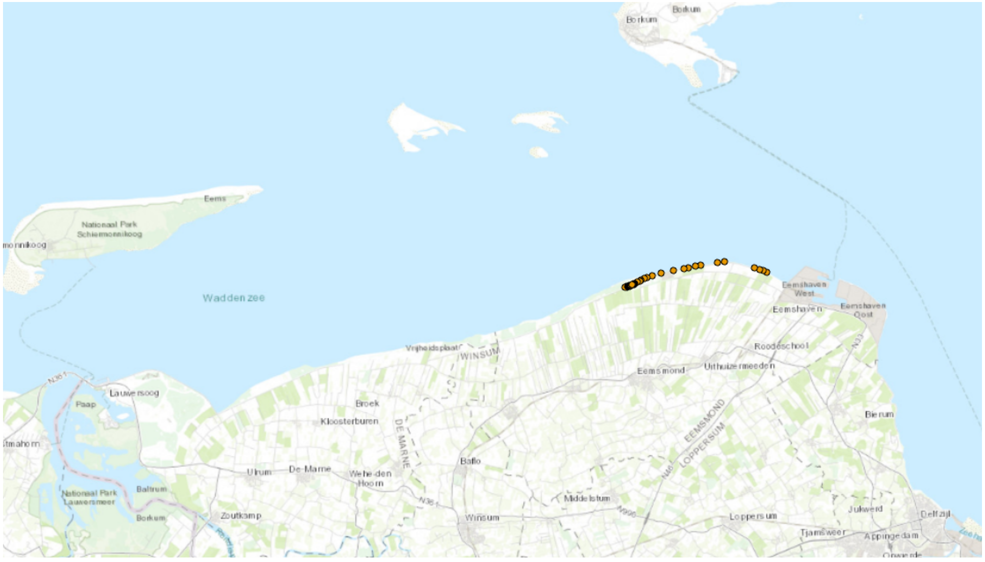

Figure I.32: Flotsam line trajectory corresponding to the high water of 13 January 2017

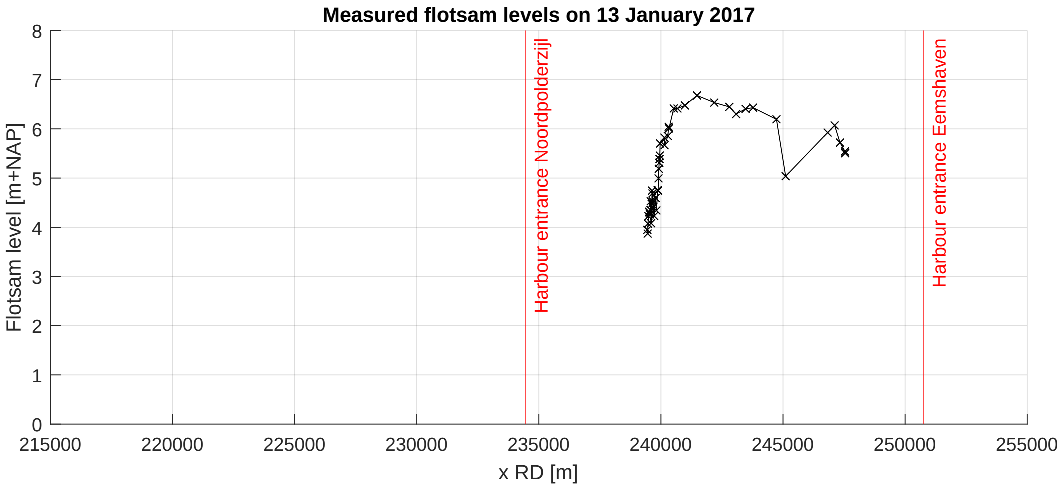

Figure I.33: Flotsam line corresponding to the high water of 13 January 2017

I.7. 8 January 2019

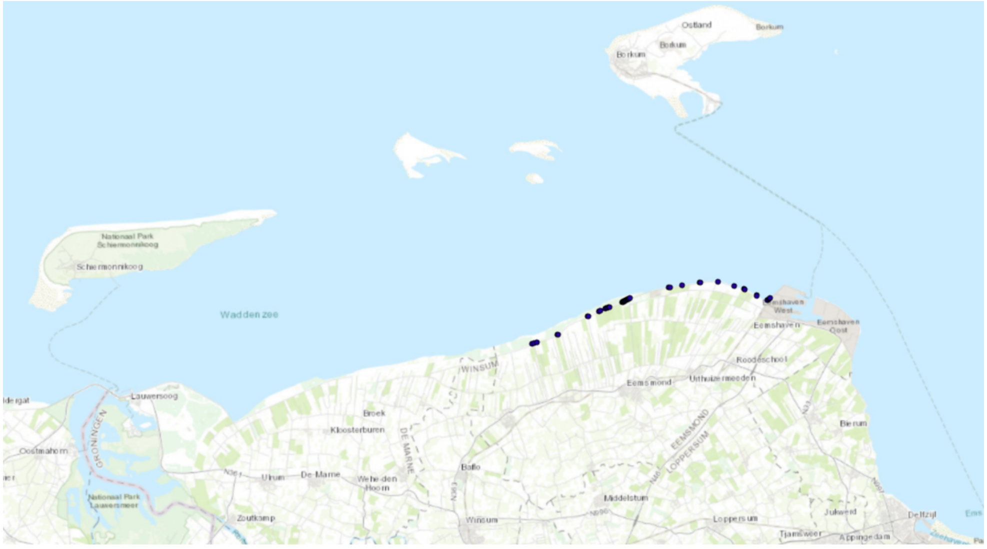

Figure I.34: Flotsam line trajectory corresponding to the high water of 8 January 2019

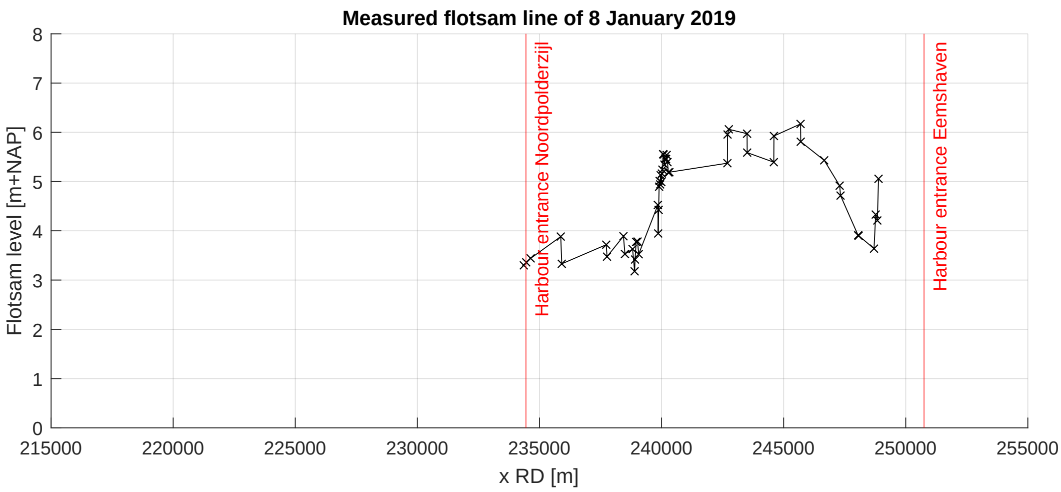

Figure I.35: Flotsam line corresponding to the high water of 8 January 2019

II

Dike-foreshore properties

In this section the properties of the considered dike-foreshore trajectory (x RD = 220 to 250 km) is presented. In Figure II.1 the applied dike slope to perform the wave run-up calculation is shown. This is followed by the dike orientation for the same considered trajectory (Figure II.2). The determined reduction factor for oblique wave incidence (γ_β) is related to the dike orientation and the direction (DIR) of the incoming waves. These reduction factors corresponding to the highest maximum wave run-up of each hindcast are shown in Figure II.3. In the end, a 1D bathymetry corresponding to the HRbasis locations is shown in Figure II.4.

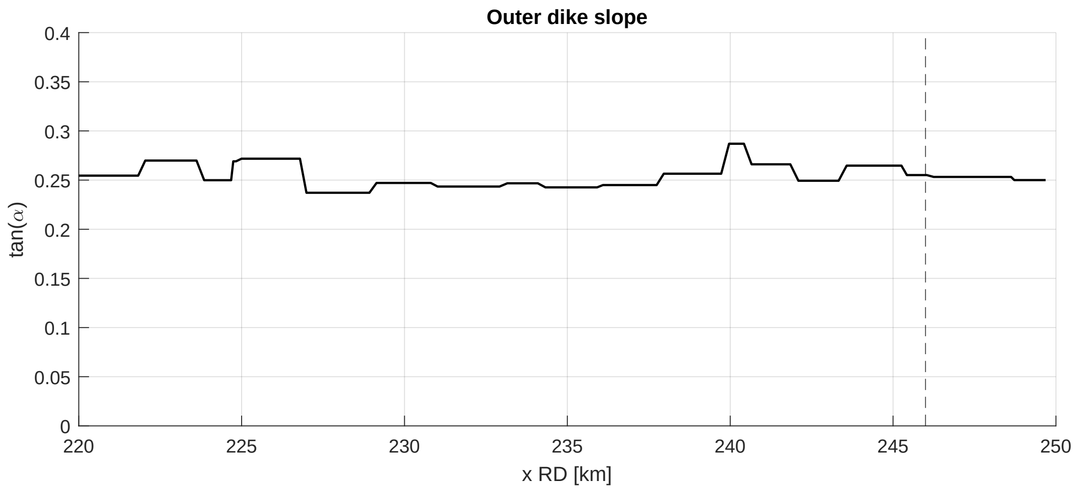

Figure II.1: Dike slope derived from files supplied by HKV. The dashed line at x RD = 246 km corresponds to the location of the measurement pole Uithuizerwad.

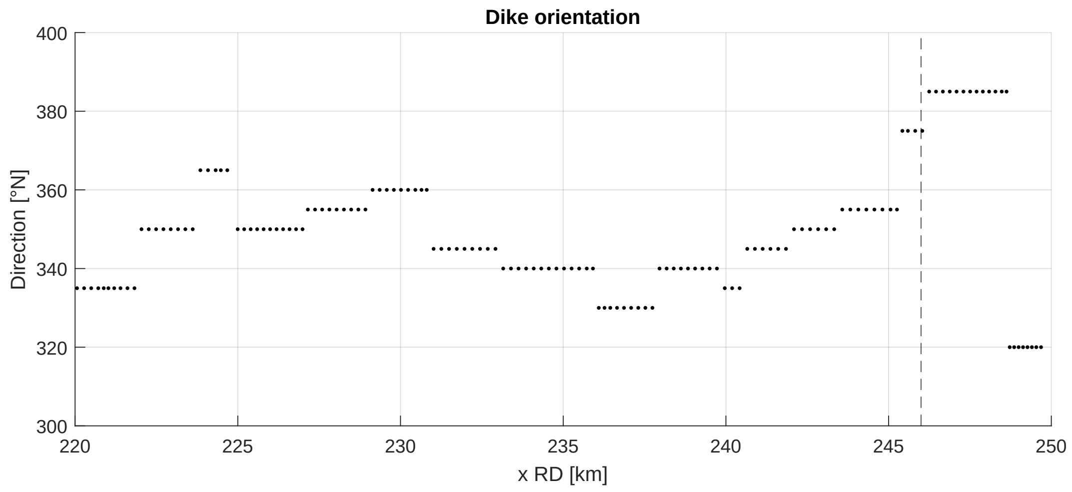

Figure II.2: Dike orientation derived from files supplied by HKV. The dashed line at x RD = 246 km corresponds to the location of the measurement pole Uithuizerwad.

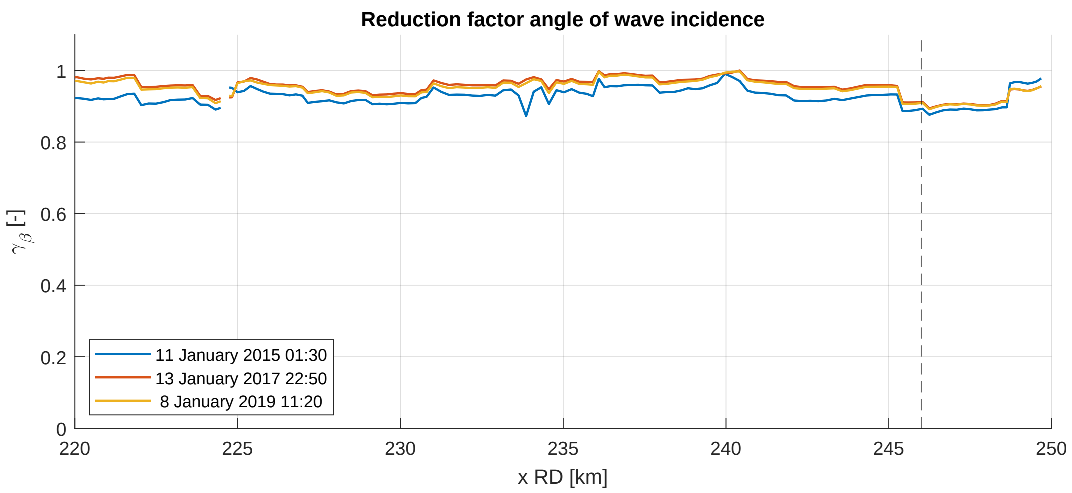

Figure II.3: Calculated reduction factor to account for angle of wave incidence. The dashed line at x RD = 246 km corresponds to the location of the measurement pole Uithuizerwad.

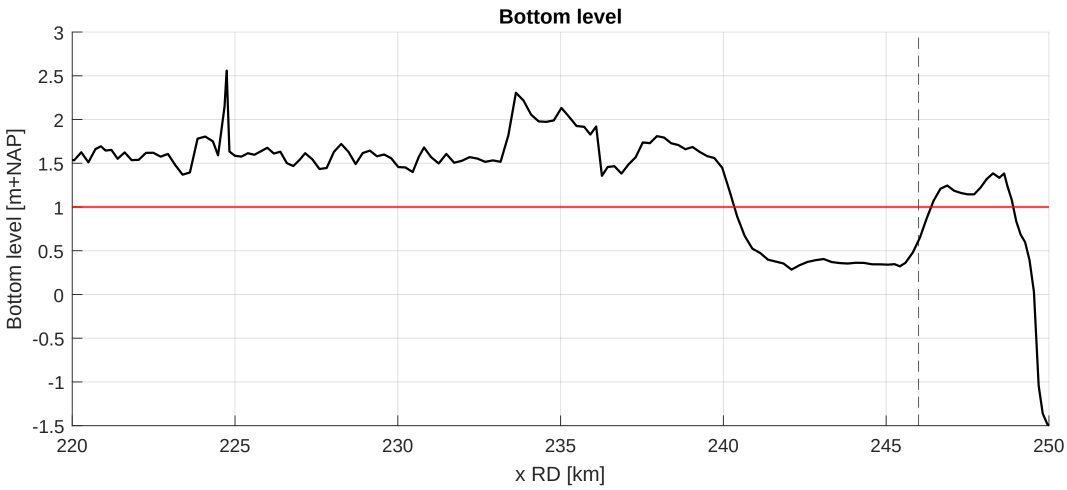

Figure II.4: Bottom levels for HRbasis set. Salt marshes are present for bottom levels higher than 1.0 m+NAP (red line). The dashed line at x RD = 246 km corresponds to the location of the measurement pole Uithuizerwad.

III

Model results 2015

Table III.1: Definitions of variables in SWAN

Parameter	Meaning
XP	X-coordinate [m]
YP	Y-coordinate [m]
DEPTH	water depth [m]
HS	significant wave height [m]
RTP	relative peak period [s]
TPS	smoothed peak period [s]
TMM10	mean absolute wave period (m_{-1}/m_0) [s]
TM01	mean absolute wave period (m_0/m_1) [s]
TM02	mean absolute wave period $(m_0/m_2)^{0.5}$ [s]
DIR	mean wave direction [°N]
DSPR	directional spreading [°]
WLEN	mean wavelength [m]
DISSIP	energy dissipation per unit time [W/m2]
DHS	the difference in significant wave height as computed in the last two iterations
DRTM01	the difference in average wave period (RTM01) as computed in the last two iterations
WATLEV	water level [m+NAP]
WIND	wind velocity [m/s]
VEL	current velocity [m/s]
BOTLEV	bottom level [m+NAP]
QB	Fraction of breaking waves

III.1. Water level

Measured water levels are plotted against calculated levels with WAQUA (dcsmv6-zunov4) in Figure IV.1. The following locations are shown in Figure IV.1: Huibertgat, Wierumergronden, Nes, Schiermonnikoog, Lauwersoog, Eemshaven, Delfzijl, Nieuwe Statenzijl.

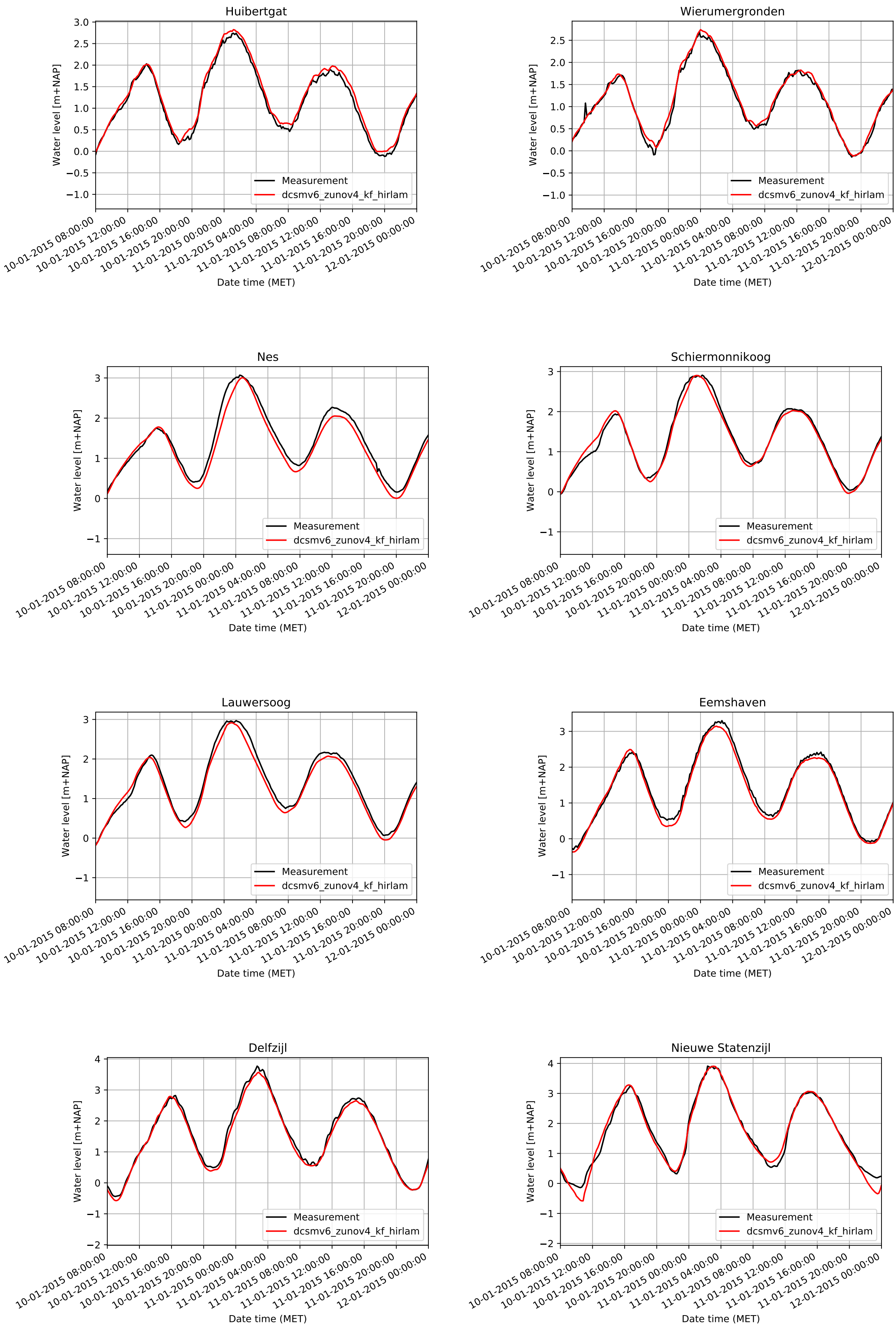

Figure III.1: Comparison between measured and modelled water levels for hindcast 2015.

III.2. Wind

Measured wind speed(Figure III.2) and direction(Figure III.3) are plotted against calculated HIRLAM wind speed and direction. The following locations are shown in Figure III.2 and Figure III.3: Huibertgat, Amelander Westgat (AWG), Lauwersoog, and Nieuwe Beerta. No measurements were available for Huibertgat.

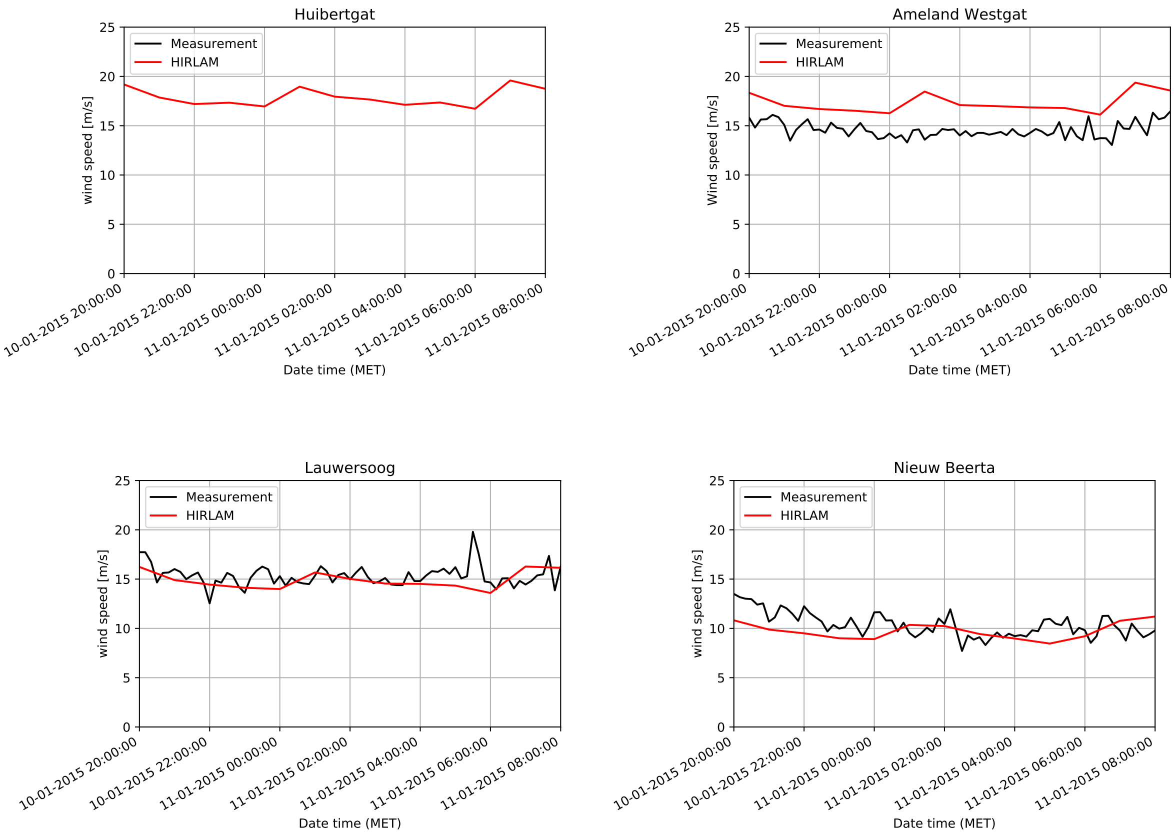

Figure III.2: Comparison between measured and HIRLAM wind speed for hindcast 2015.

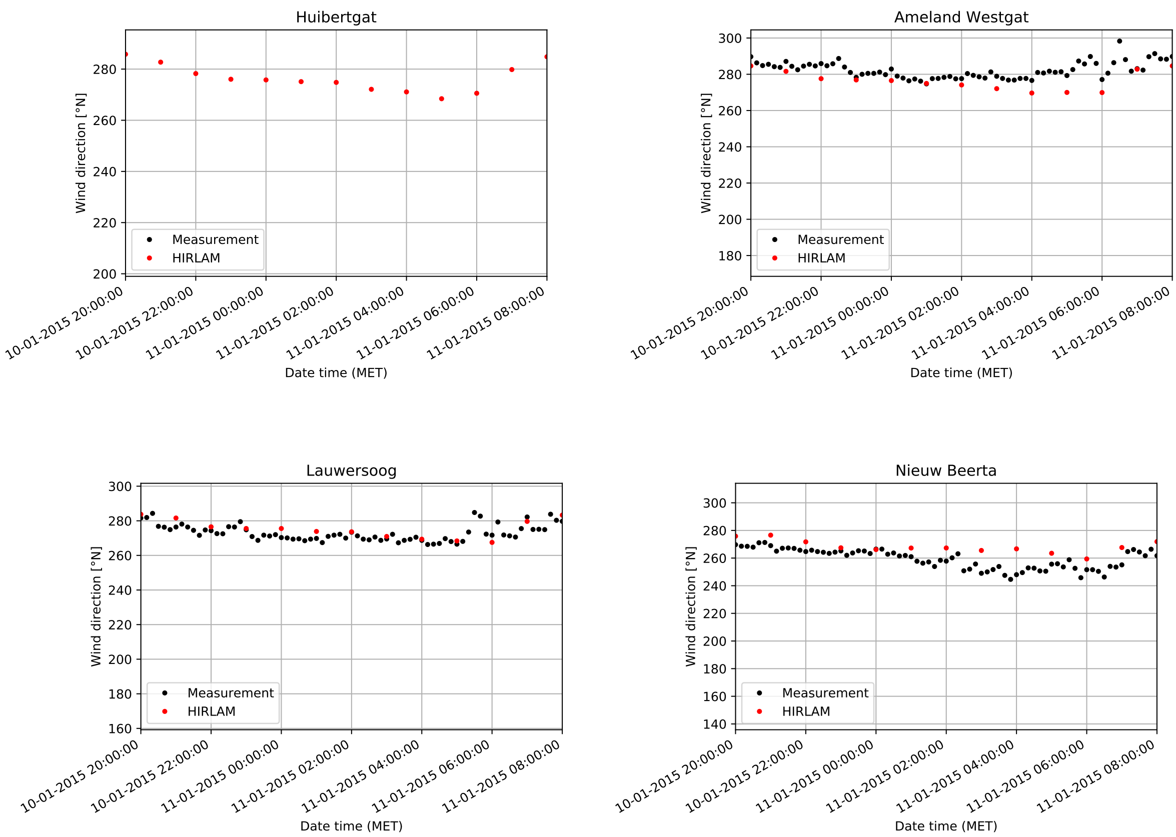

Figure III.3: Comparison between measured and HIRLAM wind direction for hindcast 2015.

III.3. SWAN spatial fields

Results hindcast (001): 11 January 2015 01:10, Grid G3, SWAN 40.72ABCDE

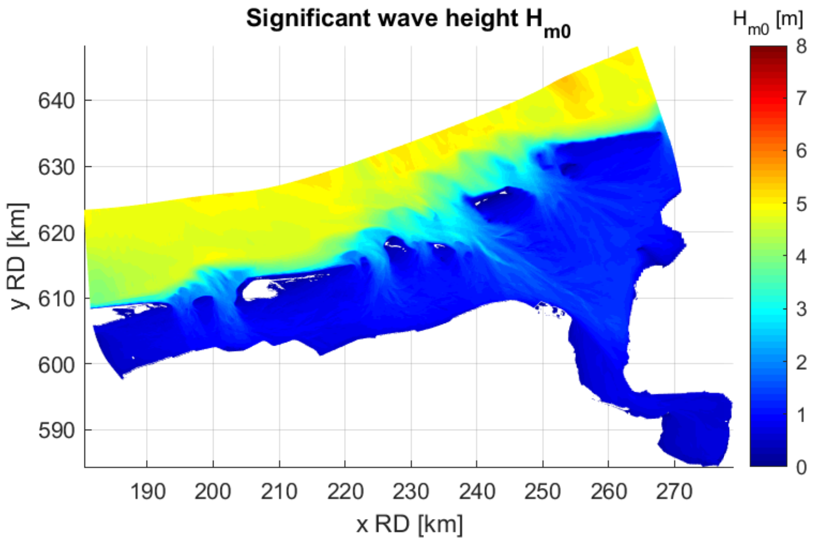

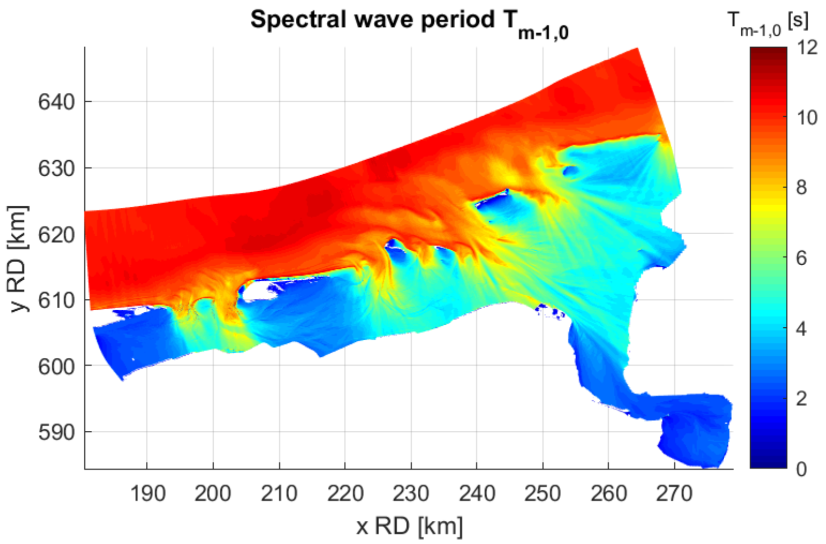

Figure III.4: Variation of significant wave height H_{m0} and spectral wave period $T_{\mathrm{m\text{-}1,0}}$ for G3 grid, 11 January 2015 01:10

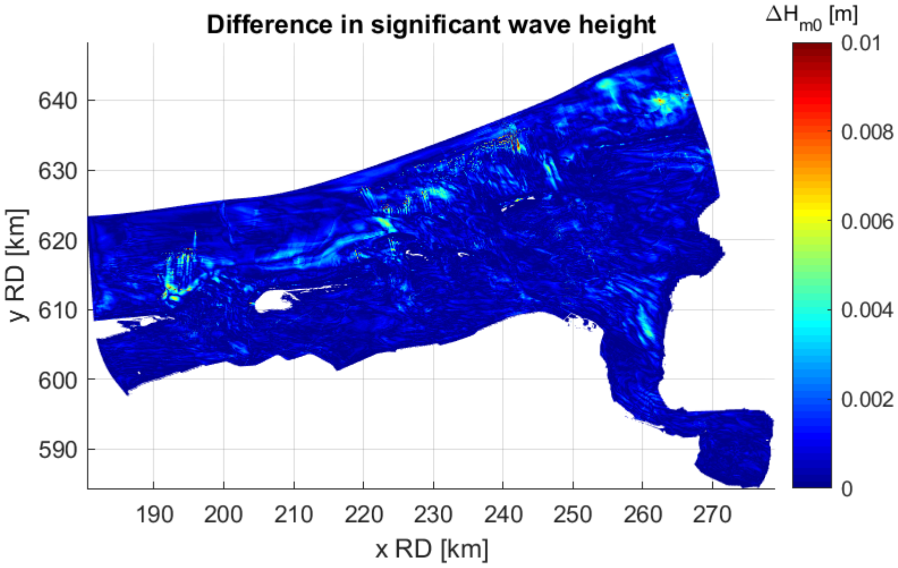

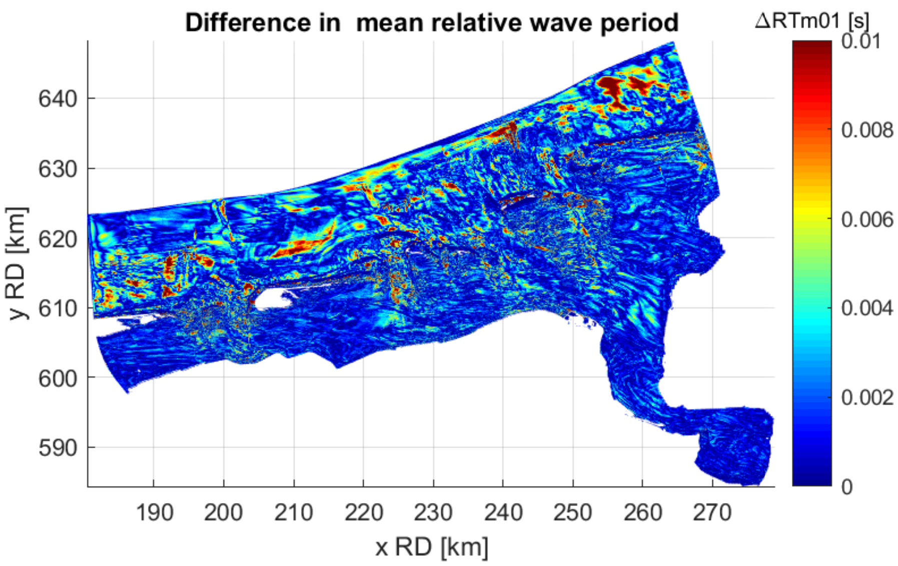

Figure III.5: Difference of significant wave height H_{m0} and relative spectral wave period RT_{m01} as computed in the last two iterations for G3 grid, 11 January 2015 01:10

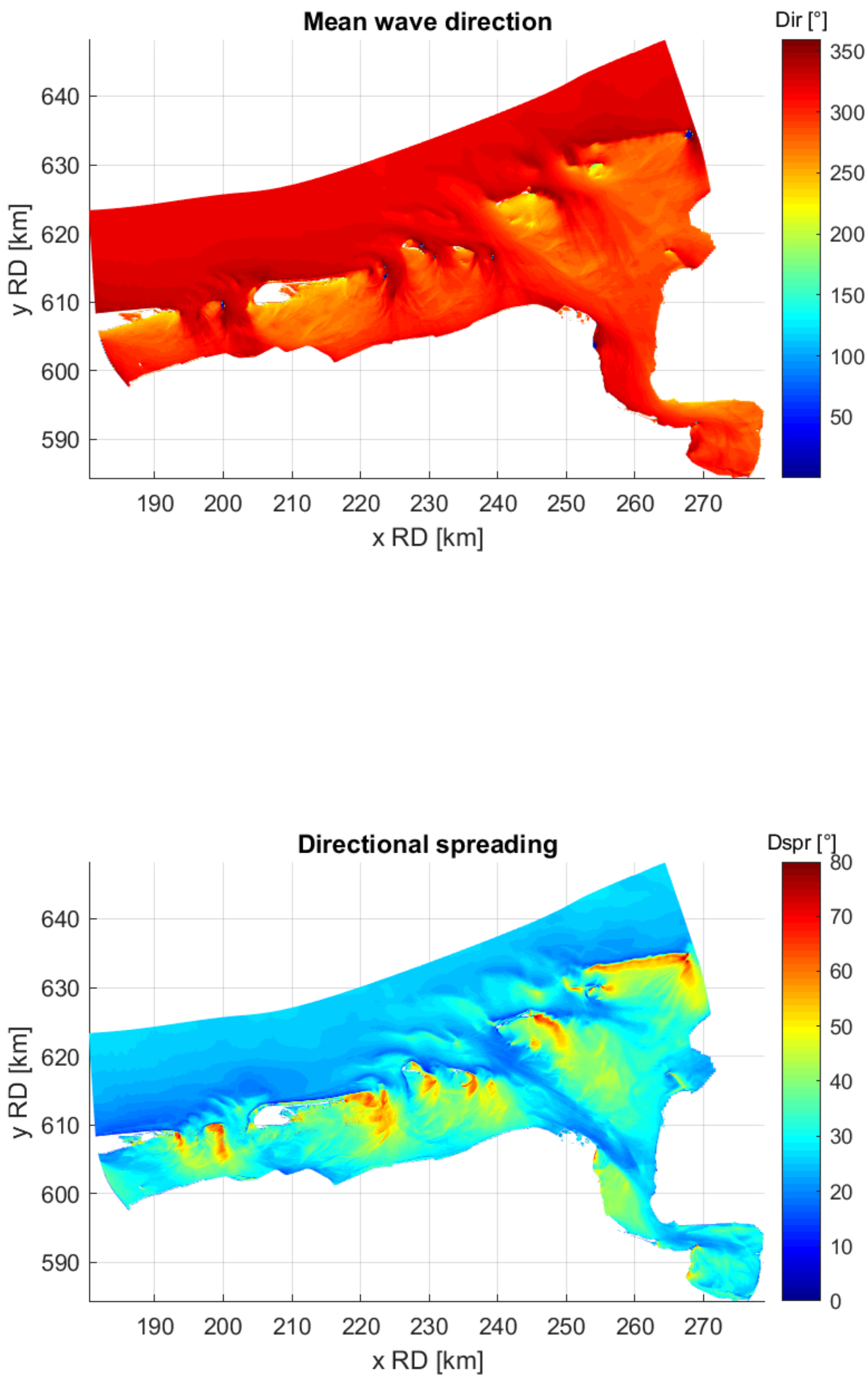

Figure III.6: Variation of mean wave direction DIR and directional spreading Dspr for G3 grid, 11 January 2015 01:10

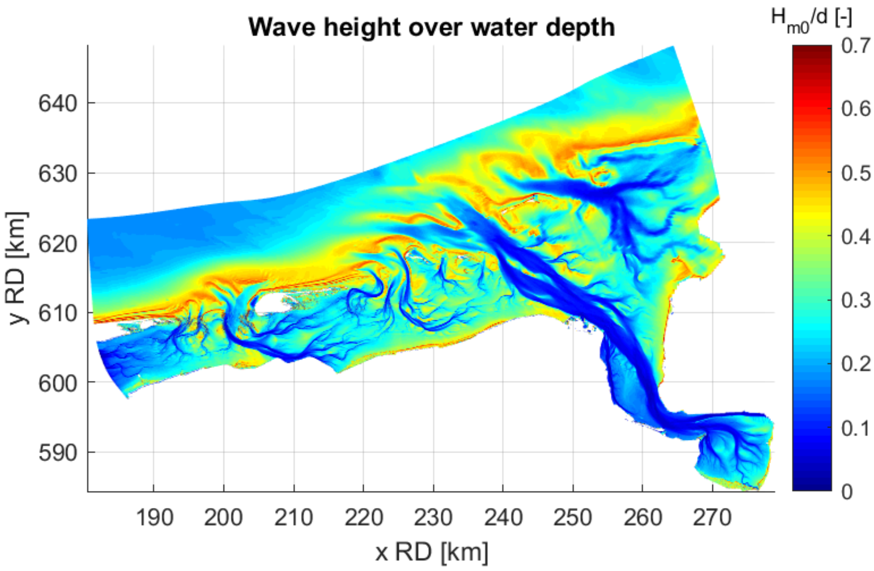

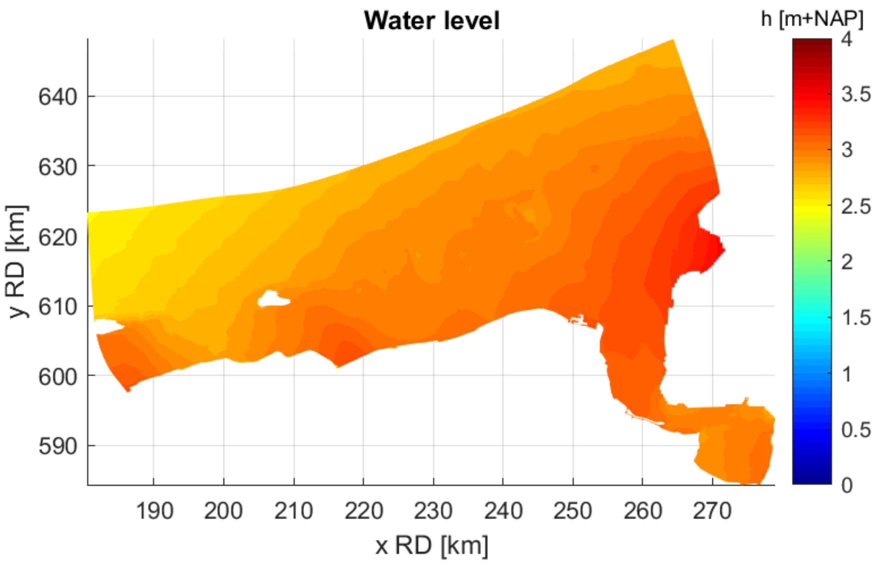

Figure III.7: Variation of the ratio H_{m0}/d and water level h for G3 grid, 11 January 2015 01:10

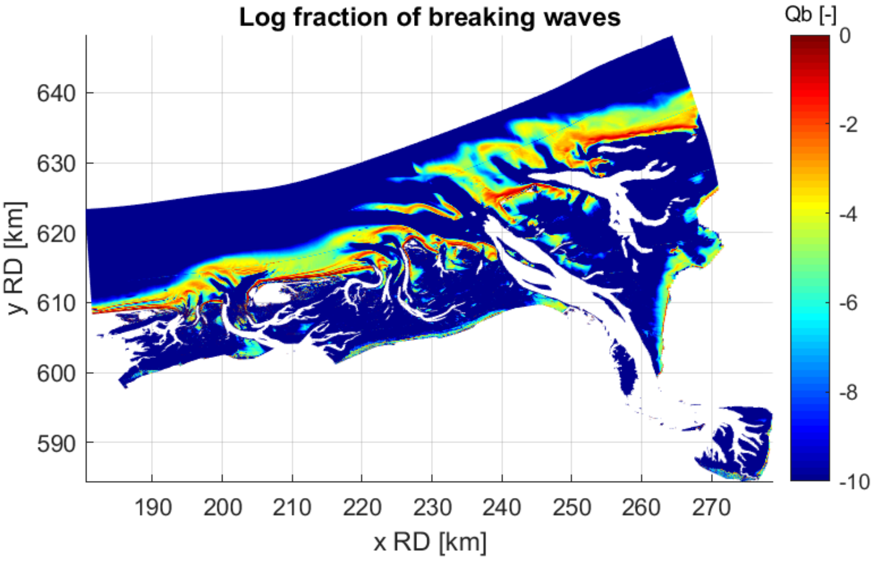

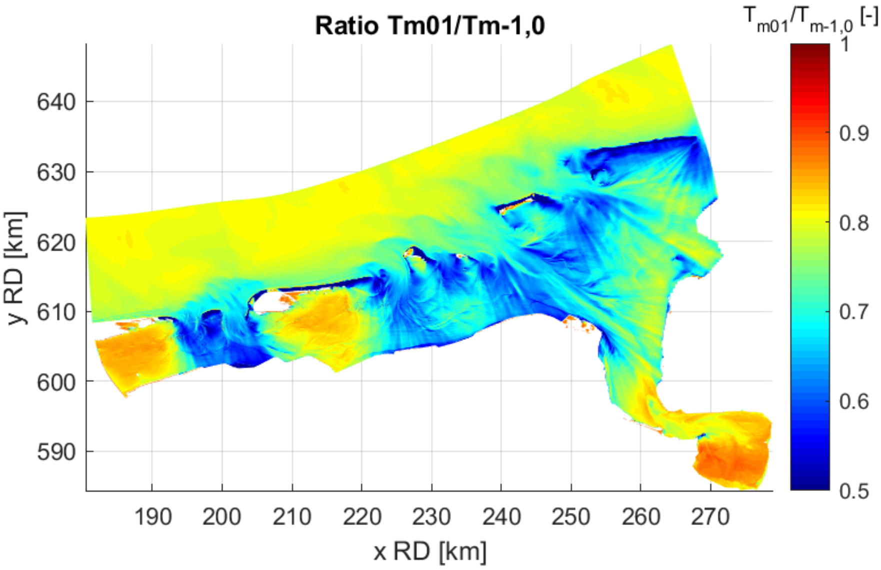

Figure III.8: The variation of breaking waves and ratio $T_{\mathrm{m01}}\,/\,T_{\mathrm{m\text{-}1,0}}$ for G3 grid, 11 January 2015 01:10

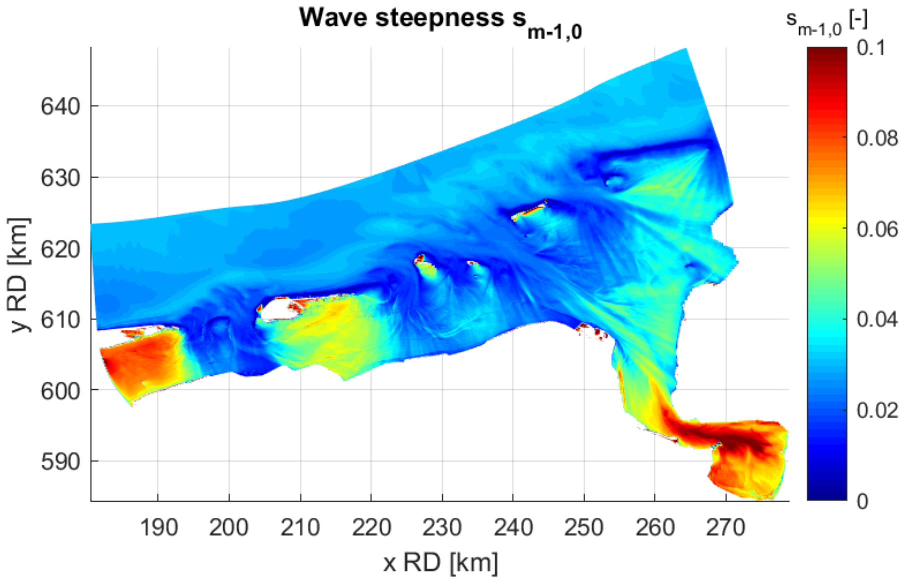

Figure III.9: The variation of wave steepness ($s_{m-1,0}$) for G3 grid, 11 January 2015 01:10.

Results hindcast (002): 11 January 2015 01:30, Grid G3, SWAN 40.72ABCDE

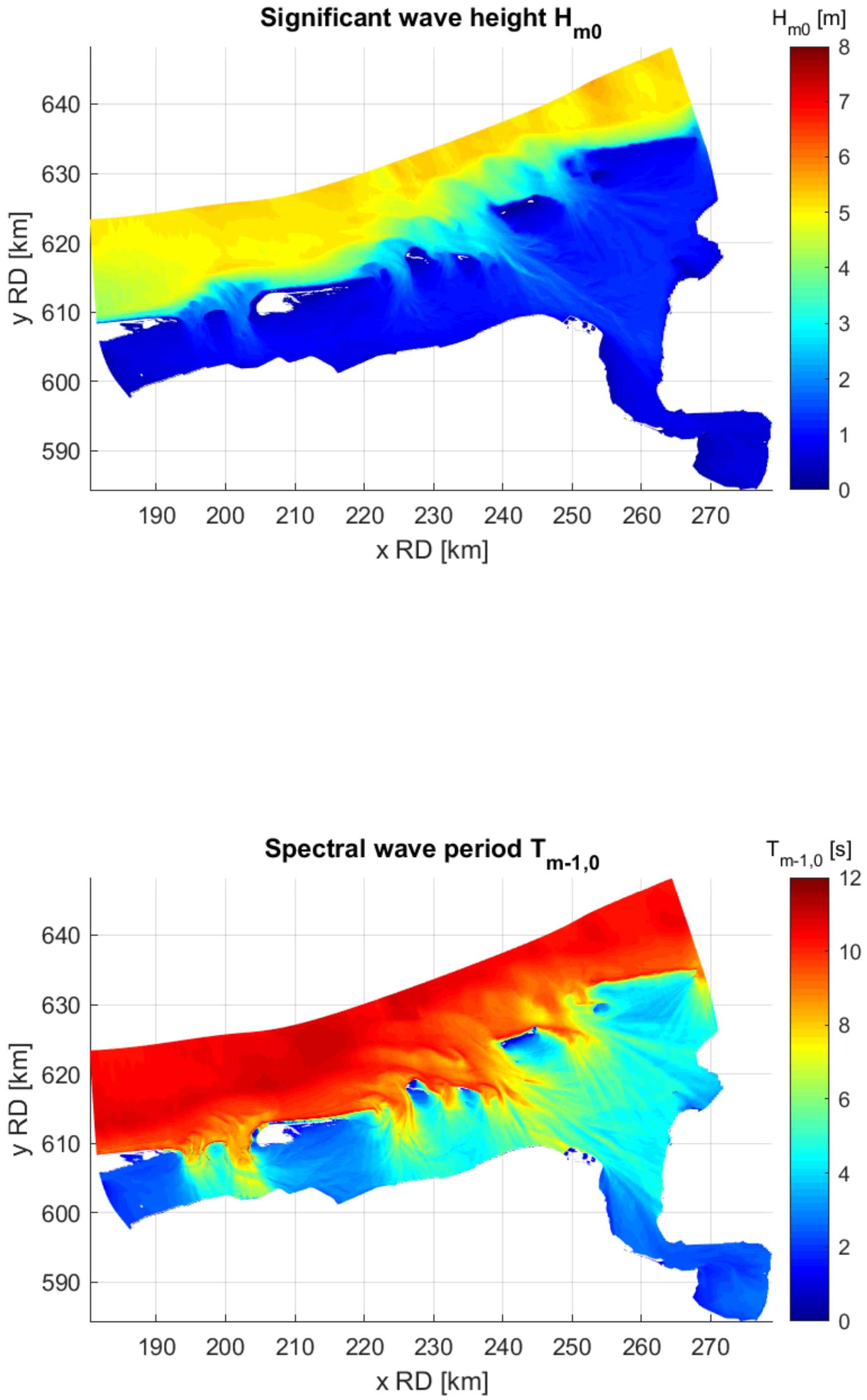

Figure III.10: Variation of significant wave height H_{m0} and spectral wave period $T_{\mathrm{m-1,0}}$ for G3 grid, 11 January 2015 01:30

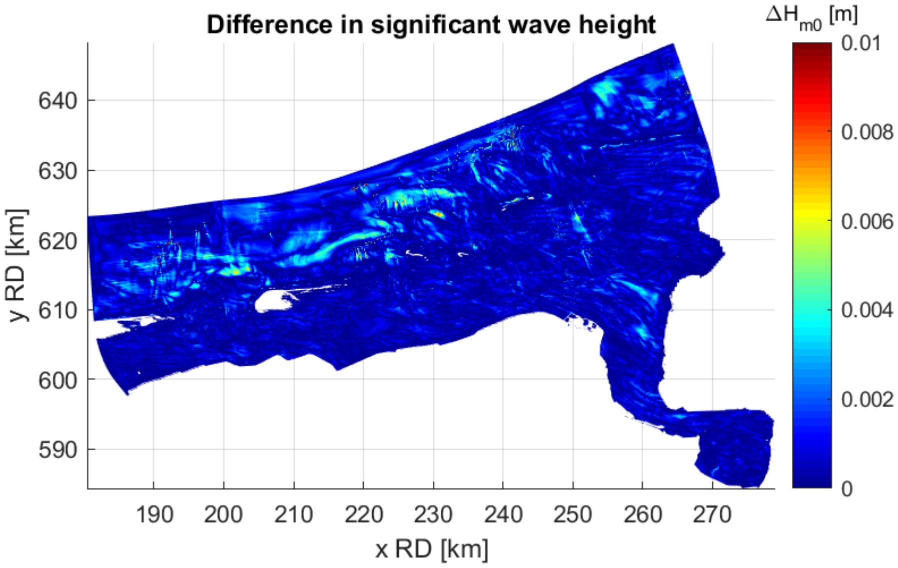

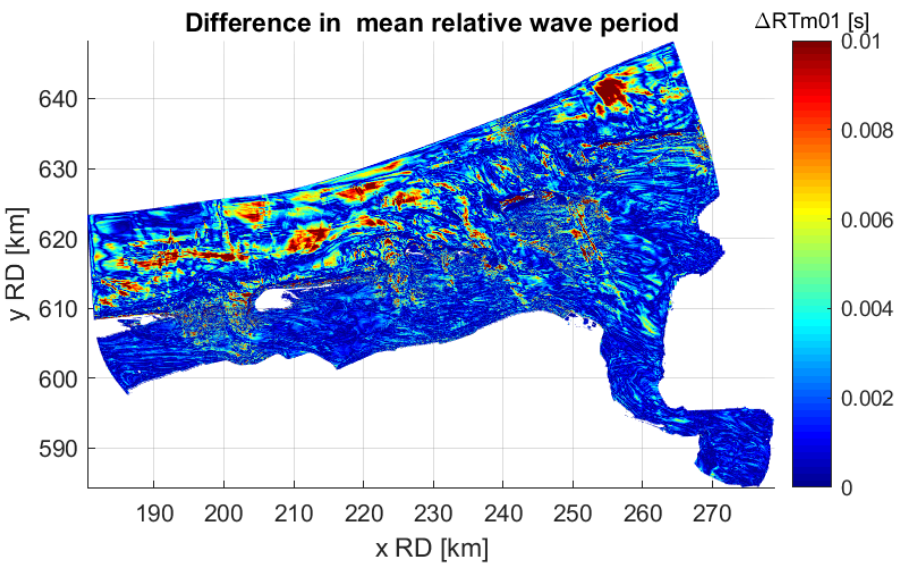

Figure III.11: Difference of significant wave height H_{m0} and relative spectral wave period RT_{m01} as computed in the last two iterations for G3 grid, 11 January 2015 01:30

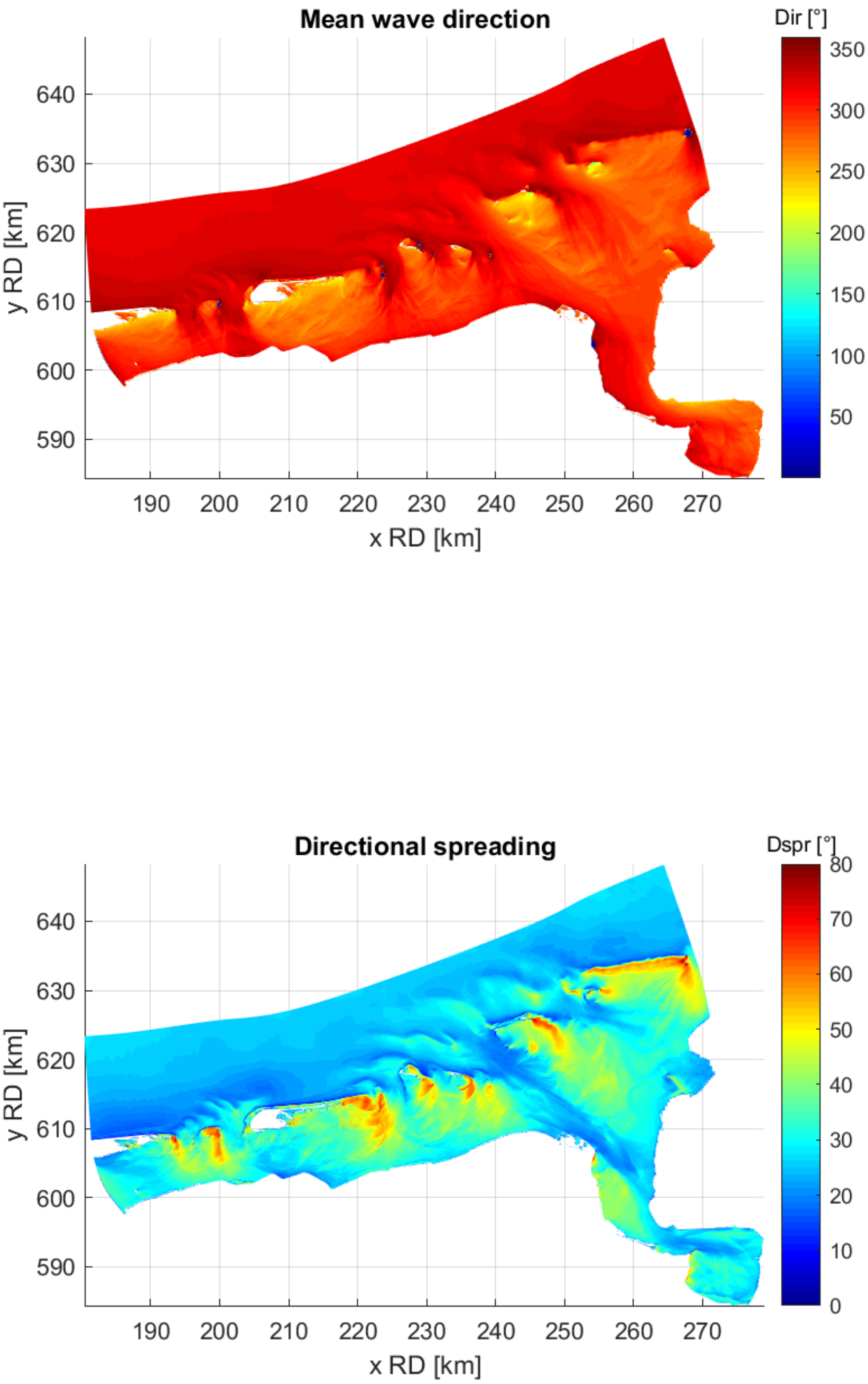

Figure III.12: Variation of mean wave direction DIR and directional spreading Dspr for G3 grid, 11 January 2015 01:30

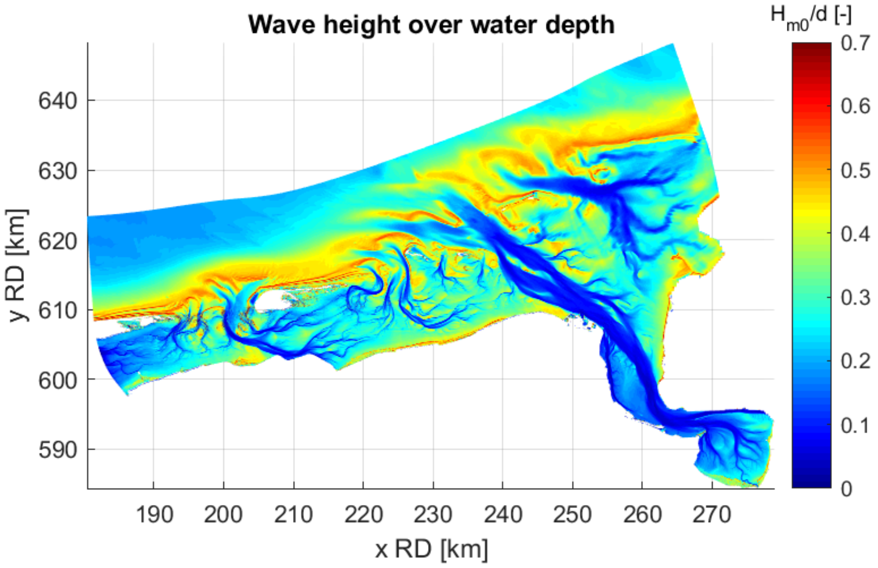

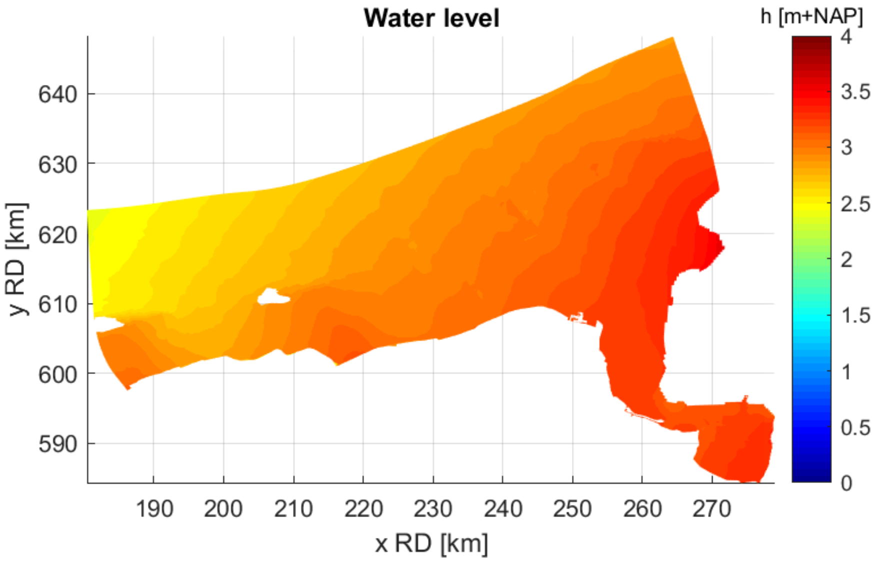

Figure III.13: Variation of the ratio $H_{\mathrm{m0}}/\mathrm{d}$ and water level h for G3 grid, 11 January 2015 01:30

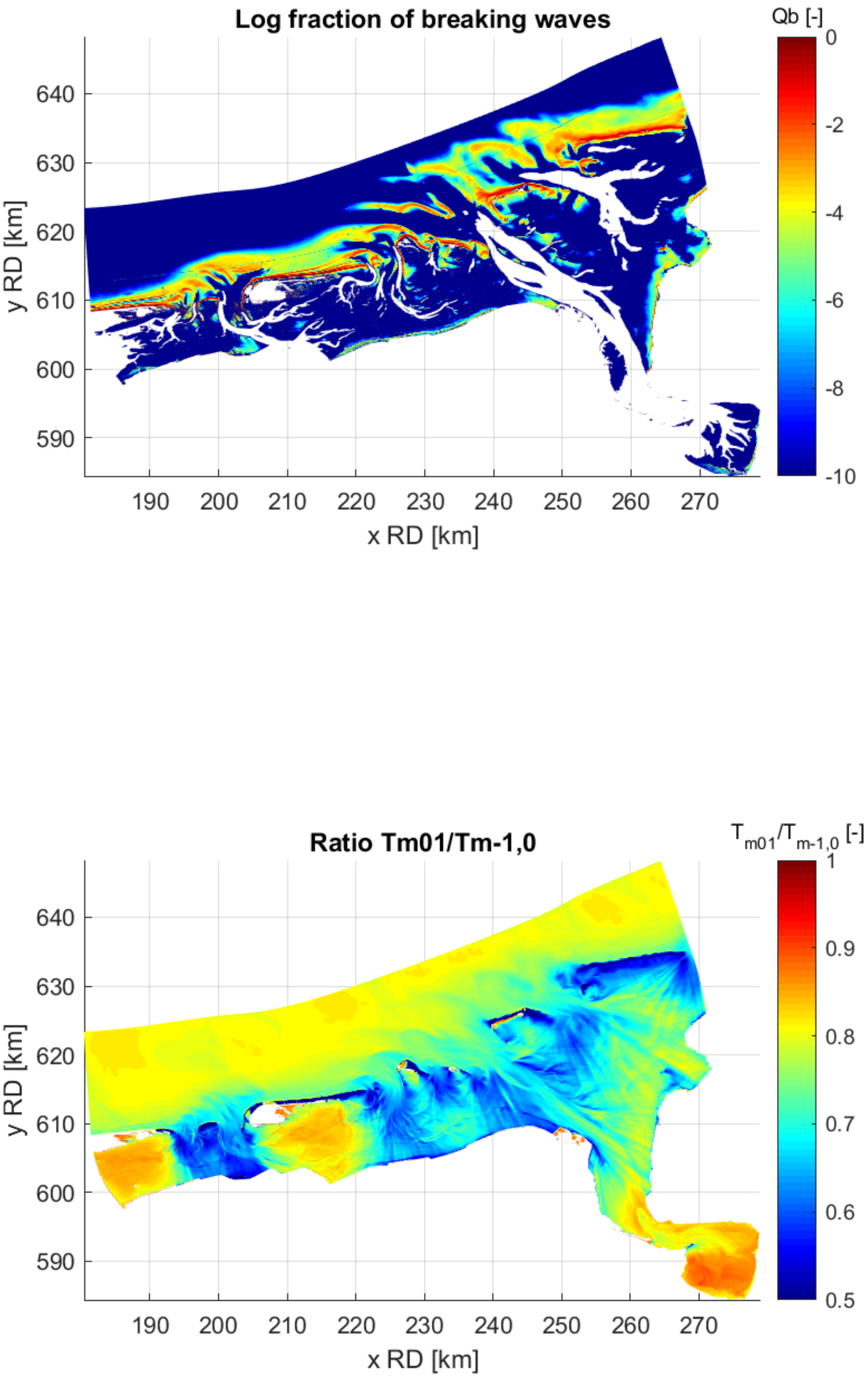

Figure III.14: The variation of breaking waves for G3 grid and ratio $T_{\mathrm{m}01}\,/\,T_{\mathrm{m}\text{-}1,0}$ for G3 grid, 11 January 2015 01:30

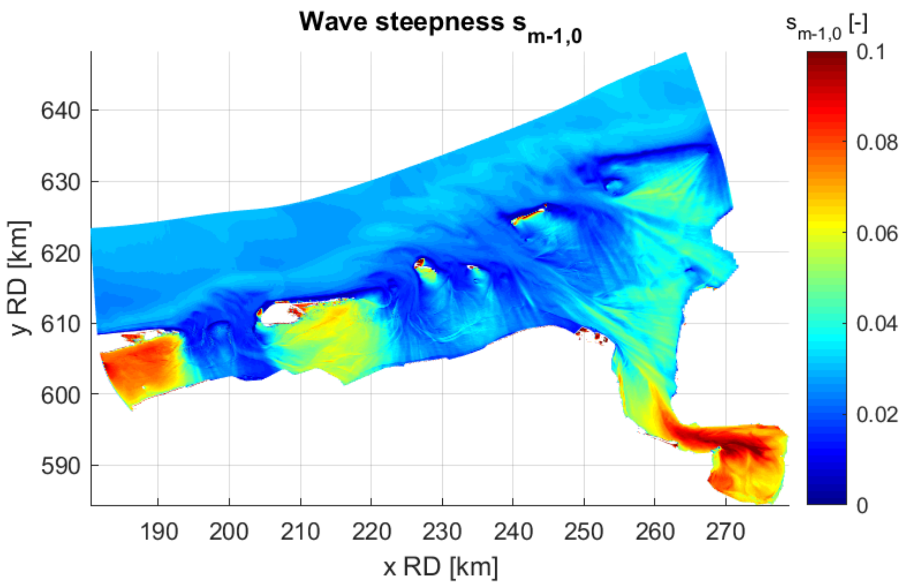

Figure III.15: The variation of wave steepness ($s_{m-1,0}$) for G3 grid, 11 January 2015 01:30.

Results hindcast (003): 11 January 2015 02:10, Grid G3, SWAN 40.72ABCDE

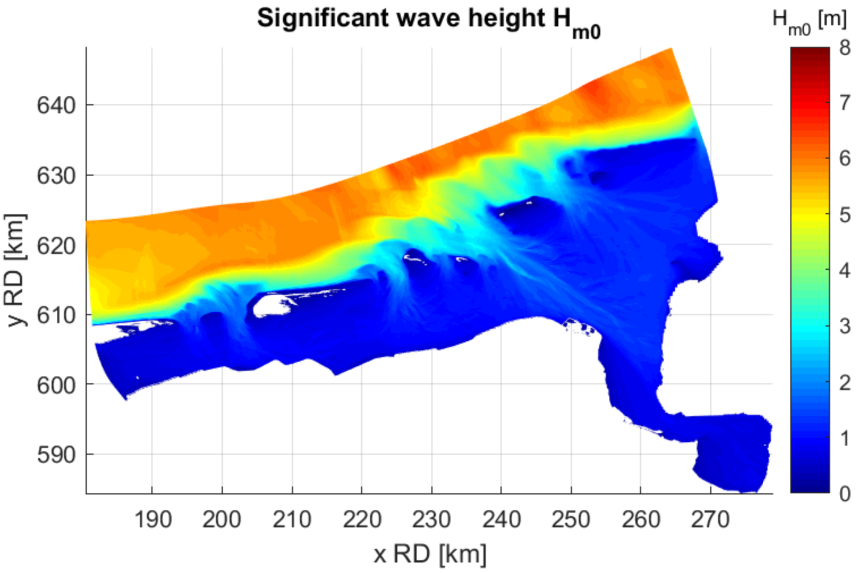

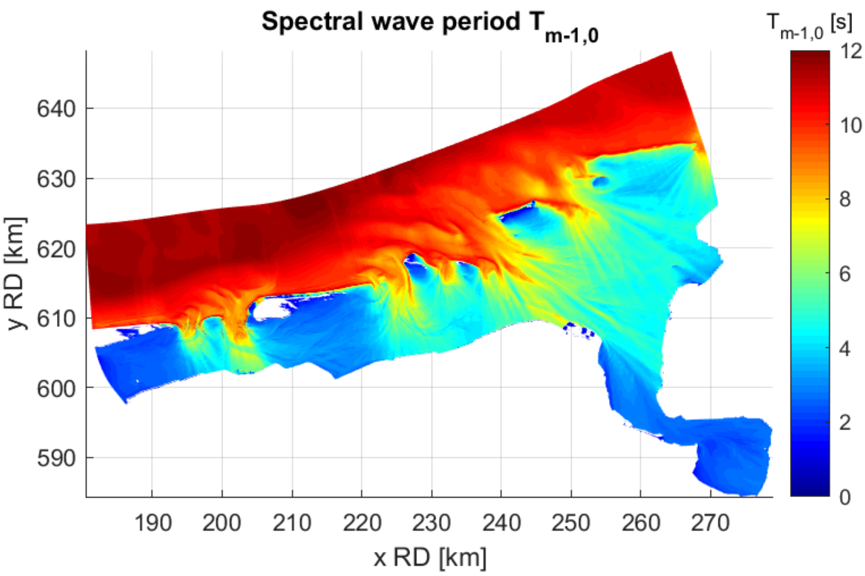

Figure III.16: Variation of significant wave height H_{m0} and spectral wave period $T_{\mathrm{m-1,0}}$ for G3 grid, 11 January 2015 02:10

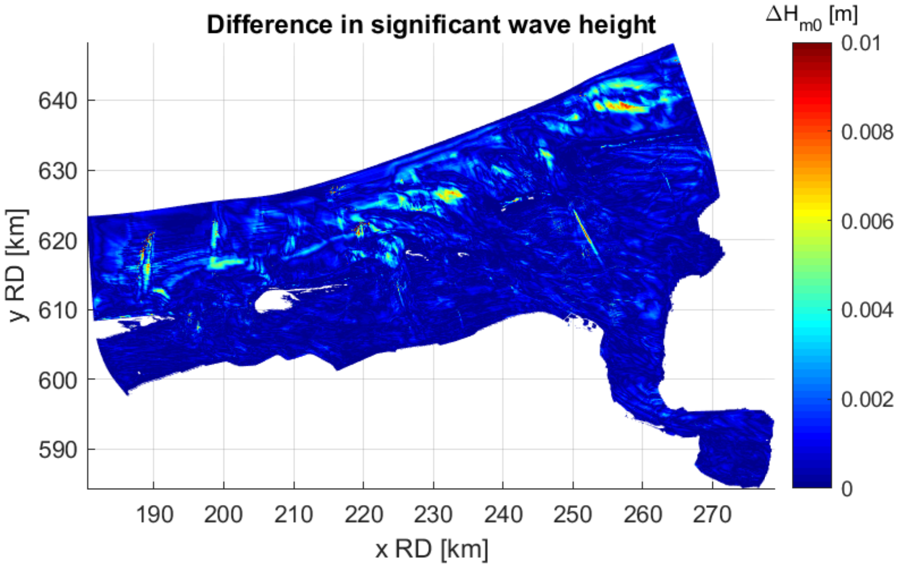

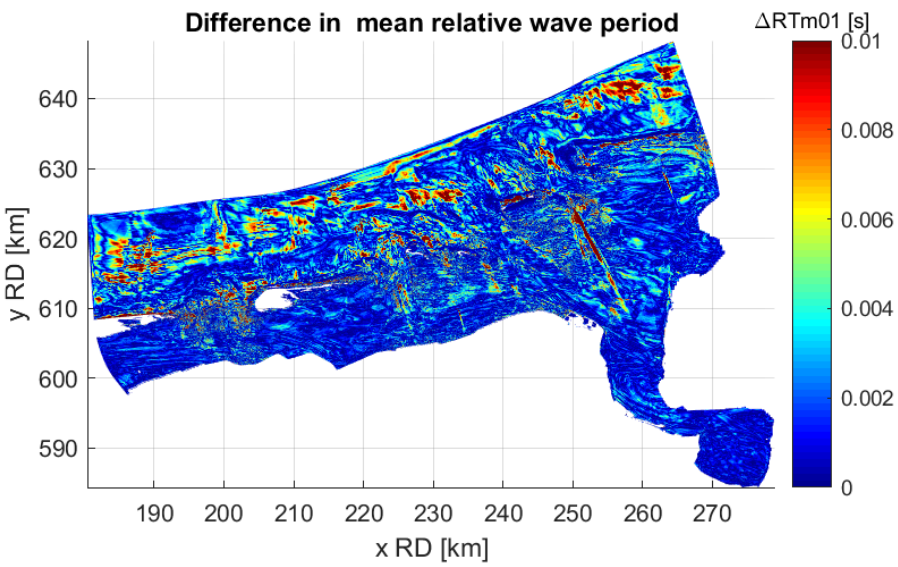

Figure III.17: Difference of significant wave height H_{m0} and relative spectral wave period RT_{m01} as computed in the last two iterations for G3 grid, 11 January 2015 02:10

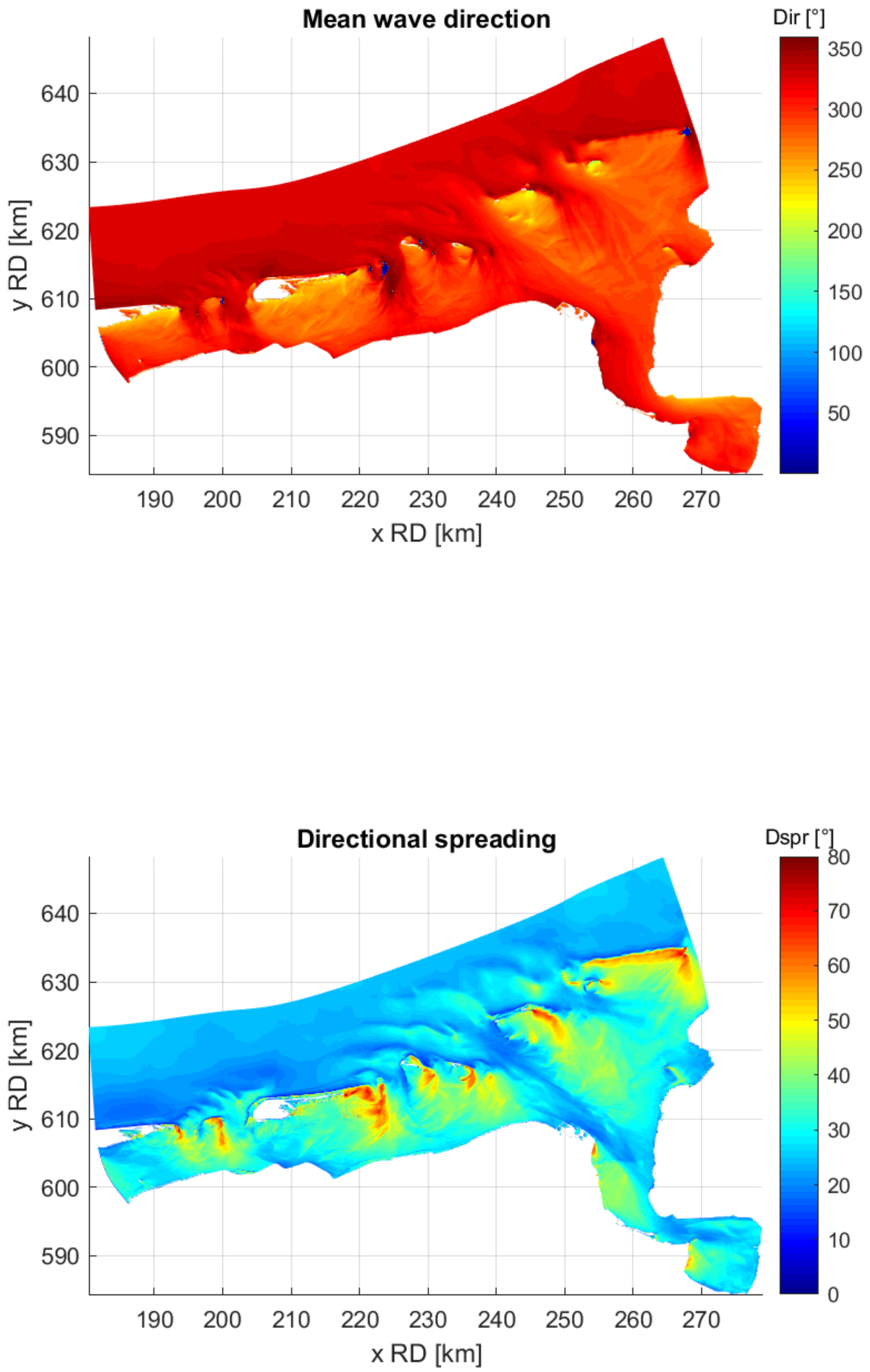

Figure III.18: Variation of mean wave direction DIR and directional spreading Dspr for G3 grid, 11 January 2015 02:10

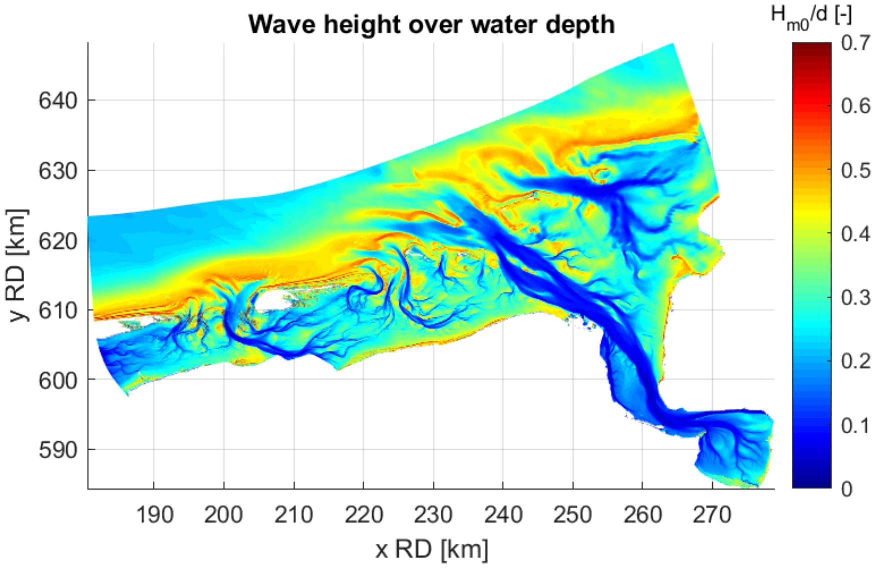

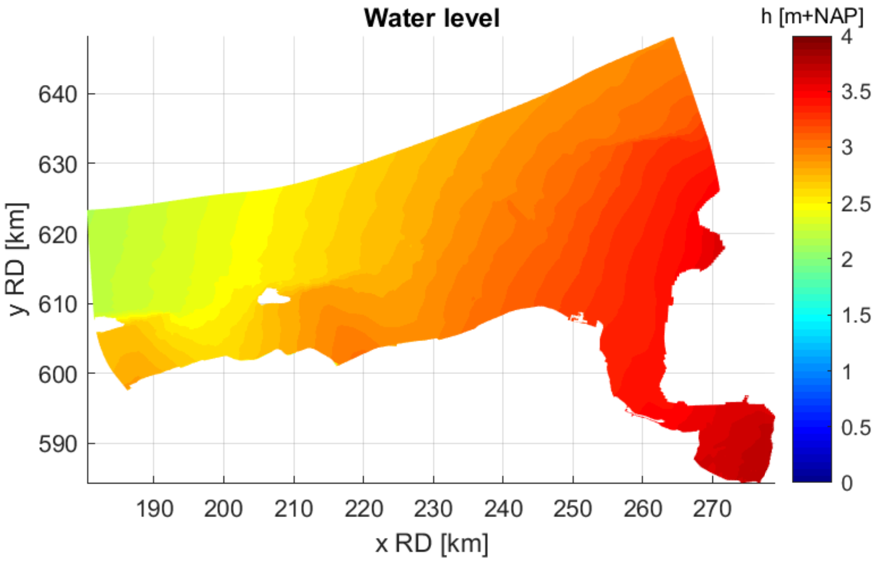

Figure III.19: Variation of the ratio $H_{\mathrm{m0}}/\mathrm{d}$ and water level h for G3 grid, 11 January 2015 02:10

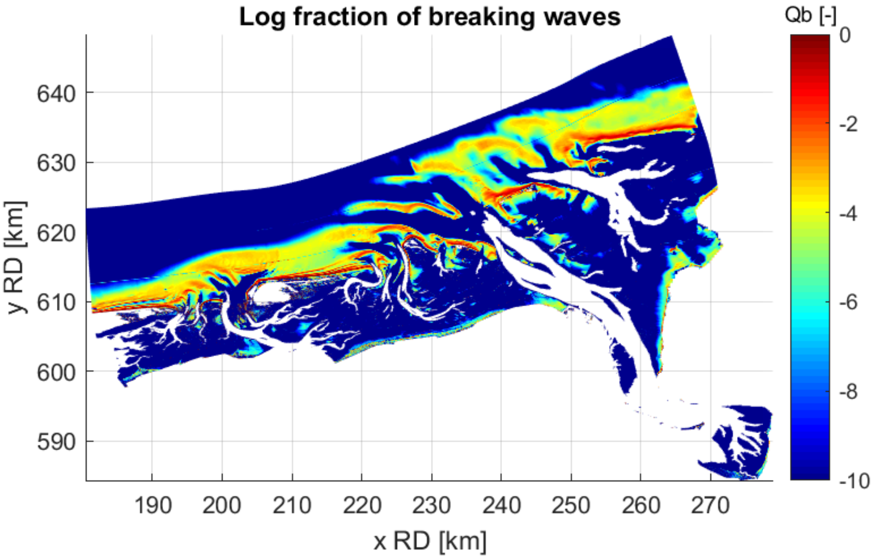

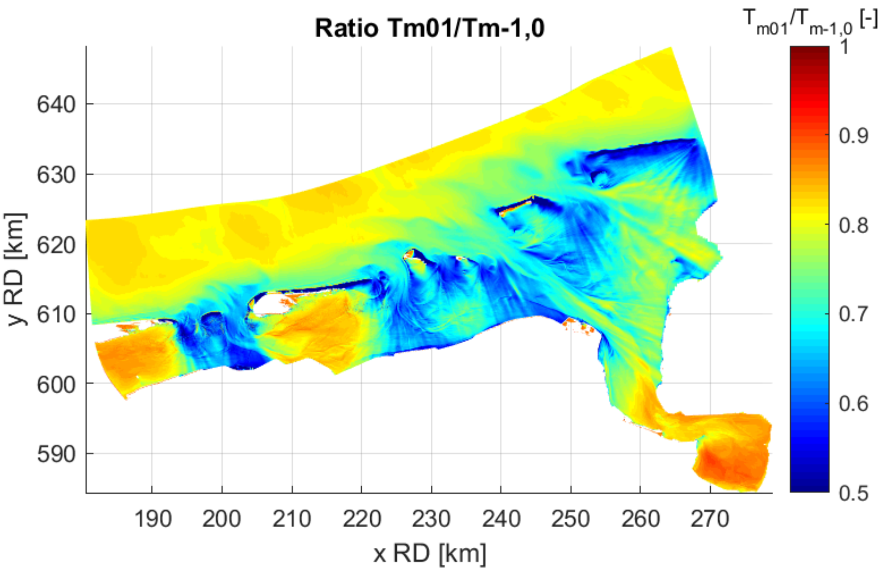

Figure III.20: The variation of breaking waves for G3 grid and ratio $T_{\mathrm{m01}}\,/\,T_{\mathrm{m\text{-}1,0}}$ for G3 grid, 11 January 2015 02:10

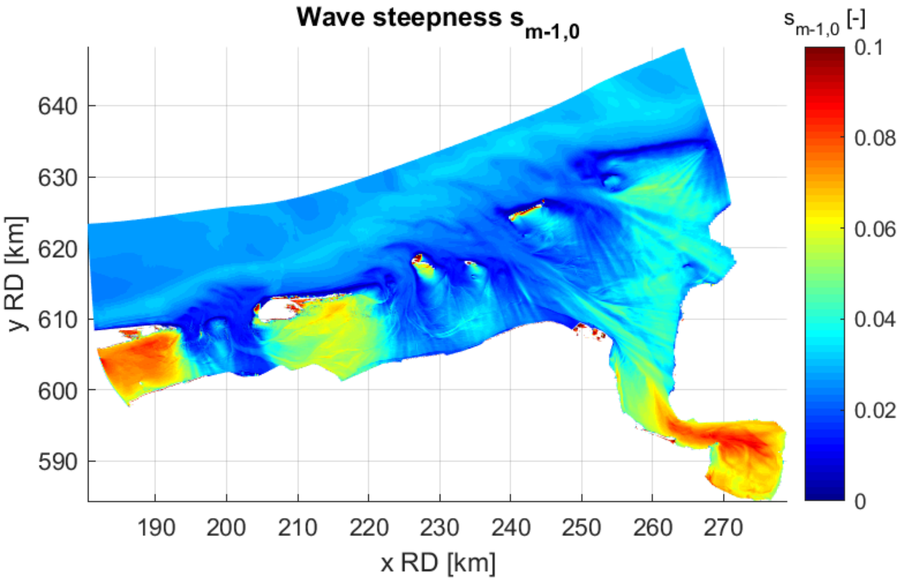

Figure III.21: The variation of wave steepness ($s_{m-1,0}$) for G3 grid, 11 January 2015 02:10

Results hindcast (004): 11 January 2015 02:40, Grid G3, SWAN 40.72ABCDE

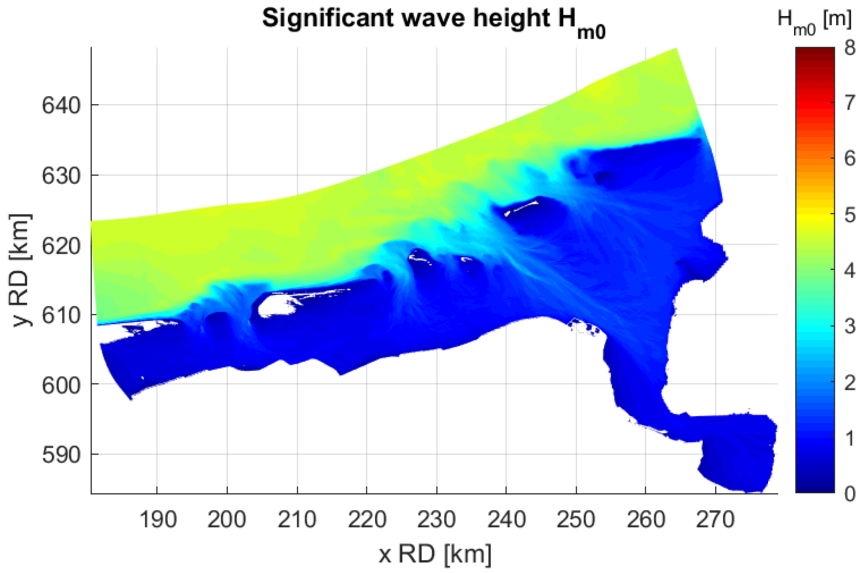

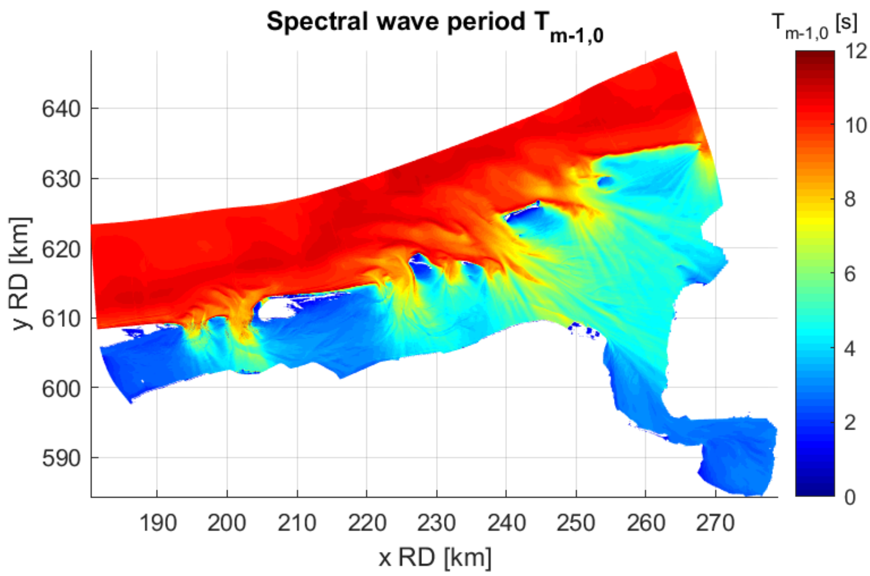

Figure III.22: Variation of significant wave height H_{m0} and spectral wave period $T_{\mathrm{m\text{-}1,0}}$ for G3 grid, 11 January 2015 02:40

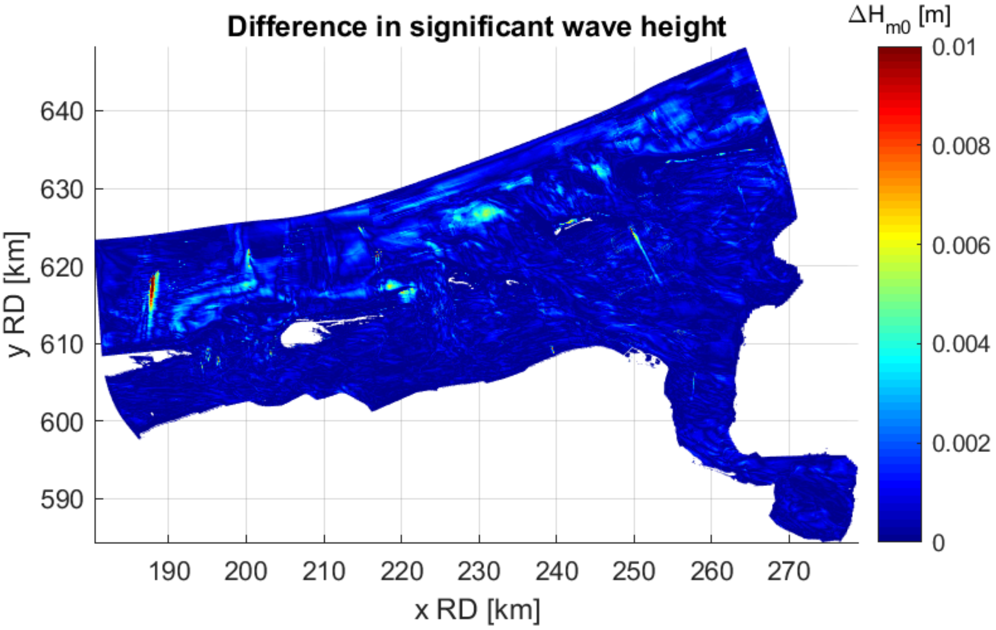

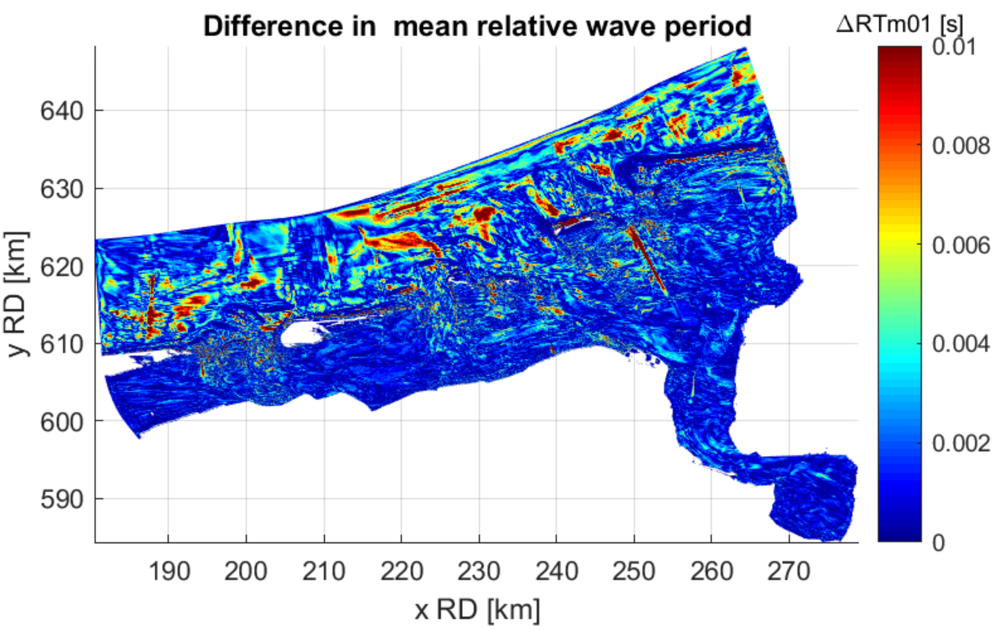

Figure III.23: Difference of significant wave height H_{m0} and relative spectral wave period RT_{m01} as computed in the last two iterations for G3 grid, 11 January 2015 02:40

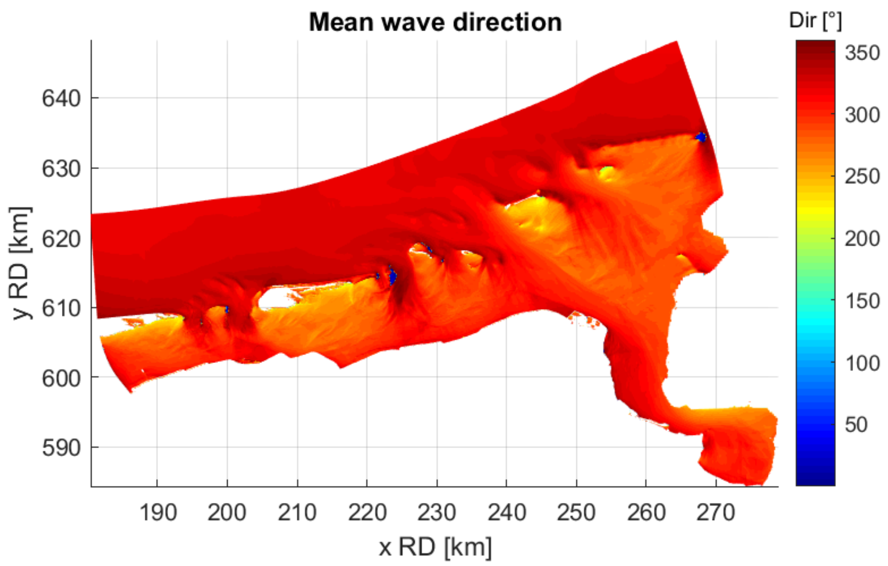

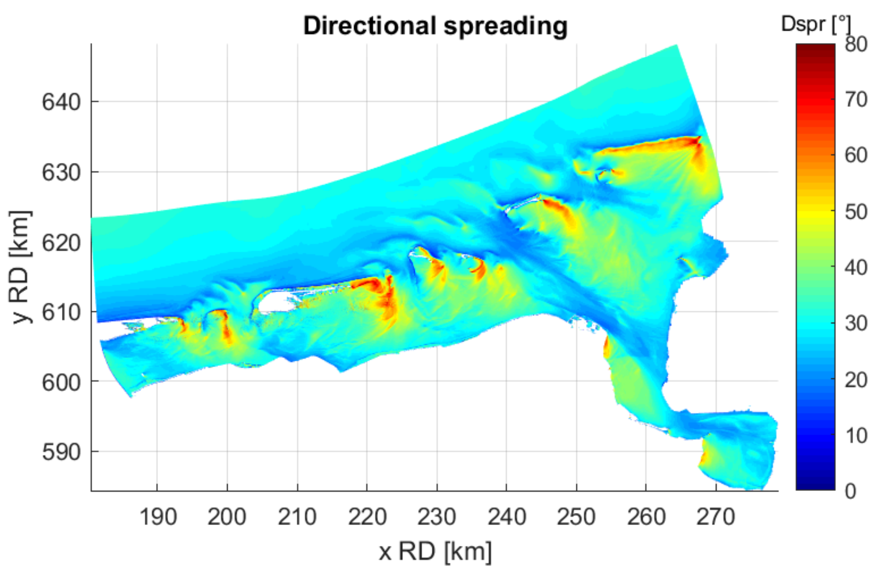

Figure III.24: Variation of mean wave direction DIR and directional spreading Dspr for G3 grid, 11 January 2015 02:40

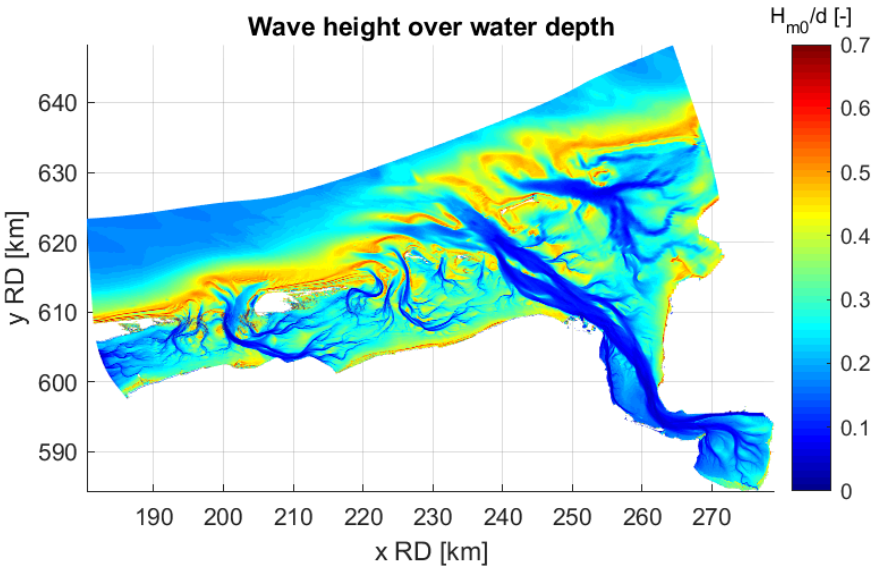

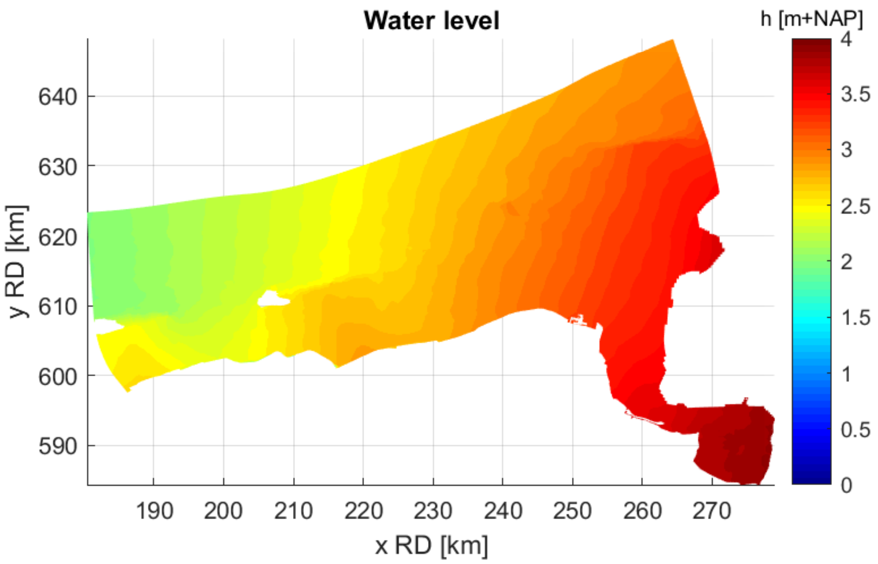

Figure III.25: Variation of the ratio $H_{\mathrm{m0}}/\mathrm{d}$ and water level h for G3 grid, 11 January 2015 02:40

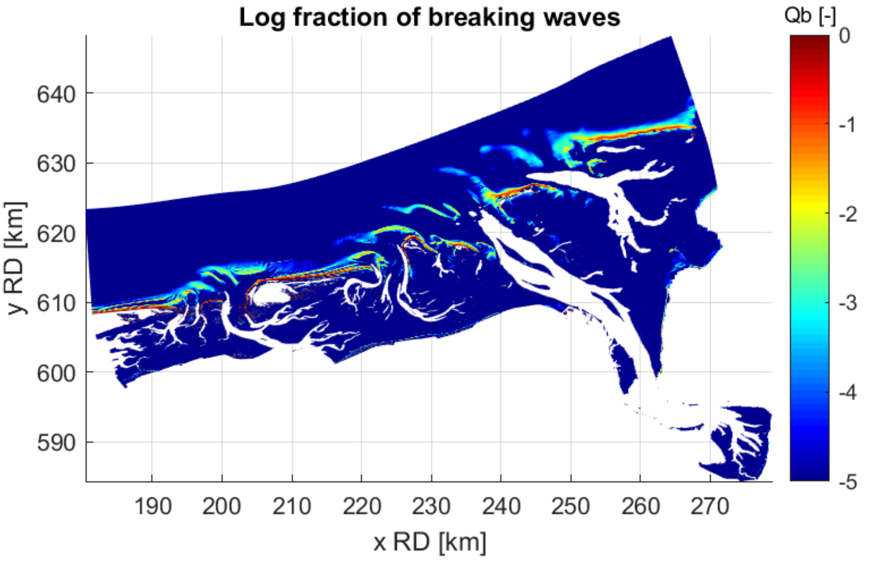

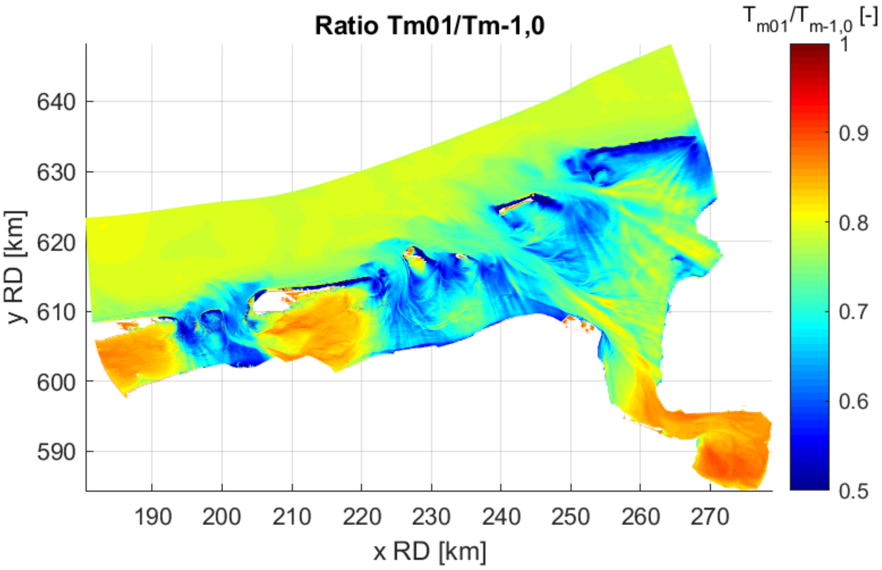

Figure III.26: The variation of breaking waves for G3 grid and ratio $T_{\mathrm{m01}}\,/\,T_{\text{m-1,0}}$ for G3 grid, 11 January 2015 02:40

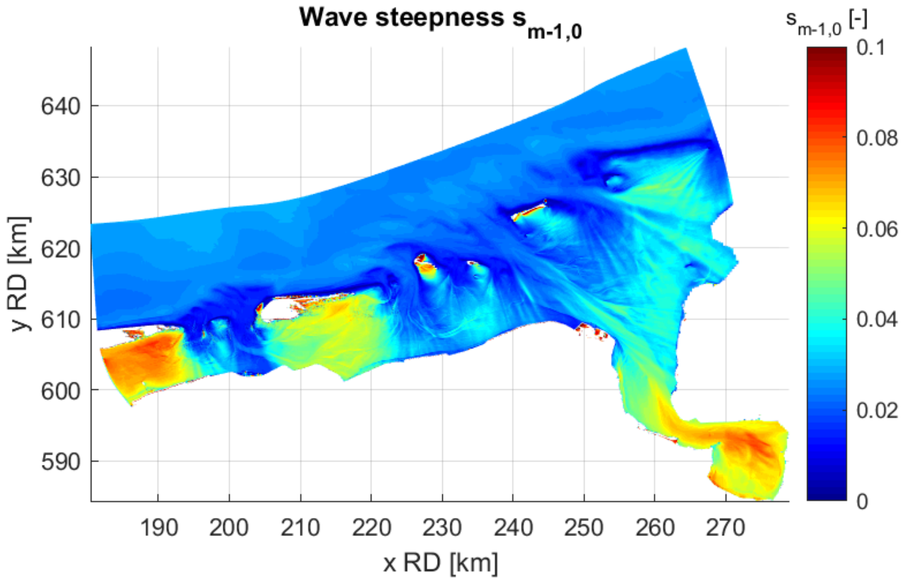

Figure III.27: The variation of wave steepness ($s_{m-1,0}$) for G3 grid, 11 January 2015 02:40

III.4. Variance density spectra

Measured variance density spectra are compared with calculated SWAN spectra. This is shown in Figures III.28, III.29 and III.30 for offshore locations Schiermonnikoog Noord (SMN1), Borkum Noord (BRKN1) and Westereems West (WEW1). In Figure III.31, SWAN variance density spectra are plotted for measurement locations in the Eastern Wadden Sea. For these locations no measurements were requested.

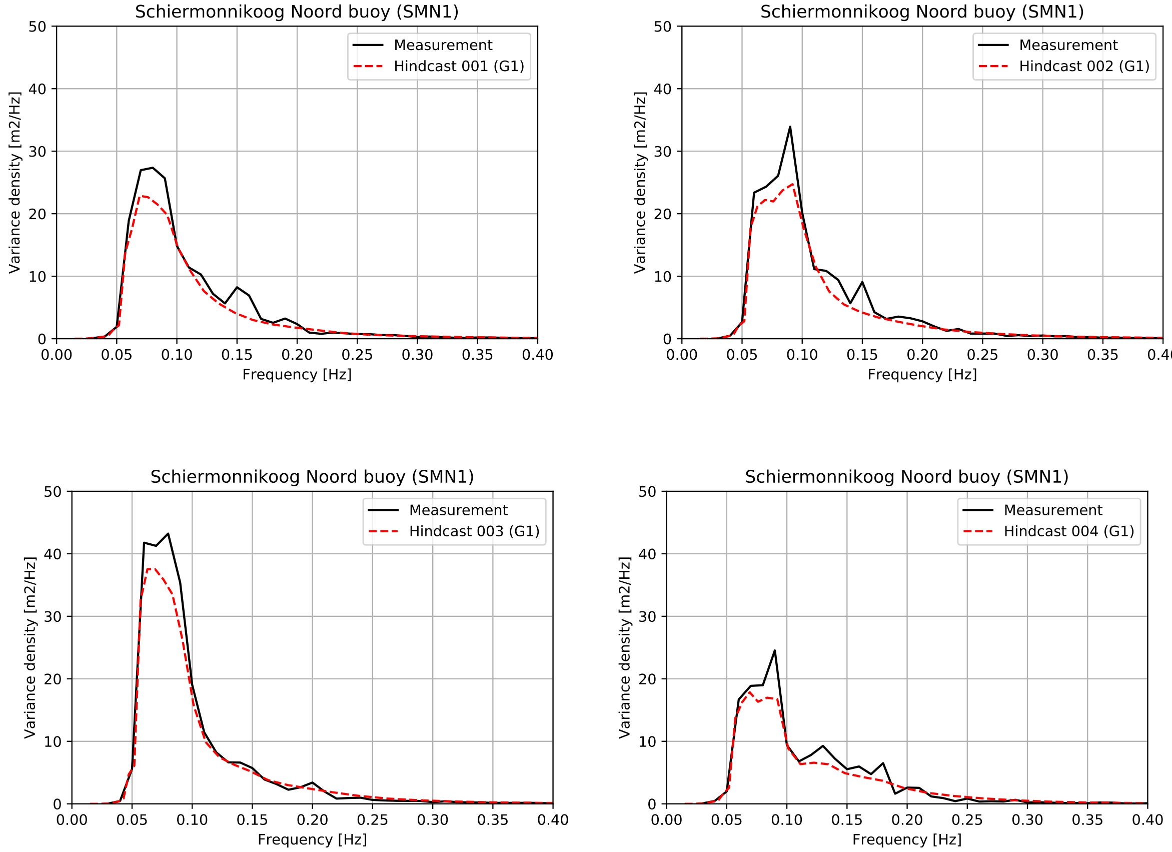

Figure III.28: Measured wave spectra at Schiermonnikoog Noord buoy compared to SWAN hindcast 2015

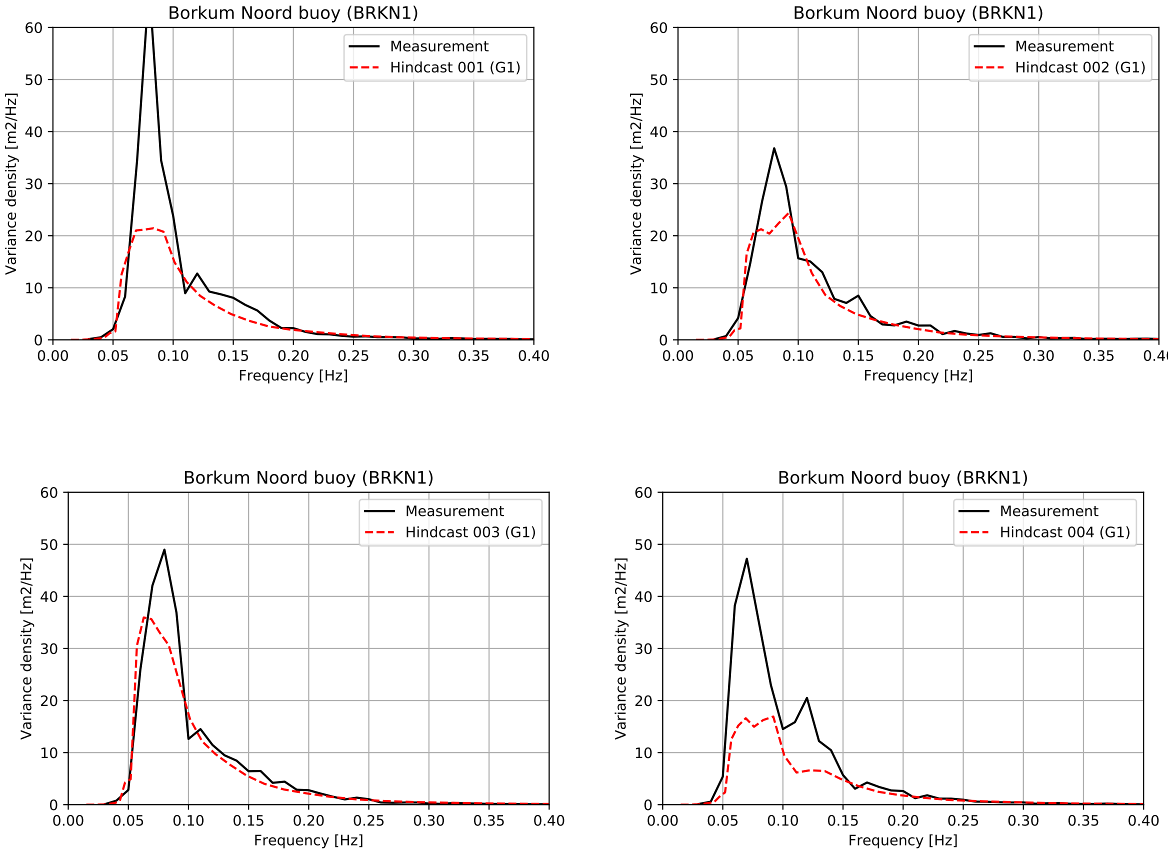

Figure III.29: Measured wave spectra at Borkum Noord buoy compared to SWAN hindcast 2015

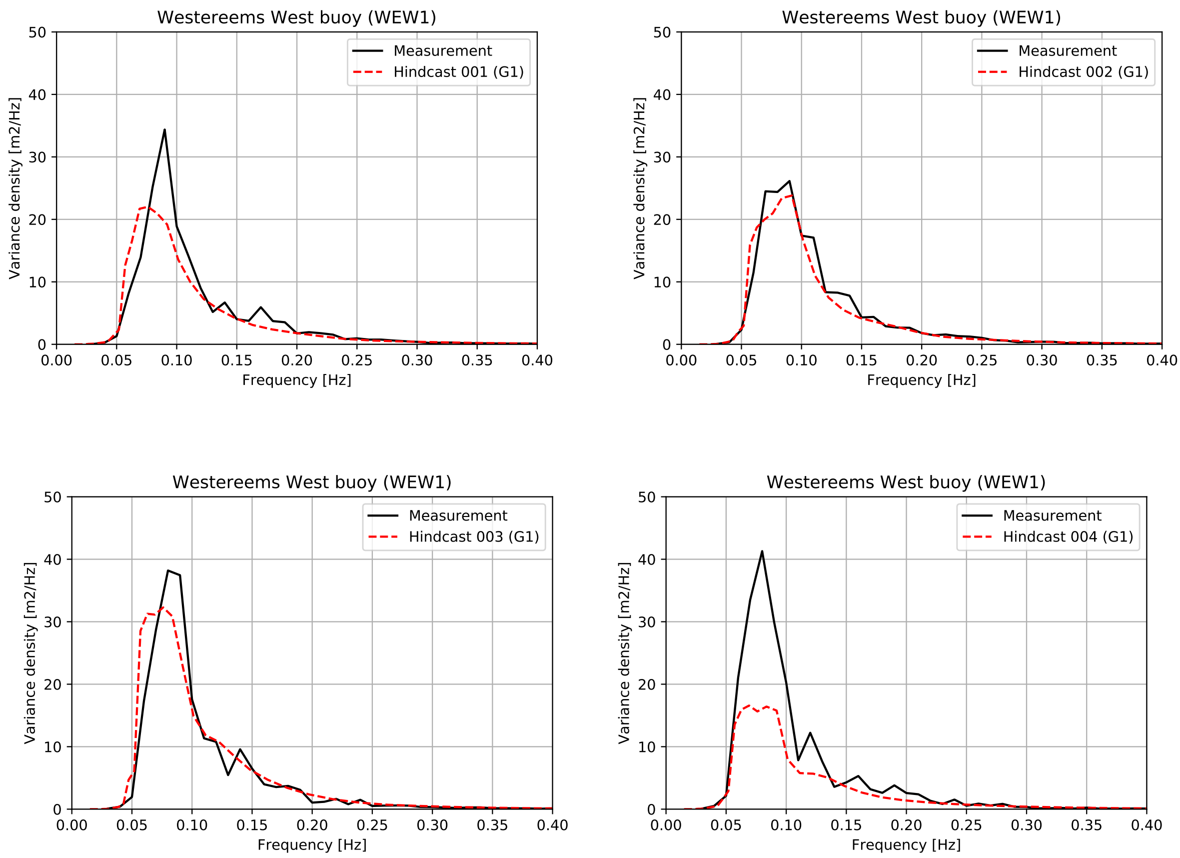

Figure III.30: Measured wave spectra at Westereems West buoy compared to SWAN hindcast 2015

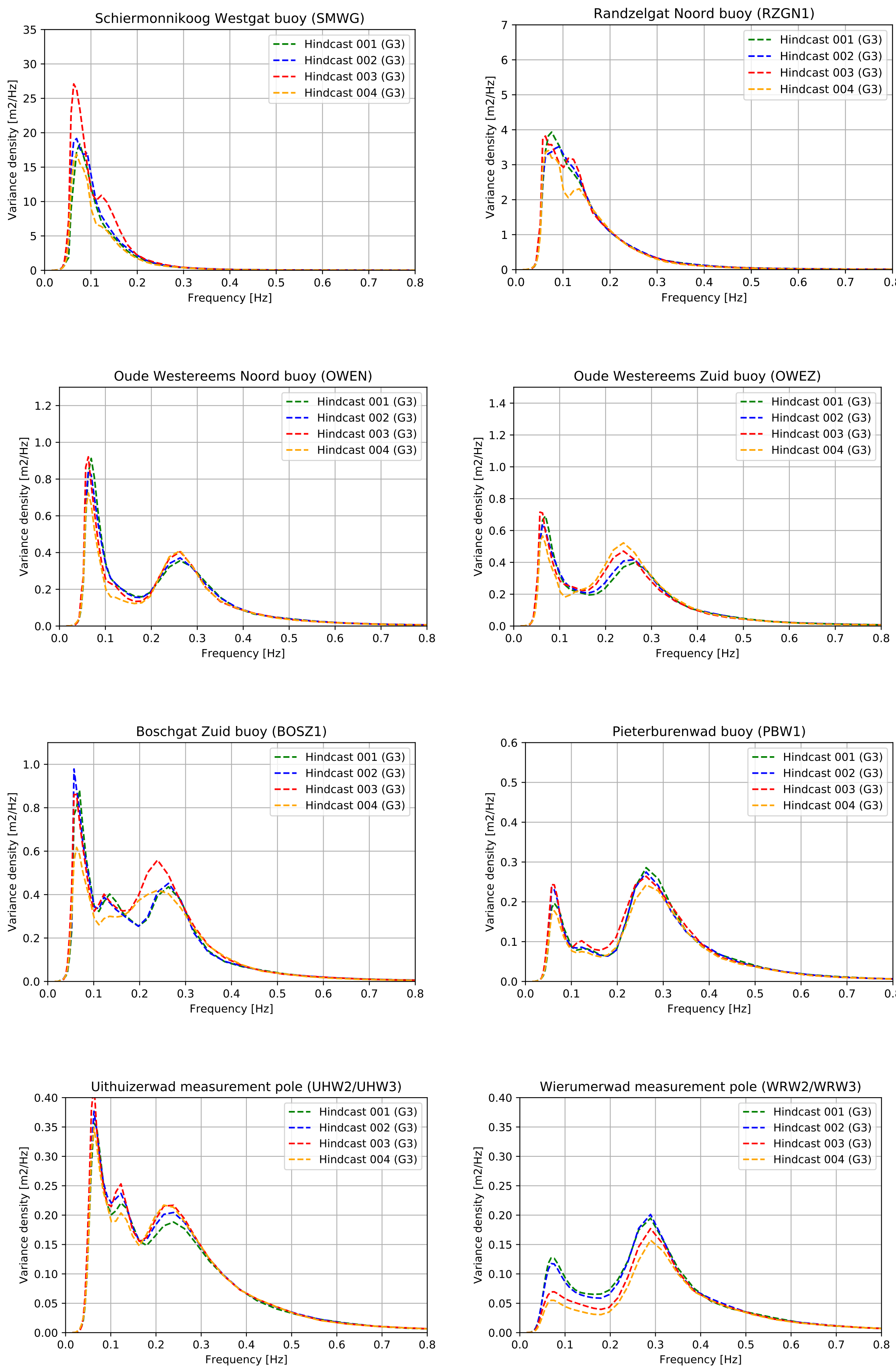

Figure III.31: Wave spectra of variance density from SWAN hindcast 2015

Table III.2: Measured spectral wave height H_{m0} [m] compared to SWAN output for 11 January 2015

Hindcast 11-01-2015 Locations	X	Y	Measured [m] 01:10	Model 001 (G1) 01:10	Model 001 (G3) 01:10	Measured [m] 01:30	Model 002 (G1) 01:30	Model 002 (G3) 01:30	Measured [m] 02:10	Model 003 (G1) 02:10	Model 003 (G3) 02:10	Measured [m] 02:40	Model 004 (G1) 02:40	Model 004 (G3) 02:40
Ameland Westgat	191767	611861		4.5209	4.51566		4.73792	4.71345		4.81759	4.85204		4.38814	4.18928
Boschgat Zuid	226200	612700	1.39	-9	1.44426	1.47	-9	1.44418	1.41	-9	1.52053	1.47	-9	1.40969
Huibertgat	221990	621330		4.5675	4.56546		4.66705	4.68237		4.84499	4.91653		4.10397	4.14059
Lauwers Oost	225500	617700		-9	-9		-9	-9		-9	-9		-9	-9
Oude Westereems Noord	240557	614915	1.07	-9	1.34065	1.12	-9	1.33367	1.14	-9	1.31345	1.1	-9	1.26115
Oude Westereems Zuid	243806	612177	1.17	-9	1.36713	1.26	-9	1.37879	1.21	-9	1.39882	1.2	-9	1.40128
Pieterburenwad	225792	608394	0.96	-9	1.01341	1.01	-9	1.00756	0.9	-9	1.02981	0.91	-9	0.96917
Randzelgat Noord	237439	621340	2.1	2.18023	2.77056	2.1	2.20357	2.75924	2.22	2.23362	2.77756	2.11	2.21713	2.62152
Schiermonnikoog Noord	206527	623484	5.85	5.02329	4.88108	5.74	5.29569	5.14048	6.2	6.02624	5.82942	5.67	4.76282	4.59031
Schiermonnikoog Westgat	195585	615149	4.93	4.78594	4.67005	5.21	5.02488	4.97293	5.52	5.49669	5.5089	5.39	4.48719	4.48905
Uithuizerwad (Radac)	245996	609772	-	-9	1.06861	-	-9	1.09293	-	-9	1.10581	-	-9	1.07822
Uithuizerwad (Etrometa)	245996	609772	0.67	-9	1.06861	0.67	-9	1.09293	0.73	-9	1.10581	0.73	-9	1.07822
Westereems Oost	230086	626634	4.76	4.7702	4.68552	4.65	4.89139	4.7599	4.47	5.05277	4.82984	4.87	4.46983	4.29539
Westereems West	219900	626397	5.32	4.94084	4.85664	5.34	5.15409	5.03414	5.57	5.92218	5.84	5.55	4.41835	4.38006
Wierumergronden	192882	614562		4.65762	4.58265		4.90851	4.83343		5.75568	5.63856		4.42163	4.37185
Wierumerwad (Radac)	199957	602618	-	-9	0.9013	0.74	-9	0.89142	-	-9	0.82431	-	-9	0.78099
Wierumerwad (Etrometa)	199957	602618	1.86	-9	0.9013	2.09	-9	0.89142	1.34	-9	0.82431	0	-9	0.78099

Table III.3: Measured spectral wave period $T_{m-1,0}$ [s] compared to SWAN output for 11 January 2015

Hindcast 11-01-2015 Locations	X	Y	Measured [s] 01:20	Model 001 (G1) 01:20	Model 001 (G3) 01:20	Measured [s] 01:30	Model 002 (G1) 01:30	Model 002 (G3) 01:30	Measured [s] 02:10	Model 003 (G1) 02:10	Model 003 (G3) 02:10	Measured [s] 02:40	Model 004 (G1) 02:40	Model 004 (G3) 02:40
Ameland Westgat	191767	611861		9.754	9.7169		9.8261	9.7653		9.8987	10.296		9.7497	10.3374
Boschgat Zuid	226200	612700	5.4	-9	6.9605	5.6	-9	7.055	5.8	-9	6.7854	5.9	-9	6.4608
Huibertgat	221990	621330		10.1343	10.0142		10.1671	10.0988		10.4373	10.4173		10.135	10.56
Lauwers Oost	225500	617700	7.9	7.5779	7.888	7.9	7.5479	8.0129	7.7	7.2611	7.862	7.4	7.299	7.8933
Oude Westereems Noord	240557	614915	4	-9	7.0958	4.3	-9	7.0465	4	-9	7.1043	4	-9	6.6809
Oude Westereems Zuid	243806	612177	4.1	-9	6.4748	4.1	-9	6.3928	4.1	-9	6.5047	4.2	-9	5.9818
Pieterburenwad	225792	608394	4.4	-9	5.0515	4.5	-9	5.2224	4.6	-9	5.3613	4.3	-9	5.0463
Randzelgat Noord	237439	621340	7.6	7.2675	8.7527	7.7	7.3409	8.6959	7.3	7.5313	8.9572	7.2	7.4198	8.7526
Schiermonnikoog Noord	206527	623484	10.7	10.7467	10.4735	10.7	10.7839	10.6409	11.7	11.5866	11.5378	11	10.2778	10.2923
Schiermonnikoog Westgat	195585	615149	11.1	10.3705	10.2321	11.1	10.4178	10.4997	11.7	10.7344	10.8369	11.6	10.5028	10.6257
Uithuizerwad (Radac)	245996	609772	-	-9	6.4487	-	-9	6.472	-	-9	6.6021	-	-9	6.3392
Uithuizerwad (Etrometa)	245996	609772	4.9	-9	6.4487	5	-9	6.472	4.9	-9	6.6021	4.9	-9	6.3392
Westereems Oost	230086	626634	10	9.8723	9.6497	10.2	9.959	9.6768	10.8	10.2615	9.9923	10.7	10.2565	10.0801
Westereems West	219900	626397	10.4	10.6729	10.4576	10.5	10.7458	10.5468	11	11.2229	11.1803	10.7	10.805	10.6974
Wierumergronden	192882	614562		10.432	10.3545		10.6119	10.6082		10.7843	11.0789		10.4899	10.6687
Wierumerwad (Radac)	199957	602618	-	-9	4.8645	4.5	-9	4.763	-	-9	4.2756	-	-9	4.0147
Wierumerwad (Etrometa)	199957	602618	5.3	-9	4.8645	4.9	-9	4.763	5.3	-9	4.2756	11.3	-9	4.0147

III.5. Results at HRbasis locations

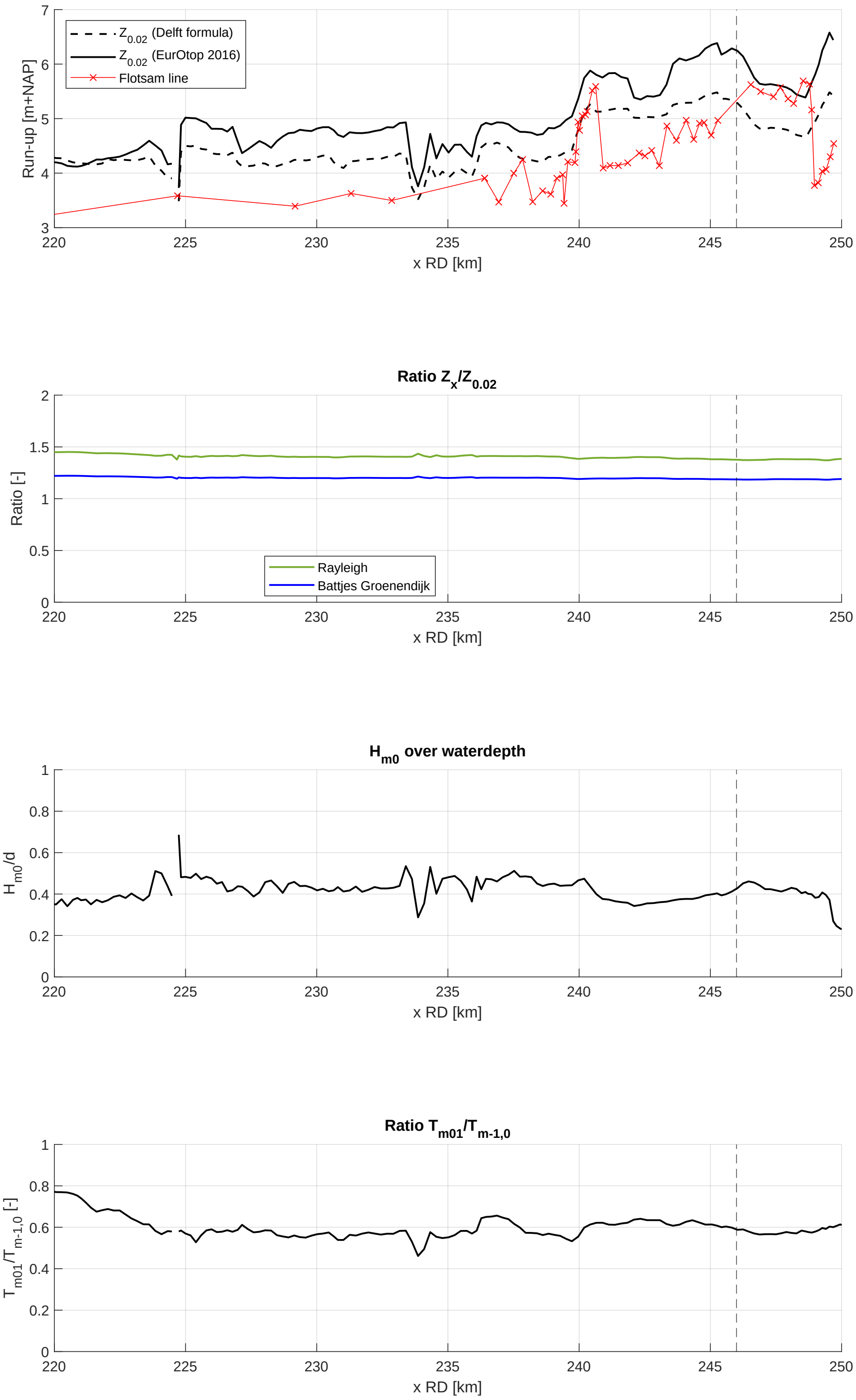

Figure III.32: Results at HRbasis locations for highest wave run-up at 11 January 2015 01:30.

IV

Model results 2017

IV.1. Water level

Measured water levels are plotted against calculated levels from WAQUA (dcsmv6-zunov4) in Figure IV.1. The following locations are shown in Figure IV.1: Huibertgat, Wierumergronden, Nes, Schiermonnikoog, Lauwersoog, Eemshaven, Delfzijl, Nieuwe Statenzijl.

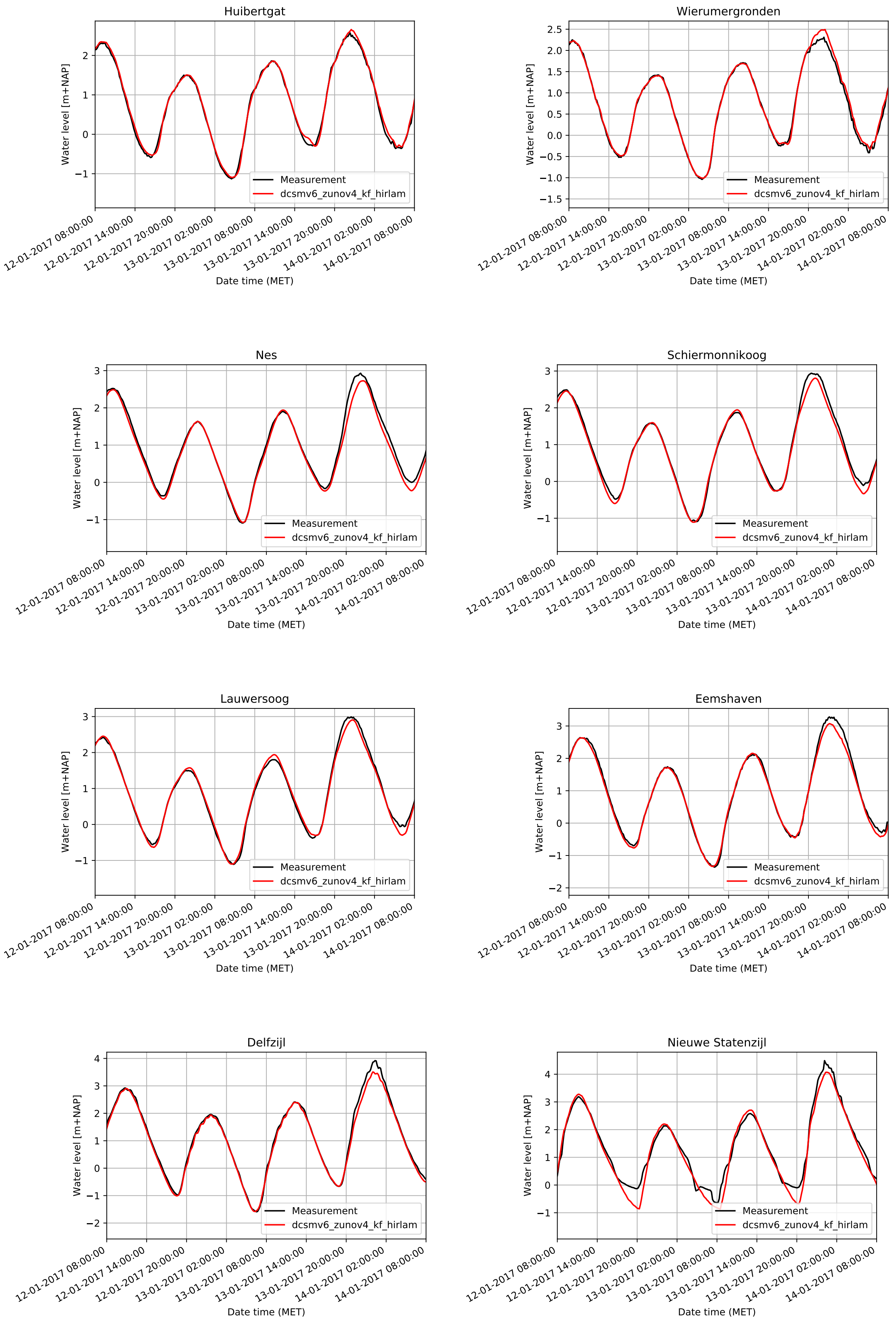

Figure IV.1: Comparison between measured and modelled water levels for hindcast 2017.

IV.2. Wind

Measured wind speed(Figure IV.2) and direction(Figure IV.3) are plotted against calculated HIRLAM wind speed and direction. The following locations are shown in Figure IV.2 and Figure IV.3: Huibertgat, Amelander Westgat (AWG), Lauwersoog, and Nieuwe Beerta.

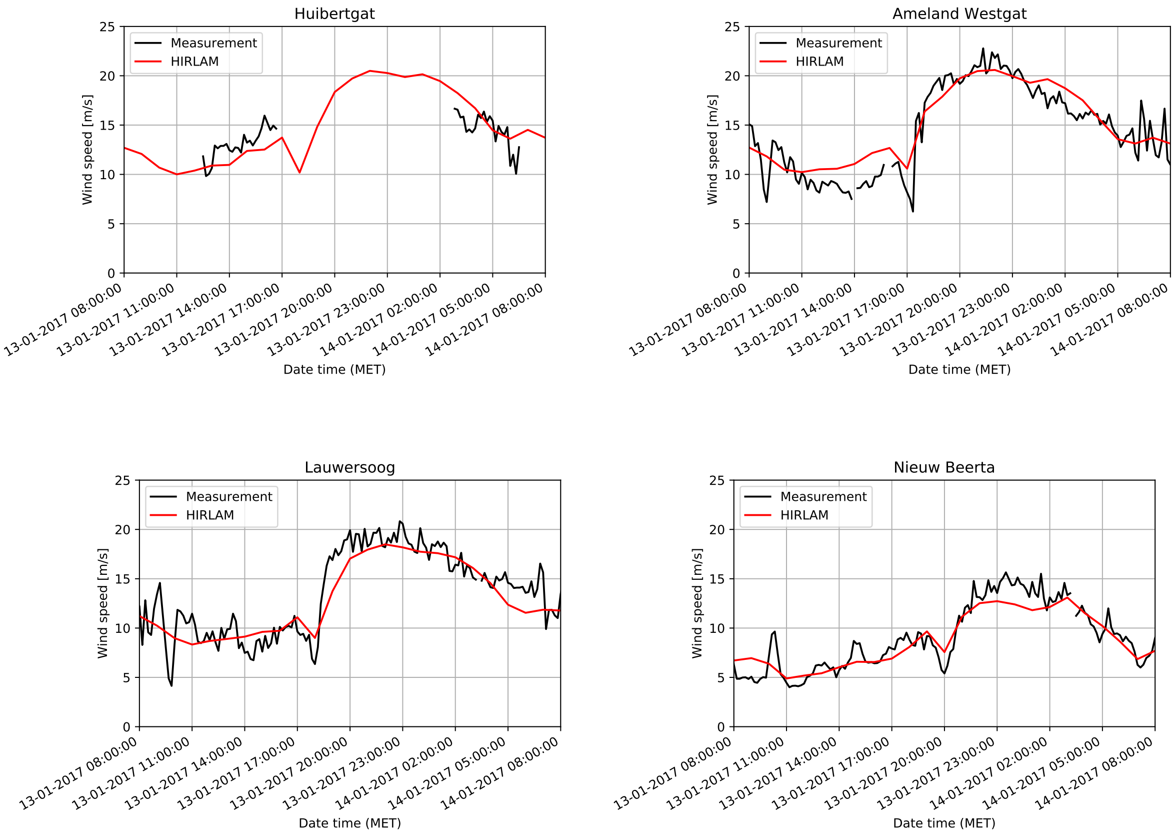

Figure IV.2: Comparison between measured and HIRLAM wind speed for hindcast 2017.

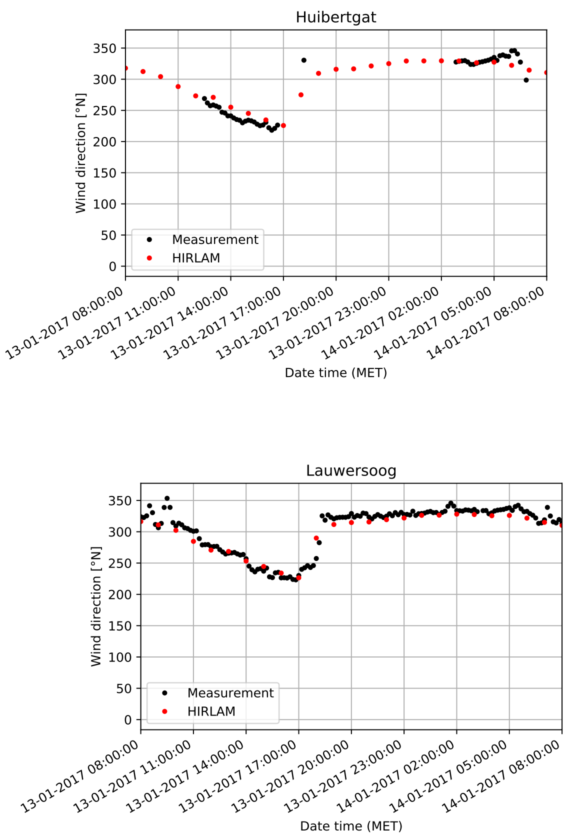

Figure IV.3: Comparison between measured and HIRLAM wind direction for hindcast 2017.

IV.3. Different computational settings

The hindcast of 13 January 2017 was initially performed with a criterion of 99.0 % of accepted points. The convergence behaviour was checked by performing a test run with a stricter criterion of 99.8 %. The difference between these criteria for hindcast 004 with npnts = 99.0% and npnts =99.8% is shown in Figure IV.4 and Figure IV.5.

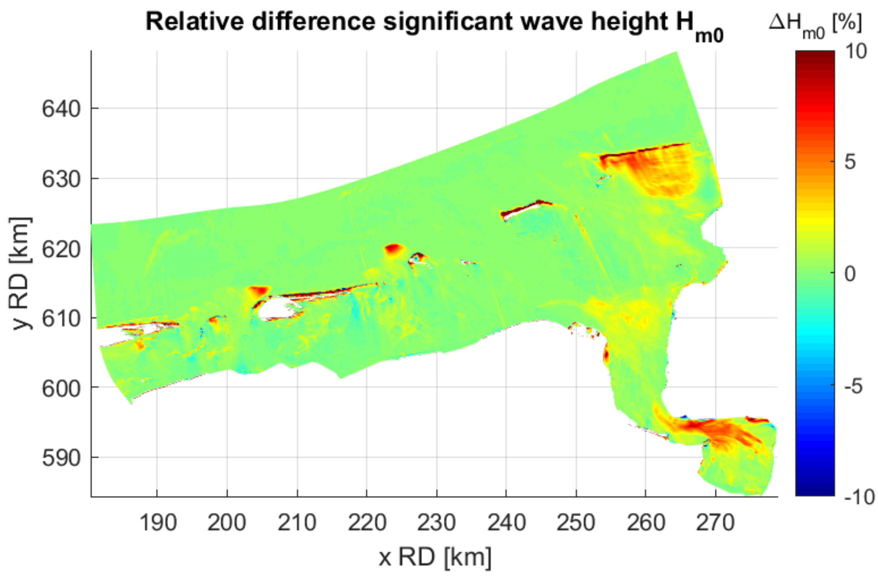

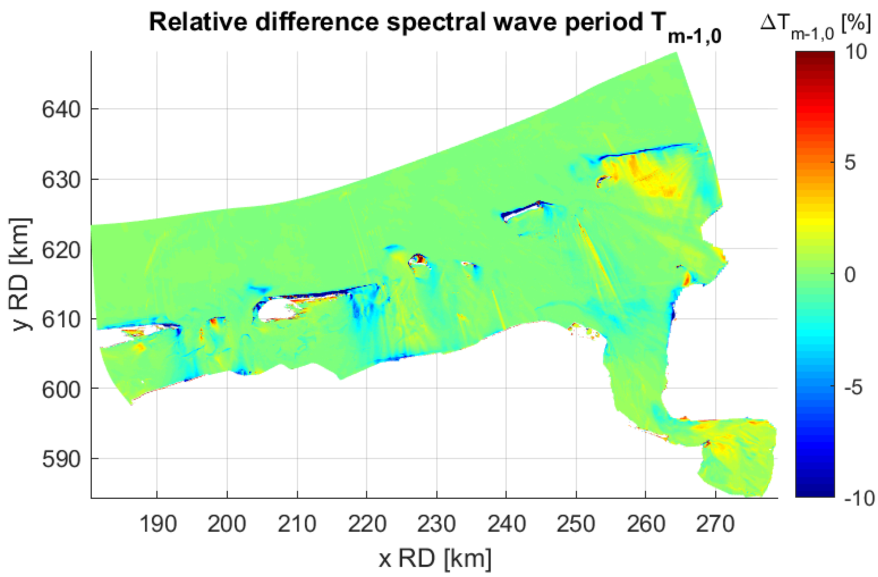

Figure IV.4: Relative difference in significant wave height H_{m0} and spectral wave period $T_{\mathrm{m\text{-}1,0}}$ as result of using npnts = 99.8% instead of npnts = 99.0% for G3 grid, 13 January 2017 23:00

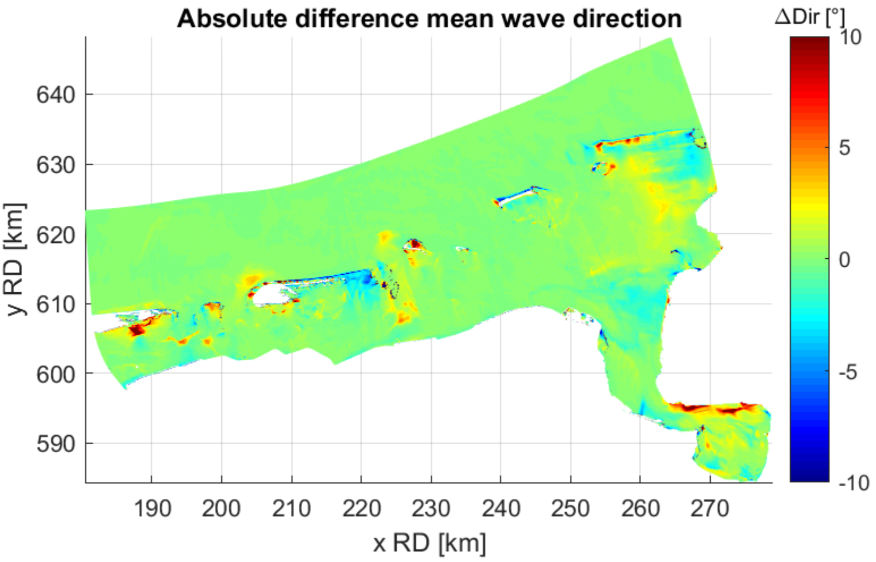

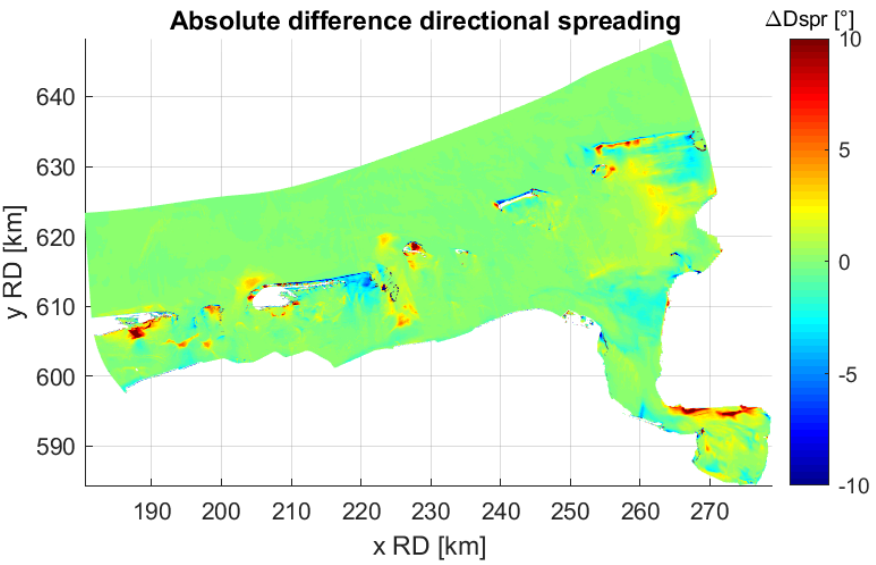

Figure IV.5: Absolute difference in mean wave direction Dir and directional spreading Dspr as result of using npnts = 99.8% instead of npnts = 99.0% for G3 grid, 13 January 2017 23:00

IV.4. SWAN spatial fields

Results hindcast (001): 13 January 2017 22:20, Grid G3, SWAN 40.72ABCDE

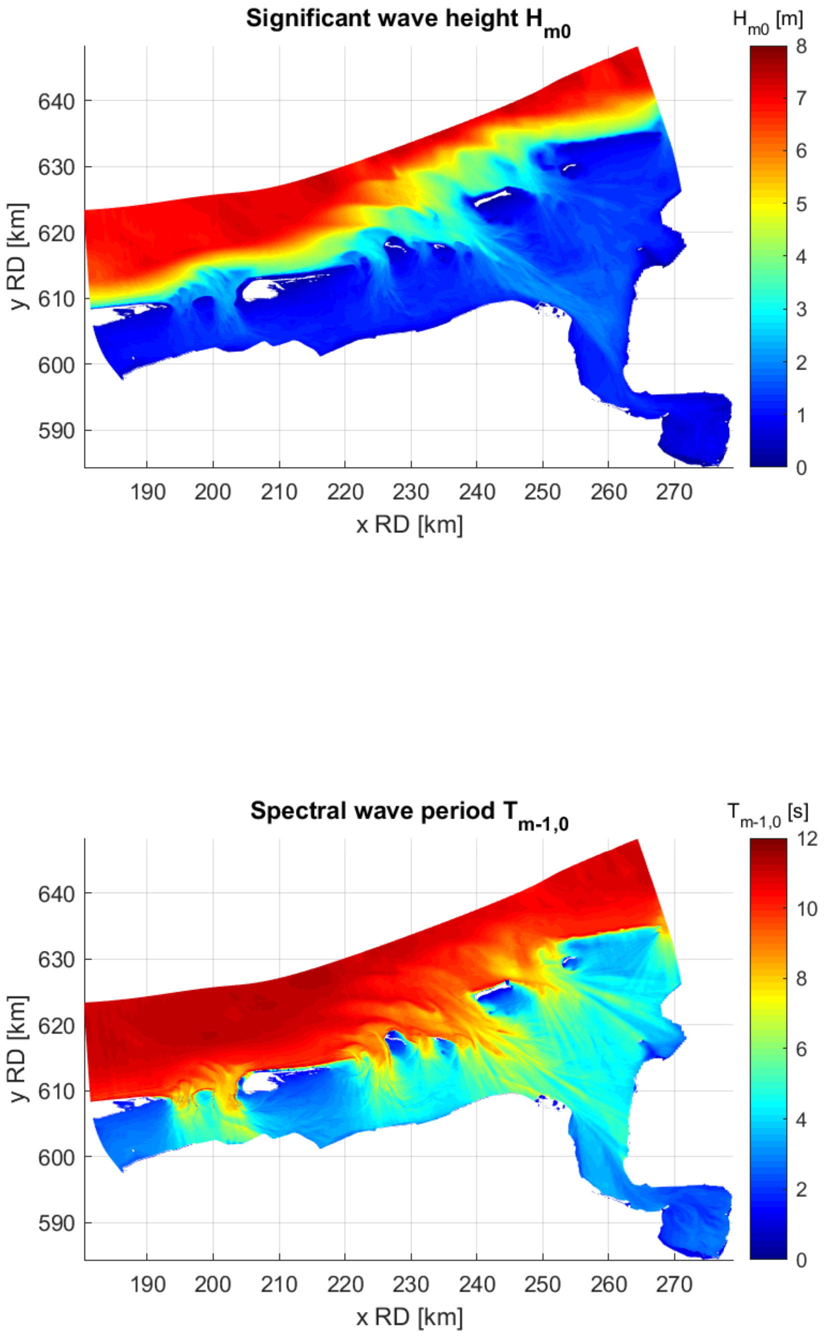

Figure IV.6: Variation of significant wave height H_{m0} and spectral wave period $T_{m-1,0}$ for G3 grid, 13 January 2017 22:20

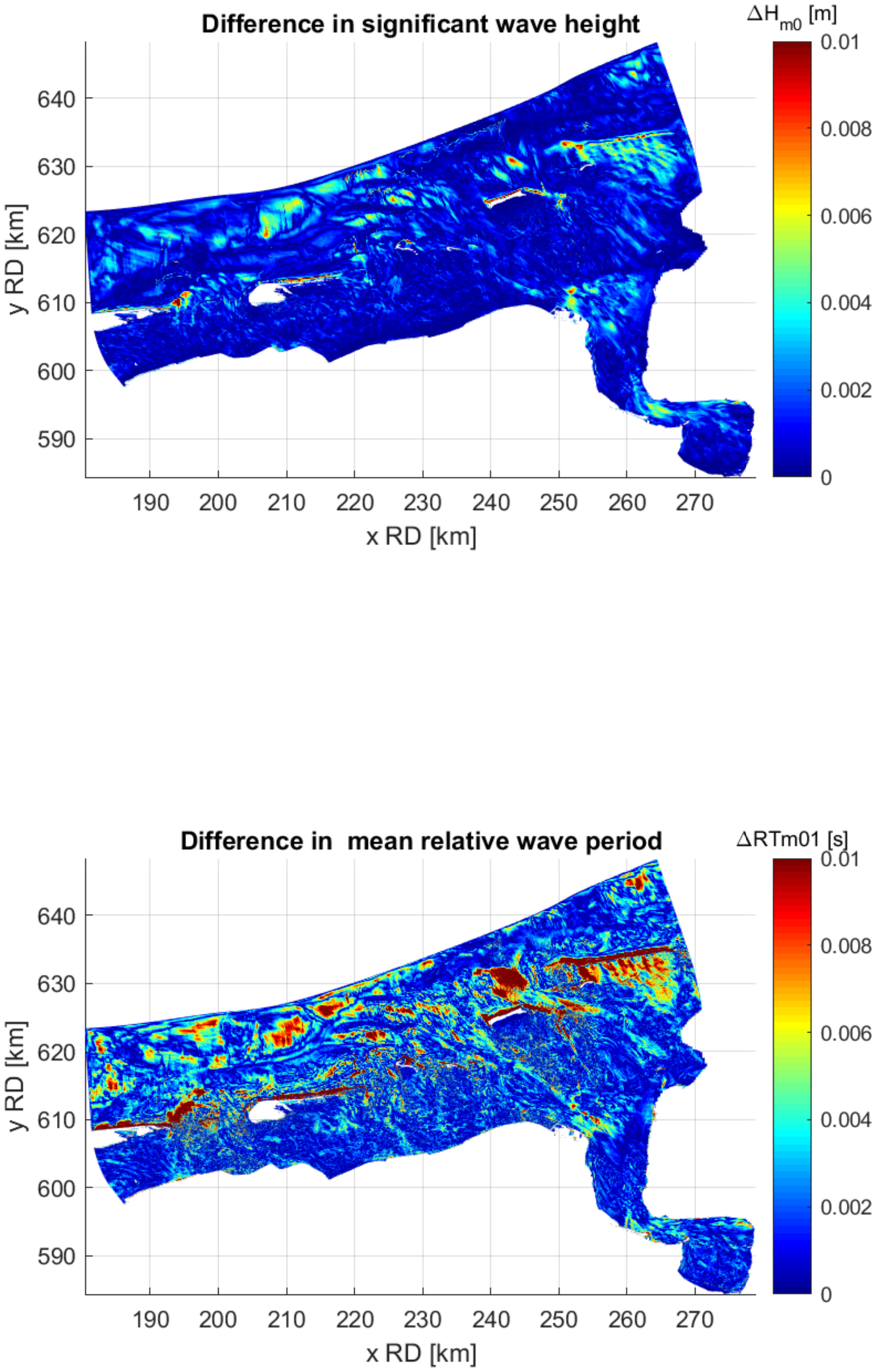

Figure IV.7: Difference of significant wave height H_{m0} and relative spectral wave period RT_{m01} as computed in the last two iterations for G3 grid, 13 January 2017 22:20

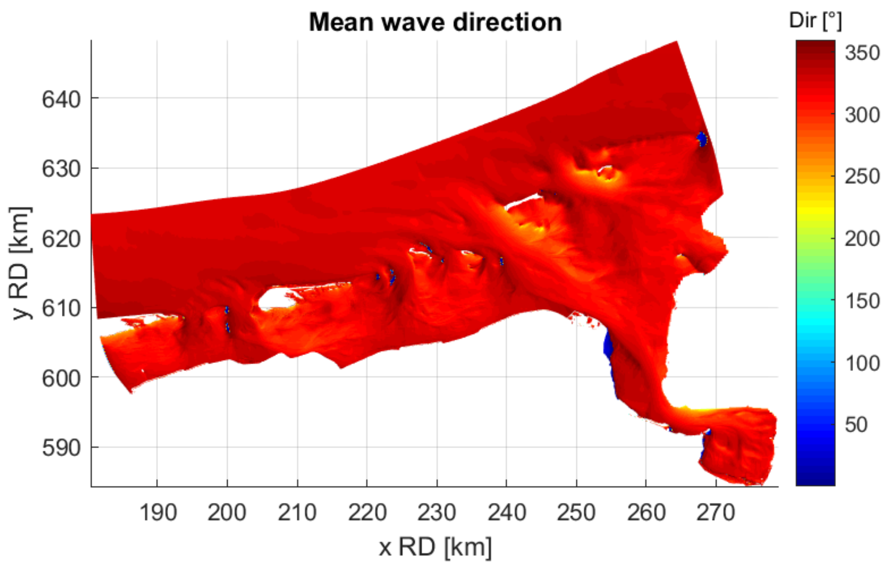

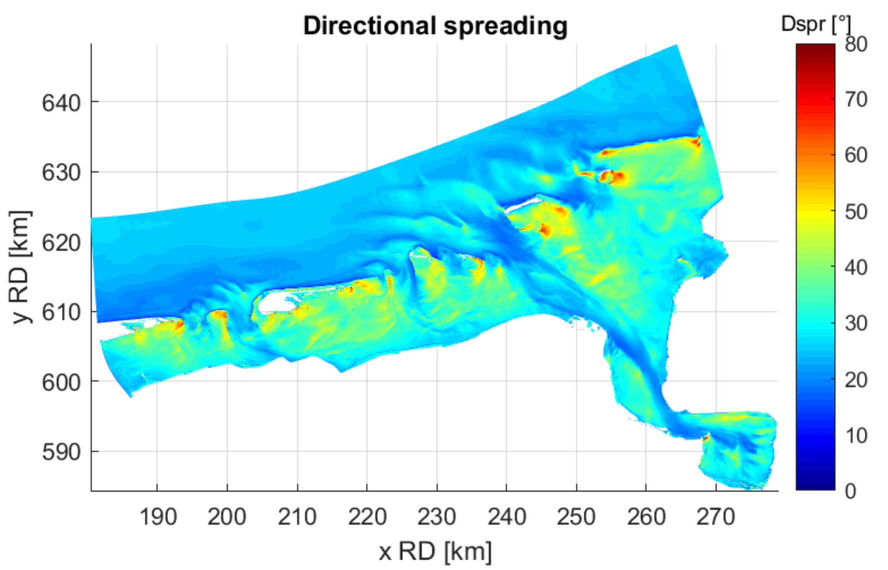

Figure IV.8: Variation of mean wave direction DIR and directional spreading Dspr for G3 grid, 13 January 2017 22:20

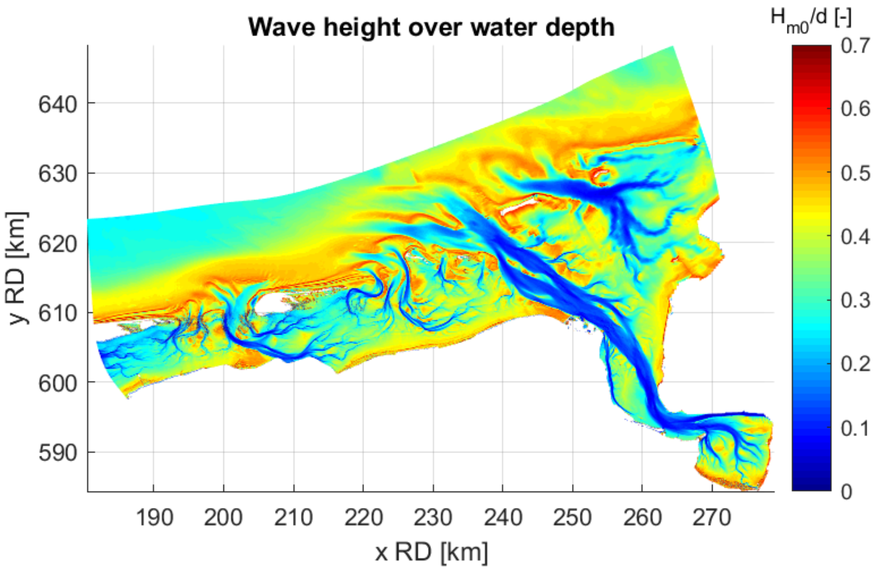

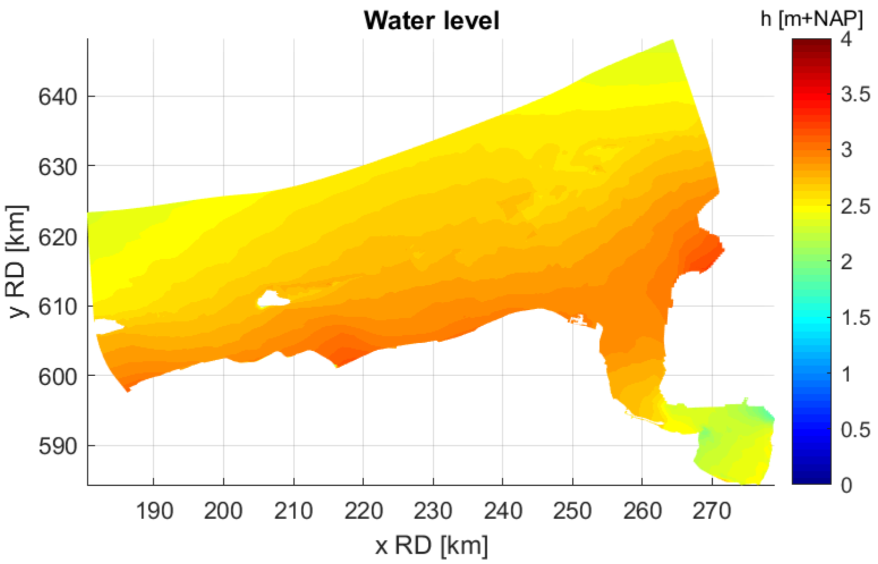

Figure IV.9: Variation of the ratio $H_{\mathrm{m0}}/\mathrm{d}$ and water level h for G3 grid, 13 January 2017 22:20

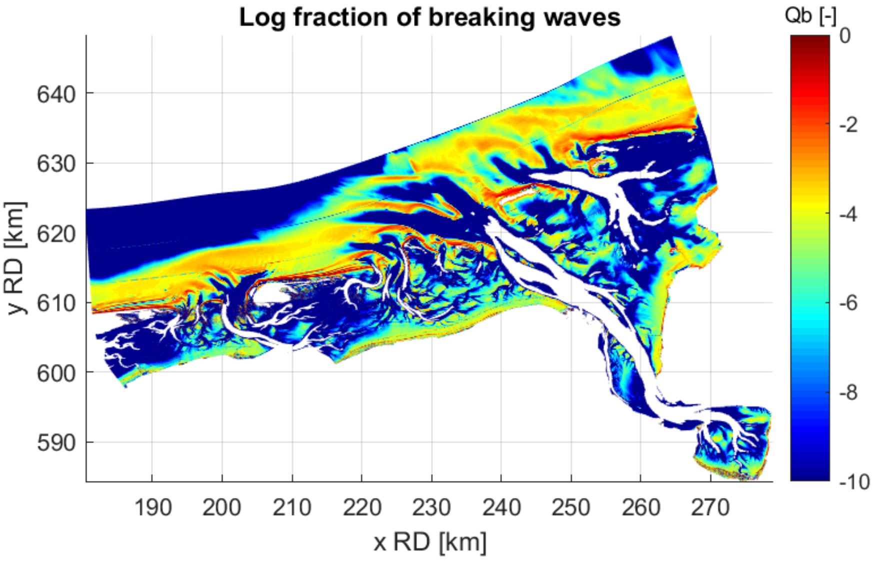

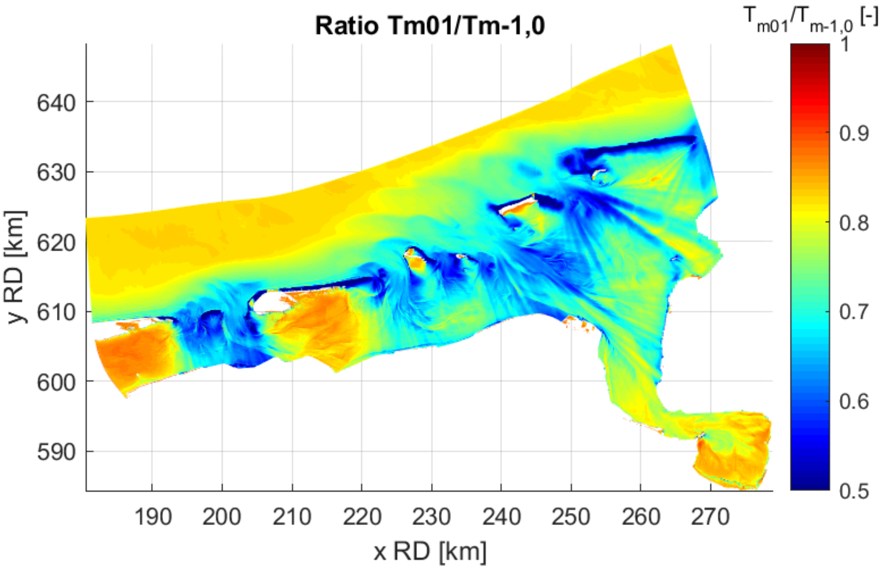

Figure IV.10: The variation of breaking waves and ratio $T_{\mathrm{m01}}/T_{\mathrm{m\text{-}1,0}}$ for G3 grid, 13 January 2017 22:20

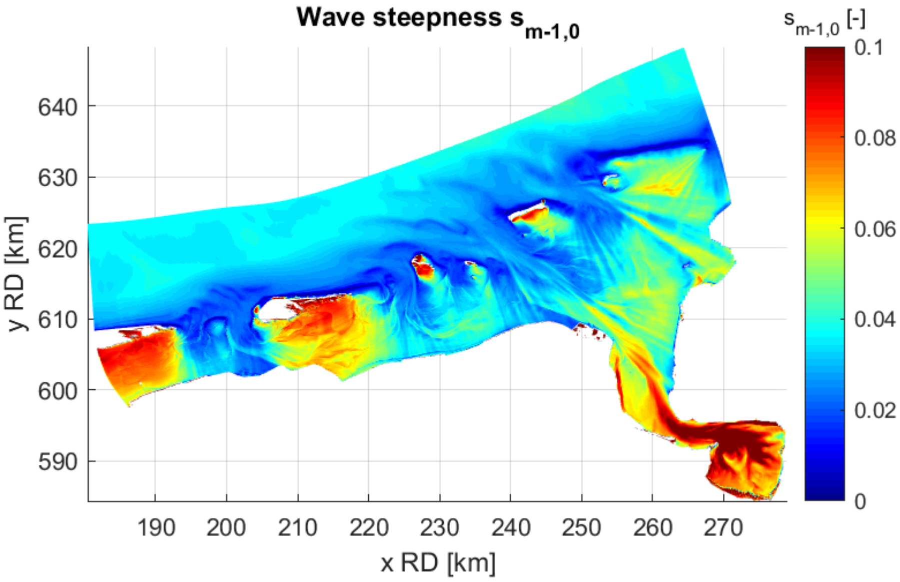

Figure IV.11: The variation of wave steepness ($s_{m-1,0}$) for G3 grid, 13 January 2017 22:20

Results hindcast (002): 13 January 2017 22:30, Grid G3, SWAN 40.72ABCDE

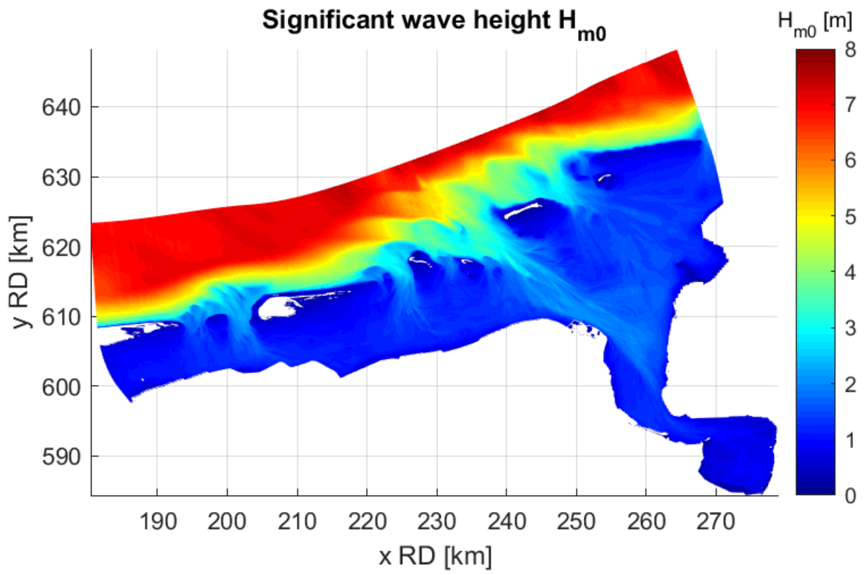

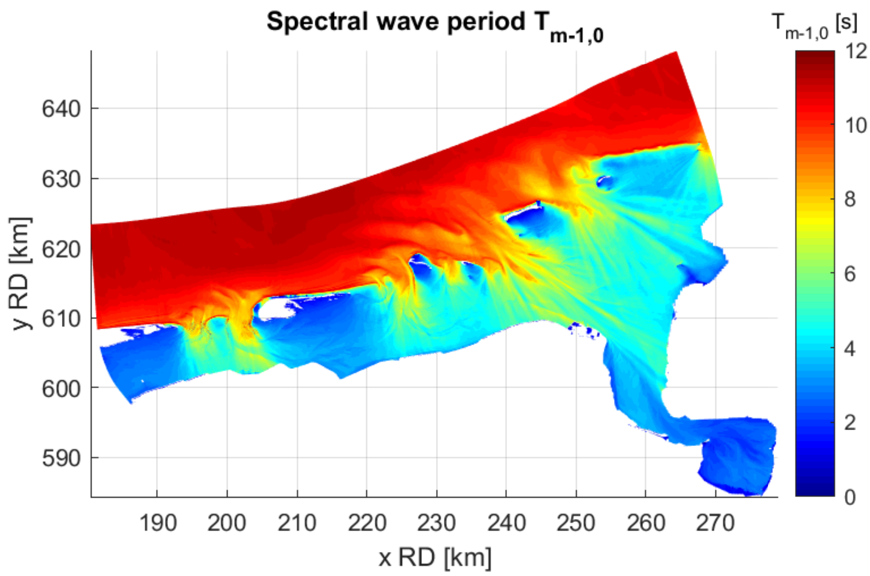

Figure IV.12: Variation of significant wave height H_{m0} and spectral wave period $T_{\text{m-1,0}}$ for G3 grid, 13 January 2017 22:30

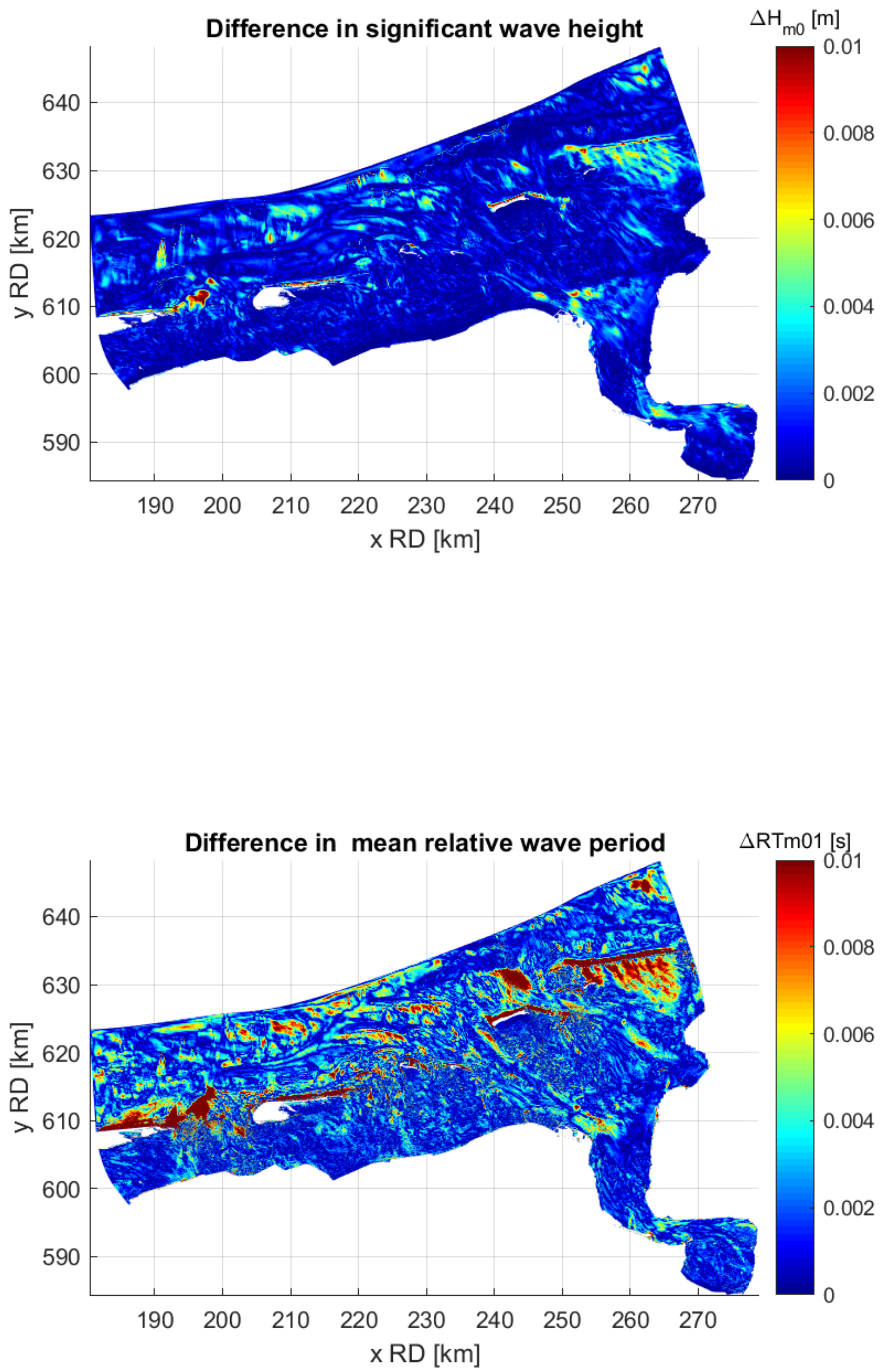

Figure IV.13: Difference of significant wave height H_{m0} and relative spectral wave period RT_{m01} as computed in the last two iterations for G3 grid, 13 January 2017 22:30

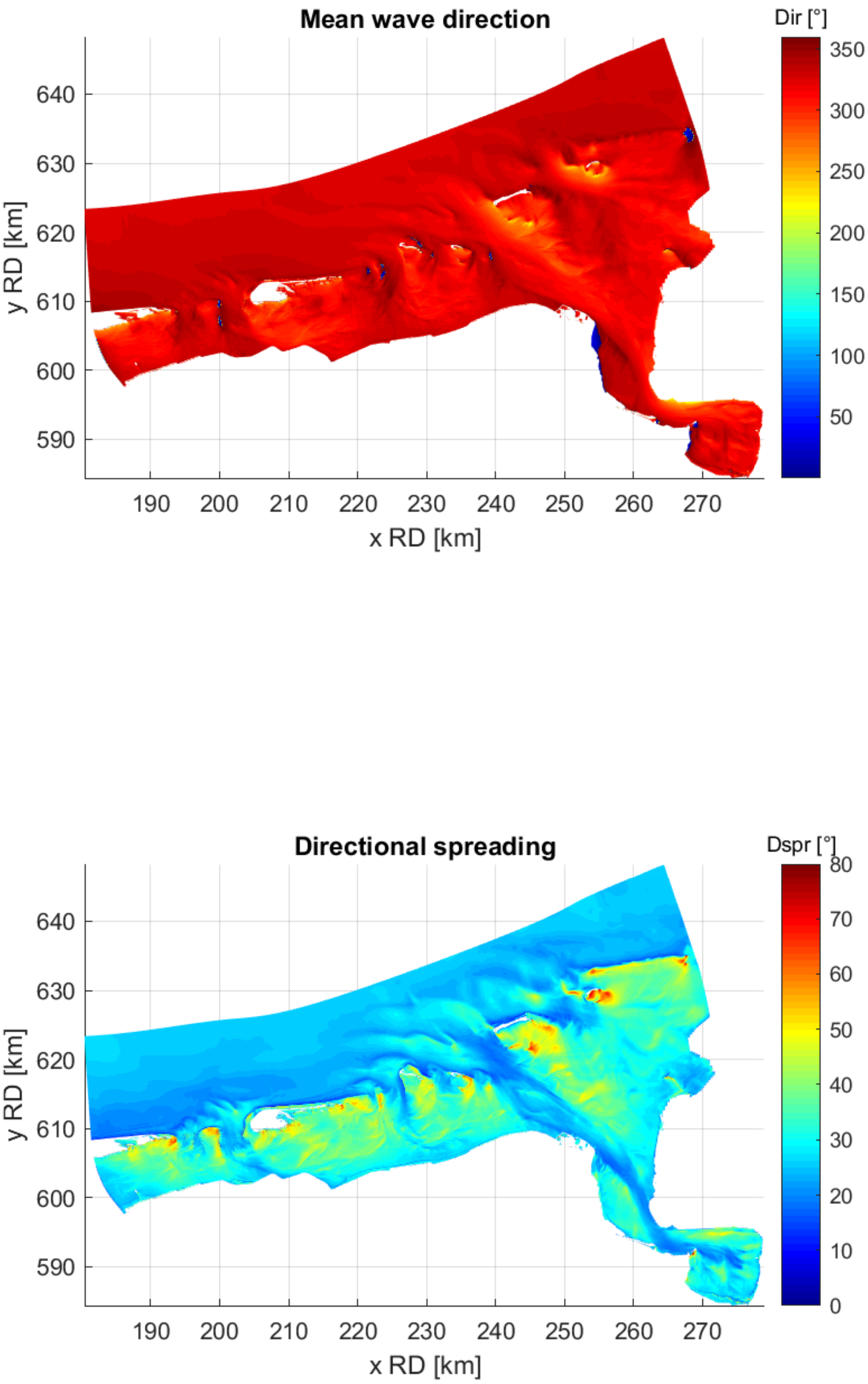

Figure IV.14: Variation of mean wave direction DIR and directional spreading Dspr for G3 grid, 13 January 2017 22:30

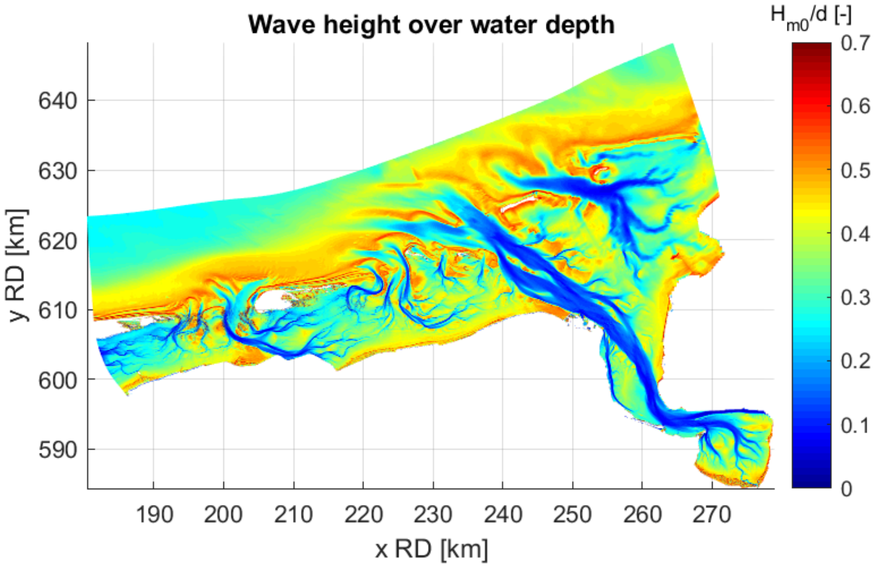

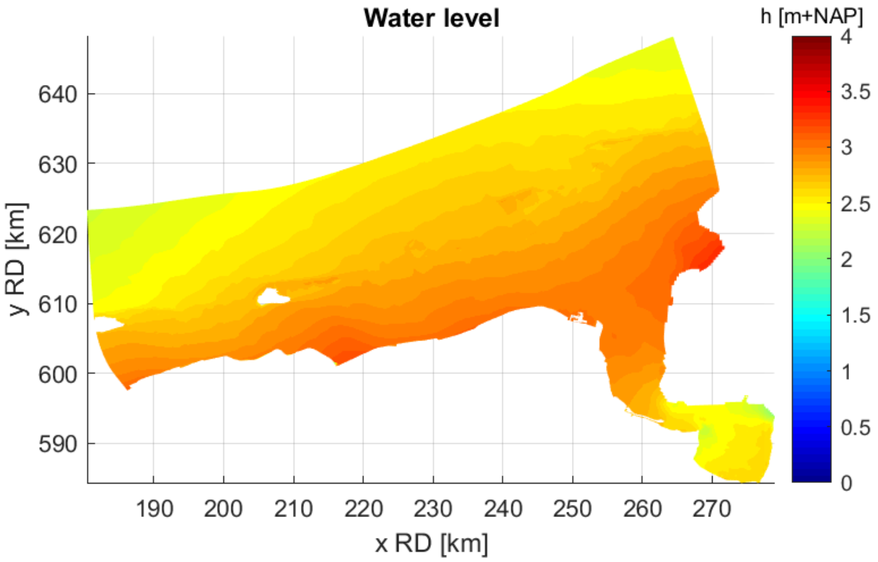

Figure IV.15: Variation of the ratio $H_{\mathrm{m0}}/\mathrm{d}$ and water level$h$ for G3 grid, 13 January 2017 22:30

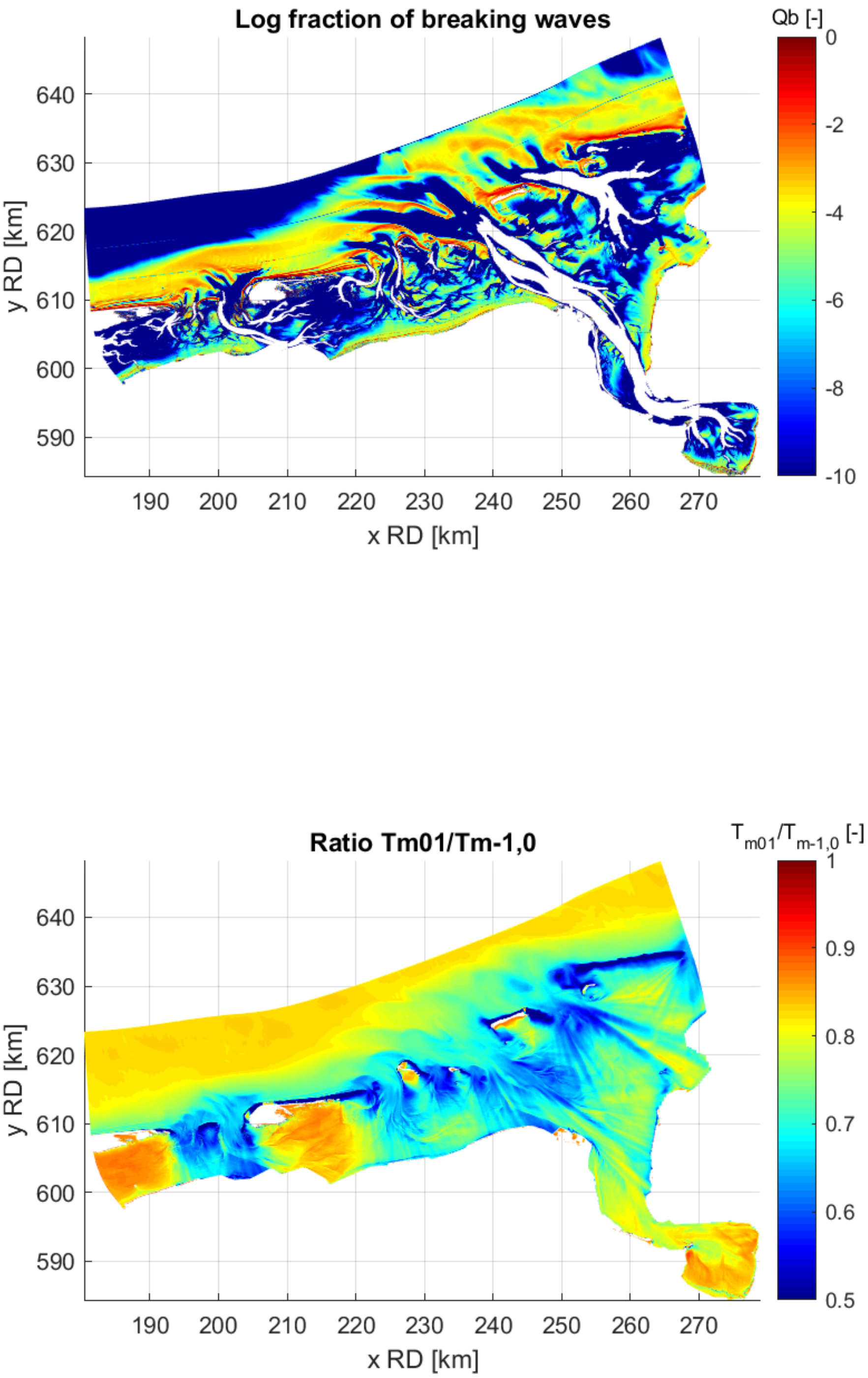

Figure IV.16: The variation of breaking waves and ratio $T_{\mathrm{m01}}/T_{\mathrm{m\text{-}1,0}}$ for G3 grid, 13 January 2017 22:30

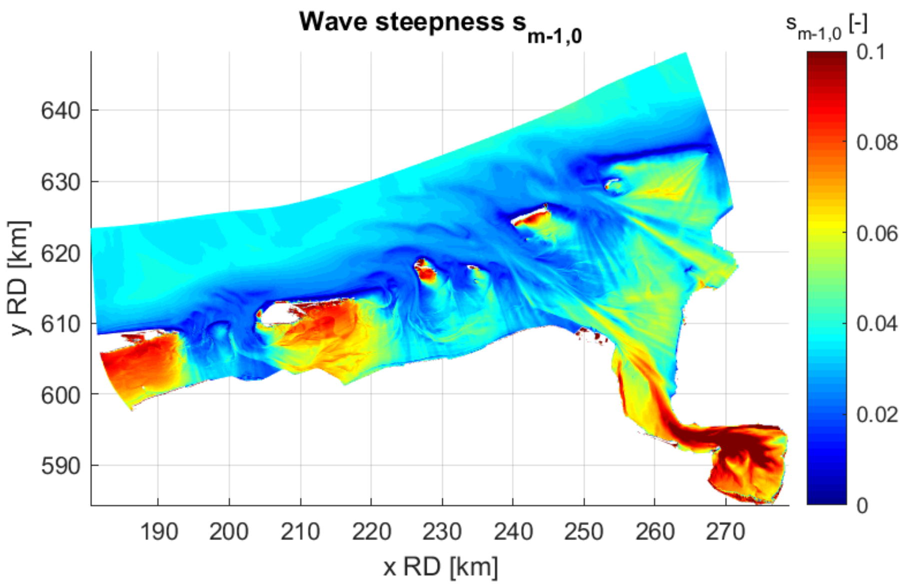

Figure IV.17: The variation of wave steepness ($s_{m-1,0}$) for G3 grid, 13 January 2017 22:30

Results hindcast (003): 13 January 2017 22:50, Grid G3, SWAN 40.72ABCDE

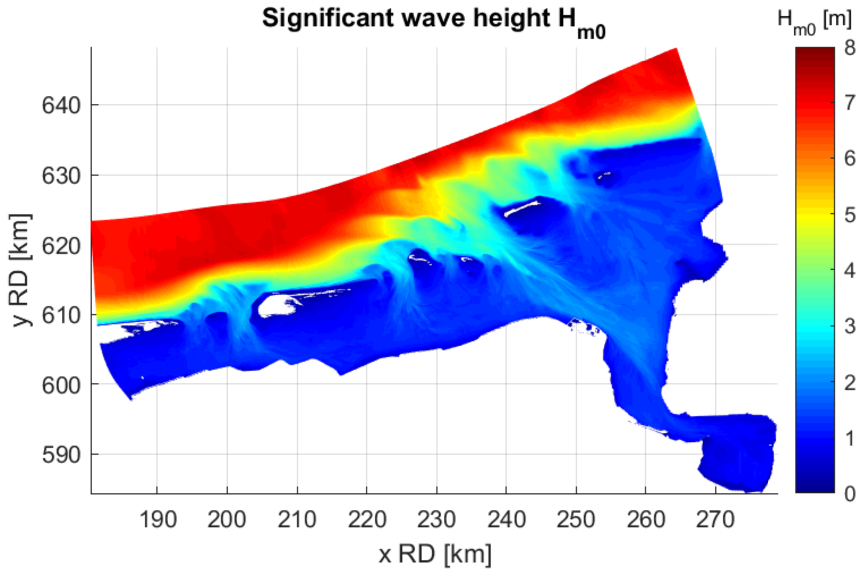

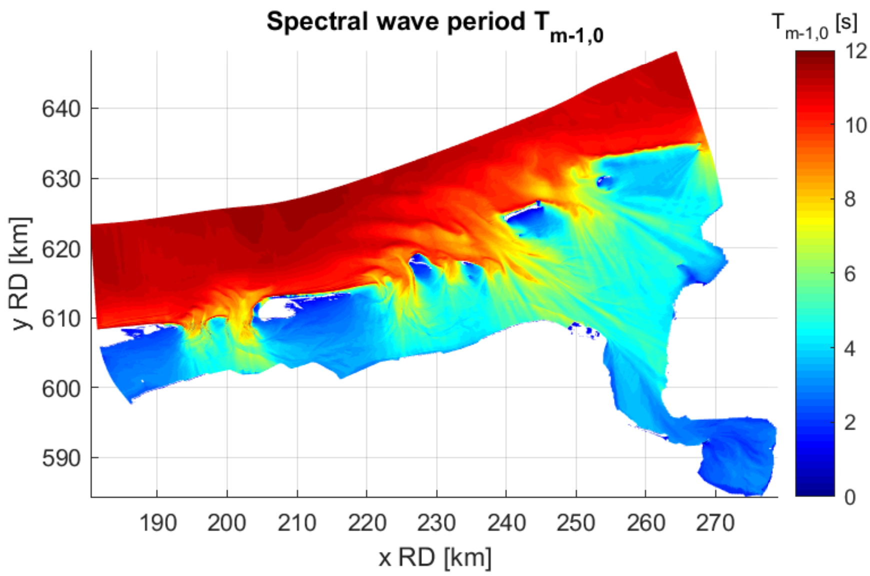

Figure IV.18: Variation of significant wave height H_{m0} and spectral wave period $T_{\mathrm{m\text{-}1,0}}$ for G3 grid, 13 January 2017 22:50

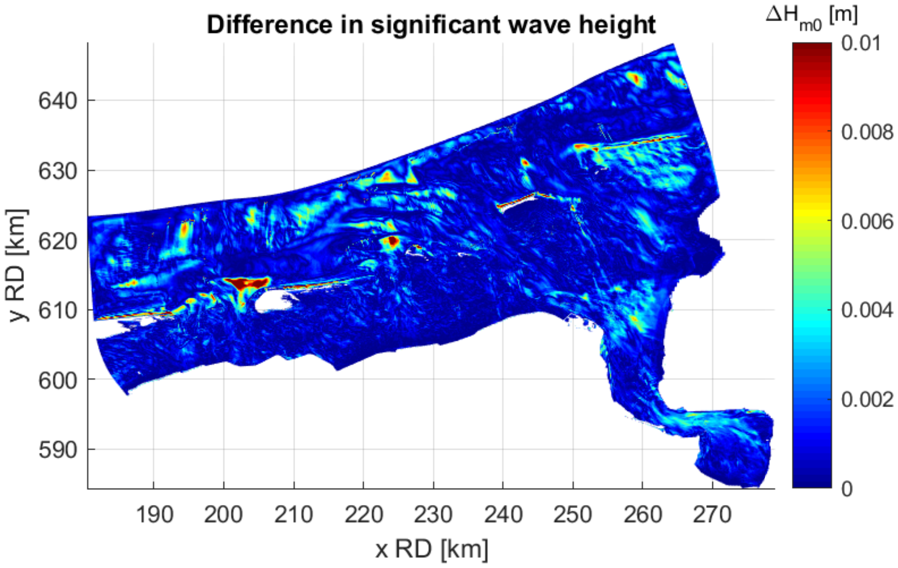

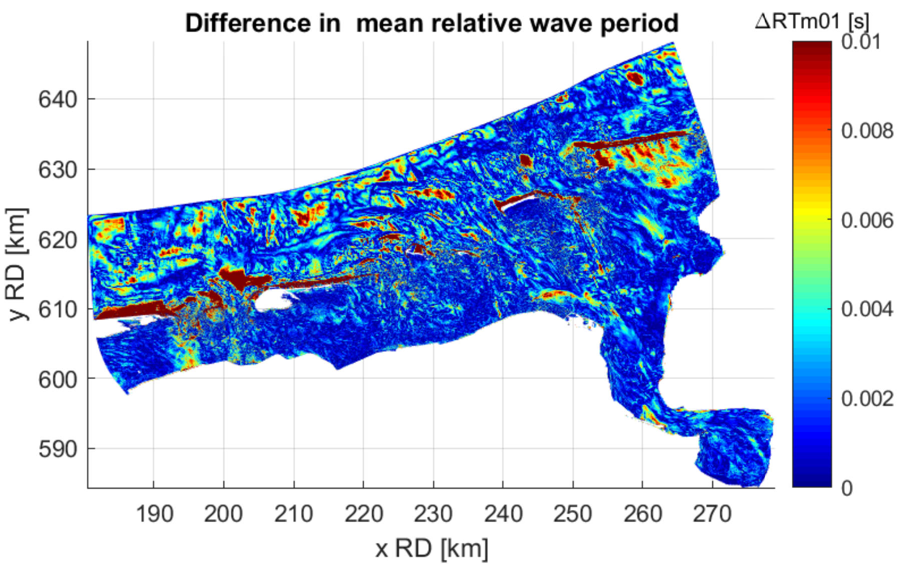

Figure IV.19: Difference of significant wave height H_{m0} and relative spectral wave period RT_{m01} as computed in the last two iterations for G3 grid, 13 January 2017 22:50

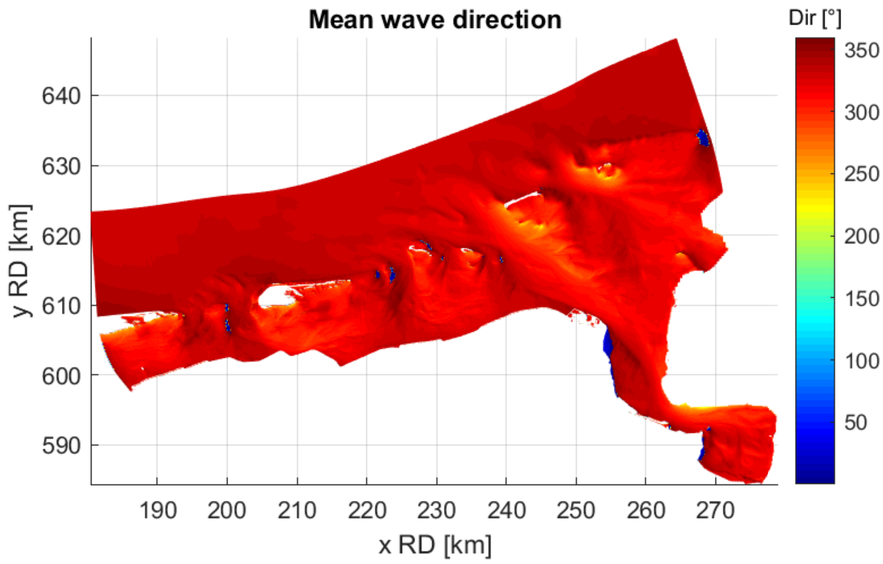

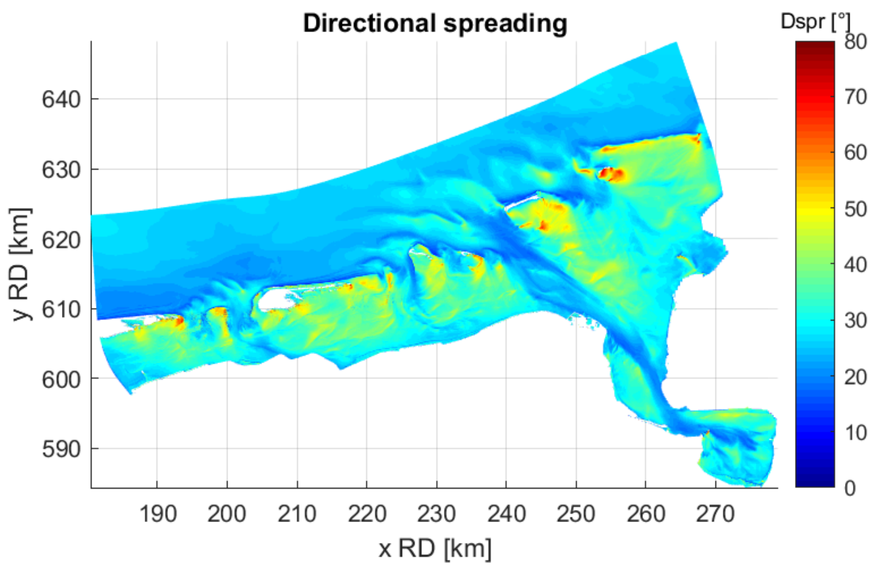

Figure IV.20: Variation of mean wave direction DIR and directional spreading Dspr for G3 grid, 13 January 2017 22:50

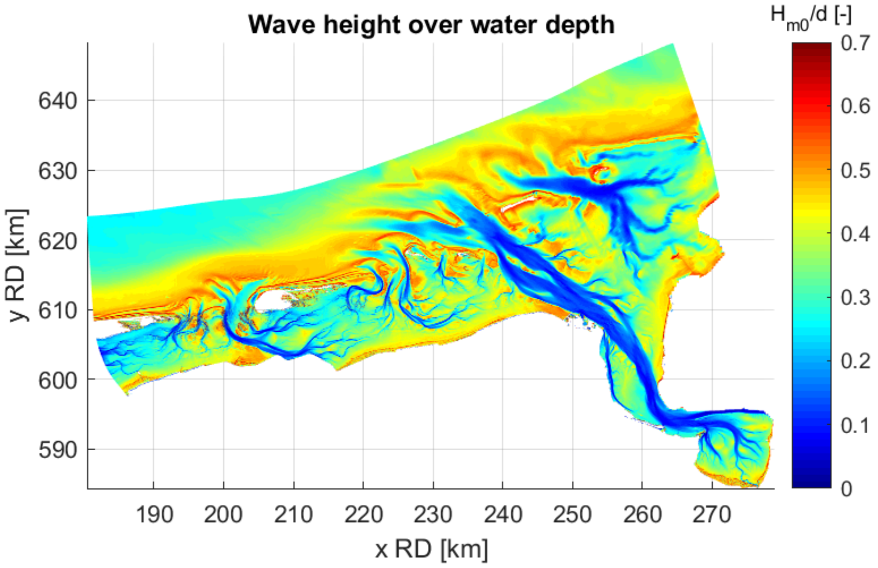

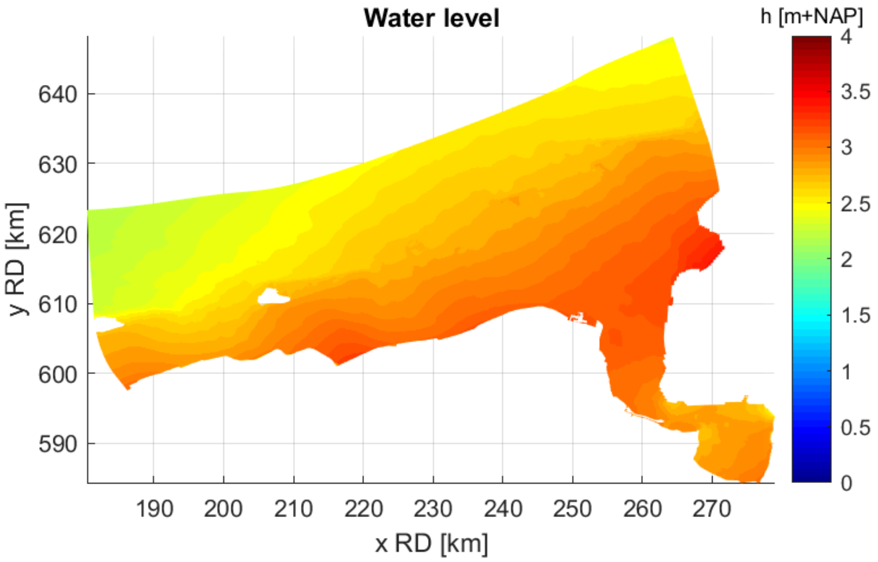

Figure IV.21: Variation of the ratio $H_{\mathrm{m0}}/\mathrm{d}$ and water level h for G3 grid, 13 January 2017 22:50

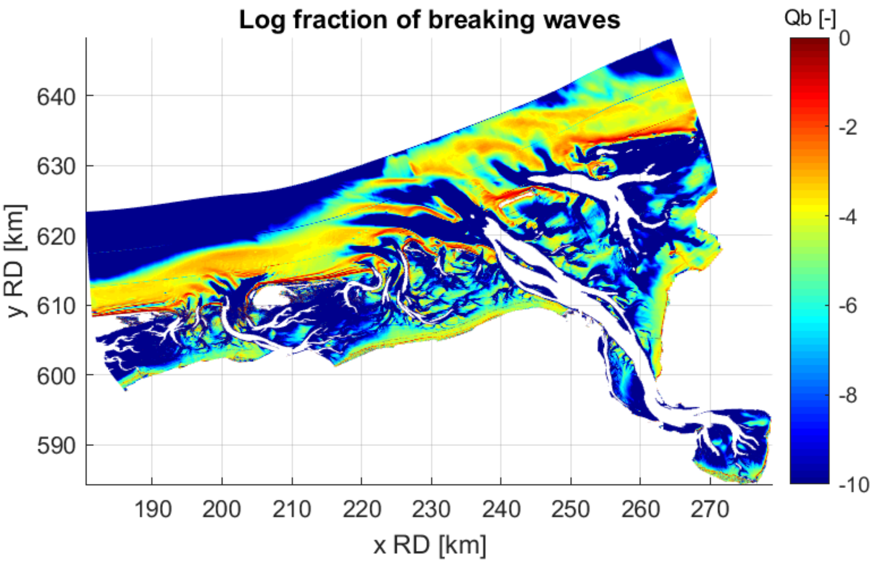

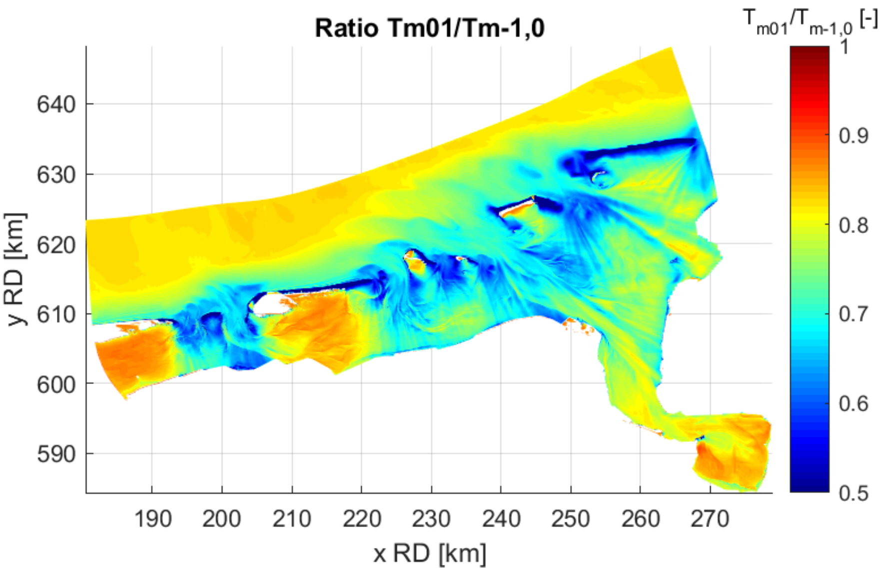

Figure IV.22: The variation of breaking waves and ratio $T_{\mathrm{m01}} / T_{\mathrm{m\text{-}1,0}}$ for G3 grid, 13 January 2017 22:50

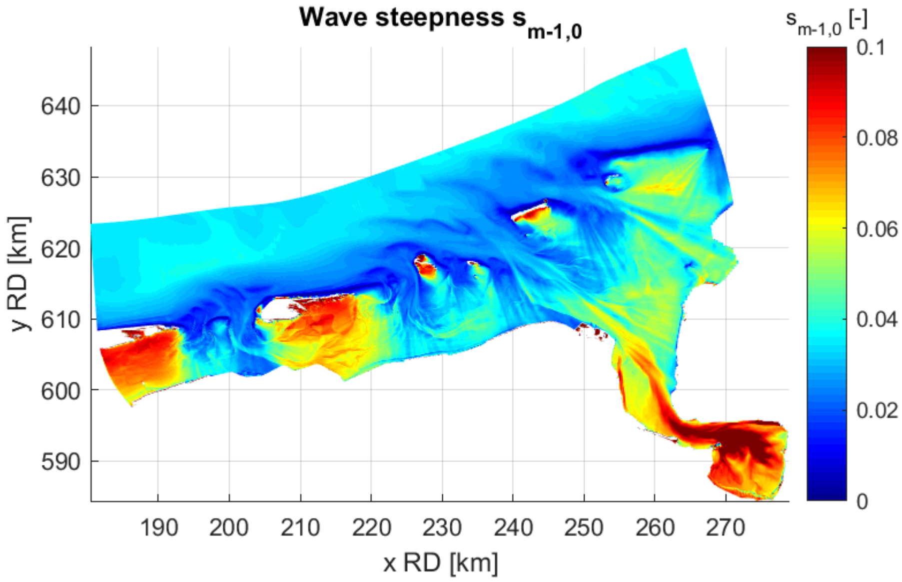

Figure IV.23: The variation of wave steepness ($s_{m-1,0}$) for G3 grid, 13 January 2017 22:50

Results hindcast (004): 13 January 2017 23:00, Grid G3, SWAN 40.72ABCDE

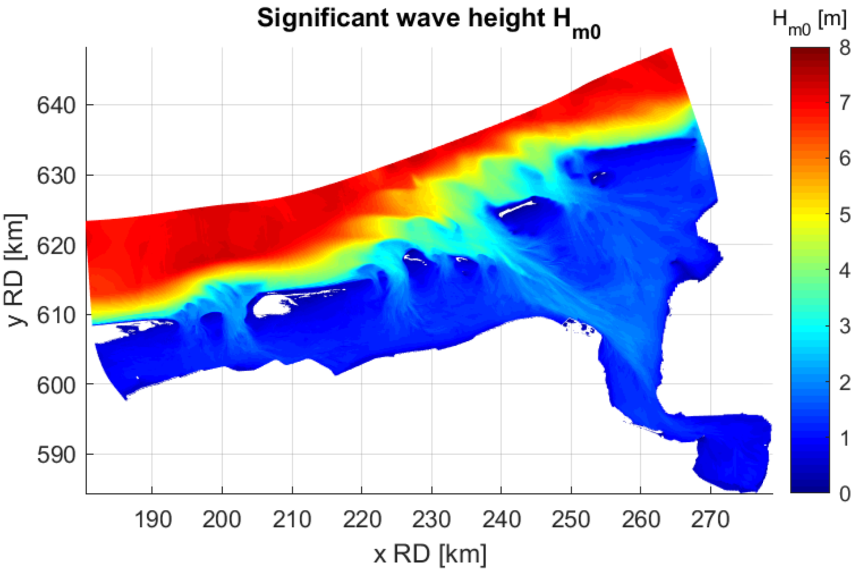

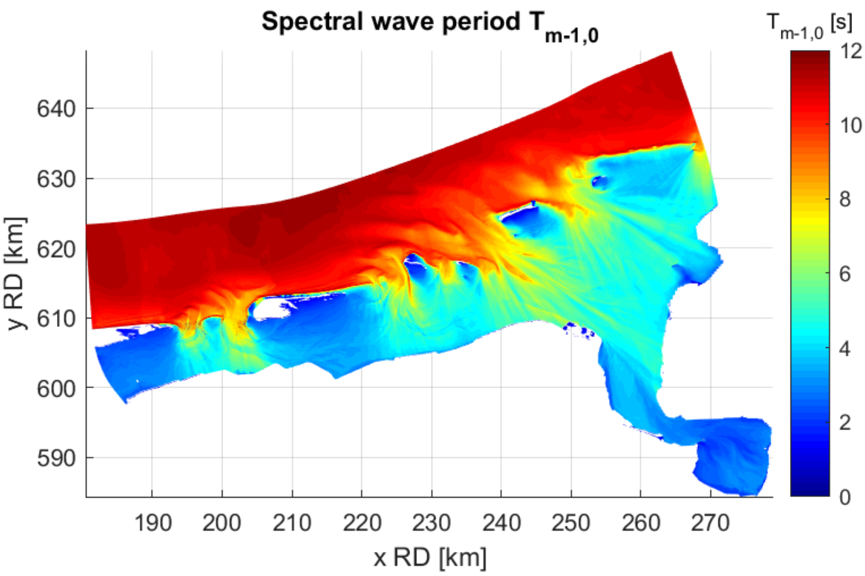

Figure IV.24: Variation of significant wave height H_{m0} and spectral wave period $T_{m\text{-}1,0}$ for G3 grid, 13 January 2017 23:00

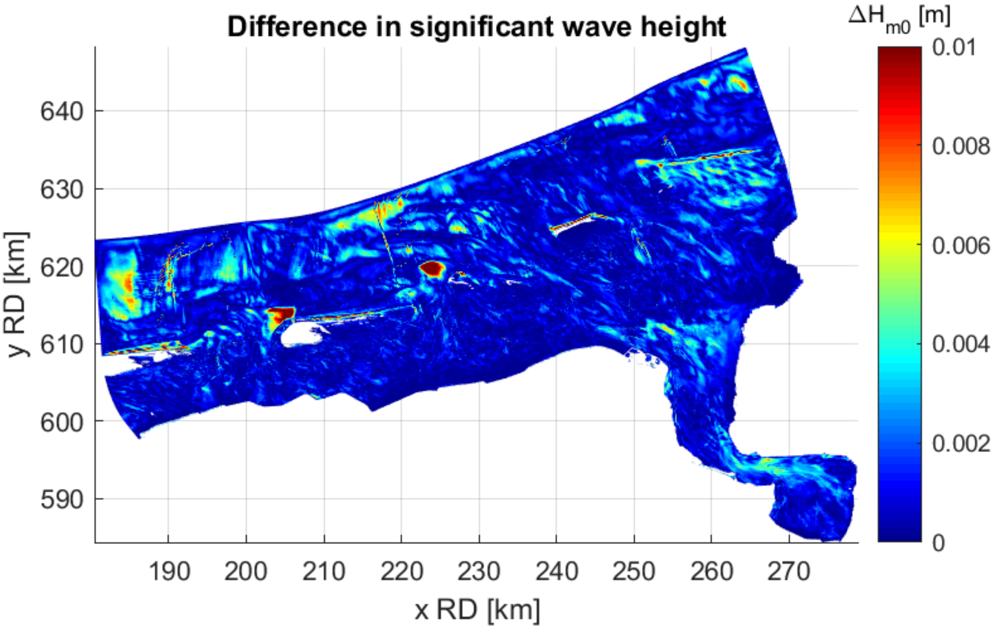

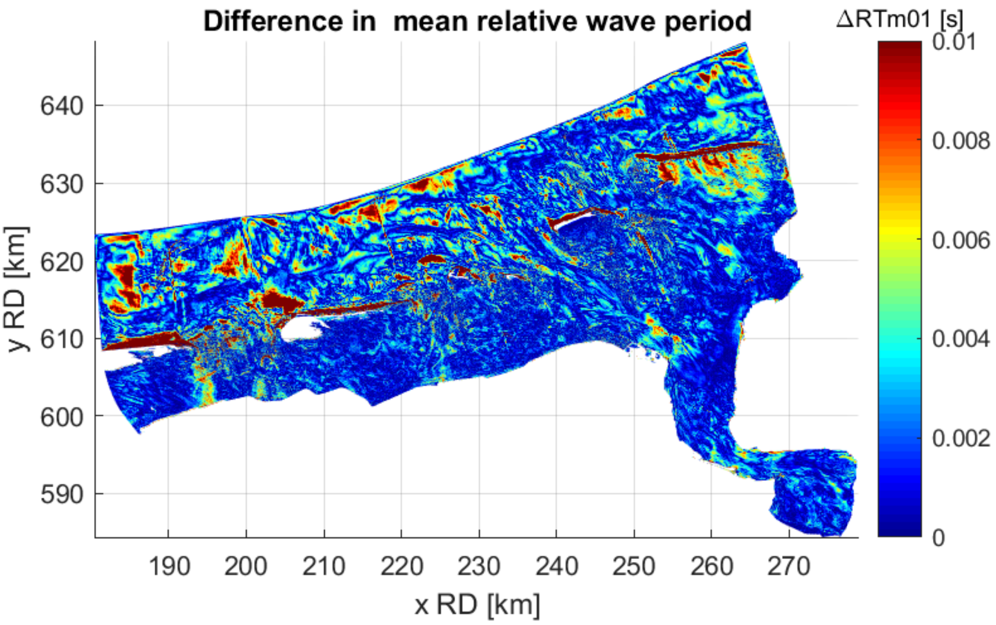

Figure IV.25: Difference of significant wave height H_{m0} and relative spectral wave period RT_{m01} as computed in the last two iterations for G3 grid, 13 January 2017 23:00

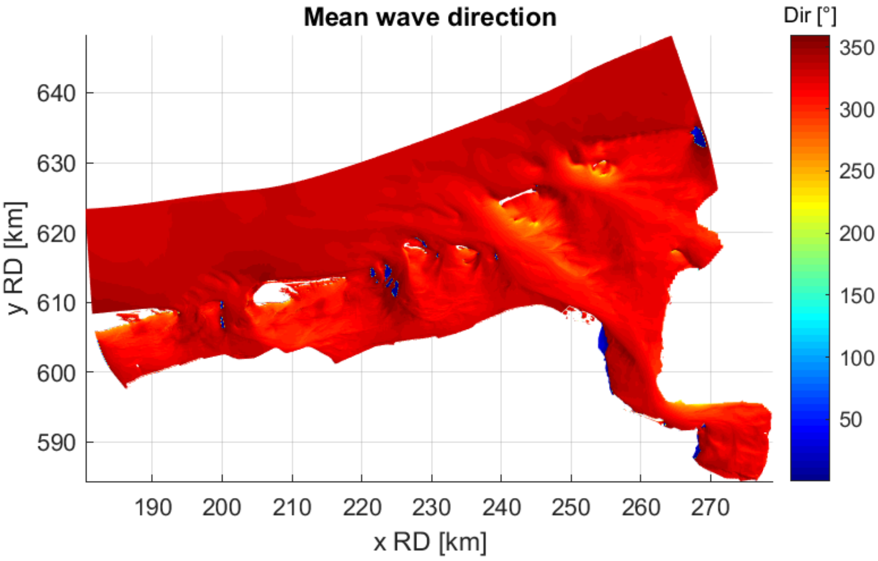

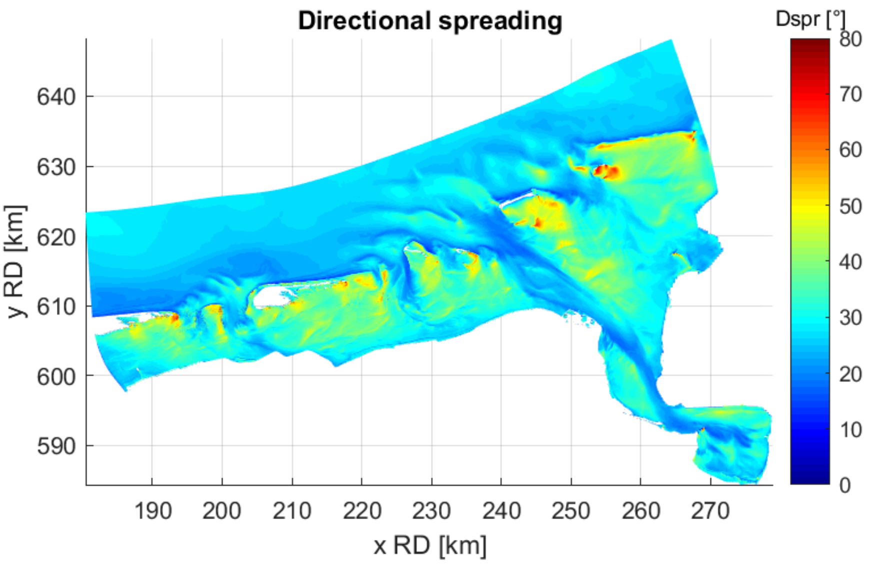

Figure IV.26: Variation of mean wave direction DIR and directional spreading Dspr for G3 grid, 13 January 2017 23:00

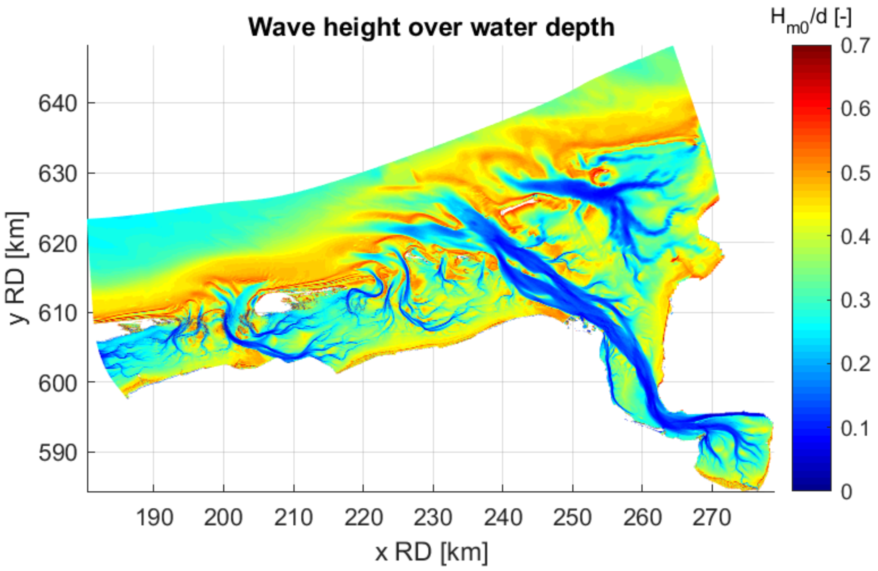

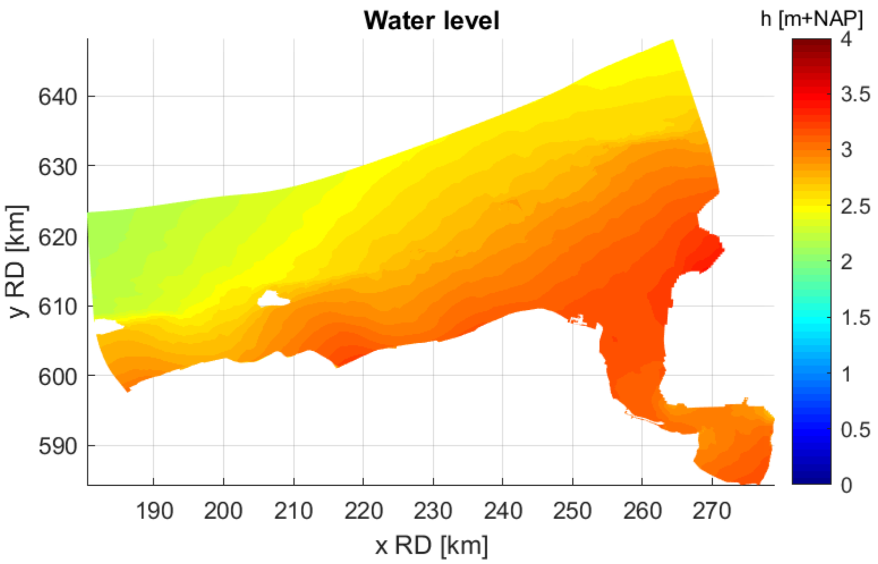

Figure IV.27: Variation of the ratio $H_{\mathrm{m0}}/\mathrm{d}$ and water level h for G3 grid, 13 January 2017 23:00

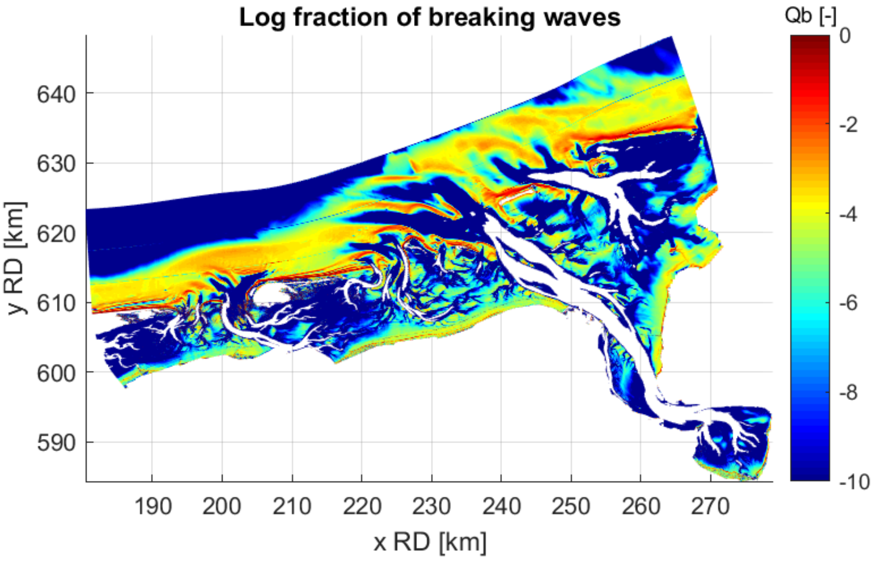

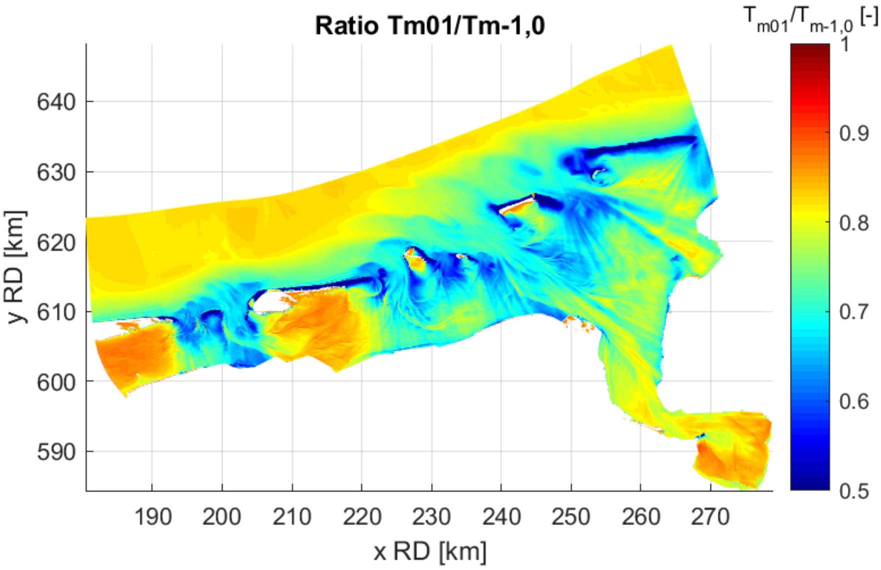

Figure IV.28: The variation of breaking waves and ratio $T_{\mathrm{m01}}\,/\,T_{\mathrm{m\text{-}1,0}}$ for G3 grid, 13 January 2017 23:00

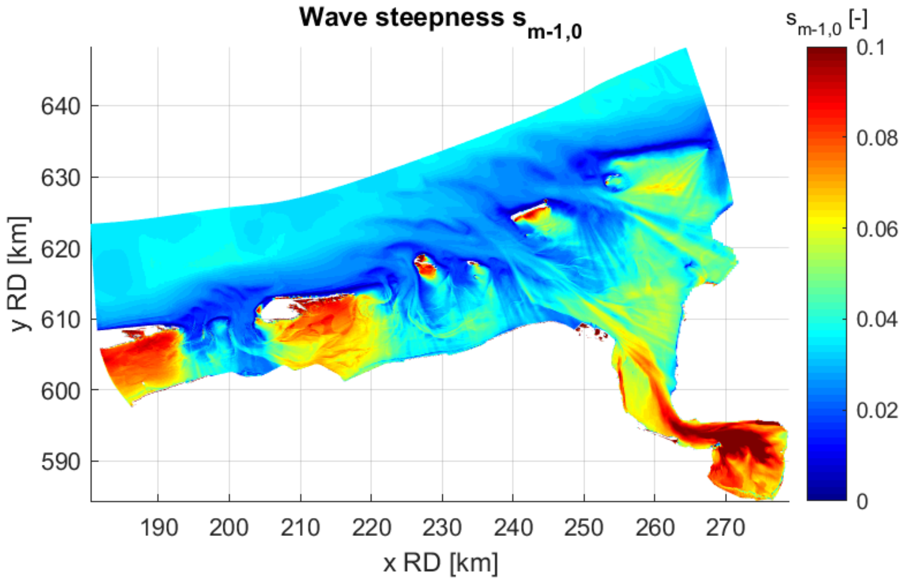

Figure IV.29: The variation of wave steepness ($s_{m-1,0}$) for G3 grid, 13 January 2017 23:00

IV.5. Variance density spectra

Measured variance density spectra are compared with calculated SWAN spectra. This is shown in Figure IV.30 for offshore locations Schiermonnikoog Noord (SMN1), Borkum Noord (BRKN1) and Westereems West (WEW1). In Figure IV.31, SWAN variance density spectra are plotted for measurement locations in the Eastern Wadden Sea. For these locations no measurements were requested

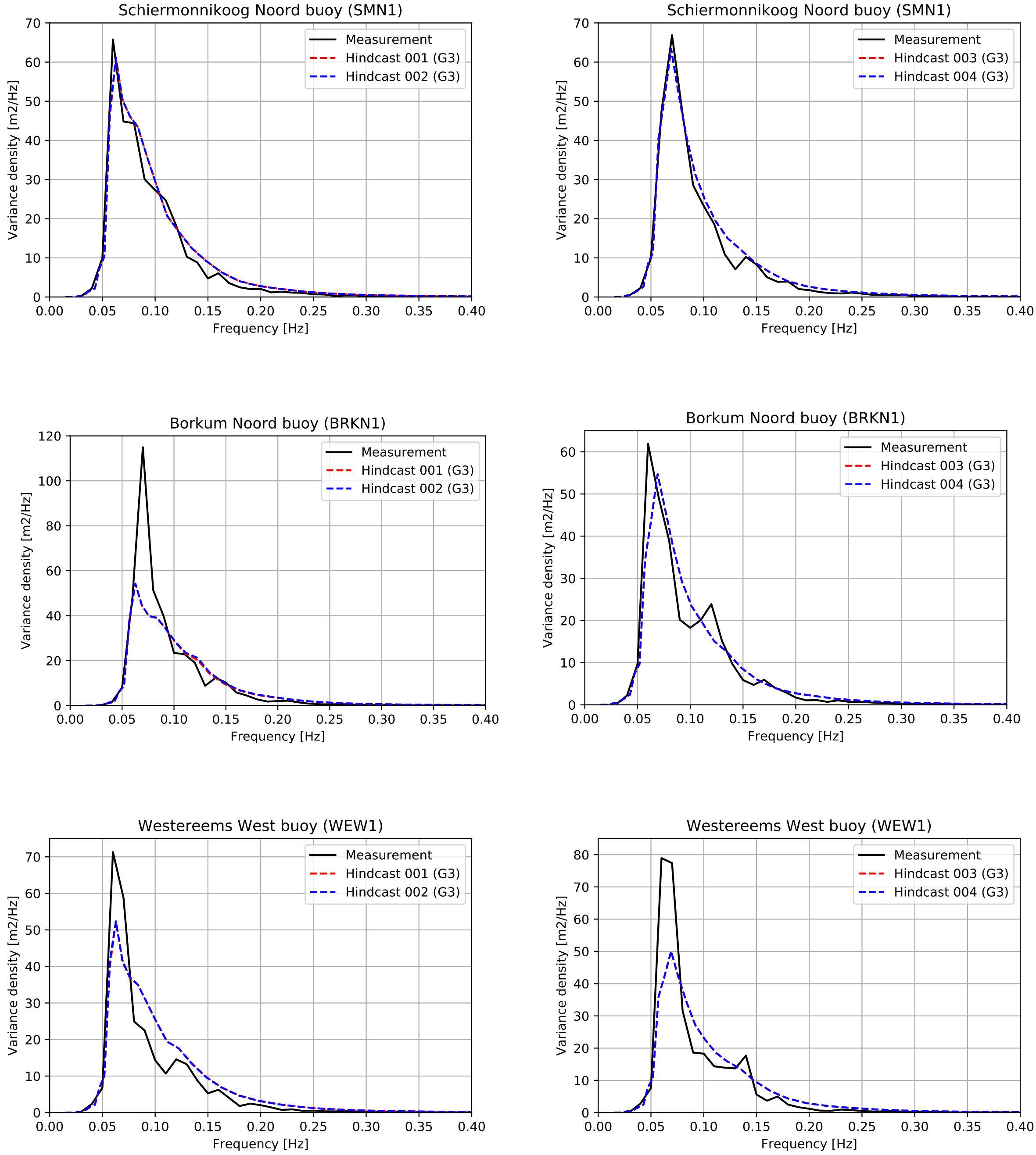

Figure IV.30: Measured wave spectra compared to SWAN hindcast 2017

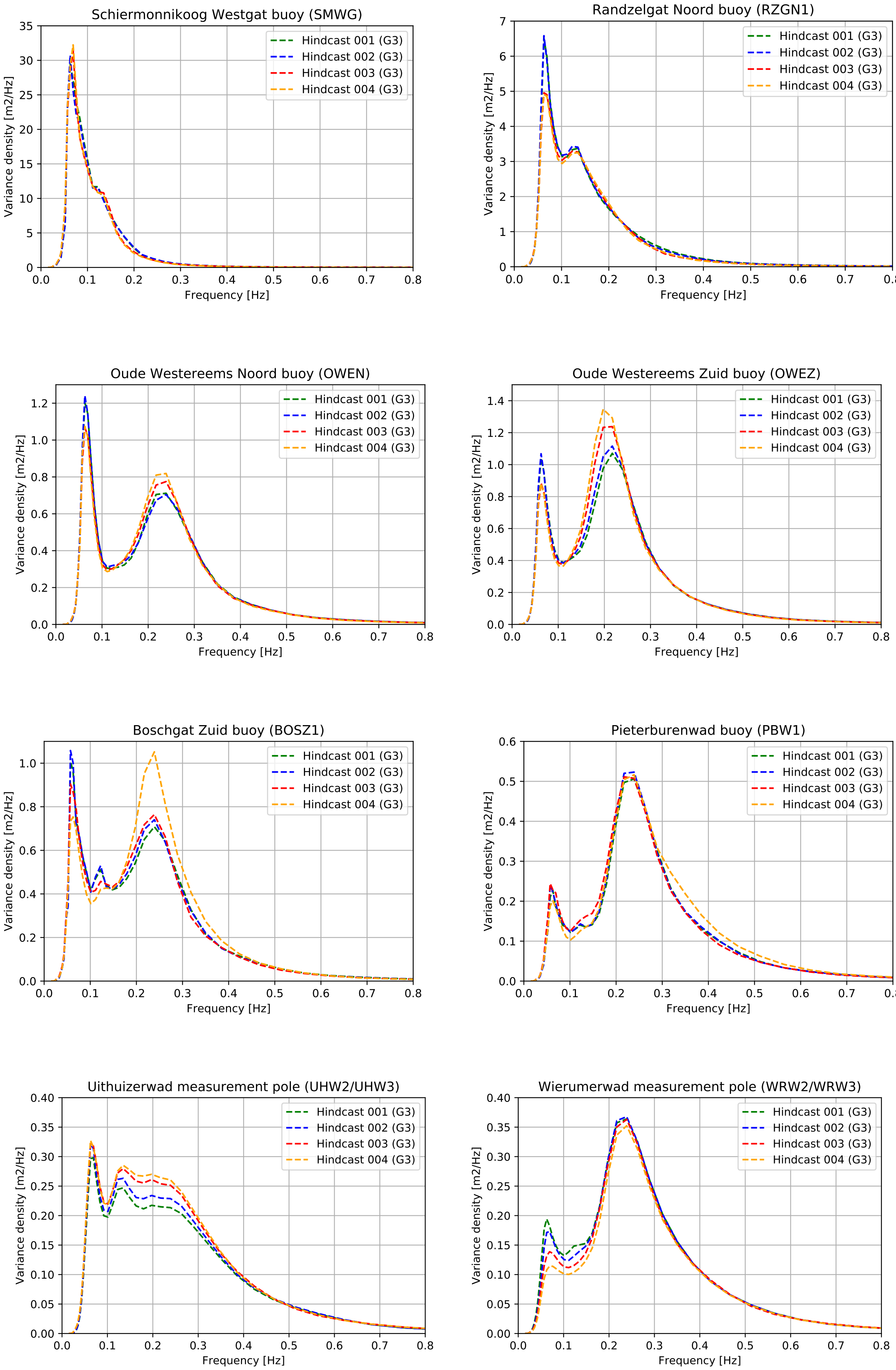

Figure IV.31: Wave spectra of variance density from SWAN hindcast 2017

Table IV.1: Measured spectral wave height H_{m0} [m] compared to SWAN output for 13 January 2017

Hindcast 13-01-2017 Locations	X	Y	Measured [m] 22:20	Model 001 (G1) 22:20	Model 001 (G3) 22:20	Measured [m] 22:30	Model 002 (G1) 22:30	Model 002 (G3) 22:30	Measured [m] 22:50	Model 003 (G1) 22:50	Model 003 (G3) 22:50	Measured [m] 23:00	Model 004 (G1) 23:00	Model 004 (G3) 23:00
Ameland Westgat	191767	611861	-	5.02044	4.99126	-	4.97238	4.95542	-	4.92792	4.94992	-	4.88442	4.96068
Boschgat Zuid	226200	612700	1.58	-	1.72932	1.51	-	1.73766	1.47	-	1.7296	1.41	-	1.83203
Huibertgat	221990	621330	-	5.32157	5.40775	-	5.28259	5.36829	-	5.2023	5.28199	-	5.16959	5.26779
Lauwers Oost	225500	617700	1.82	2.23053	2.37854	1.94	2.2366	2.37549	99999	2.20844	2.35418	99999	2.22521	2.40019
Oude Westereems Noord	240557	614915	1.24	-	1.7183	1.22	-	1.71769	1.31	-	1.72479	1.25	-	1.73288
Oude Westereems Zuid	243806	612177	-	-	1.9029	-	-	1.92262	-	-	1.95269	-	-	1.96946
Pieterburenwad	225792	608394	1.08	-	1.30962	1.13	-	1.3201	1.14	-	1.32376	1.11	-	1.35504
Randzelgat Noord	237439	621340	2.38	2.57049	3.2816	2.42	2.58711	3.27622	2.53	2.60202	3.1774	2.43	2.61982	3.16268
Schiermonnikoog Noord	206527	623484	7.51	7.41422	7.13139	7.12	7.41472	7.18234	7.07	7.30833	7.18637	7	7.30097	7.17261
Schiermonnikoog Westgat	195585	615149	999999999	5.77532	5.7478	999999999	5.74214	5.71535	15.26	5.67539	5.67567	16.76	5.64043	5.6764
Uithuizerwad (Radac)	245996	609772	1.06	-	1.1599	1.09	-	1.1894	1.08	-	1.22461	1.1	-	1.23553
Uithuizerwad (Etrometa)	245996	609772	1.21	-	1.1599	1.17	-	1.1894	1.02	-	1.22461	1.03	-	1.23553
Westereems Oost	230086	626634	4.19	5.36799	5.11915	4.17	5.37568	5.10053	4.37	5.2899	5.03639	4.44	5.27181	5.01929
Westereems West	219900	626397	6.76	7.06712	6.90835	6.67	7.06156	6.93671	7.29	6.97975	6.87531	7.17	6.96962	6.8626
Wierumergronden	192882	614562	-	6.3211	6.31838	-	6.28515	6.32978	-	6.28925	6.26448	-	6.28245	6.21716
Wierumerwad (Radac)	199957	602618	1.15	-	1.21686	1.09	-	1.20809	1.09	-	1.18619	1.01	-	1.15875
Wierumerwad (Etrometa)	199957	602618	1.48	-	1.21686	1.44	-	1.20809	1.4	-	1.18619	1.34	-	1.15875

Table IV.2: Measured spectral wave period $T_{\mathrm{m-1,0}}$ [s] compared to SWAN output for 13 January 2017

Hindcast 13-01-2017 Locations	X	Y	Measured [s] 22:20	Model 001 (G1) 22:20	Model 001 (G3) 22:20	Measured [s] 22:30	Model 002 (G1) 22:30	Model 002 (G3) 22:30	Measured [s] 22:50	Model 003 (G1) 22:50	Model 003 (G3) 22:50	Measured [s] 23:00	Model 004 (G1) 23:00	Model 004 (G3) 23:00
Ameland Westgat	191767	611861	12	10.3938	10.3577	12.3	10.3435	10.1072	12.7	10.1581	10.3183	12.4	10.1314	10.5778
Boschgat Zuid	226200	612700		-9	6.4383		-9	6.4522		-9	6.4399		-9	5.8825
Huibertgat	221990	621330		10.4093	10.3389		10.4804	10.4359		10.5339	10.5563		10.5852	10.6608
Lauwers Oost	225500	617700		7.3185	7.9259		7.3536	7.9497		7.2806	7.9949		6.8948	7.5292
Oude Westereems Noord	240557	614915		-9	6.6035		-9	6.6428		-9	6.4646		-9	6.4401
Pieterburenwad	225792	608394	4	-9	4.871	4	-9	4.8967	4	-9	5.0566	4	-9	4.6601
Randzelgat Noord	237439	621340	-	6.7313	8.6921	7.1	6.7823	8.7658	8	6.9223	8.6059	8	6.9378	8.591
Schiermonnikoog	209221	609493		2.4693	2.4096		2.4919	2.4203		2.5199	2.4518		2.5093	2.4762
Schiermonnikoog Noord	206527	623484	12.2	11.5256	11.2687	12.1	11.5541	11.2205	12.1	11.6485	11.3562	12.1	11.6413	11.3706
Schiermonnikoog Westgat	195585	615149		10.8248	10.7516		10.7866	10.7235	20.9	10.8755	11.0083	20.1	10.9773	11.1574
Uithuizerwad(Radac)	245996	609772	4.9	-9	5.8419	4.5	-9	5.8871	5.2	-9	5.9096	5.2	-9	5.903
Uithuizerwad(Etrometa)	245996	609772	5	-9	5.8419	4.6	-9	5.8871	5.1	-9	5.9096	5.2	-9	5.903
Westereems Oost	230086	626634	11.4	10.4196	10.0062	10.8	10.4353	10.0472	10.8	10.4256	10.1424	10.7	10.4503	10.1858
Westereems West	219900	626397	12.8	11.1998	10.9405	12.5	11.2357	11.0442	12.6	11.2526	11.1717	12.6	11.2846	11.2435
Wierumergronden	192882	614562		10.89	10.8103		10.9009	10.7236		10.8865	10.9652		10.8668	11.1183
Wierumerwad (Radac)	199957	602618	4.5	-9	5.0021	4.6	-9	4.8682	4.4	-9	4.7038	4.5	-9	4.5467
Wierumerwad (Etrometa)	199957	602618	4.5	-9	5.0021	4.6	-9	4.8682	4.4	-9	4.7038	4.5	-9	4.5467

IV.6. Results at HRbasis locations

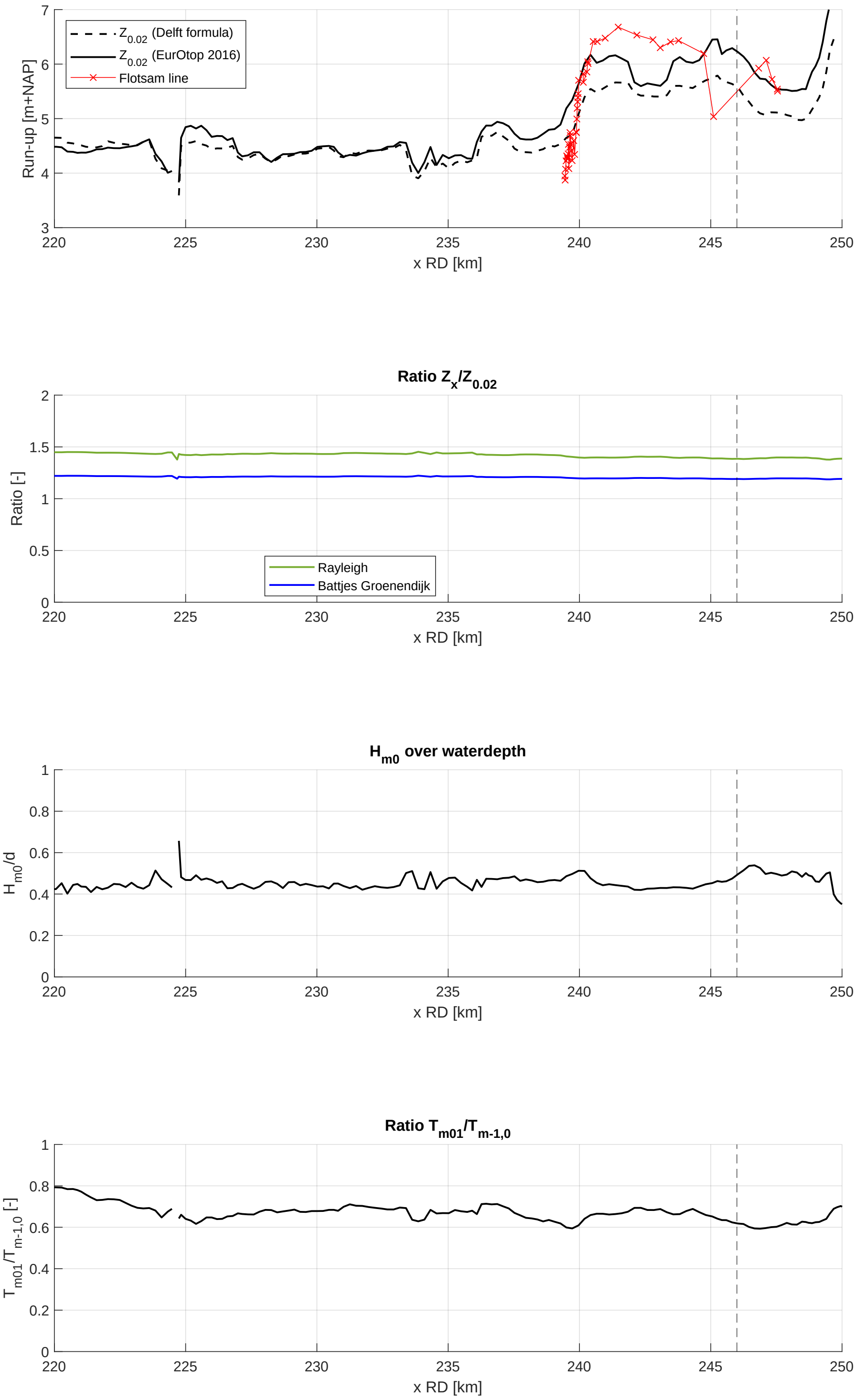

Figure IV.32: Results at HRbasis locations for highest wave run-up at 13 January 2017 22:50.

IV.7. SWAN template file grid G1

In this section a SWAN template file for computations with grid G1 is presented.

```
$************************ G1_13012017_002 ***********************

PROJ 'HW-13012017' '002'
'G1_13012017_002'

$*******************MODEL INPUT************************

MODE STAT
SET MAXERR=2 NAUTICAL

CGRID CURVILINEAR 2362 573 EXCE 0.0 0.0 CIRCLE 36 0.015 1.00
READ  COORD 1. '/home/jvanlente/SWAN/2017/AlgemeenInvoer/WADOUT1A.GRD' IDLA=4
NHEDF=0  NHEDVEC=1 FREE

INP  BOTTOM CURVILINEAR 0. 0. 2362 573 EXCE -999.
READ BOTTOM 1. '/home/jvanlente/SWAN/2017/AlgemeenInvoer/WADOUT1B.BOT' IDLA=4
NHEDF=0 FREE

INP  WLEV CURVILINEAR 0. 0. 2362 573
READ WLEV 1. '/home/jvanlente/SWAN/2017/IN/002/G1_13012017_002.lev' IDLA=4
NHEDF=0 FREE

INP  CURRENT CURVILINEAR 0. 0. 2362 573
READ CURRENT 1. '/home/jvanlente/SWAN/2017/IN/002/G1_13012017_002.cur' IDLA=4
NHEDF=0 FREE


WIND 20.36 318.97

$************************* BOUNDARY CONDITIONS ****************************

$ North East Boundary
BOUN SEGMENT XY 282428.31 634645.25 280596.4062 644230.6875 VAR &
FILE 0 '/home/jvanlente/SWAN/2017/IN/002/G1_13012017_002_SON1.SP1' 1 9758.920
&
       '/home/jvanlente/SWAN/2017/IN/002/G1_13012017_002_SON2.SP1' 1

BOUN SEGMENT XY 280596.4062 644230.6875 276884.09 663655.25 VAR &
FILE 0 '/home/jvanlente/SWAN/2017/IN/002/G1_13012017_002_SON3.SP1' 1 19775.87
&
       '/home/jvanlente/SWAN/2017/IN/002/G1_13012017_002_SON4.SP1' 1


$ Northern Boundary Eastern part
BOUN SEGMENT XY 276884.09 663655.25 203628.313 638071.313 CONST &
FILE '/home/jvanlente/SWAN/2017/IN/002/G1_13012017_002_SON5.SP1' 1

$ Northern Boundary Northern Part
BOUN SEGMENT XY 203628.313 638071.313 99404.328 593119.750 VAR &
```

```
FILE 0 '/home/jvanlente/SWAN/2017/IN/002/G1_13012017_002_SON6.SP1' 1
117336.765 &
       '/home/jvanlente/SWAN/2017/IN/002/G1_13012017_002_ELD6.SP1' 1

$ Northern Boundary Western part
BOUN SEGMENT XY 99404.328 593119.750 81746.85 556658.13 CONST &
FILE '/home/jvanlente/SWAN/2017/IN/002/G1_13012017_002_ELD5.SP1' 1


$ South Western Boundary
BOUN SEGMENT XY 81746.85 556658.13 101026.4531 550303.5 VAR &
FILE 0 '/home/jvanlente/SWAN/2017/IN/002/G1_13012017_002_ELD4.SP1' 1
20305.674 &
       '/home/jvanlente/SWAN/2017/IN/002/G1_13012017_002_ELD3.SP1' 1

BOUN SEGMENT XY 101026.4531 550303.5 109757.7812 547901.875 VAR &
FILE 0 '/home/jvanlente/SWAN/2017/IN/002/G1_13012017_002_ELD2.SP1' 1
9002.2764 &
       '/home/jvanlente/SWAN/2017/IN/002/G1_13012017_002_ELD1.SP1' 1

$******************************** PHYSICS ***********************************

GEN3 WESTH
WCAP WESTH cds2=5.00000e-05 br=0.00175000 p0=4.00000 powst=0.00000
powk=0.00000  &
          nldisp=0.00000 cds3=0.800000 powfsh=1.00000
QUAD iquad=2 lambda=0.250000 Cnl4=3.00000e+07
LIMITER ursell=10.0000 qb=1.00000
FRIC JONSWAP cfjon=0.0380000
BREA WESTH alpha=0.960000 pown=2.50000 bref=-1.39630 shfac=500.000
TRIAD trfac=0.10000 cutfr=2.50000

$************************** NUMERIEKE PARAMETERS ****************************

NUM STOPC dabs=0.00  drel=0.01  curvat=0.001  npnts=99.  STAT mxitst=80
alfa=0.001

$***************************** OUTPUT ***************************************

POINTS 'PRvwG2'    FILE
'/home/jvanlente/SWAN/2017/AlgemeenInvoer/G1LocRvwG2.pnt'
POINTS 'PRvwG3'    FILE
'/home/jvanlente/SWAN/2017/AlgemeenInvoer/G1LocRvwG3.pnt'
POINTS 'PELD'      FILE '/home/jvanlente/SWAN/2017/AlgemeenInvoer/ELD.PNT'
POINTS 'PSON'      FILE '/home/jvanlente/SWAN/2017/AlgemeenInvoer/SON.PNT'
POINTS 'P04'       FILE
'/home/jvanlente/SWAN/2017/AlgemeenInvoer/Pbuoys_2004.PNT'
POINTS 'P05'       FILE
'/home/jvanlente/SWAN/2017/AlgemeenInvoer/Pbuoys_2005.PNT'
```

```
POINTS 'P06'       FILE
'/home/jvanlente/SWAN/2017/AlgemeenInvoer/Pbuoys_2006.PNT'
POINTS 'P07'       FILE
'/home/jvanlente/SWAN/2017/AlgemeenInvoer/Pbuoys_2007.PNT'
POINTS 'P08'       FILE
'/home/jvanlente/SWAN/2017/AlgemeenInvoer/Pbuoys_2008.PNT'
POINTS 'MLOW'       FILE
'/home/jvanlente/SWAN/2017/AlgemeenInvoer/M_locations_OW.PNT'
POINTS 'FS'       FILE
'/home/jvanlente/SWAN/2017/AlgemeenInvoer/FS_locations_OW.PNT'


TABLE 'PRvwG2' HEAD
'/home/jvanlente/SWAN/2017/OUT/002/PRvwG2_G1_13012017_002.TAB' &
        XP YP DEP HS RTP TPS TMM10 TM01 TM02 DIR DSPR WLEN DISS DHS DRTM01
WATLEV WIND VEL

TABLE 'PRvwG3' HEAD
'/home/jvanlente/SWAN/2017/OUT/002/PRvwG3_G1_13012017_002.TAB' &
        XP YP DEP HS RTP TPS TMM10 TM01 TM02 DIR DSPR WLEN DISS DHS DRTM01
WATLEV WIND VEL

TABLE 'PELD' HEAD '/home/jvanlente/SWAN/2017/OUT/002/ELD_G1_13012017_002.TAB'
&
        XP YP DEP HS RTP TPS TMM10 TM01 TM02 DIR DSPR WLEN DISS DHS DRTM01
WATLEV WIND VEL

TABLE 'PSON' HEAD '/home/jvanlente/SWAN/2017/OUT/002/SON_G1_13012017_002.TAB'
&
        XP YP DEP HS RTP TPS TMM10 TM01 TM02 DIR DSPR WLEN DISS DHS DRTM01
WATLEV WIND VEL

TABLE 'P04' HEAD '/home/jvanlente/SWAN/2017/OUT/002/P04_G1_13012017_002.TAB'
&
        XP YP DEP HS RTP TPS TMM10 TM01 TM02 DIR DSPR WLEN DISS DHS DRTM01
WATLEV WIND VEL

TABLE 'P05' HEAD '/home/jvanlente/SWAN/2017/OUT/002/P05_G1_13012017_002.TAB'
&
        XP YP DEP HS RTP TPS TMM10 TM01 TM02 DIR DSPR WLEN DISS DHS DRTM01
WATLEV WIND VEL

TABLE 'P06' HEAD '/home/jvanlente/SWAN/2017/OUT/002/P06_G1_13012017_002.TAB'
&
        XP YP DEP HS RTP TPS TMM10 TM01 TM02 DIR DSPR WLEN DISS DHS DRTM01
WATLEV WIND VEL

TABLE 'P07' HEAD '/home/jvanlente/SWAN/2017/OUT/002/P07_G1_13012017_002.TAB'
&
```

```
        XP YP DEP HS RTP TPS TMM10 TM01 TM02 DIR DSPR WLEN DISS DHS DRTM01
WATLEV WIND VEL

TABLE 'P08' HEAD '/home/jvanlente/SWAN/2017/OUT/002/P08_G1_13012017_002.TAB'
&
        XP YP DEP HS RTP TPS TMM10 TM01 TM02 DIR DSPR WLEN DISS DHS DRTM01
WATLEV WIND VEL

TABLE 'MLOW' HEAD
'/home/jvanlente/SWAN/2017/OUT/002/MLOW_G1_13012017_002.TAB' &
        XP YP DEP HS RTP TPS TMM10 TM01 TM02 DIR DSPR WLEN DISS DHS DRTM01
WATLEV WIND VEL

TABLE 'FS' HEAD '/home/jvanlente/SWAN/2017/OUT/002/FS_G1_13012017_002.TAB' &
        XP YP DEP HS RTP TPS TMM10 TM01 TM02 DIR DSPR WLEN DISS DHS DRTM01
WATLEV WIND VEL

BLOCK 'COMPGRID' NOHEAD
'/home/jvanlente/SWAN/2017/OUT/002/G1_13012017_002.mat' &
       LAYOUT 3 XP YP DEPTH HSIG RTP TPS TMM10 TM01 TM02 DIR DSPR WLEN &
       DHS DRTM01 WATLEV WIND VEL DISSIP

$SPECOUT 'PRvwG2'  SPEC1D ABS
'/home/jvanlente/SWAN/2017/IN/G2/002/PRvwG2_G1_13012017_002.SP1'
SPECOUT 'PRvwG3'  SPEC1D ABS
'/home/jvanlente/SWAN/2017/IN/G3/002/PRvwG3_G1_13012017_002.SP1'
SPECOUT 'PRvwG2'  SPEC1D ABS
'/home/jvanlente/SWAN/2017/OUT/002/PRvwG2_G1_13012017_002.SP1'
SPECOUT 'PRvwG3'  SPEC1D ABS
'/home/jvanlente/SWAN/2017/OUT/002/PRvwG3_G1_13012017_002.SP1'
SPECOUT 'PELD'    SPEC1D ABS
'/home/jvanlente/SWAN/2017/OUT/002/ELD_G1_13012017_002.SP1'
SPECOUT 'PSON'    SPEC1D ABS
'/home/jvanlente/SWAN/2017/OUT/002/SON_G1_13012017_002.SP1'
SPECOUT 'P04'     SPEC1D ABS
'/home/jvanlente/SWAN/2017/OUT/002/P04_G1_13012017_002.SP1'
SPECOUT 'P05'     SPEC1D ABS
'/home/jvanlente/SWAN/2017/OUT/002/P05_G1_13012017_002.SP1'
SPECOUT 'P06'     SPEC1D ABS
'/home/jvanlente/SWAN/2017/OUT/002/P06_G1_13012017_002.SP1'
SPECOUT 'P07'     SPEC1D ABS
'/home/jvanlente/SWAN/2017/OUT/002/P07_G1_13012017_002.SP1'
SPECOUT 'P08'     SPEC1D ABS
'/home/jvanlente/SWAN/2017/OUT/002/P08_G1_13012017_002.SP1'
SPECOUT 'MLOW'     SPEC1D ABS
'/home/jvanlente/SWAN/2017/OUT/002/MLOW_G1_13012017_002.SP1'
SPECOUT 'FS'     SPEC1D ABS
'/home/jvanlente/SWAN/2017/OUT/002/FS_G1_13012017_002.SP1'
```

```
$SPECOUT 'PRvwG2'  SPEC2D ABS
'/home/jvanlente/SWAN/2017/IN/G2/002/PRvwG2_G1_13012017_002.SP2'
SPECOUT 'PRvwG3'  SPEC2D ABS
'/home/jvanlente/SWAN/2017/IN/G3/002/PRvwG3_G1_13012017_002.SP2'
SPECOUT 'PRvwG2'  SPEC2D ABS
'/home/jvanlente/SWAN/2017/OUT/002/PRvwG2_G1_13012017_002.SP2'
SPECOUT 'PRvwG3'  SPEC2D ABS
'/home/jvanlente/SWAN/2017/OUT/002/PRvwG3_G1_13012017_002.SP2'
SPECOUT 'PELD'    SPEC2D ABS
'/home/jvanlente/SWAN/2017/OUT/002/ELD_G1_13012017_002.SP2'
SPECOUT 'PSON'    SPEC2D ABS
'/home/jvanlente/SWAN/2017/OUT/002/SON_G1_13012017_002.SP2'
SPECOUT 'P04'     SPEC2D ABS
'/home/jvanlente/SWAN/2017/OUT/002/P04_G1_13012017_002.SP2'
SPECOUT 'P05'     SPEC2D ABS
'/home/jvanlente/SWAN/2017/OUT/002/P05_G1_13012017_002.SP2'
SPECOUT 'P06'     SPEC2D ABS
'/home/jvanlente/SWAN/2017/OUT/002/P06_G1_13012017_002.SP2'
SPECOUT 'P07'     SPEC2D ABS
'/home/jvanlente/SWAN/2017/OUT/002/P07_G1_13012017_002.SP2'
SPECOUT 'P08'     SPEC2D ABS
'/home/jvanlente/SWAN/2017/OUT/002/P08_G1_13012017_002.SP2'
SPECOUT 'MLOW'     SPEC2D ABS
'/home/jvanlente/SWAN/2017/OUT/002/MLOW_G1_13012017_002.SP2'
SPECOUT 'FS'     SPEC2D ABS
'/home/jvanlente/SWAN/2017/OUT/002/FS_G1_13012017_002.SP2'


TEST 1 0 POINTS XY    &
103572 553057 &
105804 555349 &
108408 558232 &
120055 577807 &
120398 578495 &
120989 579751 &
133612 591889 &
135018 592861 &
136905 594067 &
138533 595073 &
139420 595609 &
167045 605483 &
168146 605679 &
169209 605923 &
194583 609265 &
196534 609493 &
200590 609982 &
201884 610145 &
203043 610341 &
222764 614427 &
226331 615559 &
```

```
230288 616918 &
236580 619126 &
241833 621391 &
246050 623203 &
249747 624901 &
253818 626829 &
257969 628867 &
264456 631698 &
272628 634416 &
278985 636001 &
 PAR '/home/jvanlente/SWAN/2017/OUT/002/G1_13012017_002.PAR'

COMPUTE

$HOTFILE 'G1_13012017_002.hot'

STOP
```

IV.8. SWAN template file grid G3

In this section a SWAN template file for computations with grid G3 is presented.

```
$************************ G3_13012017_002 ***********************

PROJ 'HW-13012017' '002'
'G3_13012017_002'

$*******************MODEL INPUT*************************

MODE STAT
SET MAXERR=2 NAUTICAL

CGRID CURVILINEAR 989 1257 EXCE 0.0 0.0 CIRCLE 36 0.015 1.00
READ  COORD 1. '/home/jvanlente/SWAN/2017/AlgemeenInvoer/Wadgrid3b.grd'
IDLA=4 NHEDF=0  NHEDVEC=1 FREE

INP  BOTTOM CURVILINEAR 0. 0. 989 1257 EXCE -999.
READ BOTTOM 1. '/home/jvanlente/SWAN/2017/AlgemeenInvoer/Wadbot3b.bot' IDLA=4
NHEDF=0 FREE

INP  WLEV CURVILINEAR 0. 0. 989 1257
READ WLEV 1. '/home/jvanlente/SWAN/2017/IN/G3/002/G3_13012017_002.lev' IDLA=4
NHEDF=0 FREE

INP  CURRENT CURVILINEAR 0. 0. 989 1257
READ CURRENT 1. '/home/jvanlente/SWAN/2017/IN/G3/002/G3_13012017_002.cur'
IDLA=4 NHEDF=0 FREE

WIND 20.36 318.97

$************************** BOUNDARY CONDITIONS **************************

BOUNDNEST1 NEST
'/home/jvanlente/SWAN/2017/IN/G3/002/PRvwG3_G1_13012017_002.SP2'  OPEN

$******************************** PHYSICS ********************************

GEN3 WESTH
WCAP WESTH cds2=5.00000e-05 br=0.00175000 p0=4.00000 powst=0.00000
powk=0.00000  &
          nldisp=0.00000 cds3=0.800000 powfsh=1.00000
QUAD iquad=2 lambda=0.250000 Cnl4=3.00000e+07
LIMITER ursell=10.0000 qb=1.00000
FRIC JONSWAP cfjon=0.0380000
BREA WESTH alpha=0.960000 pown=2.50000 bref=-1.39630 shfac=500.000
TRIAD trfac=0.10000 cutfr=2.50000

$************************* NUMERIEKE PARAMETERS **************************
```

```
NUM STOPC dabs=0.00  drel=0.01  curvat=0.001  npnts=99.  STAT mxitst=80
alfa=0.001  REFRL 0.2  2

$******************************* OUTPUT *********************************

POINTS 'HRb'  FILE  '/home/jvanlente/SWAN/2017/AlgemeenInvoer/HRbasis.pnt'
POINTS 'HRe'  FILE  '/home/jvanlente/SWAN/2017/AlgemeenInvoer/HRextra.pnt'
POINTS 'HR50' FILE  '/home/jvanlente/SWAN/2017/AlgemeenInvoer/HR50m.pnt'
POINTS 'P04'  FILE
'/home/jvanlente/SWAN/2017/AlgemeenInvoer/Pbuoys_2004.PNT'
POINTS 'P05'  FILE
'/home/jvanlente/SWAN/2017/AlgemeenInvoer/Pbuoys_2005.PNT'
POINTS 'P06'  FILE
'/home/jvanlente/SWAN/2017/AlgemeenInvoer/Pbuoys_2006.PNT'
POINTS 'P07'  FILE
'/home/jvanlente/SWAN/2017/AlgemeenInvoer/Pbuoys_2007.PNT'
POINTS 'P08'  FILE
'/home/jvanlente/SWAN/2017/AlgemeenInvoer/Pbuoys_2008.PNT'
POINTS 'MLOW'       FILE
'/home/jvanlente/SWAN/2017/AlgemeenInvoer/M_locations_OW.PNT'
POINTS 'FS'       FILE
'/home/jvanlente/SWAN/2017/AlgemeenInvoer/FS_locations_OW.PNT'

TABLE 'HRb' HEAD
'/home/jvanlente/SWAN/2017/OUT/G3/002/HRbasis_G3_13012017_002.TAB' &
        XP YP DEP HS RTP TPS TMM10 TM01 TM02 DIR DSPR WLEN DISS DHS DRTM01 &
        WATLEV WIND VEL BOTLEV QB

TABLE 'HRe' HEAD
'/home/jvanlente/SWAN/2017/OUT/G3/002/HRextra_G3_13012017_002.TAB' &
        XP YP DEP HS RTP TPS TMM10 TM01 TM02 DIR DSPR WLEN DISS DHS DRTM01 &
        WATLEV WIND VEL BOTLEV QB

TABLE 'HR50' HEAD
'/home/jvanlente/SWAN/2017/OUT/G3/002/HR50_G3_13012017_002.TAB' &
        XP YP DEP HS RTP TPS TMM10 TM01 TM02 DIR DSPR WLEN DISS DHS DRTM01 &
        WATLEV WIND VEL BOTLEV QB

TABLE 'P04' HEAD
'/home/jvanlente/SWAN/2017/OUT/G3/002/P04_G3_13012017_002.TAB' &
        XP YP DEP HS RTP TPS TMM10 TM01 TM02 DIR DSPR WLEN DISS DHS DRTM01 &
        WATLEV WIND VEL BOTLEV QB

TABLE 'P05' HEAD
'/home/jvanlente/SWAN/2017/OUT/G3/002/P05_G3_13012017_002.TAB' &
        XP YP DEP HS RTP TPS TMM10 TM01 TM02 DIR DSPR WLEN DISS DHS DRTM01 &
        WATLEV WIND VEL BOTLEV QB

TABLE 'P06' HEAD
'/home/jvanlente/SWAN/2017/OUT/G3/002/P06_G3_13012017_002.TAB' &
```

```
        XP YP DEP HS RTP TPS TMM10 TM01 TM02 DIR DSPR WLEN DISS DHS DRTM01 &
        WATLEV WIND VEL BOTLEV QB

TABLE 'P07' HEAD
'/home/jvanlente/SWAN/2017/OUT/G3/002/P07_G3_13012017_002.TAB' &
        XP YP DEP HS RTP TPS TMM10 TM01 TM02 DIR DSPR WLEN DISS DHS DRTM01 &
        WATLEV WIND VEL BOTLEV QB

TABLE 'P08' HEAD
'/home/jvanlente/SWAN/2017/OUT/G3/002/P08_G3_13012017_002.TAB' &
        XP YP DEP HS RTP TPS TMM10 TM01 TM02 DIR DSPR WLEN DISS DHS DRTM01 &
        WATLEV WIND VEL BOTLEV QB

TABLE 'MLOW' HEAD
'/home/jvanlente/SWAN/2017/OUT/G3/002/MLOW_G3_13012017_002.TAB' &
        XP YP DEP HS RTP TPS TMM10 TM01 TM02 DIR DSPR WLEN DISS DHS DRTM01
WATLEV WIND VEL

TABLE 'FS' HEAD '/home/jvanlente/SWAN/2017/OUT/G3/002/FS_G3_13012017_002.TAB'
&
        XP YP DEP HS RTP TPS TMM10 TM01 TM02 DIR DSPR WLEN DISS DHS DRTM01
WATLEV WIND VEL

BLOCK 'COMPGRID' NOHEAD
'/home/jvanlente/SWAN/2017/OUT/G3/002/G3_13012017_002.mat' &
       LAYOUT 3 XP YP DEPTH HSIG RTP TPS TMM10 TM01 TM02 DIR DSPR WLEN &
       DHS DRTM01 WATLEV WIND VEL DISSIP BOTLEV QB

SPECOUT 'HRb'  SPEC1D ABS
'/home/jvanlente/SWAN/2017/OUT/G3/002/HRbasis_G3_13012017_002.SP1'
SPECOUT 'HRe'  SPEC1D ABS
'/home/jvanlente/SWAN/2017/OUT/G3/002/HRextra_G3_13012017_002.SP1'
SPECOUT 'HR50' SPEC1D ABS
'/home/jvanlente/SWAN/2017/OUT/G3/002/HR50_G3_13012017_002.SP1'
SPECOUT 'P04'  SPEC1D ABS
'/home/jvanlente/SWAN/2017/OUT/G3/002/P04_G3_13012017_002.SP1'
SPECOUT 'P05'  SPEC1D ABS
'/home/jvanlente/SWAN/2017/OUT/G3/002/P05_G3_13012017_002.SP1'
SPECOUT 'P06'  SPEC1D ABS
'/home/jvanlente/SWAN/2017/OUT/G3/002/P06_G3_13012017_002.SP1'
SPECOUT 'P07'  SPEC1D ABS
'/home/jvanlente/SWAN/2017/OUT/G3/002/P07_G3_13012017_002.SP1'
SPECOUT 'P08'  SPEC1D ABS
'/home/jvanlente/SWAN/2017/OUT/G3/002/P08_G3_13012017_002.SP1'
SPECOUT 'MLOW' SPEC1D ABS
'/home/jvanlente/SWAN/2017/OUT/G3/002/MLOW_G3_13012017_002.SP1'
SPECOUT 'FS' SPEC1D ABS
'/home/jvanlente/SWAN/2017/OUT/G3/002/FS_G3_13012017_002.SP1'
```

```
SPECOUT 'HRb'  SPEC2D ABS
'/home/jvanlente/SWAN/2017/OUT/G3/002/HRbasis_G3_13012017_002.SP2'
SPECOUT 'HRe'  SPEC2D ABS
'/home/jvanlente/SWAN/2017/OUT/G3/002/HRextra_G3_13012017_002.SP2'
SPECOUT 'HR50' SPEC2D ABS
'/home/jvanlente/SWAN/2017/OUT/G3/002/HR50_G3_13012017_002.SP2'
SPECOUT 'P04'  SPEC2D ABS
'/home/jvanlente/SWAN/2017/OUT/G3/002/P04_G3_13012017_002.SP2'
SPECOUT 'P05'  SPEC2D ABS
'/home/jvanlente/SWAN/2017/OUT/G3/002/P05_G3_13012017_002.SP2'
SPECOUT 'P06'  SPEC2D ABS
'/home/jvanlente/SWAN/2017/OUT/G3/002/P06_G3_13012017_002.SP2'
SPECOUT 'P07'  SPEC2D ABS
'/home/jvanlente/SWAN/2017/OUT/G3/002/P07_G3_13012017_002.SP2'
SPECOUT 'P08'  SPEC2D ABS
'/home/jvanlente/SWAN/2017/OUT/G3/002/P08_G3_13012017_002.SP2'
SPECOUT 'MLOW' SPEC2D ABS
'/home/jvanlente/SWAN/2017/OUT/G3/002/MLOW_G3_13012017_002.SP2'
SPECOUT 'FS' SPEC2D ABS
'/home/jvanlente/SWAN/2017/OUT/G3/002/FS_G3_13012017_002.SP2'


TEST 1 0 POINTS XY   &
187516.00  598960.00 &
194245.00  601082.00 &
200611.00  602531.00 &
207049.00  603287.00 &
213520.00  603255.00 &
219625.00  602713.00 &
225993.00  604547.00 &
232919.00  605438.00 &
239965.00  608542.00 &
247299.00  609282.00 &
252045.00  608679.00 &
253949.55  603481.76 &
255679.00  597365.00 &
261125.00  593872.00 &
265920.00  591720.00 &
267473.00  587908.00 &
273124.00  584797.00 &
208002.00  609787.00 &
182672.10  605722.89 &
 PAR '/home/jvanlente/SWAN/2017/OUT/G3/002/G3_13012017_002.PAR'

COMPUTE

STOP
```

V
Model results 2019

V.1. Water level

Measured water levels are plotted against calculated levels from WAQUA (dcsmv6-zunov4) in Figure V.1. The following locations are shown in Figure V.1: Huibertgat, Wierumergronden, Nes, Schiermonnikoog, Lauwersoog, Eemshaven, Delfzijl, Nieuwe Statenzijl.

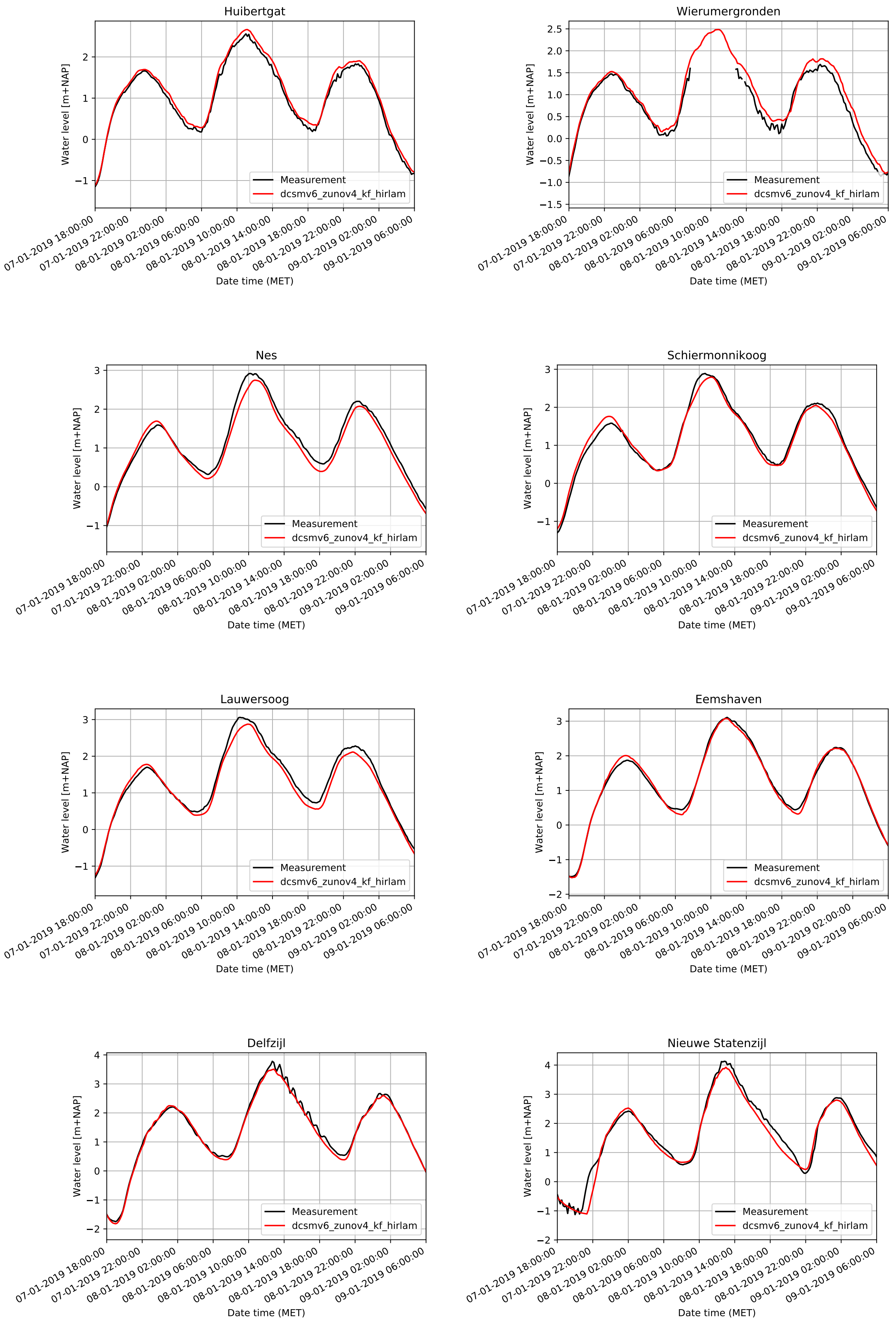

Figure V.1: Comparison between measured and modelled water levels for hindcast 2019.

V.2. Wind

Measured wind speed(Figure V.2) and direction(Figure V.3) are plotted against calculated HIRLAM wind speed and direction. The following locations are shown in Figure V.2 and Figure V.3: Huibertgat, Amelander Westgat (AWG), Lauwersoog, and Nieuwe Beerta.

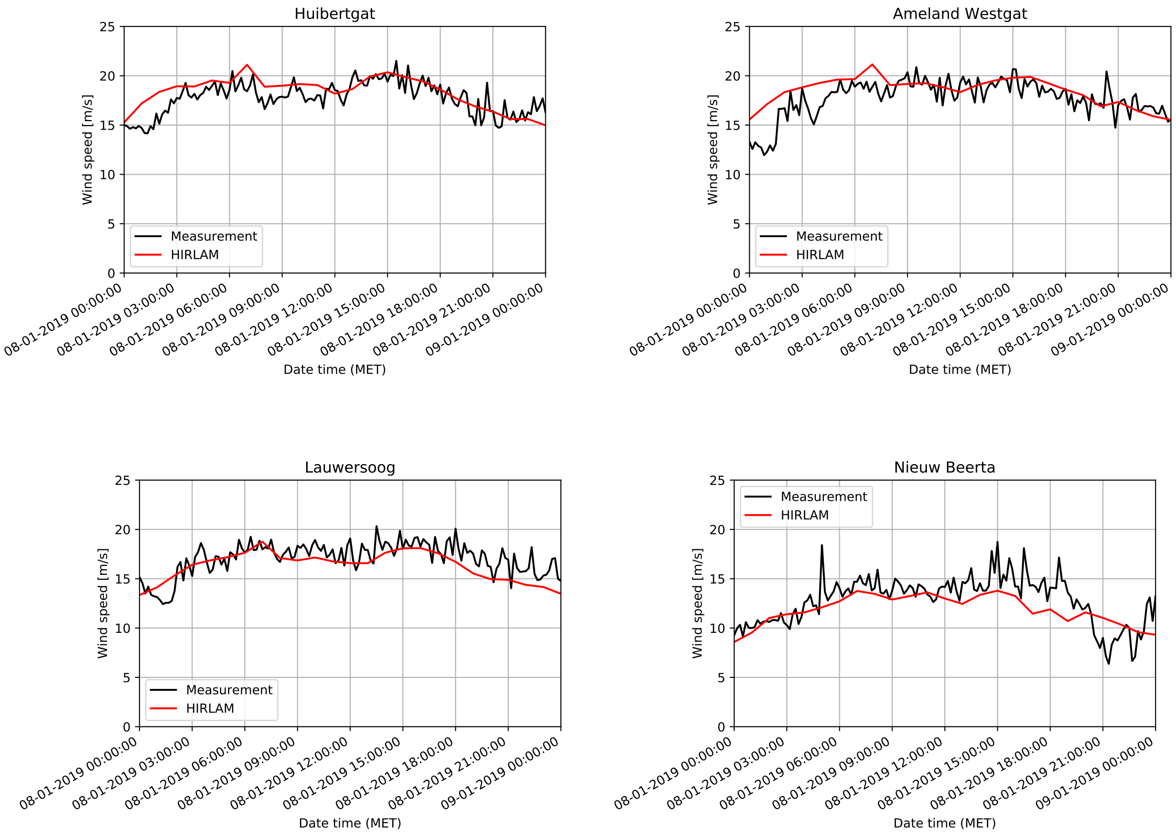

Figure V.2: Comparison between measured and HIRLAM wind speed for hindcast 2019.

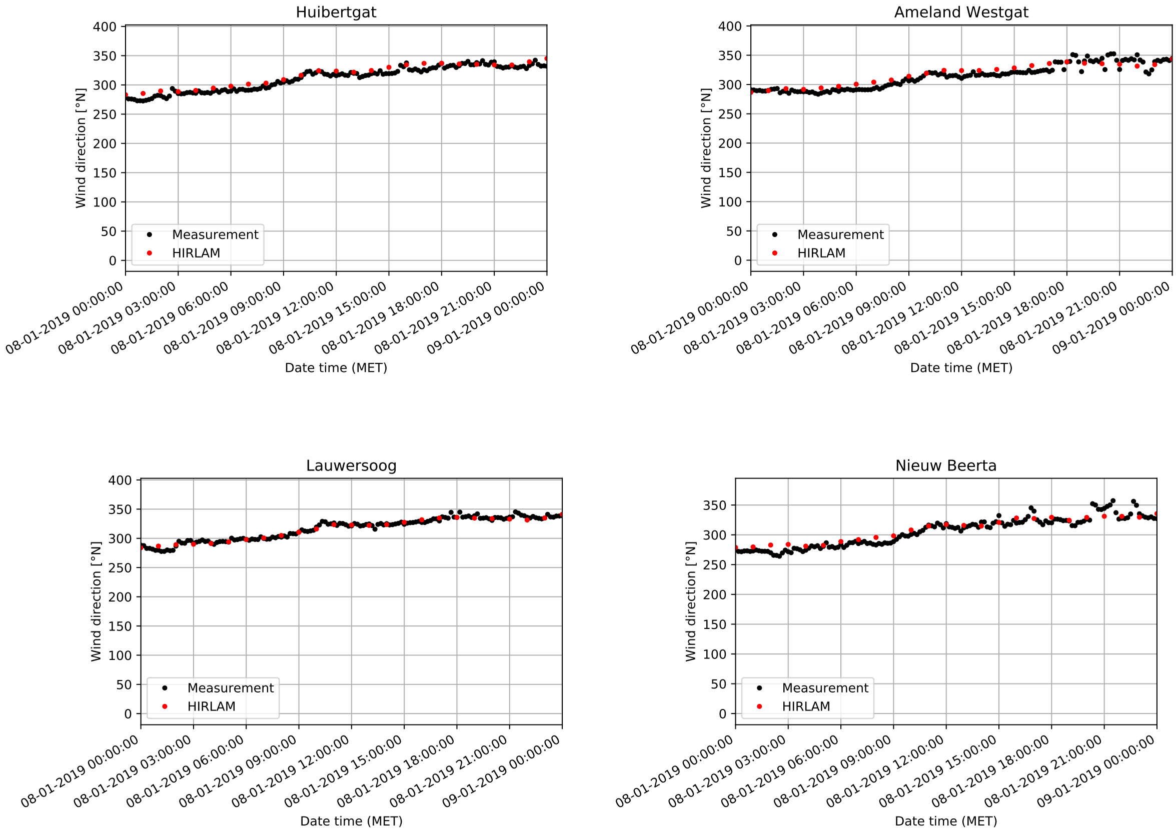

Figure V.3: Comparison between measured and HIRLAM wind direction for hindcast 2019.

V.3. SWAN spatial fields

Results hindcast (001): 8 January 2019 11:20, Grid G3, SWAN 40.72ABCDE

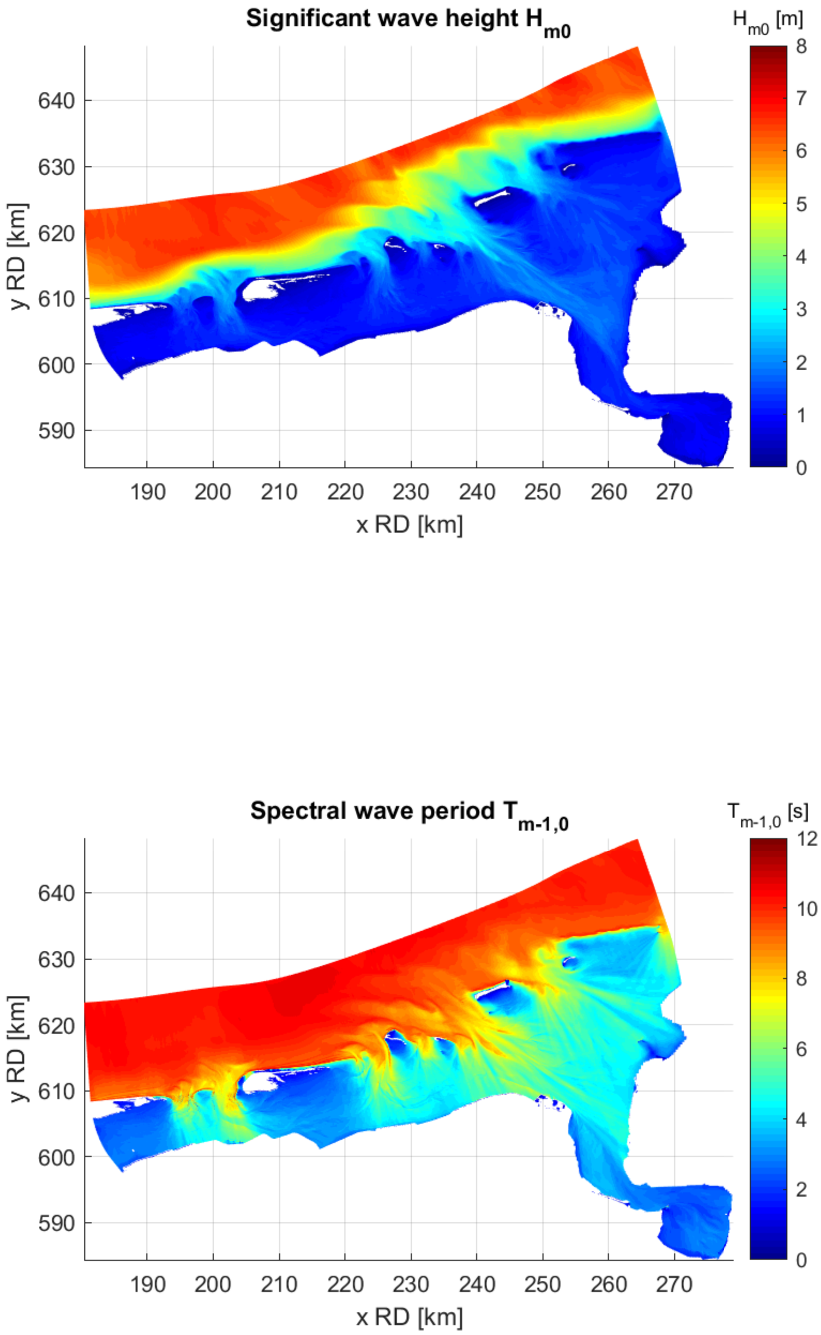

Figure V.4: Variation of significant wave height H_{m0} and spectral wave period $T_{\mathrm{m\text{-}1,0}}$ for G3 grid, 8 January 2019 11:20

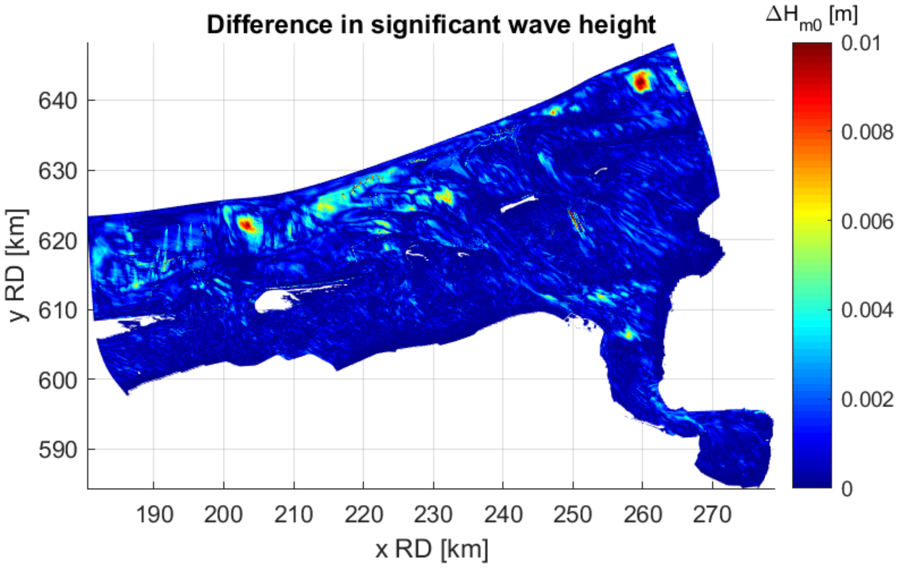

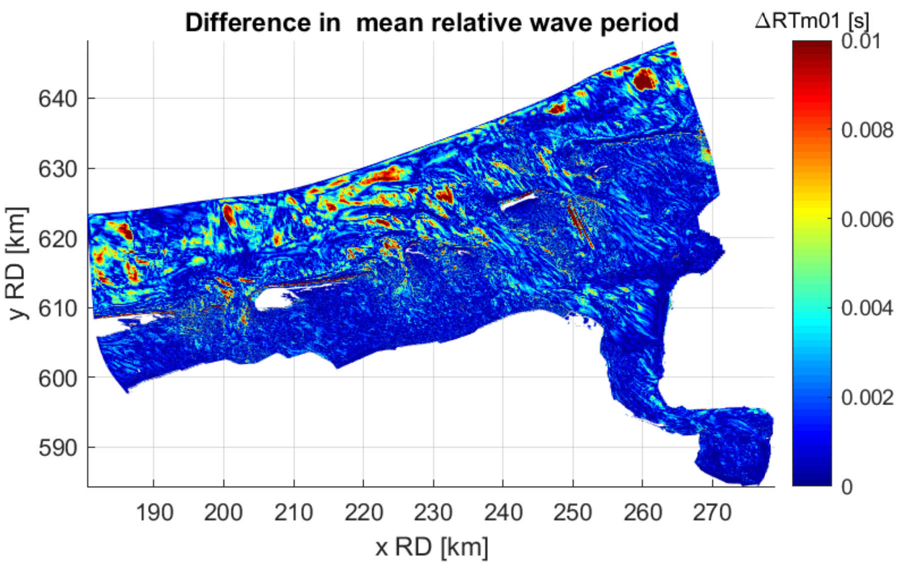

Figure V.5: Difference of significant wave height H_{m0} and relative spectral wave period RT_{m01} as computed in the last two iterations for G3 grid, 8 January 2019 11:20

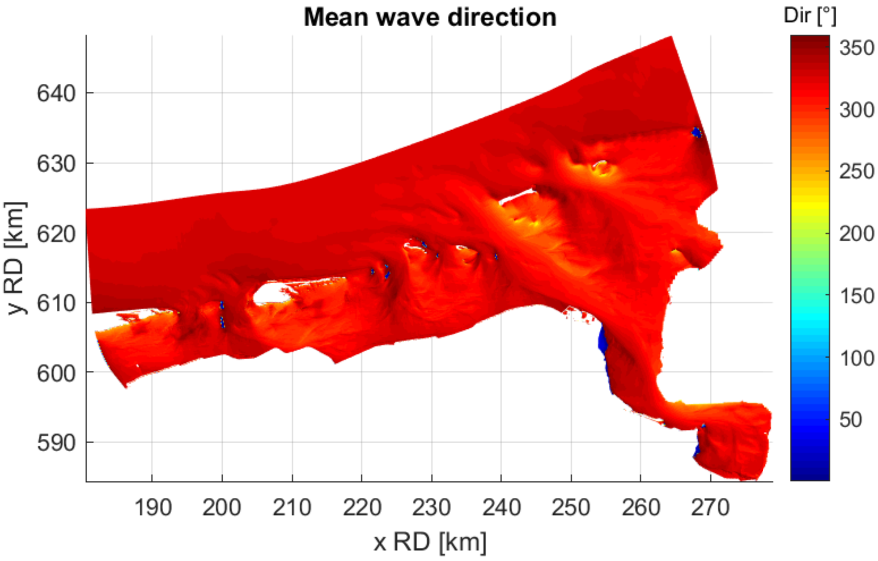

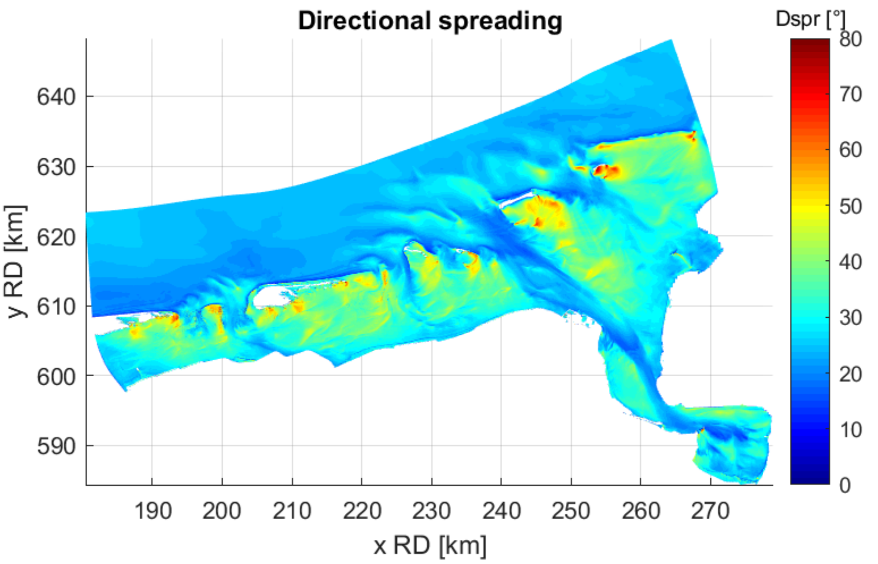

Figure V.6: Variation of mean wave direction DIR and directional spreading Dspr for G3 grid, 8 January 2019 11:20

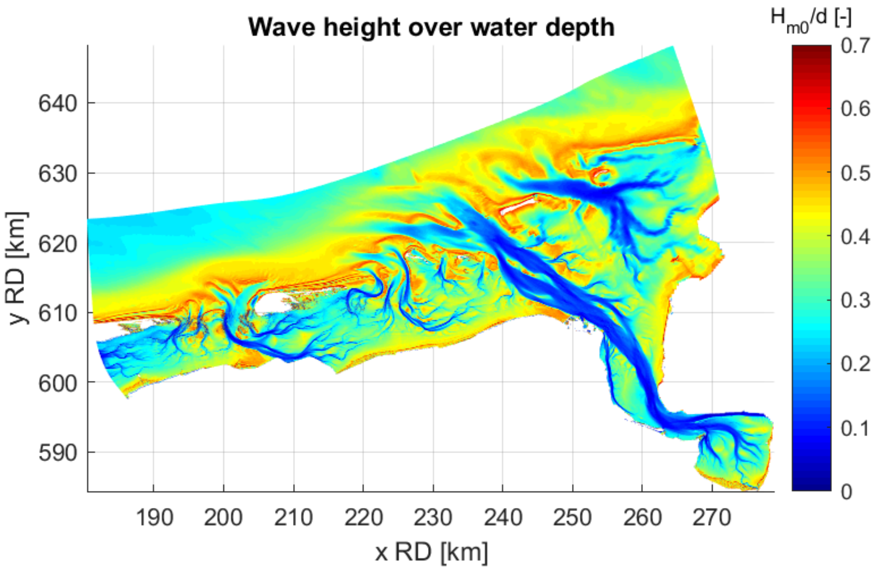

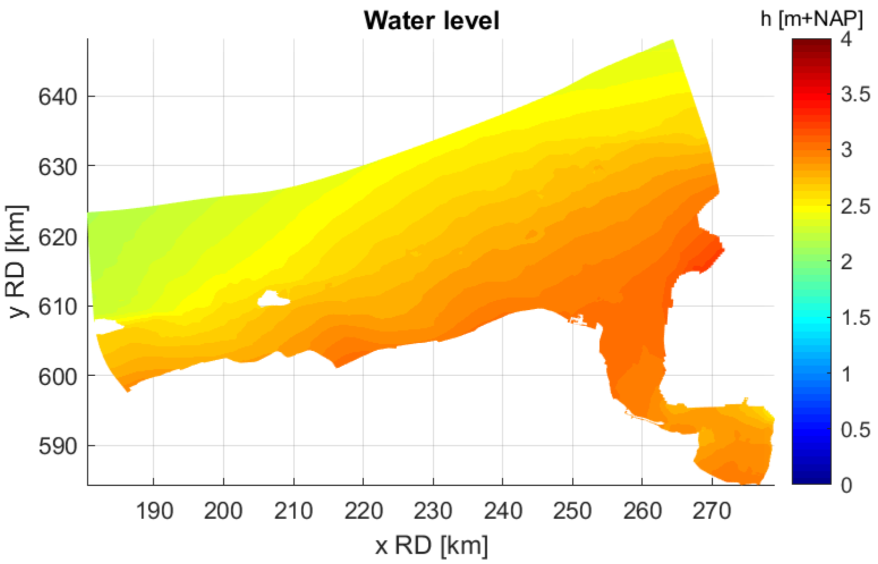

Figure V.7: Variation of the ratio $H_{\mathrm{m0}}/\mathrm{d}$ and water level h for G3 grid, 8 January 2019 11:20

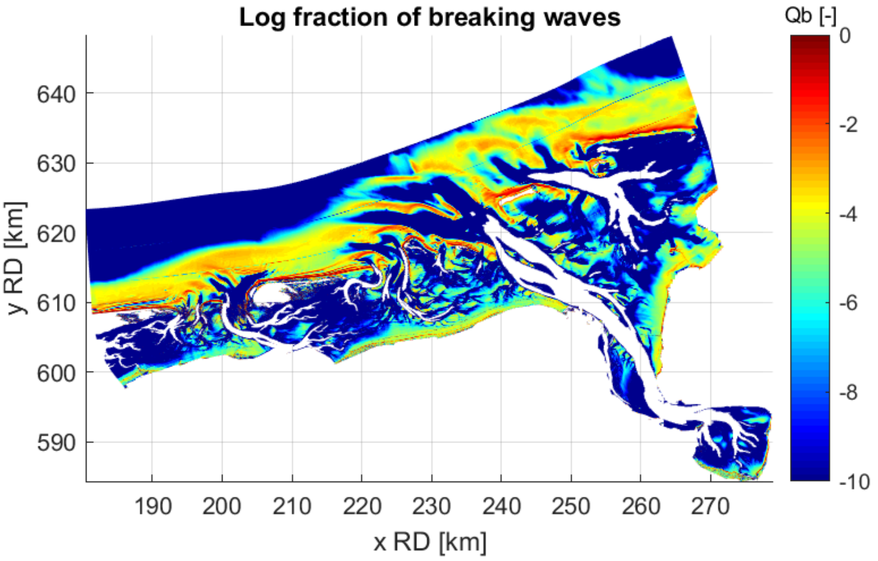

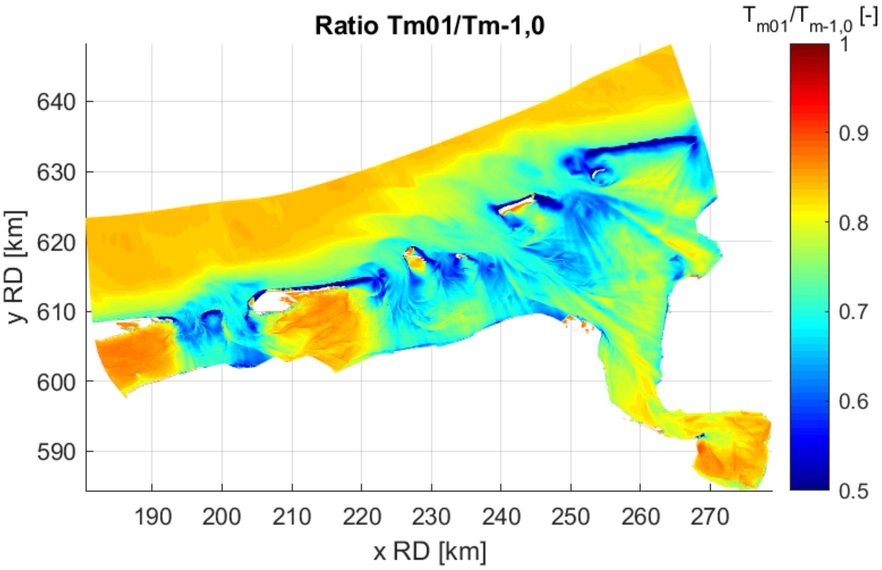

Figure V.8: The variation of breaking waves and ratio $T_{\mathrm{m01}}/T_{\mathrm{m\text{-}1,0}}$ for G3 grid, 8 January 2019 11:20

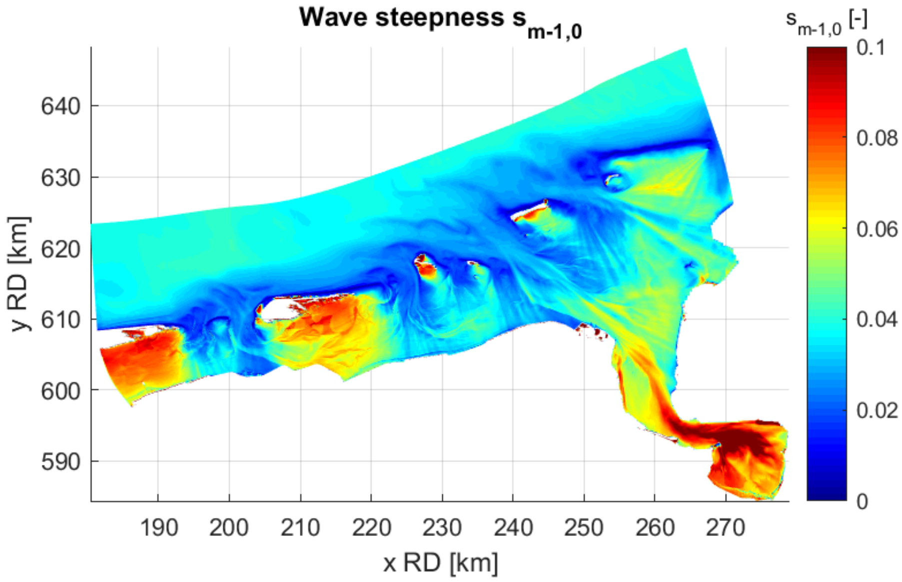

Figure V.9: The variation of wave steepness ($s_{m-1,0}$) for G3 grid, 8 January 2019 11:20

Results hindcast (002): 8 January 2019 11:40, Grid G3, SWAN 40.72ABCDE

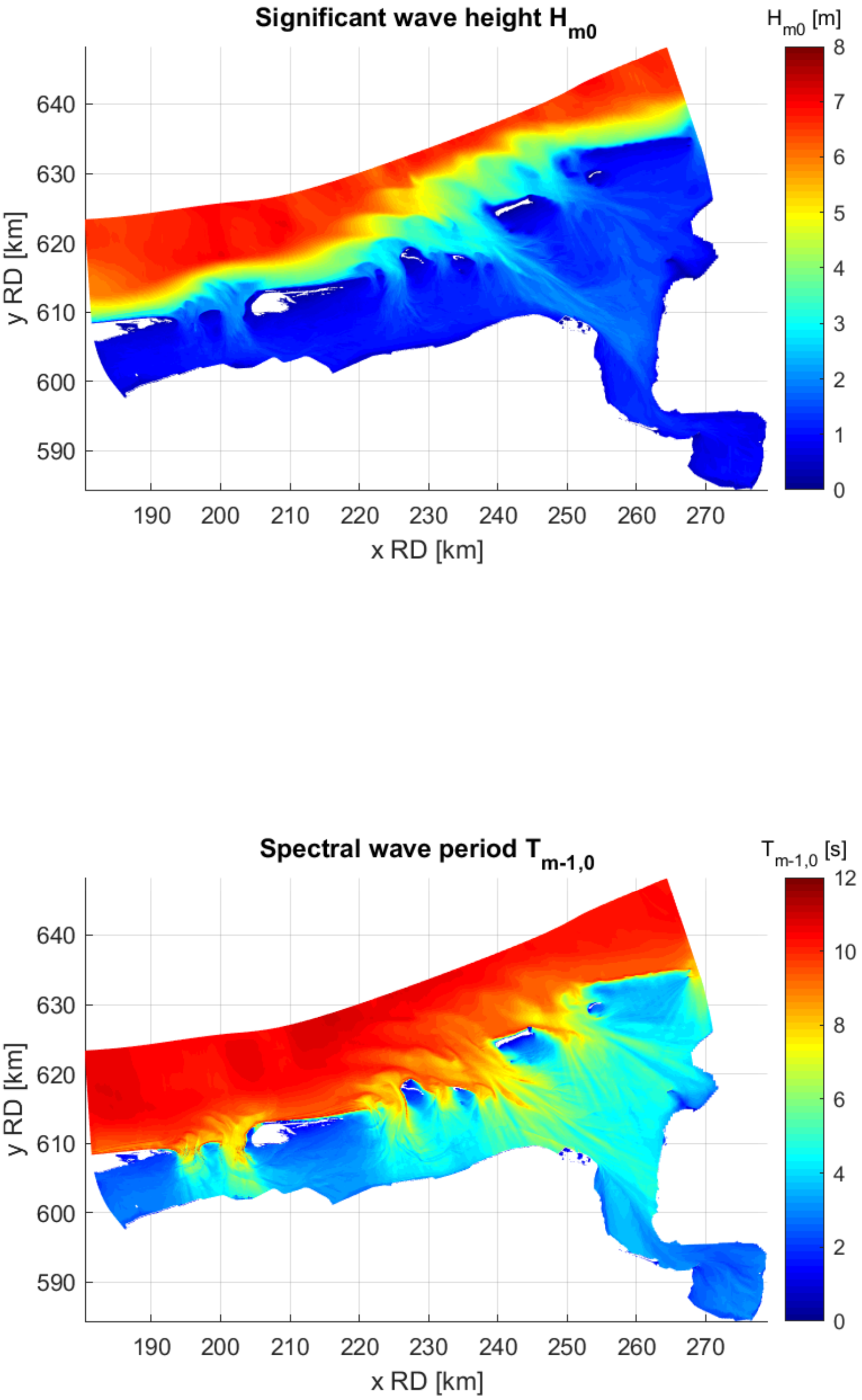

Figure V.10: Variation of significant wave height H_{m0} and spectral wave period $T_{\mathrm{m\text{-}1,0}}$ for G3 grid, 8 January 2019 11:40

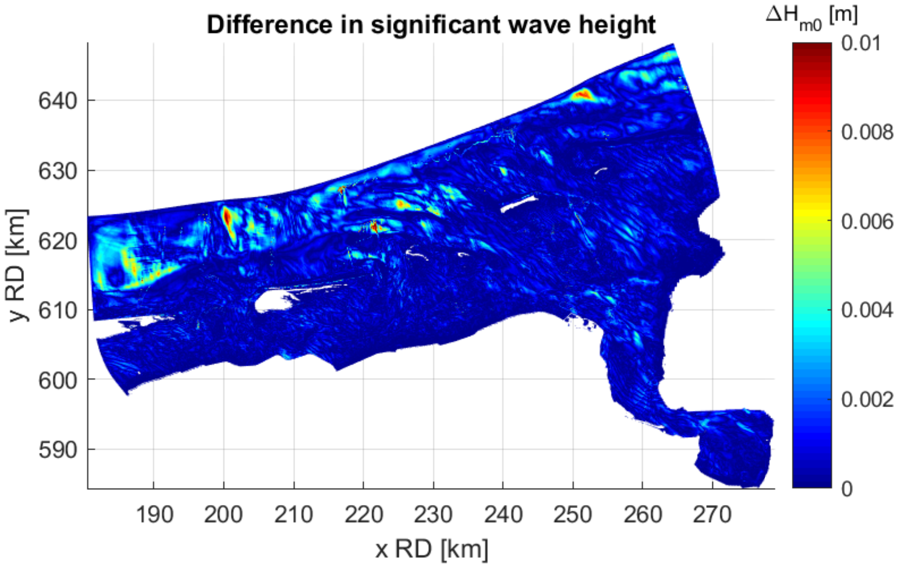

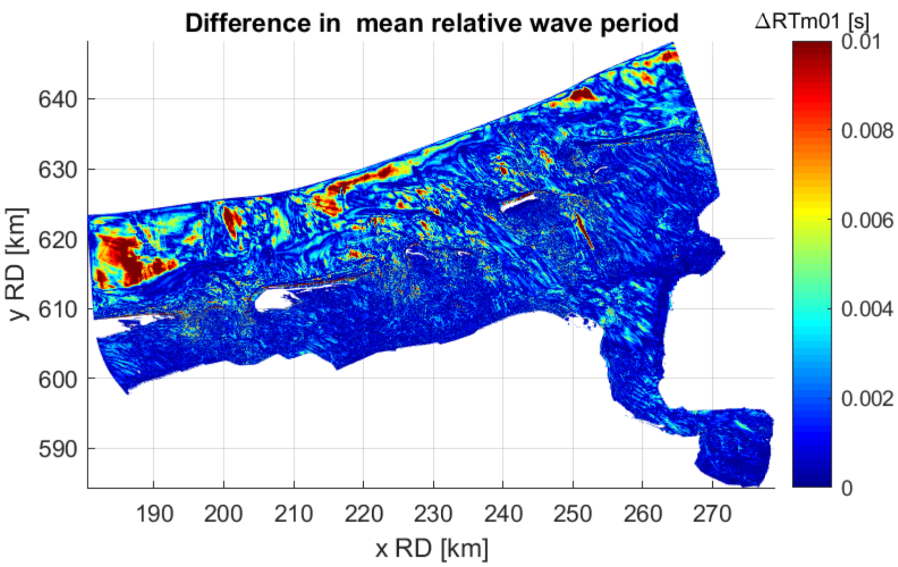

Figure V.11: Difference of significant wave height H_{m0} and relative spectral wave period RT_{m01} as computed in the last two iterations for G3 grid, 8 January 2019 11:40

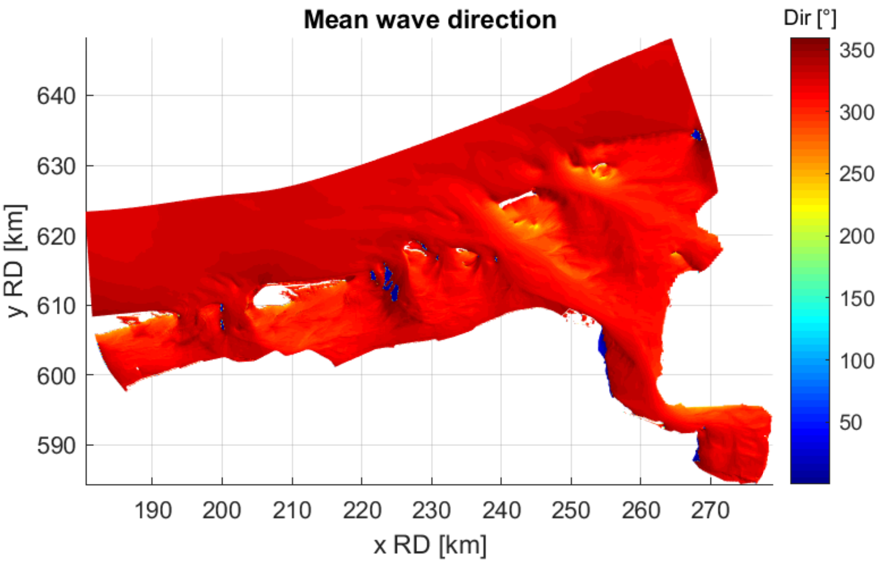

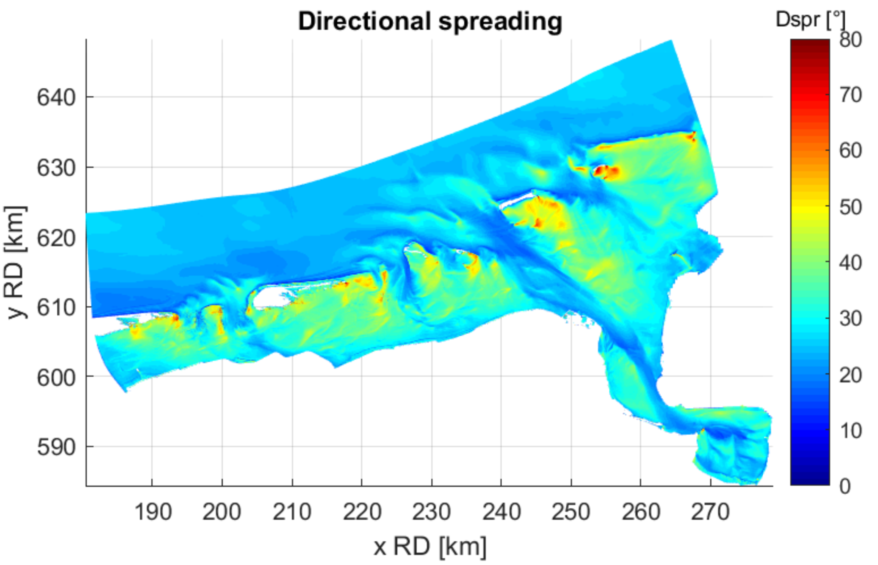

Figure V.12: Variation of mean wave direction DIR and directional spreading Dspr for G3 grid, 8 January 2019 11:40

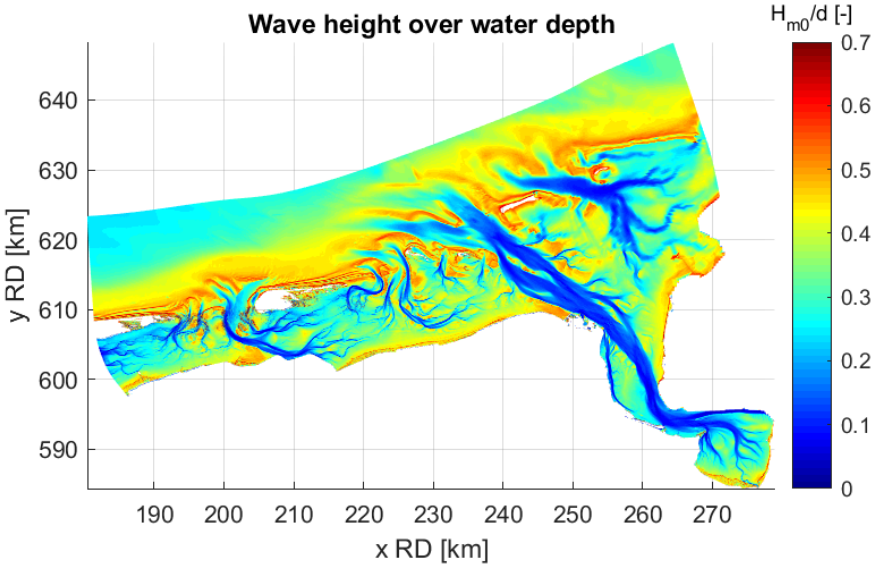

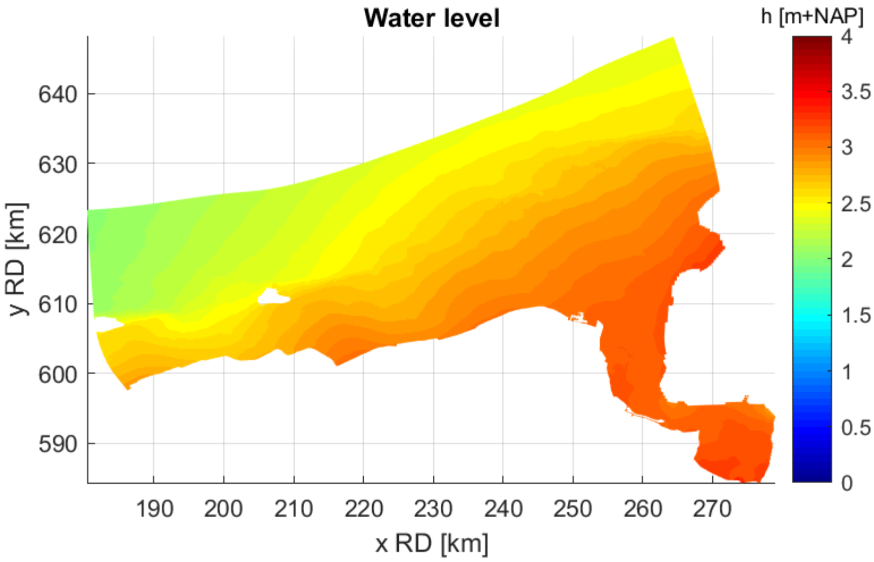

Figure V.13: Variation of the ratio $H_{\mathrm{m0}}/\mathrm{d}$ and water level h for G3 grid, 8 January 2019 11:40

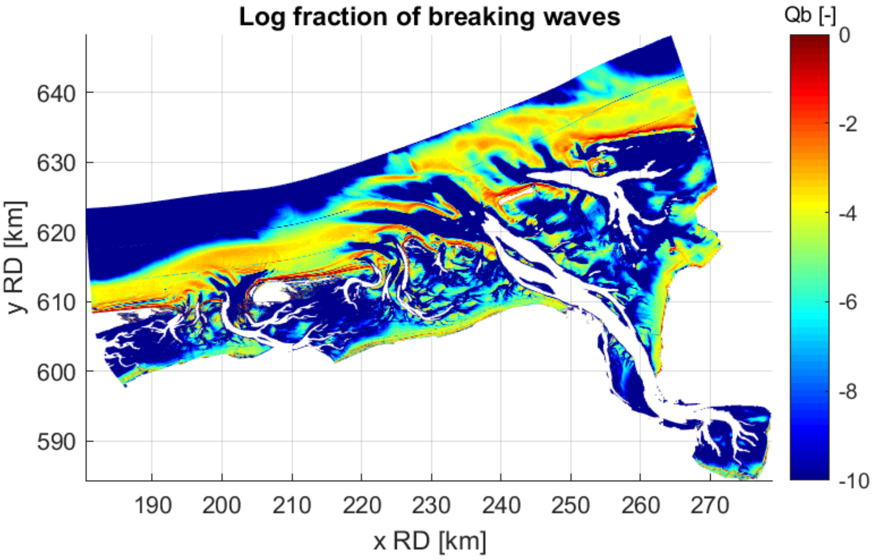

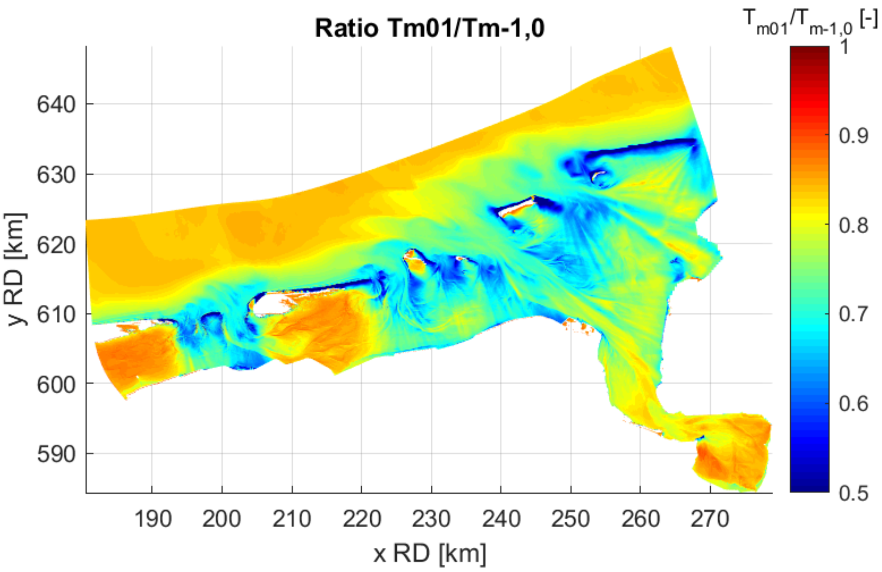

Figure V.14: The variation of breaking waves and ratio $T_{\mathrm{m01}}\,/\,T_{\mathrm{m\text{-}1,0}}$ for G3 grid, 8 January 2019 11:40

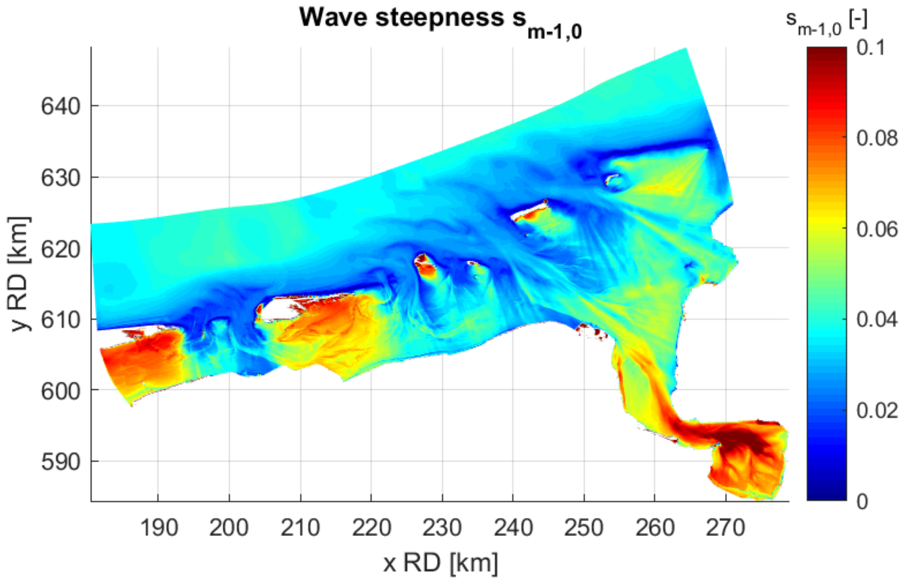

Figure V.15: The variation of wave steepness ($s_{m-1,0}$) for G3 grid, 8 January 2019 11:40

Results hindcast (003): 8 January 2019 11:50, Grid G3, SWAN 40.72ABCDE

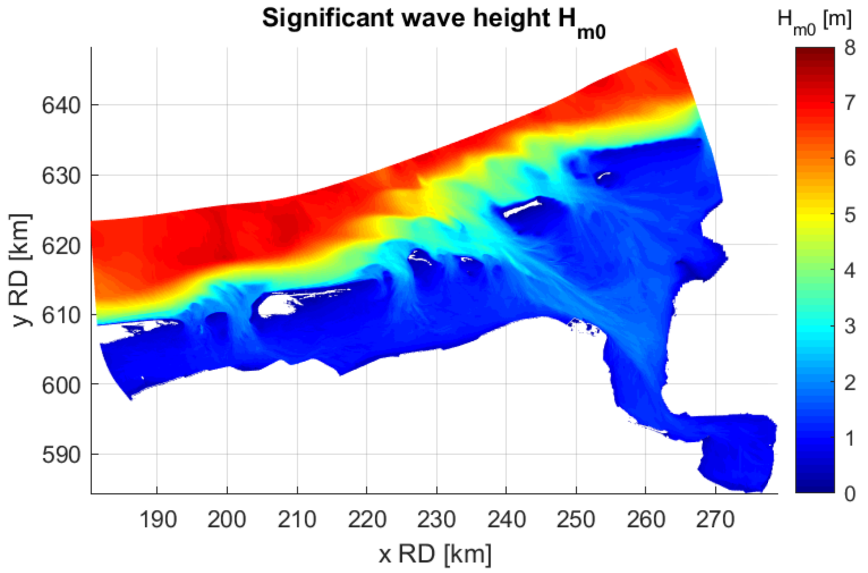

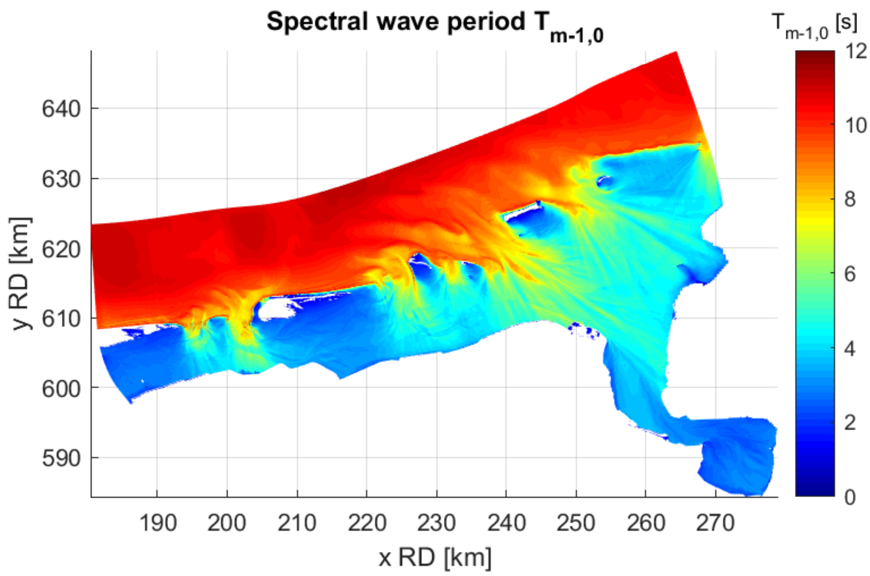

Figure V.16: Variation of significant wave height H_{m0} and spectral wave period $T_{\mathrm{m\text{-}1,0}}$ for G3 grid, 8 January 2019 11:50

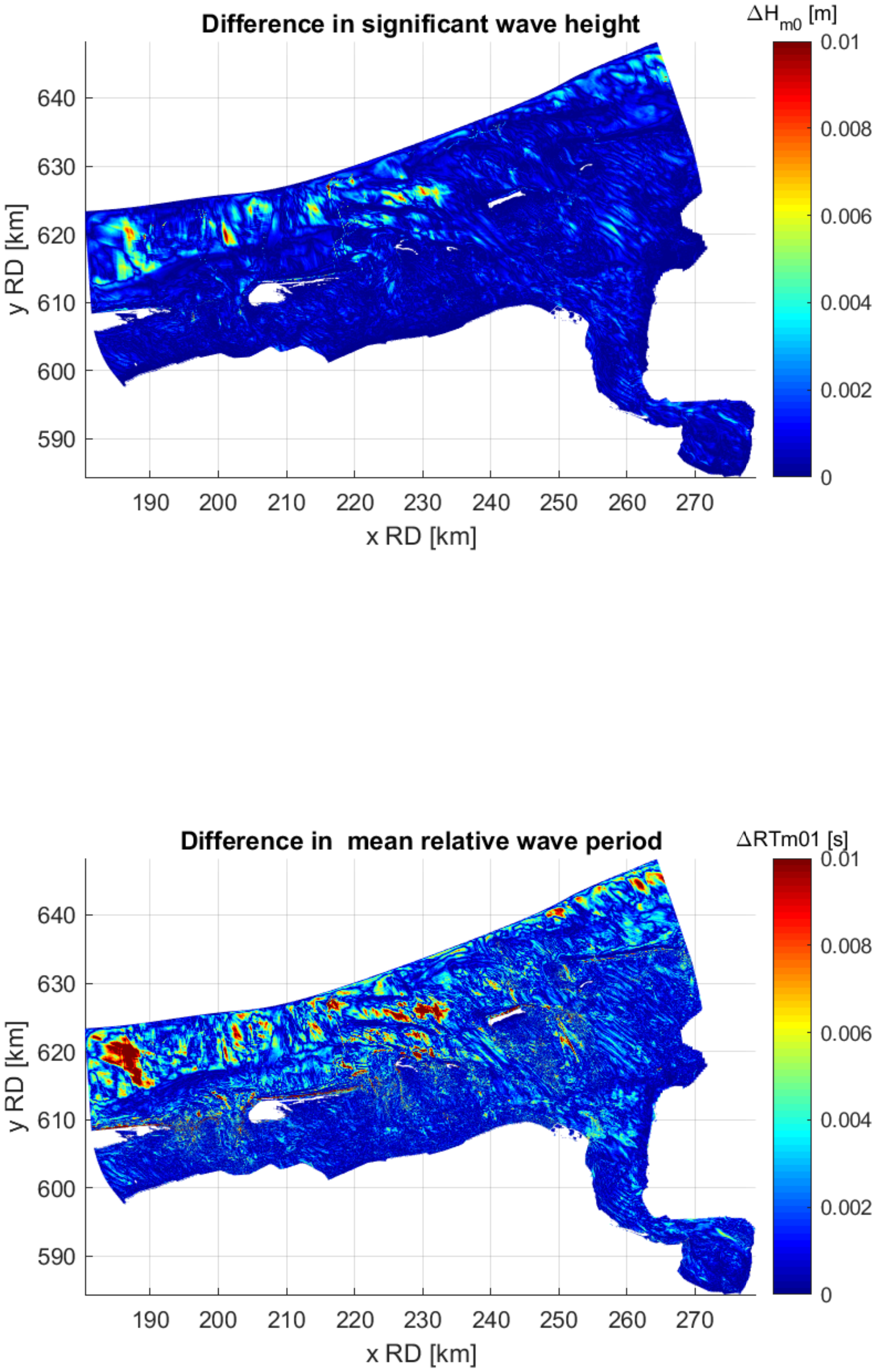

Figure V.17: Difference of significant wave height H_{m0} and relative spectral wave period RT_{m01} as computed in the last two iterations for G3 grid, 8 January 2019 11:50

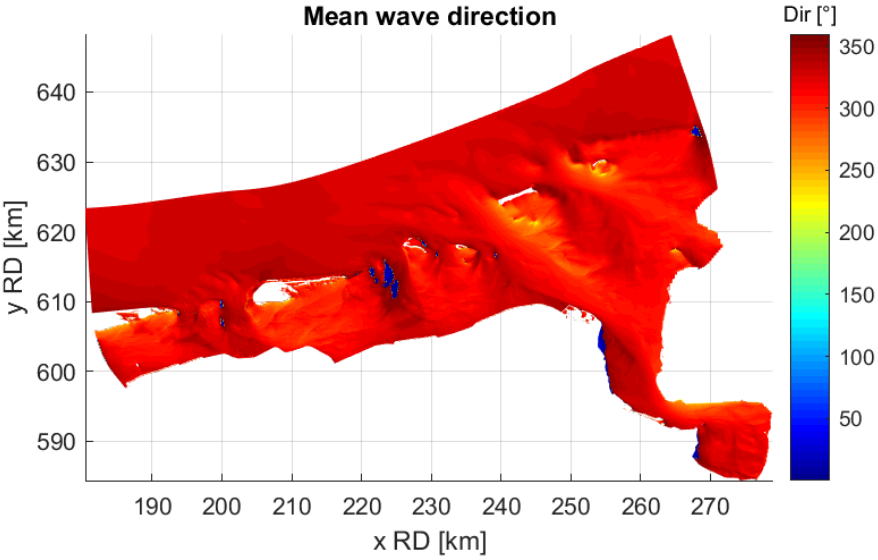

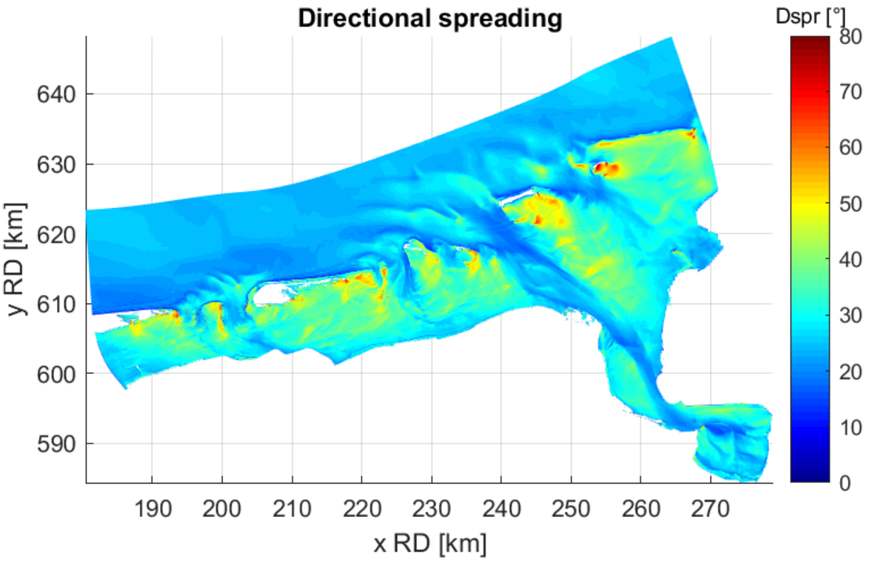

Figure V.18: Variation of mean wave direction DIR and directional spreading Dspr for G3 grid, 8 January 2019 11:50

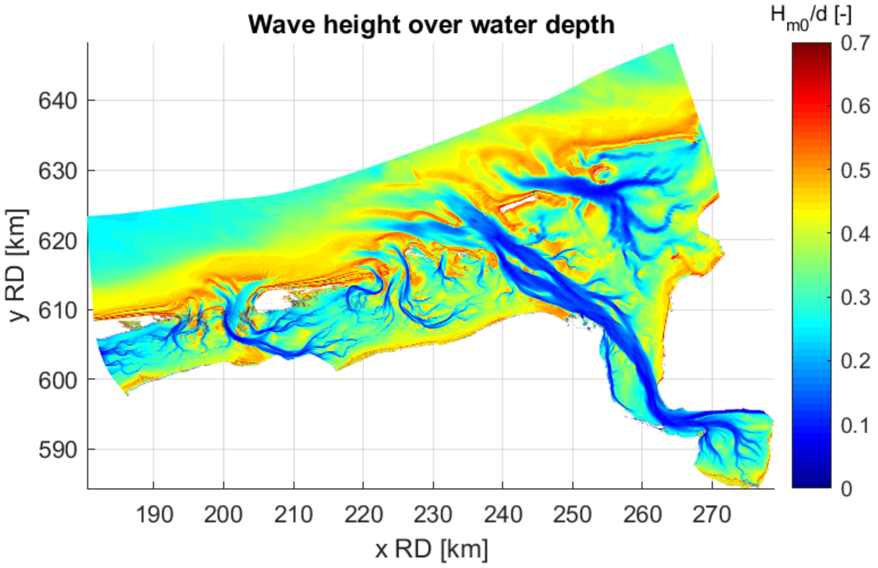

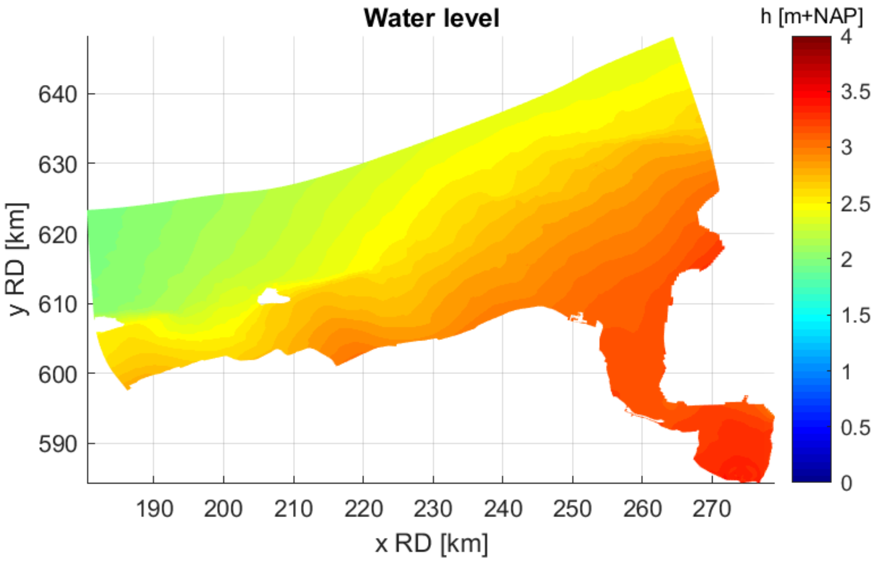

Figure V.19: Variation of the ratio $H_{\mathrm{m0}}/\mathrm{d}$ and water level h for G3 grid, 8 January 2019 11:50

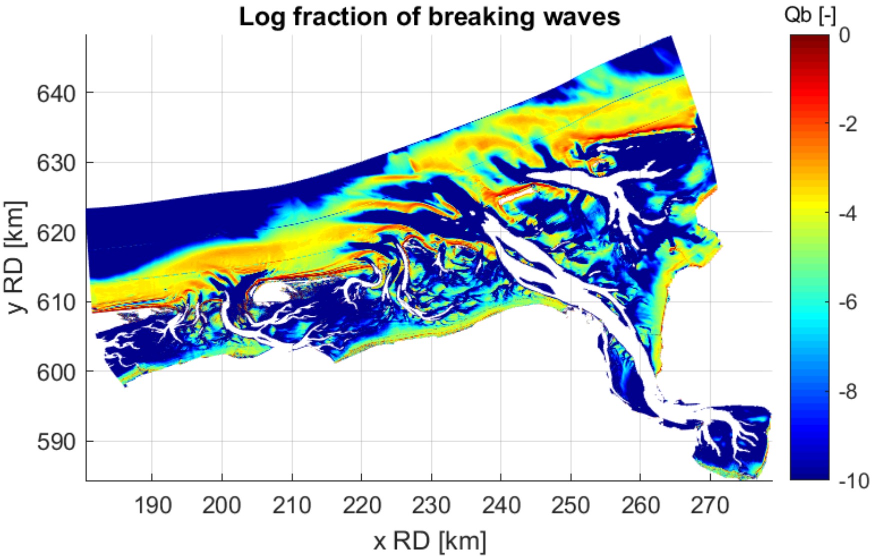

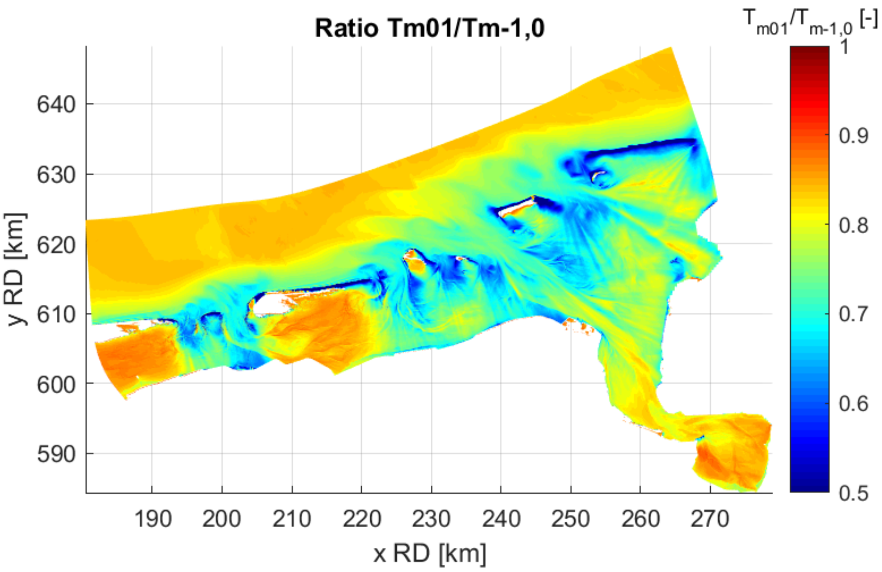

Figure V.20: The variation of breaking waves and ratio $T_{\mathrm{m01}}\,/\,T_{\mathrm{m\text{-}1,0}}$ for G3 grid, 8 January 2019 11:50

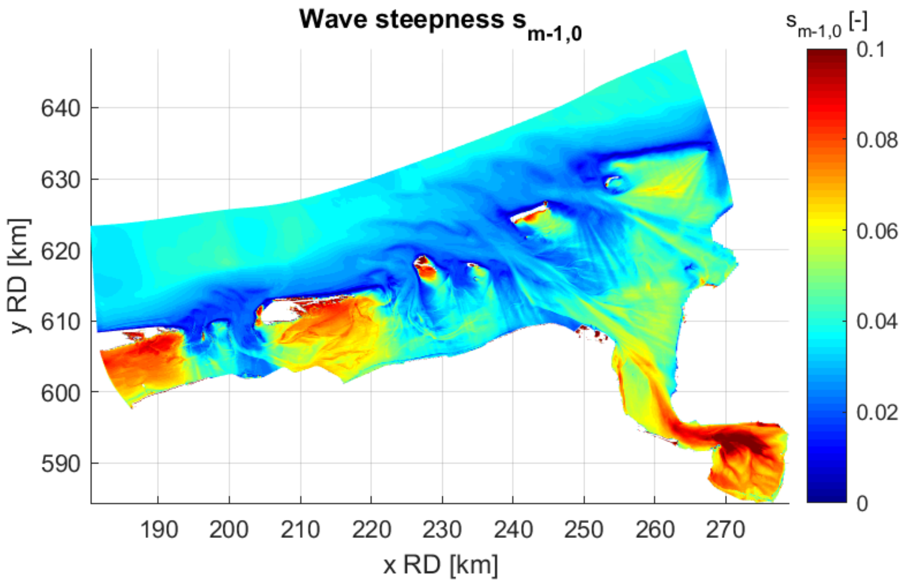

Figure V.21: The variation of wave steepness ($s_{m-1,0}$) for G3 grid, 8 January 2019 11:50

Results hindcast (004): 8 January 2019 13:10, Grid G3, SWAN 40.72ABCDE

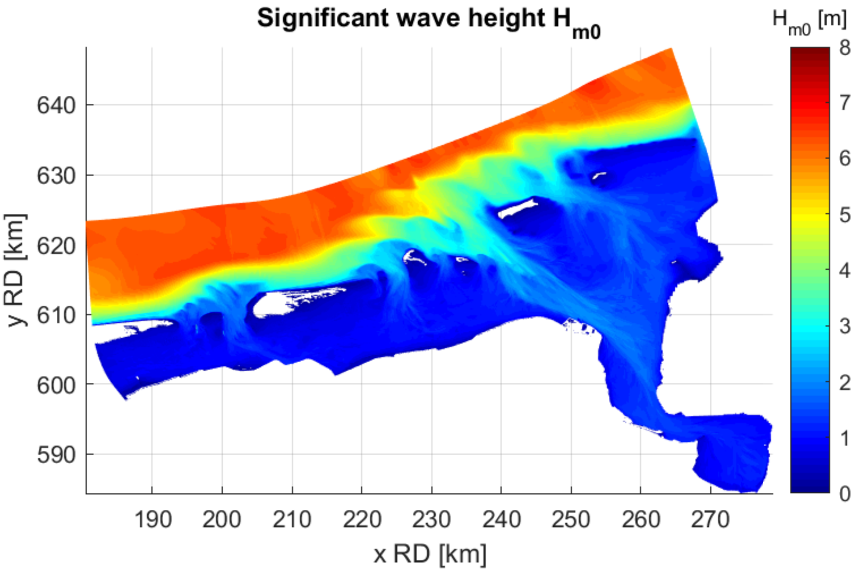

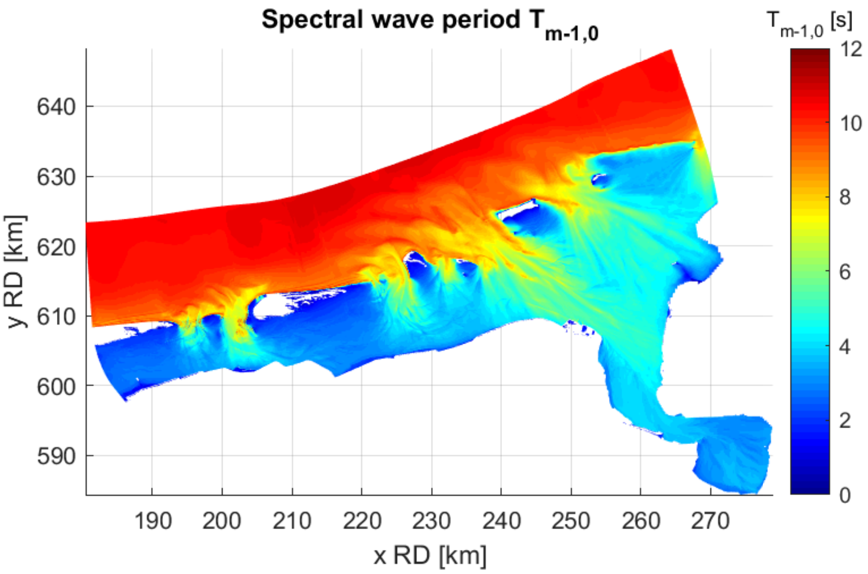

Figure V.22: Variation of significant wave height H_{m0} and spectral wave period $T_{\mathrm{m-1,0}}$ for G3 grid, 8 January 2019 13:10

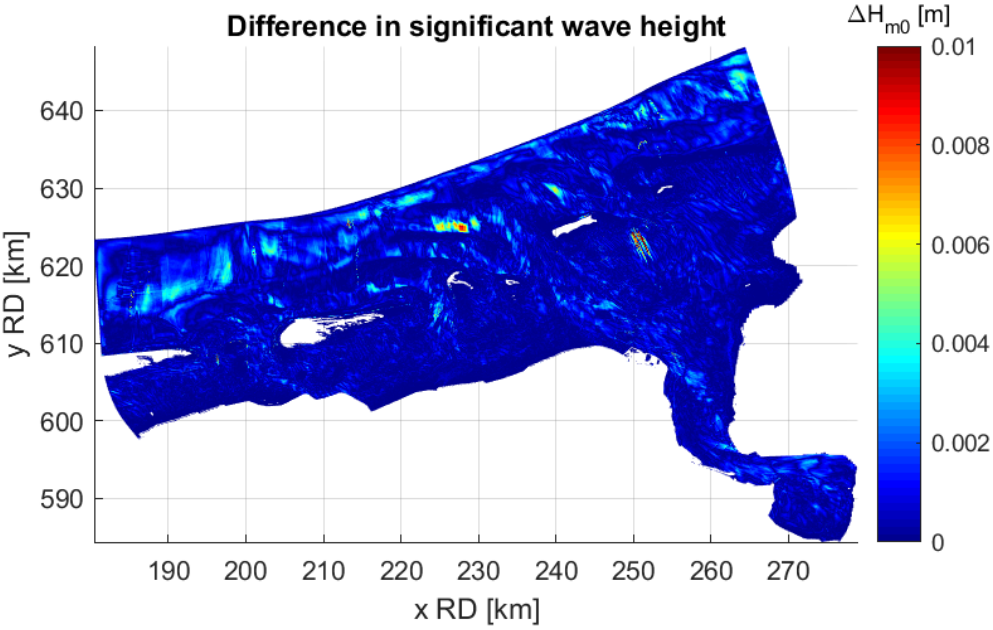

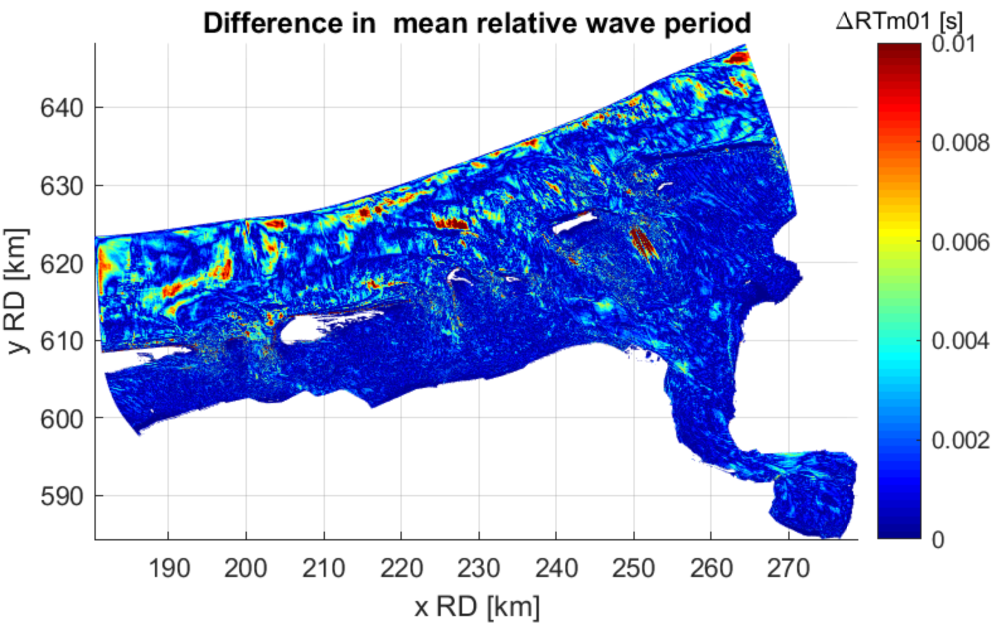

Figure V.23: Difference of significant wave height H_{m0} and relative spectral wave period RT_{m01} as computed in the last two iterations for G3 grid, 8 January 2019 13:10

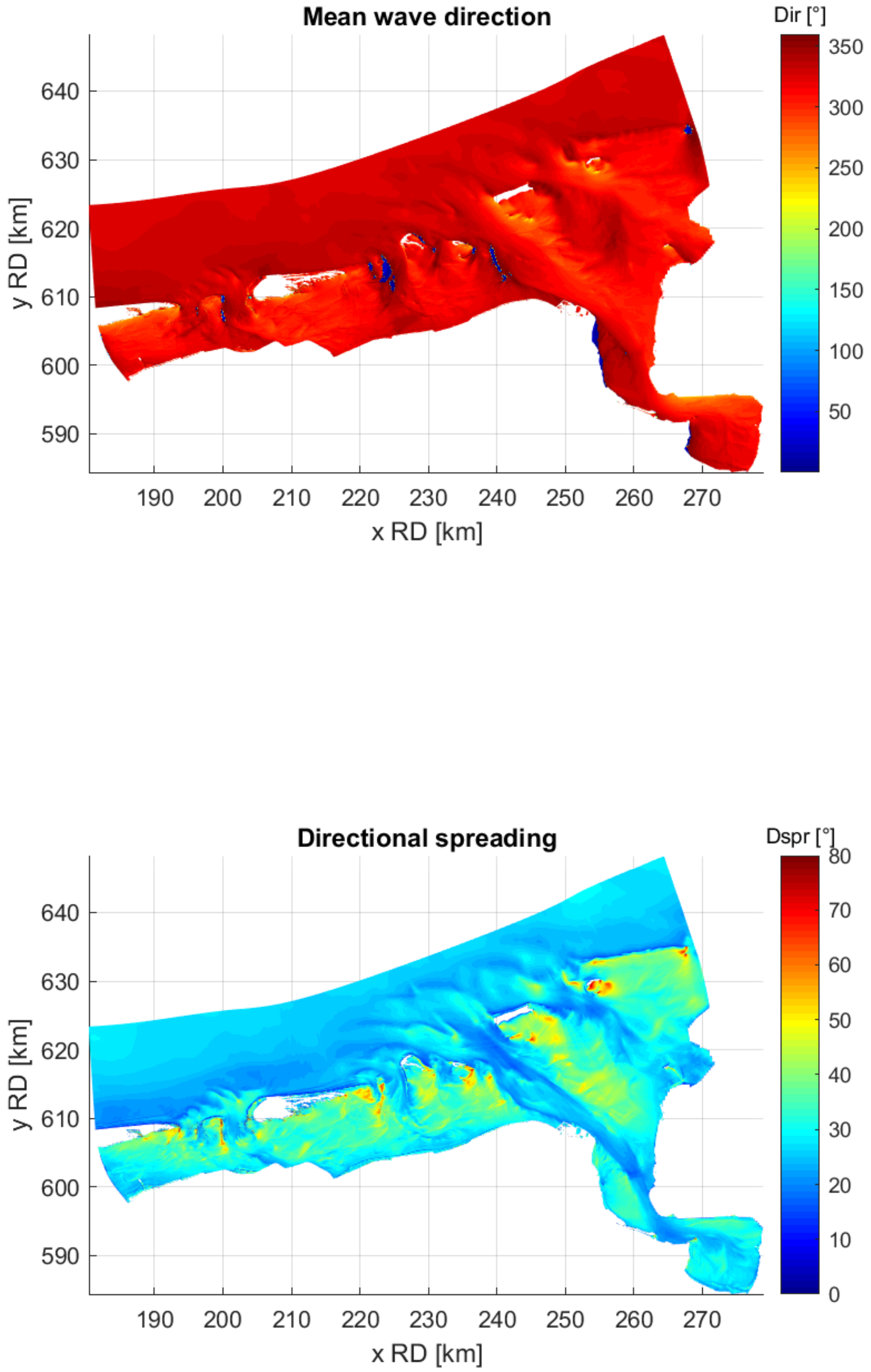

Figure V.24: Variation of mean wave direction DIR and directional spreading Dspr for G3 grid, 8 January 2019 13:10

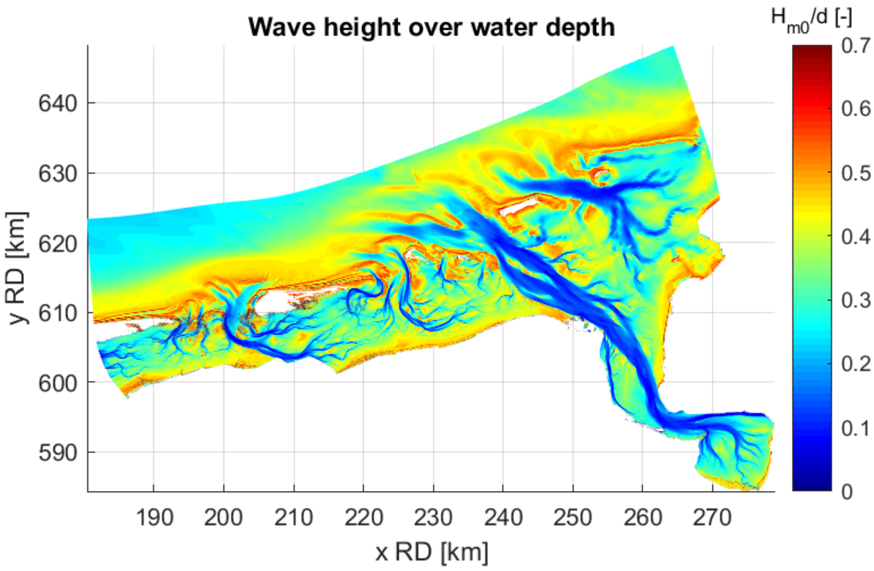

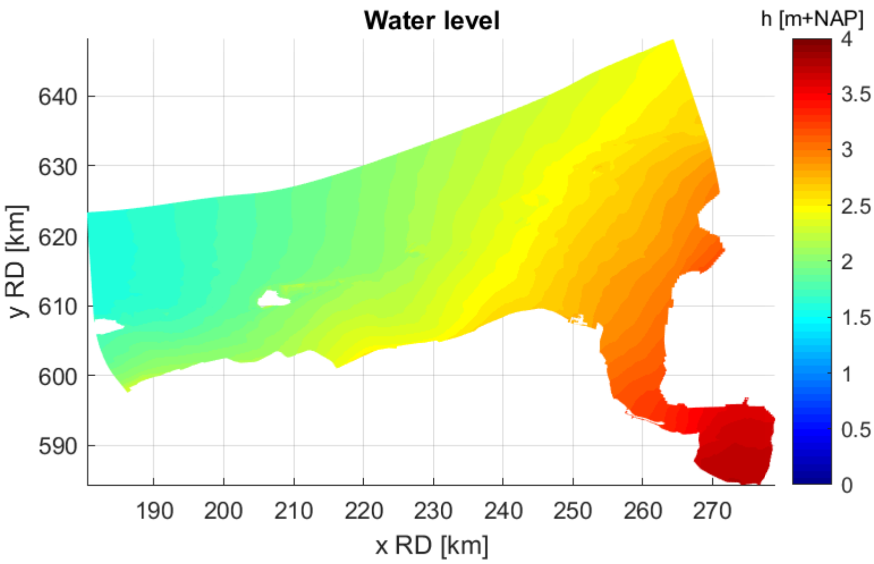

Figure V.25: Variation of the ratio $H_{\mathrm{m0}}/\mathrm{d}$ and water level h for G3 grid, 8 January 2019 13:10

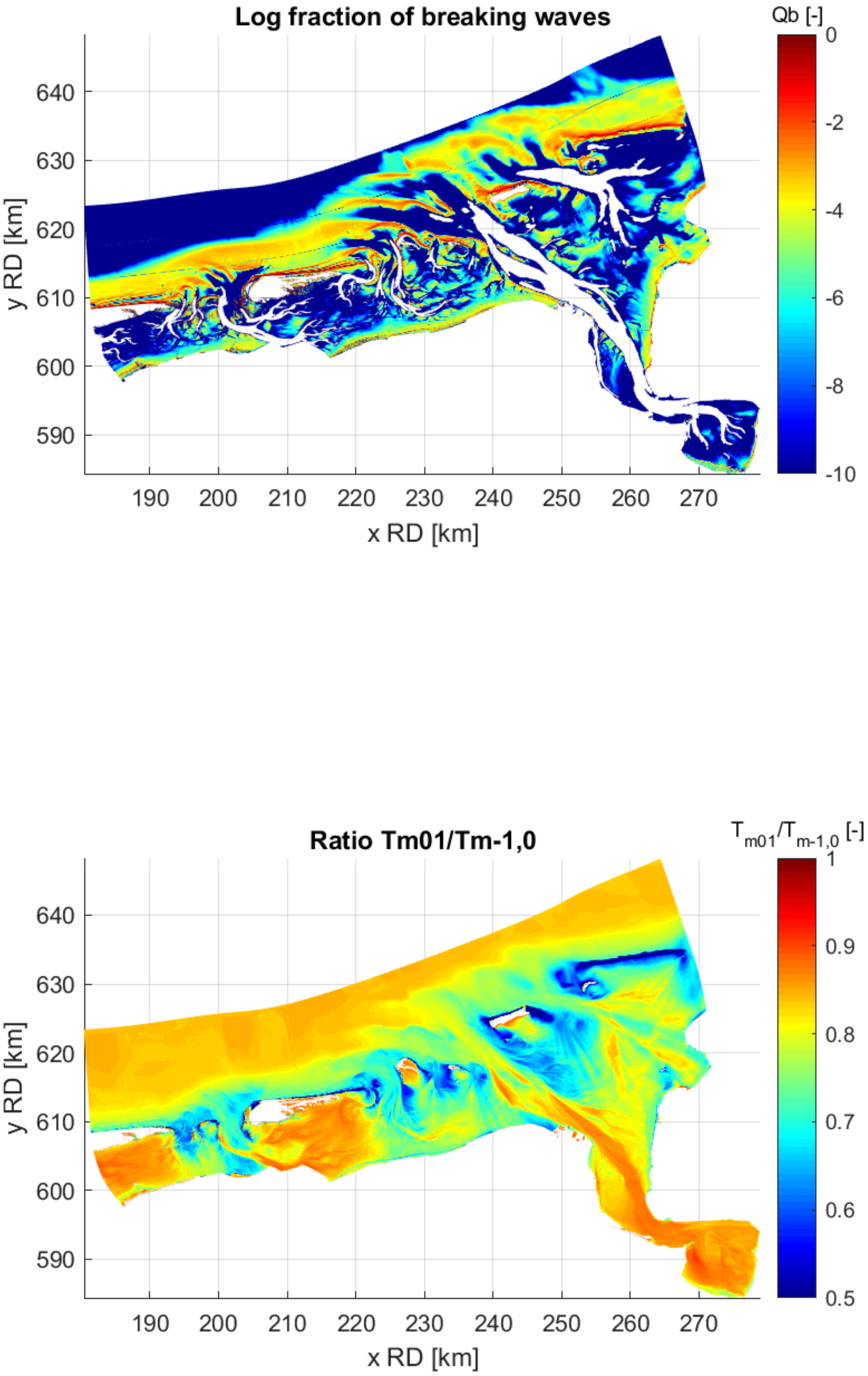

Figure V.26: The variation of breaking waves and ratio $T_{\mathrm{m01}}\,/\,T_{\mathrm{m\text{-}1,0}}$ for G3 grid, 8 January 2019 13:10

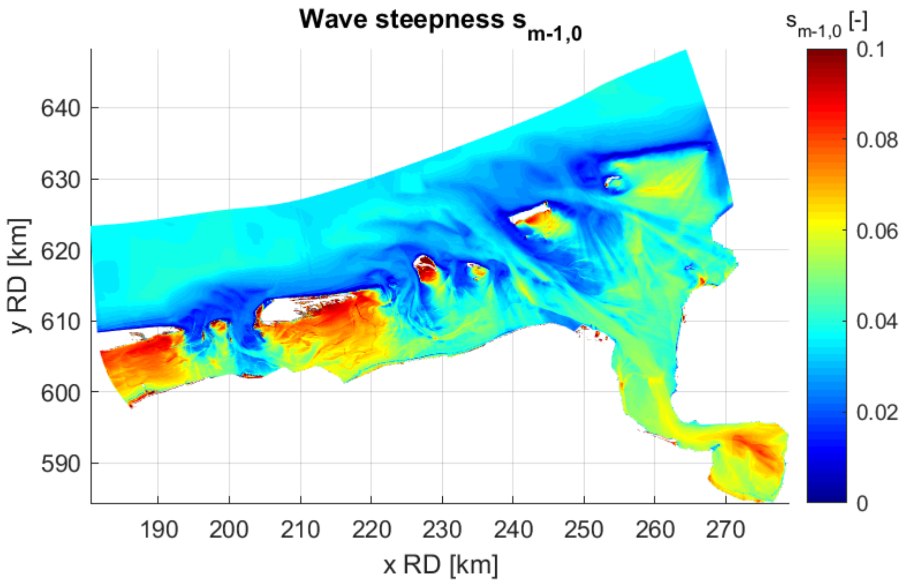

Figure V.27: The variation of wave steepness ($s_{m-1,0}$) for G3 grid, 8 January 2019 13:10

V.4. Variance density spectra

Measured variance density spectra are compared with calculated SWAN spectra. This is shown in Figures V.28 and V.29 for offshore locations Schiermonnikoog Noord (SMN1) and Westereems West (WEW1). In Figure V.30, SWAN variance density spectra are plotted for measurement locations in the Eastern Wadden Sea. For these locations no measurements were requested

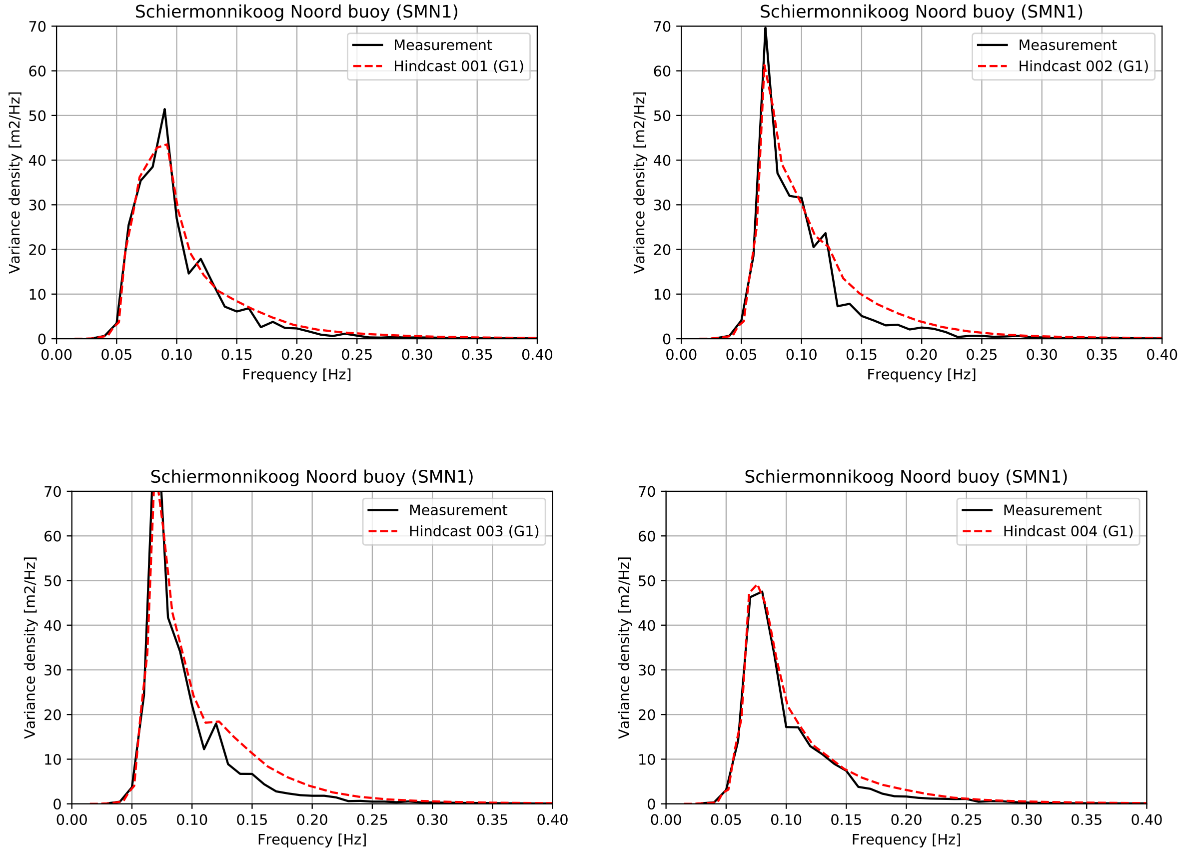

Figure V.28: Measured wave spectra at Schiermonnikoog Noord buoy compared to SWAN hindcast 2019

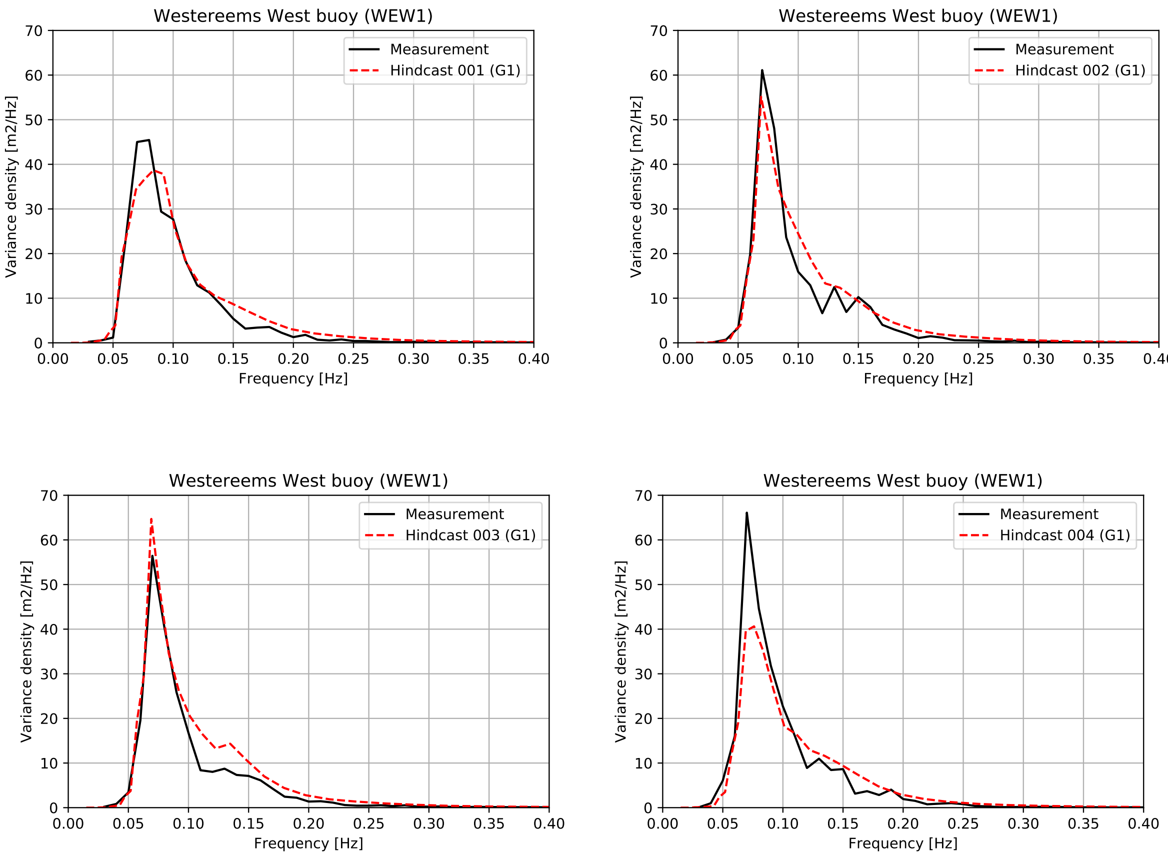

Figure V.29: Measured wave spectra at Westereems West buoy compared to SWAN hindcast 2019

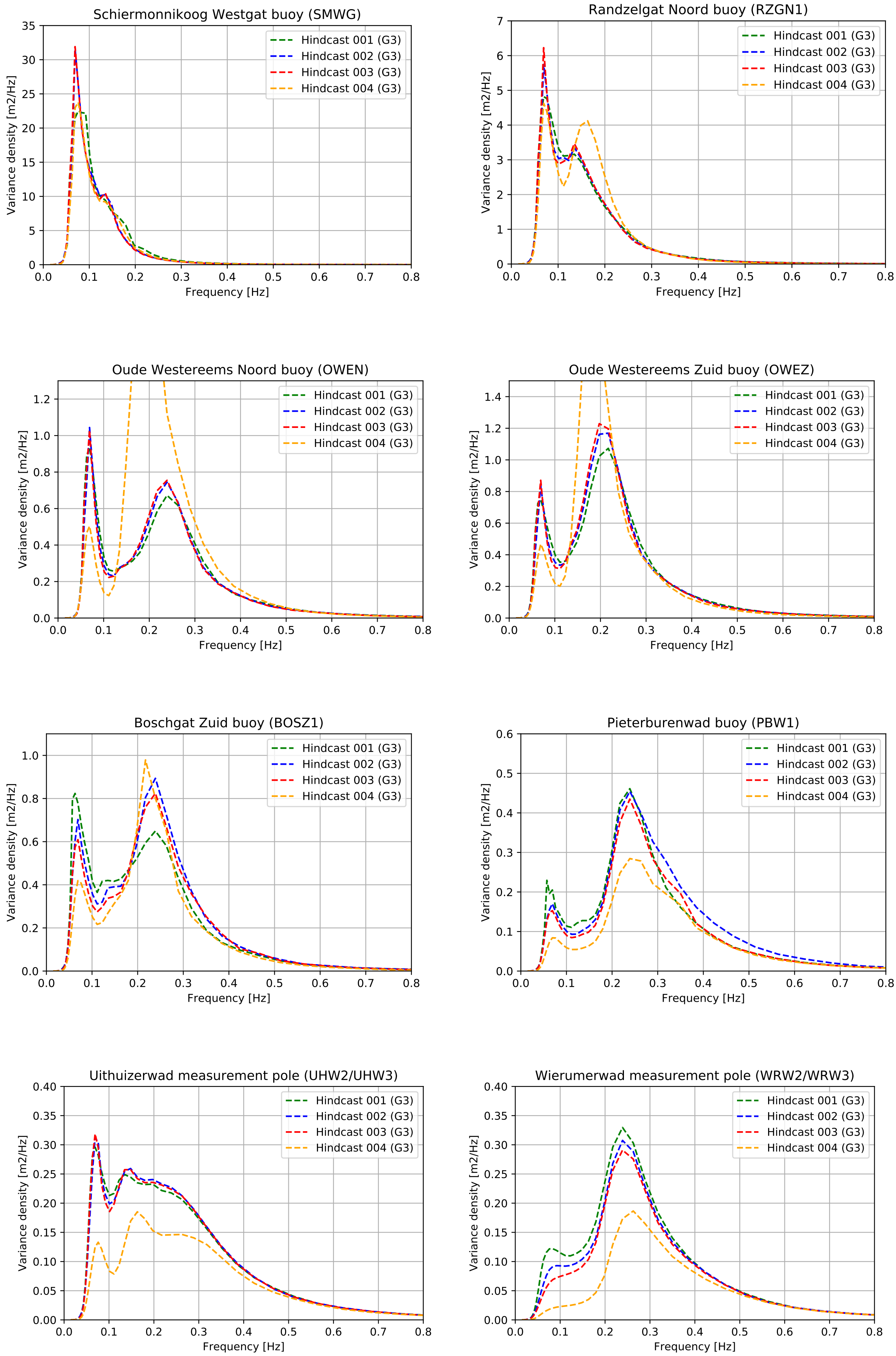

Figure V.30: Wave spectra of variance density from SWAN hindcast 2019

Table V.1: Measured spectral wave height H_{m0} [m] compared to SWAN output for 8 January 2019

Hindcast 08-01-2019 Locations	X	Y	Measured [m] 11:20	Model 001 (G1) 11:20	Model 001 (G3) 11:20	Measured [m] 11:40	Model 002 (G1) 11:40	Model 002 (G3) 11:40	Measured [m] 11:50	Model 003 (G1) 11:50	Model 003 (G3) 11:50	Measured [m] 13:10	Model 004 (G1) 13:10	Model 004 (G3) 13:10
Ameland Westgat	191767	611861	-	4.76912	4.76875	-	4.68675	4.69312	-	4.63942	4.69606	-	4.44976	4.42613
Boschgat Zuid	226200	612700	1.28	-9	1.6472	1.34	-9	1.71267	1.34	-9	1.66579	1.21	-9	1.56405
Huibertgat	221990	621330	-	4.97879	5.03943	-	4.90932	4.97	-	4.88905	4.99548	-	4.95217	4.98722
Lauwers Oost	225500	617700	-	2.18817	2.31009	-	2.07635	2.22825	-	2.03552	2.19642	-	1.81541	1.98274
Oude Westereems Noord	240557	614915	1.09	-9	1.61036	1.03	-9	1.60945	0.97	-9	1.60843	0.9	-9	2.07827
Oude Westereems Zuid	243806	612177	1.31	-9	1.8353	1.3	-9	1.84788	1.33	-9	1.85647	1.24	-9	1.9769
Pieterburenwad	225792	608394	1.12	-9	1.23309	1.07	-9	1.28475	1.06	-9	1.19396	1.08	-9	1.04053
Randzelgat Noord	237439	621340	2.64	2.5361	3.11852	2.57	2.55621	3.09383	2.34	2.56291	3.10335	1.81	2.73054	3.2131
Schiermonnikoog Noord	206527	623484	6.53	6.7829	6.57697	6.72	7.19779	6.95343	6.86	7.41055	7.13343	6.23	6.58198	6.3878
Schiermonnikoog Westgat	195585	615149	99999	5.57146	5.45719	8.96	5.4261	5.41437	99999	5.41361	5.41926	4.29	5.26166	5.19409
Uithuizerwad (Radac)	245996	609772	0.99	-9	1.16176	1.05	-9	1.16676	1.07	-9	1.16256	0.95	-9	0.96129
Uithuizerwad (Etrometa)	245996	609772	0.62	-9	1.16176	0.62	-9	1.16676	0.63	-9	1.16256	0.79	-9	0.96129
Westereems Oost	230086	626634	4.02	5.11026	4.8517	4.25	5.05871	4.80236	4.68	5.06702	4.80494	3.94	4.91421	4.72372
Westereems West	219900	626397	6.31	6.57942	6.45736	6.29	6.64218	6.54026	6.03	6.77594	6.69477	6.5	6.29043	6.28733
Wierumergronden	192882	614562	-	6.18019	6.02822	-	6.11673	5.9971	-	6.13924	6.00885	-	5.88948	5.79157
Wierumerwad (Radac)	199957	602618	-	-9	1.12307	-	-9	1.07469	-	-9	1.04608	-	-9	0.85978
Wierumerwad (Etrometa)	199957	602618	-	-9	1.12307	-	-9	1.07469	-	-9	1.04608	-	-9	0.85978

Table V.2: Measured spectral wave period $T_{\mathrm{m\text{-}1,0}}$ [s] compared to SWAN output for 8 January 2019

Hindcast 08-01-2019 Locations	X	Y	Measured [s] 11:20	Model 001 (G1) 11:20	Model 001 (G3) 11:20	Measured [s] 11:40	Model 002 (G1) 11:40	Model 002 (G3) 11:40	Measured [s] 11:50	Model 003 (G1) 11:50	Model 003 (G3) 11:50	Measured [s] 13:10	Model 004 (G1) 13:10	Model 004 (G3) 13:10
Ameland Westgat	191767	611861	-	9.3225	9.3951	-	9.4189	9.8893	-	9.564	10.0665	-	9.269	9.5683
Boschgat Zuid	226200	612700	6.6	-9	6.3885	6.3	-9	5.7221	6.8	-9	5.6516	6.1	-9	5.3901
Huibertgat	221990	621330	-	9.974	9.9056	-	10.0367	9.9846	-	10.1436	10.2223	-	9.254	9.5531
Lauwers Oost	225500	617700	7.6	7.2884	7.775	6.8	6.7016	7.3058	7	6.6937	7.3214	6.8	6.5351	7.1347
Oude Westereems Noord	240557	614915	4.7	-9	6.2807	4.5	-9	6.1428	4.6	-9	6.173	4	-9	5.2337
Oude Westereems Zuid	243806	612177	4.7	-9	5.8385	4.6	-9	5.7547	4.5	-9	5.8102	4.4	-9	5.5167
Pieterburenwad	225792	608394	3.9	-9	4.8821	3.9	-9	4.4046	3.9	-9	4.5691	3.8	-9	4.1386
Randzelgat Noord	237439	621340	8.4	6.797	8.4284	8.1	6.7956	8.3771	7.9	6.848	8.4885	7.8	6.5207	7.8328
Schiermonnikoog Noord	206527	623484	11.1	10.5902	10.3638	11.3	10.5457	10.4388	11.8	10.8486	10.7559	11.1	10.646	10.4876
Schiermonnikoog Westgat	195585	615149	99999	9.9224	10.1371	20.8	10.2988	10.3445	99999	10.4676	10.5021	11.3	9.9339	10.187
Uithuizerwad (Radac)	245996	609772	5.37	-9	5.79	5.1	-9	5.7026	5.1	-9	5.73	4.6	-9	4.8465
Uithuizerwad (Etrometa)	245996	609772	5.6	-9	5.79	5.5	-9	5.7026	5.4	-9	5.73	4.5	-9	4.8465
Westereems Oost	230086	626634	10.2	9.8865	9.5606	10.9	9.904	9.613	10.9	10.032	9.7466	10.2	9.4793	9.2801
Westereems West	219900	626397	11.2	10.532	10.3859	11.5	10.6883	10.5886	11.5	10.8786	10.8	11.5	10.4162	10.4766
Wierumergronden	192882	614562	-	9.9649	10.1584	-	10.1791	10.4242	-	10.3114	10.6046	-	9.979	10.1359
Wierumerwad (Radac)	199957	602618	4.2	-9	4.5684	4.2	-9	4.3098	4.3	-9	4.1408	3.7	-9	3.409
Wierumerwad (Etrometa)	199957	602618	4.3	-9	4.5684	4.2	-9	4.3098	4.1	-9	4.1408	3.7	-9	3.409

V.5. Results at HRbasis locations

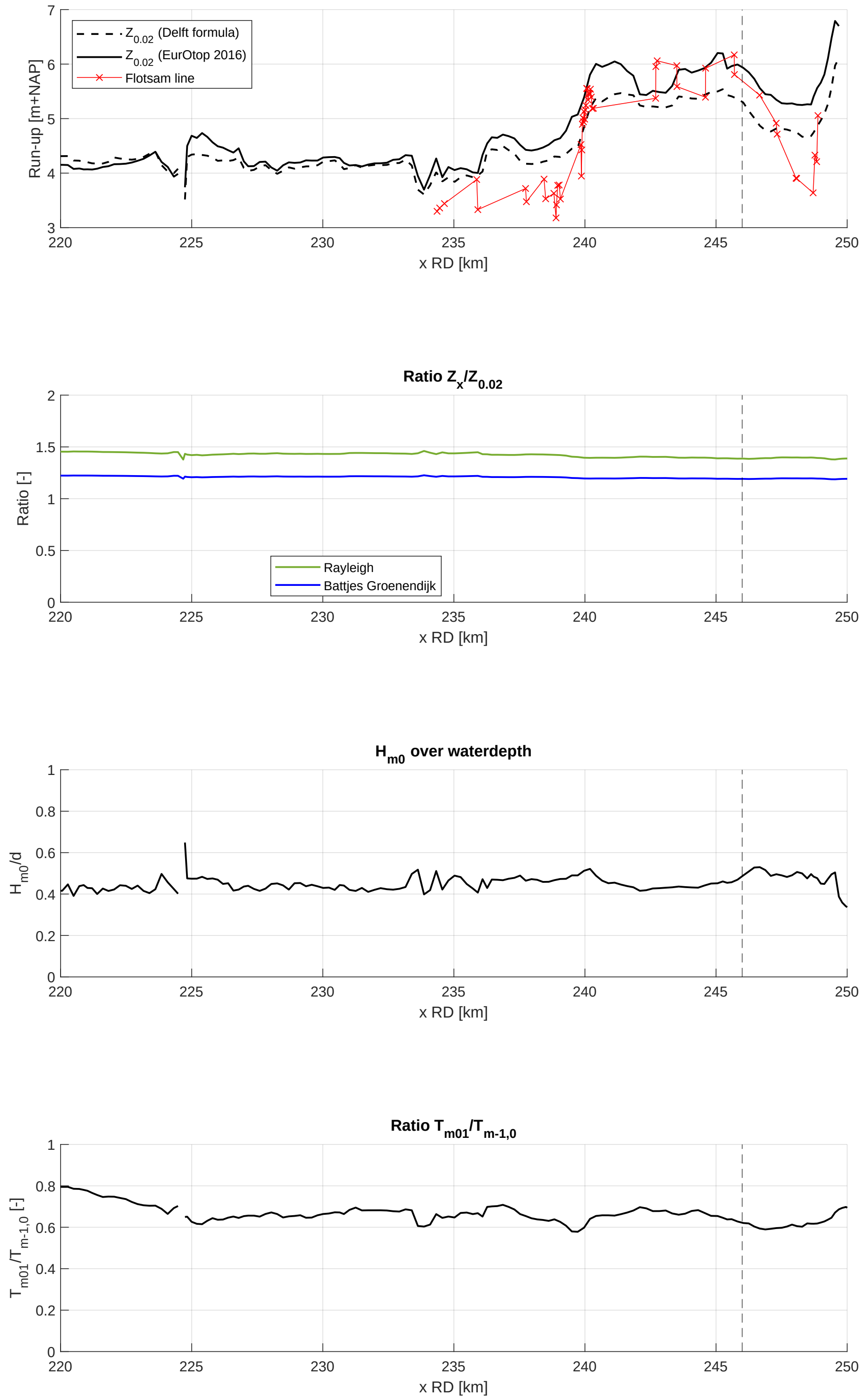

Figure V.31: Results at HRbasis locations for highest wave run-up at 8 January 2019 11:20.

VI

Wave conditions salt marsh edge 2015

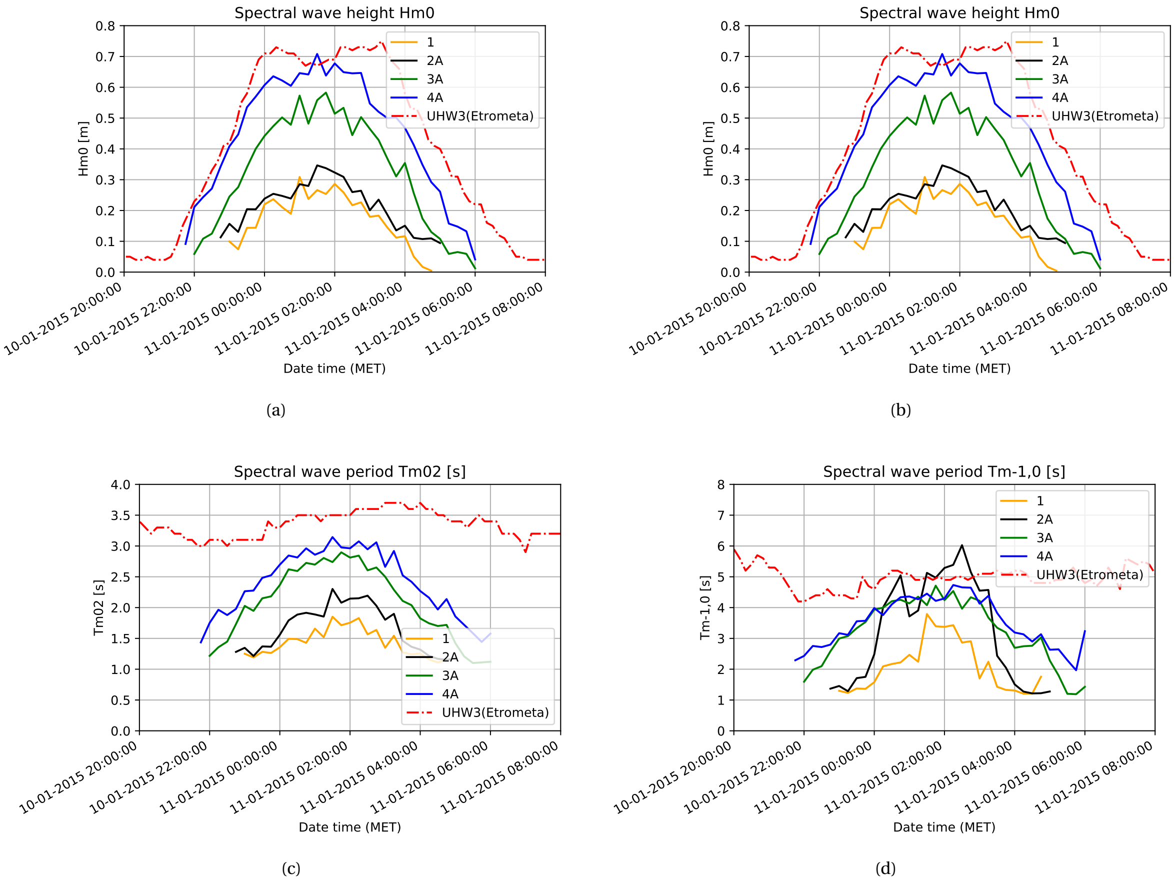

Figure VI.1: Measured data at locations 1, 2A, 3A and 4A compared to measurements at Uithuizerwad for 10/11 January 2015.

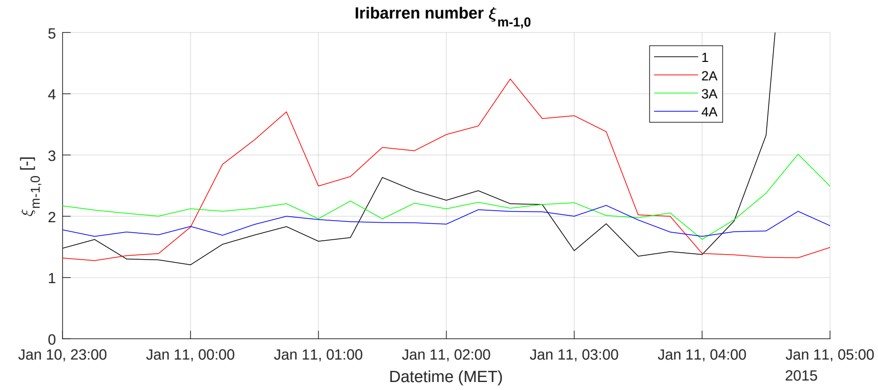

Figure VI.2: Breaker parameter based on $T_{\text{m-1,0}}$ for locations 1, 2A, 3A and 4A in 2015.

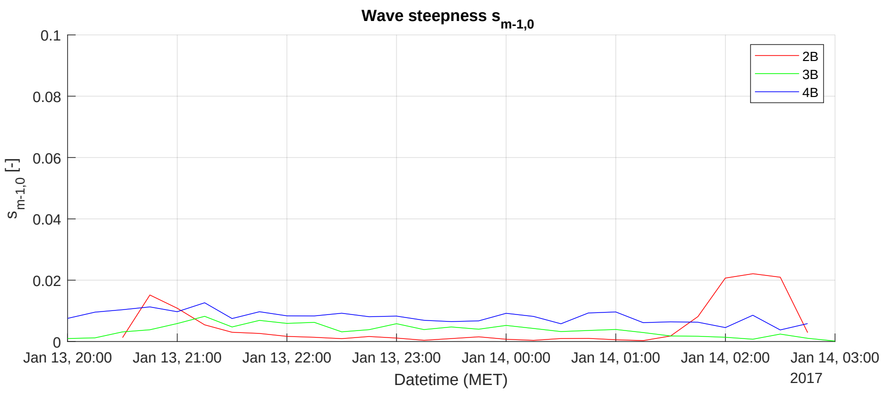

Figure VI.3: Wave steepness based on $T_{\text{m-1,0}}$ for locations 1, 2A, 3A and 4A in 2017.

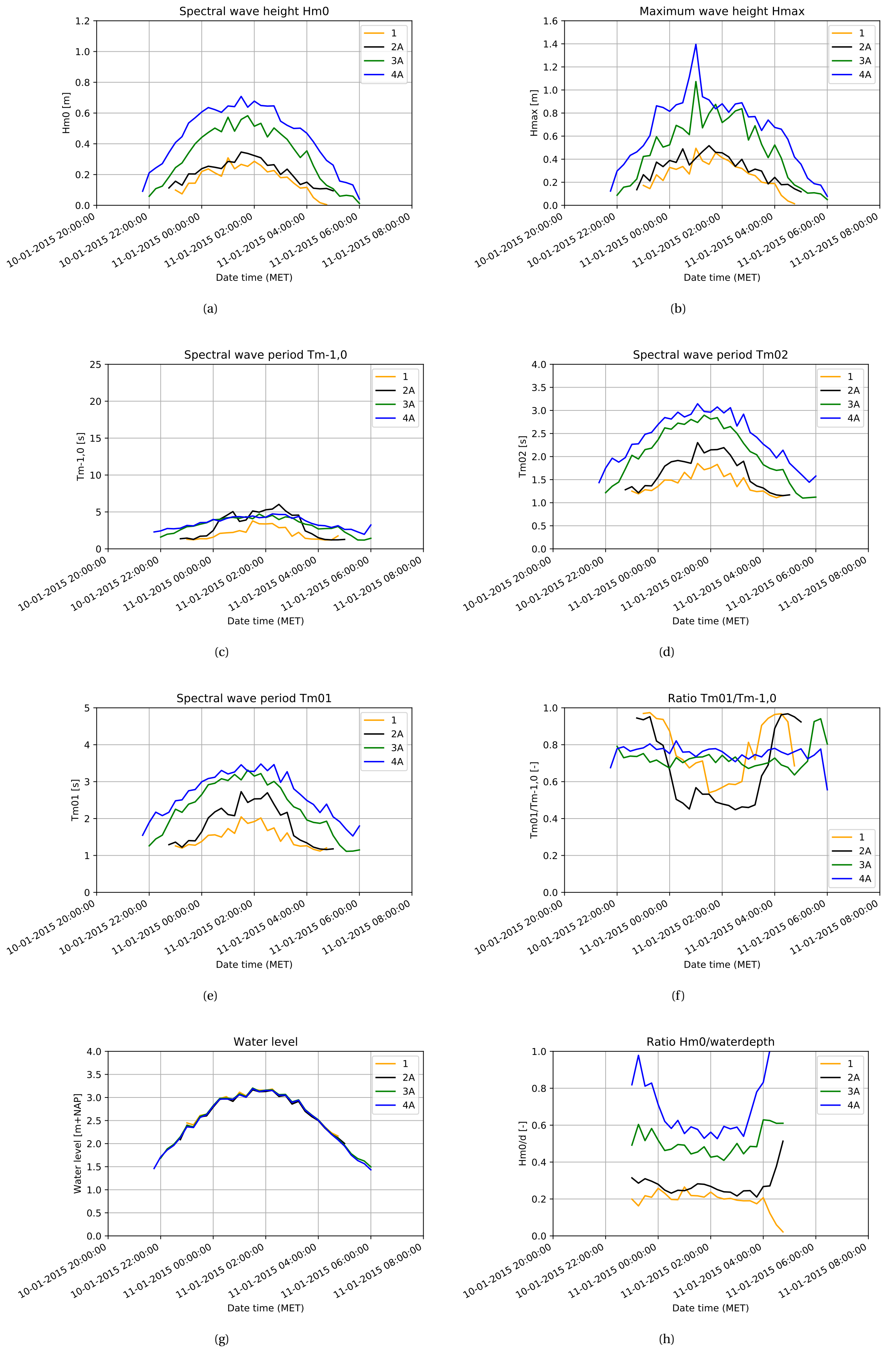

Figure VI.4: Measured properties at locations 1, 2A, 3A, 4A at 10/11 January 2015.

VII

Wave conditions salt marsh edge 2017

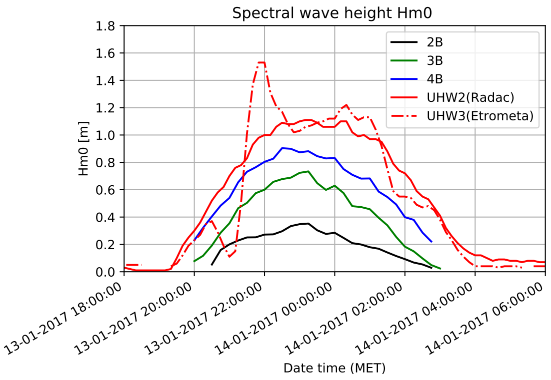

(a)

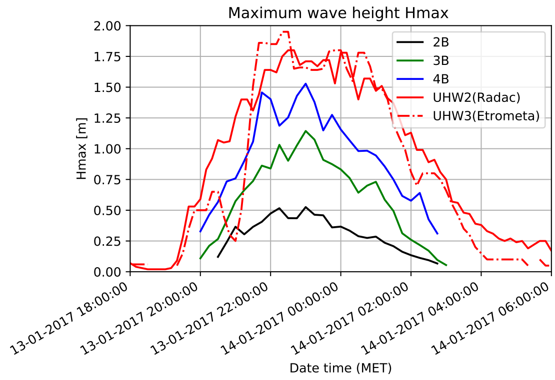

(b)

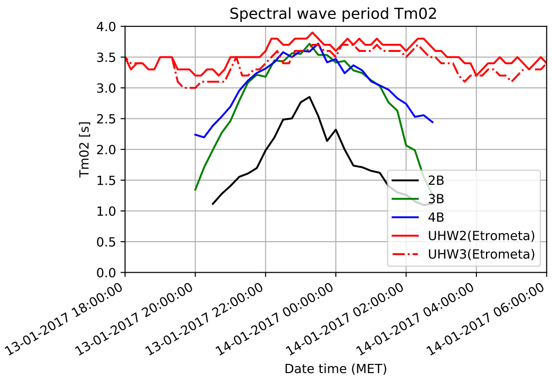

(c)

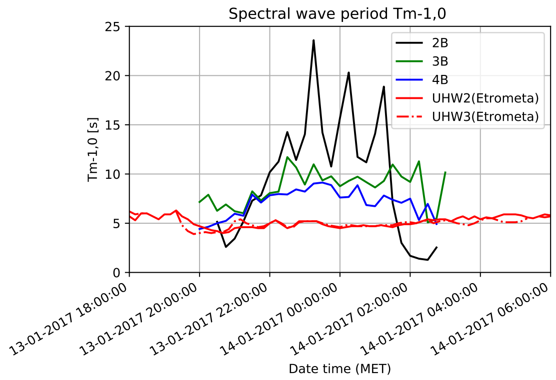

(d)

Figure VII.1: Measured data at locations 2B, 3B and 4B compared to measurements at Uithuizerwad for 13/14 January 2017.

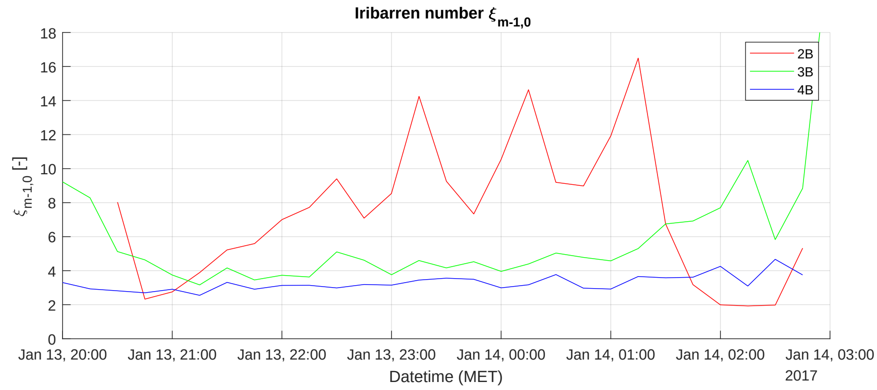

Figure VII.2: Breaker parameter based on $T_{\text{m-1,0}}$ for locations 2B, 3B and 4B in 2017.

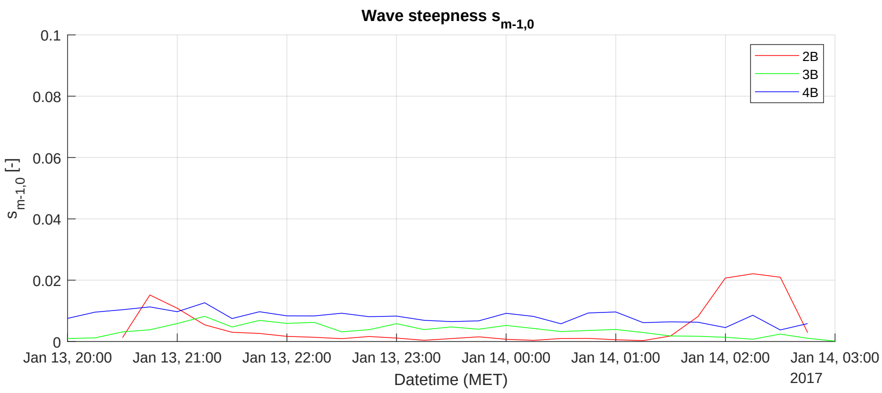

Figure VII.3: Wave steepness based on $T_{\text{m-1,0}}$ for locations 2B, 3B and 4B in 2017.

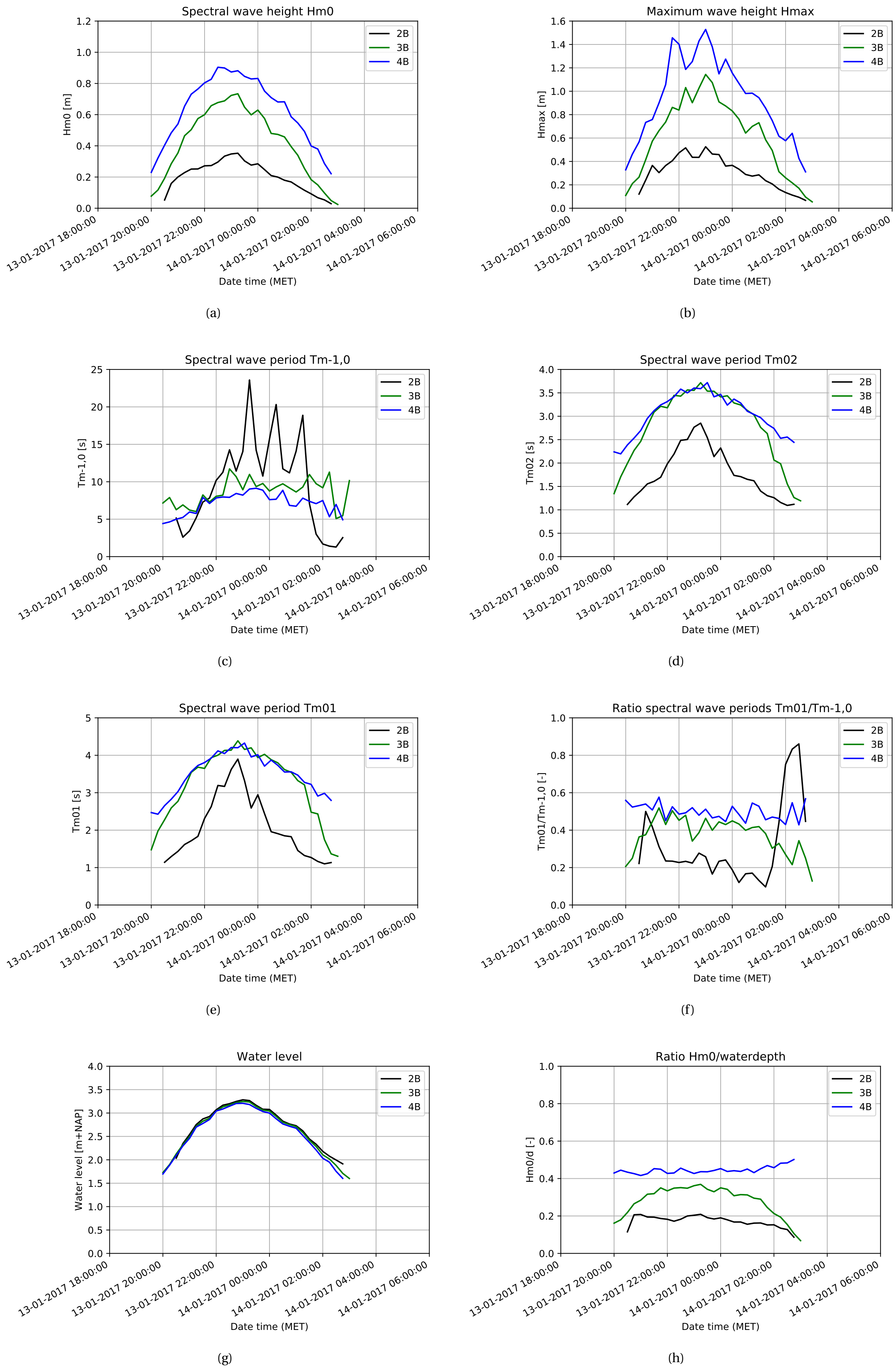

Figure VII.4: Measured properties at locations 2B, 3B and 4B at 13/14 January 2017.